UNIVERSITY OF CAPE TOWN

DEPARTMENT OF CIVIL ENGINEERING

CIV5000Z: MASTERS THESIS

Research topic:

"*Alternative patch repair materials for rebar corrosion damage*"

Compiled By: Primesh Jassa

Student Number: JSSPRI001

Supervisor: Professor Hans Beushausen

Co-Supervisor: Dr Ines Tchetgnia Ngassam

Department: Concrete materials and structural integrity research unit (CoMSIRU)

Date: May 2017

This thesis is submitted in partial fulfilment of the requirements for the degree of Master of Science in Civil Engineering

Plagiarism declaration

1. I know that plagiarism is wrong. Plagiarism is using another's work and to pretend that it is one's own.
2. I have used the Harvard Convention for citation and referencing. Each significant contribution to, and quotation in this thesis, from the work, or works of other people has been attributed and has been cited and referenced.
3. This thesis is my own work.
4. I have not allowed, and will not allow, anyone to copy my work with the intention of passing it off as his or her own work.
5. I acknowledge that copying someone else's work, or part of it, is wrong, and declare that this is my own work.
6. I know the meaning of plagiarism and declare that all the work in the document, save for that which is properly acknowledged, is my own. This thesis/dissertation has been submitted to the Turnitin module (or equivalent similarity and originality checking software) and I confirm that my supervisor has seen my report and any concerns revealed by such have been resolved with my supervisor.

Name	Student Number	Signature	Date
Primesh Jassa	JSSPRI001	Signed by candidate	20 May 2017

Dedicated to my parents for their unconditional support and sacrifices made throughout my studies.

Acknowledgements

The research conducted and presented in this thesis required assistance and information to be gathered from multiple sources. Therefore, I will sincerely like to thank the following for their support that enabled me to successfully complete this research project:

- Professor Hans Beushausen for supervising my research. It was truly a great honour working with him as he provided invaluable guidance from his vast background in the civil and concrete engineering field. He provided constant advice and motivation throughout the research project for which I am very grateful.
- Dr Ines Tchetgnia Ngassam for co-supervising my research. It was a pleasure working with her and I thank her sincerely for guiding me through my work and constantly being available for consultation.
- Concrete Materials and Structural Research Unit (CoMSIRU) for providing funding for my research. I am thankful for the opportunity to work with this research group. The information sources and networking opportunities made available through the research unit was instrumental to my studies.
- Mr Nooredien Hassen & Mr Taahir Mukaddam for organizing testing equipment and providing information and guidance in the civil engineering laboratory at the University of Cape Town (UCT).
- Mr Charles Nicholas from the civil engineering workshop at UCT who assisted in manufacturing the substrate moulds.
- The laboratory staff in the civil engineering laboratory: Mr Charlie May, Mr Elvino Witbooi, Mr Leonard Adams and Mr Chris Caesar.
- Mrs Lorraine Nkemba from the Centre for Minerals Research (UCT) for assisting with SEM sample preparation.
- Mrs Miranda Waldron from the Centre for Imaging and Analysis (UCT) for assisting with operating the SEM equipment.
- Adri Swanepoel from Dalven Products who supplied the bitumen used in this research project.
- Postgraduate colleagues from CoMSIRU who provided constant motivation and created an environment optimal for learning.
- All the authors who have been referenced in this thesis for their informative publications.

Abstract

Reinforced concrete (RC) is extensively used in the construction industry. It is particularly used to guarantee that infrastructure assets around the world last for multiple years whilst ensuring that the structural integrity and serviceability of the structure is maintained. However, in practice countless RC constructions are failing prematurely due to a large number of factors of which the corrosion of steel embedded within concrete is the most significant (Matthews *et al*., 2003). Steel corrosion is particularly pernicious to concrete due to the expansive nature of the corrosion by-products formed, which commonly leads to cracking and spalling. One of the most common methods adopted in the rehabilitation of corrosion damaged concrete is the patch repair procedure. However, in practice this method has shown to often be unreliable as a consequence of the widespread occurrence of shrinkage cracking and poor substrate-patch adhesion leading to debonding of the patch repair. From a practical point of view, such failed repair systems essentially restore the repaired concrete back to a deteriorated state. The underlying cause of poor durability in patch repairs is attributed to a range of reasons including, the lack of understanding of the substrate-patch composite system and the limited availability of appropriate design standards. Furthermore, there is a lack of understanding in the repair industry on the critical material properties actually required for durable patch repairs. There is a common belief that repairing concrete with specialised proprietary repair materials would guarantee durability. However the widespread premature failure of patch repairs conducted using such materials has proven the contrary. A proper patch repair process includes treatment of the corroded steel, adequate substrate surface preparation, installing sacrificial anodes (at least for chloride contaminated concrete) and surface coating. In principle, if this process is correctly followed then the material requirements for a durable, non-structural repair would be to fill in the cavity created by removing contaminated concrete, resist shrinkage induced cracking and/or debonding and provide protection against chloride ingress (in chloride environments). The material used for patch repairs could be any appropriate repair material and it does not specifically need to be a specialised cementitious repair mortar. This dissertation presents an understanding of the materials and issues concerning the durability and serviceability of patch repairs, with the aim of identifying alternative non-structural patch repair materials for the durable repair of corrosion-damaged concrete structures. The potential patch repair materials studied in this dissertation were rubberised waterproofing bitumen, polymer (copolymer of vinyl acetate and ethylene) with 5% cement replacement and 60%, 80% and 100% fly ash (FA) mortar. Patch repairs were conducted on substrate moulds to test application and observe cracking/debonding occurrence. Furthermore, compressive strength, durability index, accelerated drying shrinkage, restrained shrinkage, workability and SEM tests were conducted. It was concluded that the 60% FA repair material had the best overall performance with the polymer-cement concrete exhibiting good bonding and crack resistance properties. This research established that innovative alternative repair materials such as a 60% FA or polymer-cement concrete material, can be developed for non-structural patch repairs with improved long-term performance relative to conventional materials. The research has further provided a foundation for the development and design of durable repair mortars by identifying the principal material performance properties required of such materials.

Table of contents

List of figures

List of tables

List of equations

Abbreviations and symbols

CCI	Chloride conductivity index
CSH	Calcium silicate hydrates
FA	Fly ash
HAC	High alumina cement
LKD	Lime kiln dust
MDOT	Michigan Department of Transportation
MSU	Montana State University
OPC	Ordinary Portland cement
OPI	Oxygen permeability index
PC	Portland cement
RC	Reinforced concrete
RWBC	Rubberised waterproofing bitumen compound
SACP	Sacrificial anode cathodic protection systems
SEM	Scanning electron microscope
UCT	University of Cape Town
WSI	Water sorptivity index
w/b	Water to binder ratio
w/c	Water to cement ratio
mm	Millimetres
m	Metres
µm	Micrometres
^{o}C	Degrees Celsius

1 Introduction

1.1 Background

Reinforced concrete has been used in the construction industry for around 150 years. It is the most widely used material the world over. It is estimated that up to one tonne of concrete for every person on earth is consumed annually (Hendrik, 2007). It is a very resourceful composite material that is economical and abundant. This is because concrete can be easily moulded into unique shapes for many different uses. Furthermore, the raw materials needed to manufacture concrete including stone and sand are easily sourced from the earth. Concrete has a long service life and has generally proved to be resistant to harsh environmental conditions. However, concrete is a brittle material with good resistance to compressive stress but it is limited in tensional and bending strength. Additionally, concrete does not have a high fracture toughness. As a solution to this, steel is typically embedded within the concrete matrix as a reinforcement mechanism. Although, steel improves robustness and enhances the mechanical properties of the concrete, it is not inert to chemical deterioration. This introduces a serious durability concern in reinforced concrete (RC) exposed to harmful environmental conditions.

Steel used as reinforcement is prone to corrosion in the presence of oxygen, moisture and aggressive species. Corrosion is the electrochemical deterioration of materials due to reaction with substances in the environment. However, steel is naturally protected in concrete due to the alkaline environment that leads to the passivation of steel thereby, forming a protective layer against corrosion (Owens, 2009). Nevertheless, due to the effect of destructive chemical processes predominantly, carbonation and chloride ion attack, corrosion is possible (Song & Shayan, 1998). These processes further increase the severity and rate of corrosion. As a consequence of the damaging effects of reinforcement corrosion an extensive amount of prior research has been conducted to understand concrete deterioration and principles such as: the mechanism and effects of reinforcement corrosion (Browne, 1980), the rate of reinforced corrosion (Andrade & Alonso, 2001) and corrosion induced concrete cracking (Torres-Acosta & Sagues 2004; Vu *et al* 2005).

The principal cause of steel corrosion is attributed to ingress of aggressive species into concrete up to the embedded steel. The infiltration of moisture, which frequently contains harmful contaminants such as chloride ions, carbon dioxide gas and hydroxide ions, into concrete initiates the corrosion process. Corrosion chemical reactions generate a range of by-products. These products, particularly the expansive ones are most detrimental to concrete integrity. Expansive corrosion products cause extensive volume changes that result in cracking, delamination and ultimately spalling of the concrete matrix. Furthermore, cracking exacerbates concrete deterioration since aggressive media can now easily penetrate into the concrete element. Over time, this diminishes the serviceability and structural integrity of the RC element. Steel corrosion is of major concern in civil engineering due to its widespread occurrence and associated effects of concrete cracking, delamination and spalling as shown in Figure 1-1.

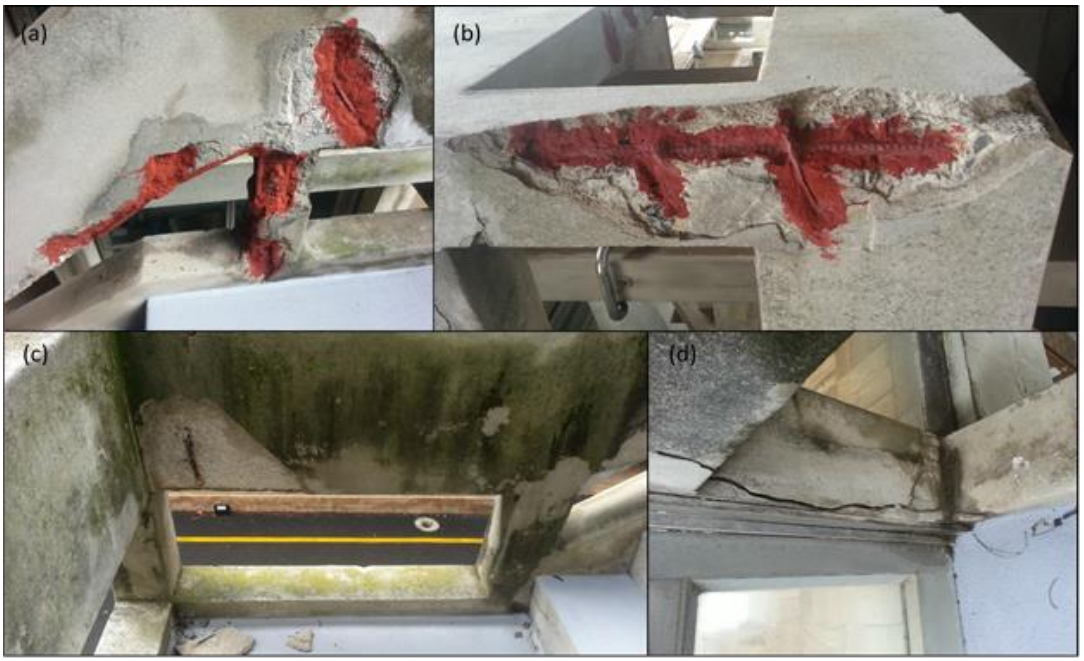

Figure 1-1: Effects of reinforcement corrosion: (a) & (b) extensive spalling exposing embedded steel (c) delamination (d) cracking (pictures taken on UCT upper campus)

Corrosion is predominantly responsible for the premature loss of durability in RC structures (Hansson *et al* 2007; Smith & Virmani 2000; Song & Shayan 1998; Cabrera 1996). Furthermore, the deterioration of concrete structures due to steel corrosion is worsened by numerous other factors including: deficient designs, poor construction methods, lack of monitoring and maintenance, exposure to aggressive environmental conditions, the use of non-durable construction materials and increases in service loads (Banthia *et al*., 2014).

Early failure of concrete due to reinforcement corrosion is an important issue because the rehabilitation of deteriorating infrastructure is a difficult task that usually has massive cost implications. For example, more than 50% of Europe's annual construction budget is used for the repair and rehabilitation of existing infrastructure (Matthews *et al*., 2003). Additionally, throughout the world there is an ever-increasing amount of ageing infrastructure. Therefore, the economic and financial costs involved in the assessment, maintenance and repair of concrete infrastructure is expected to increase further in the future.

One of the most widely applied solutions for the repair of corrosion damaged RC is the patch repair method (Courard *et al*. 2014; Beushausen & Alexander 2007). This method is commonly applied to concrete structures for addressing spalling and localised corrosion induced damage (Addis & Owens, 2009). The repair process involves the removal of defective concrete and all corrosion products followed by treatment of the corroded steel. This is done by surface coating or steel replacement in extreme cases. The removed concrete is then replaced with patch materials and finally the finished surface of the repaired concrete is typically coated. However, the lack of durability of concrete patch repairs is a common occurrence the world over. The Michigan department of transportation (MDOT) has reported that 8-10% of concrete spall repairs fail within the first year of service and that 50% fail within the first 5 years (MDOT, 1996).

A comprehensive investigation on 230 concrete structures in Europe called the ConRepNet report concluded that up to 50% of all concrete repairs had failed prematurely (Matthews *et al.*, 2003). Furthermore, the report concluded that up to 75% of all repairs failed within the first 10 years of service as illustrated in Figure 1-2 below.

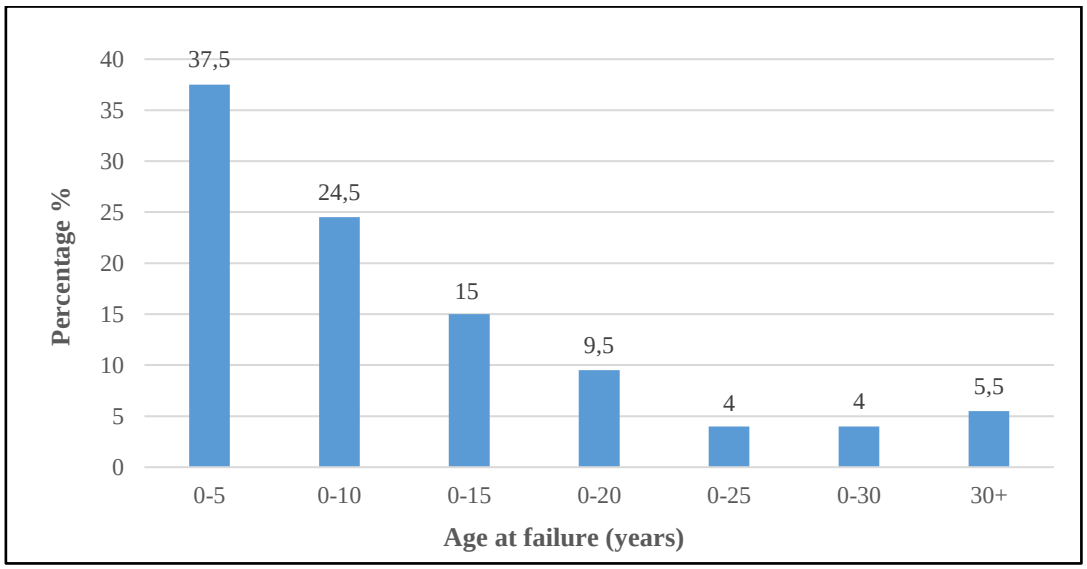

Figure 1-2: Age of concrete repair at failure (Matthews *et al.*, 2003)

This huge failure rate occurs despite the fact that numerous improvements in materials and methods have been developed. In practice, the continuation of corrosion in the adjacent substrate concrete, shrinkage induced cracking and subsequent debonding of the patch repair is widespread. These mechanisms fundamentally return the concrete integrity back to a deteriorated state. There are a multitude of underlying reasons for these failures including a lack of technical knowledge, application of substandard construction methods, poor substrate preparation, incorrect selection of repair materials, insufficient curing, time-dependent material properties, wrong diagnosis and severe environmental conditions. However, poor workmanship and differential shrinkage between the substrate and patch have been identified by Alexander & Beushausen (2009) as the chief inhibiting factors for the durability and service life performance of patch repair systems.

Essentially, a correctly applied patch repair would ensure a low failure rate. Particularly, if the corroded steel is adequately treated and the underlying cause of corrosion addressed, then the only requirement for a complete, non-structural patch repair on carbonation damaged concrete would be to fill in the cavity initially created by removing defective concrete. For non-structural repairs on carbonation damaged structures, in isolation to the integrity of the adjacent substrate, the basic purpose of the fill material selected would be to simply restore the serviceability (aesthetics) of the repaired element. Fundamentally, this can be achieved with any material which does not specifically need to be a specialised repair mortar. However, in the case of chloride ion induced corrosion, any non-structural patch repair also needs to limit the ingress of aggressive media into the repair. The material needs to have the added property of being sufficiently impermeable to chloride ions and moisture.

This difference in repair material requirement between carbonation and chloride-induced corrosion is an important aspect that must be considered. The use of highly specialised commercially available repair mortars for non-structural patch repairs is widespread in the repair industry. Besides the cost implications of using such repair mortars, this practice does not consider resource efficiency. There is a common misconception that repairing damaged concrete with specialised materials would guarantee durability. However, this approach is incorrect and points to the lack of technical understanding of the patch repair procedure. The use of specialised repair mortars for patch repairs is in many cases probably not necessary.

This is because the properties exhibited by these mortars, such as high compressive strength and high elastic modulus are not required for non-structural patch repairs. Furthermore, high mechanical performance of repair mortars may even result in a lack of performance with regards to cracking. An adequate substrate-patch bond and crack resistance are the core requirements of any material selected for a patch repair programme. A seemingly substandard repair material that meets these basic requirements has the potential to outlast specialised repair mortars in non-structural repair applications. This thesis is based on the theme of identifying such alternative materials for the durable, non-structural patch repair of corrosion damaged concrete.

1.2 Problem statement

Patch repairs have very limited performance with respect to long-term durability. Poor repair durability results in the need for frequent repairs to maintain the serviceability and structural integrity of an infrastructure asset. However, having to perform repairs of repairs is highly inefficient and has considerable economic and environmental impact. For infrastructure asset managers, the cost of concrete repair is estimated at $ 18 to $ 21 billion in the United States alone (Emmons & Sordyl, 2006) whereas, in Asia the repair and retrofitting of infrastructure is estimated to cost $ 2 trillion. In Europe, Japan, Korea and Thailand the cost of infrastructure repairs has exceeded the cost of new construction (Li & Li, 2011).

Furthermore, the amount of prior research conducted relating to specifically, the durability of repair mortars commonly used in the repair industry is highly inadequate. The widespread use of commercially available, specialised repair mortars for the patch repair of deteriorated concrete has shown no significant improvement in the long-term durability of patch repairs. This is a consequence of the limitations of using cementitious based repair materials and the limited understanding of the critical material properties actually required of patch repair materials. Adding to this issue is the fact that standards relating to concrete repair specify guidelines such as minimum compressive strength and elastic modulus which do not fundamentally correlate to improved durability, particularly in non-structural patch repairs. Furthermore, it is clear from the widespread failure of patch repairs that the specifications made by standards do not relate to actual field performance.

1.3 Justification of study

In response to the issues identified in the problem statement, there is a need to conduct new research to develop an improved understanding of:

- The underlying cause for poor durability performance of non-structural patch repairs.
- The most critical properties required of patch repair materials.
- The possibility of utilising new, seemingly substandard and unconventional repair materials for non-structural patch repairs.

1.4 Objectives of study

The primary objective of this study is to identify alternative cementitious and non-cementitious patch repair materials that could be effectively adopted in the durable, non-structural repair of corrosion damaged concrete. Specifically, this study will:

- Provide an understanding of the mechanisms and reasons behind the large failure rate of conventional patch repairs.
- Explain why it is often unnecessary to use "high-quality" and specialised proprietary repair mortars for non-structural patch repairs.
- Experimentally establish whether the materials developed through this research can be effectively and practically used in non-structural patch repairs with the aim of improving patch repair durability.

1.5 Scope and limitations of research

This study specifically investigates into the patch repair method of rehabilitating deteriorated concrete structures which is limited to:

- Non-structural patch repairs of corrosion damaged concrete.
- A patch repair with a depth of less than 50 mm and a surface area of less than $1m^2$.
- The practicality of utilising selected materials for patch repairs without considering the effect of these on the future corrosion state of the embedded steel.
- Laboratory investigations that will not model typical in-service conditions.
- All standards followed in the experimental programme were those specifically developed for concrete/cementitious materials. These same standards were also followed in working with the polymer and bitumen materials.
- A first approach, feasibility study that does not consider the optimisation (cost and mix design) of the repair materials for industry application.

1.6 Thesis outline

Chapter one provides an overview of the research topic and links it with the problem statement. The key objectives of the study and limitations are also presented. This is followed by a comprehensive review of important literature in chapter two. This chapter delves into the background details of the research topic to provide an understanding of the underlying issues concerning patch repair systems.

The chapter reviews into concrete repair durability issues, failure mechanisms and patch repair systems. Chapter two also reviews into possible materials that could be used for non-structural patch repairs based on promising prior studies that incorporated unconventional materials in the production of concrete/mortar. These materials included particularly ones that replaced cementitious material in high volumes with materials such as fly ash, lime kiln dust and polymers. Lastly, Section 2.9.3 of chapter two outlines the material performance requirements expected of an ideal non-structural patch repair material. Chapter three outlines the methodology adopted in the experimental work and details the procedures that were followed in conducting the research. The equipment and materials that were required to investigate the research topic are also specified. Chapter four presents the key results of the investigations with a discussion and analysis into the results. Conclusions drawn from the study are presented in chapter five. This chapter summarises the key findings of the research conducted followed by Section 5.2 that lists recommendations for future studies. The various sources consulted in gathering information to compile this research are acknowledged next in Chapter six with a complete list of references. Finally, supplementary material is included under Chapter seven, the appendices.

2 Literature review

2.1 Introduction

This dissertation was primarily aimed at developing alternative non-structural patch repair materials for reinforcement corrosion damaged structures. The research focused on understanding the cause of poor durability performance of patch repair systems in an effort to identify what principles and material properties are most critical to ensure patch repair durability. The most critical performance requirements for successful patch repairs were used as guidelines in developing new patch repair materials. Prior to experimental research, literature relevant to the thesis topic was reviewed which is presented in this chapter to provide a fundamental understanding of the thesis and a comprehensive framework on which to direct the research methodology. The extent to which the new materials met the performance requirements for application to non-structural patch repairs was then experimentally investigated.

Section 2.2 of this chapter presents a review into the background and the reasons behind the large failure rates of concrete repairs. Sections 2.3 and 2.4 provide an in-depth review into the fundamentals of reinforcement corrosion, particularly the deterioration mechanisms and chemical processes involved. Section 2.5 presents a review into the transport mechanisms in concrete which facilitate the movement of aggressive media in reinforced concrete. Section 2.6 delves into carbonation and chloride ion induced corrosion, which are predominantly responsible for steel deterioration in concrete. Section 2.7 reviews concrete repair according to the EN 1504 standard. Section 2.8 presents a detailed review into the patch repair procedure with an overview of the methodology and materials adopted as well as the limitations of these. The issues involved with conventional patch repairs and the effectiveness of these on carbonation and chloride ion damaged concrete is also discussed. Section 2.9 reviews literature into alternative materials and lastly, Section 2.10 presents a summary of the literature reviewed.

2.2 Concrete repair durability

2.2.1 ConRepNet report

The durability of concrete repairs has been evidently unsatisfactory throughout the construction industry around the world. The need to perform further repairs on previously repaired elements has massive time and cost implications. As a consequence of this some research effort has been directed towards concrete repair with the aim of establishing the cause of premature failure and developing possible solutions to mitigate this. One such study is the ConRepNet study conducted by Matthews *et al*. (2003) which is the most recent comprehensive study on concrete repair durability. The research was funded by the European Commission and investigated up to 230 cases of repaired concrete structures. The cases were selected from different locations around Europe with 70% of the cases from Northern Europe. The different structures examined along with the percentage distribution is depicted in Figure 2-1. These structures were selected from varying environmental conditions including urban, rural, coastal, highway and industrial conditions.

The study concluded that 50% of repaired concrete elements had failed prematurely due to a multitude of reasons. 25% were found to deteriorate within the first 5 years, 75% failed within 10 years and 95% failed within 25 years of service.

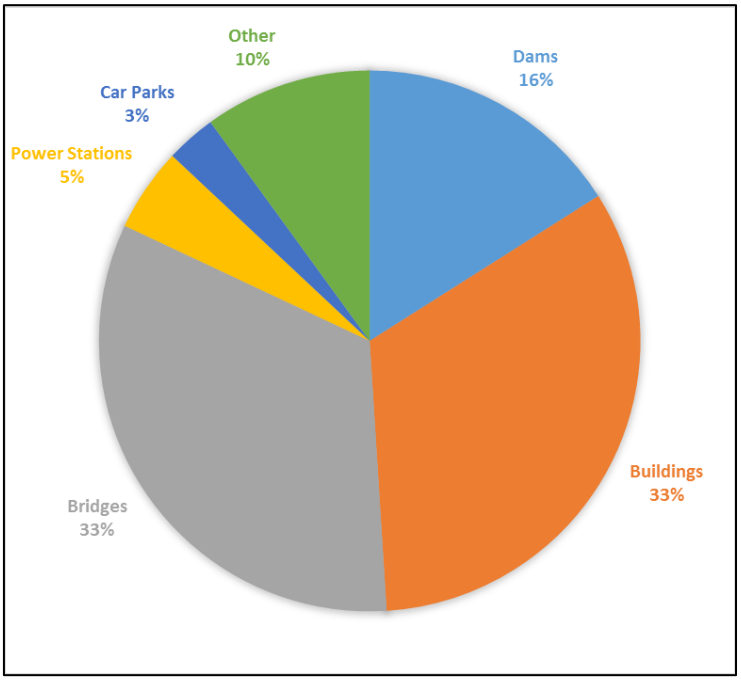

Figure 2-1: Percentage distribution of different structures (Matthews *et al.*, 2003)

2.2.1.1 Cause of failure

The ConRepNet study looked into the past performance of repaired structures to determine the reasons for failure as well as the performance of repairs in terms of time to failure. Based on the case study investigations Matthews *et al*. (2003) determined the dominant causes of concrete repair failure which are summarised in Figure 2-2. As depicted in Figure 2-2, "problems with repair materials" is directly linked to incorrect design. It is important to note that it is sometimes not the repair material but the effect of incorrect specification and wrong selection of repair materials that leads to failure. For example, utilising low strength concrete for structural repairs and using repair mortars with significant penetrability for repairs exposed to chloride ions. The "other" factors that were attributed to repair failure included undesirable service conditions such as overloading and exposure to de-icing salts as well as vandalism.

Many repairs were identified to fail due to incorrect diagnosis of the underlying mechanism of corrosion and concrete deterioration. Problems that were commonly misdiagnosed or not given proper attention included honeycombing, porous concrete, presence of chloride ions, presence of high alumina cement and not determining the original cause of cracking. With respect to incorrect design, not removing all defective concrete prior to patching, low cover, cosmetic treatment and inadequate drainage allowance were identified as the principal issues leading to failure. With continued corrosion cases, incipient anode formation was widespread due to defective concrete left untreated. Generally the study found that poor workmanship and deficient designs were key issues. Despite clear repair instructions, incorrect application of coatings was also common.

Based on these findings it can be identified that the premature failure of concrete repairs may not always be solely attributed to repair material failure, but rather the incorrect application of the repair material and not adhering to proper repair procedures. Therefore, it may be possible to substitute specialised proprietary repair materials, which are relatively expensive and exhibit unnecessary properties such as high compressive strength, with seemingly sub-standard repair materials. On condition that a repair procedure is properly executed, it is expected that such a substitute repair material would effectively serve the primary purpose of restoring the serviceability and durability of a deteriorated structure.

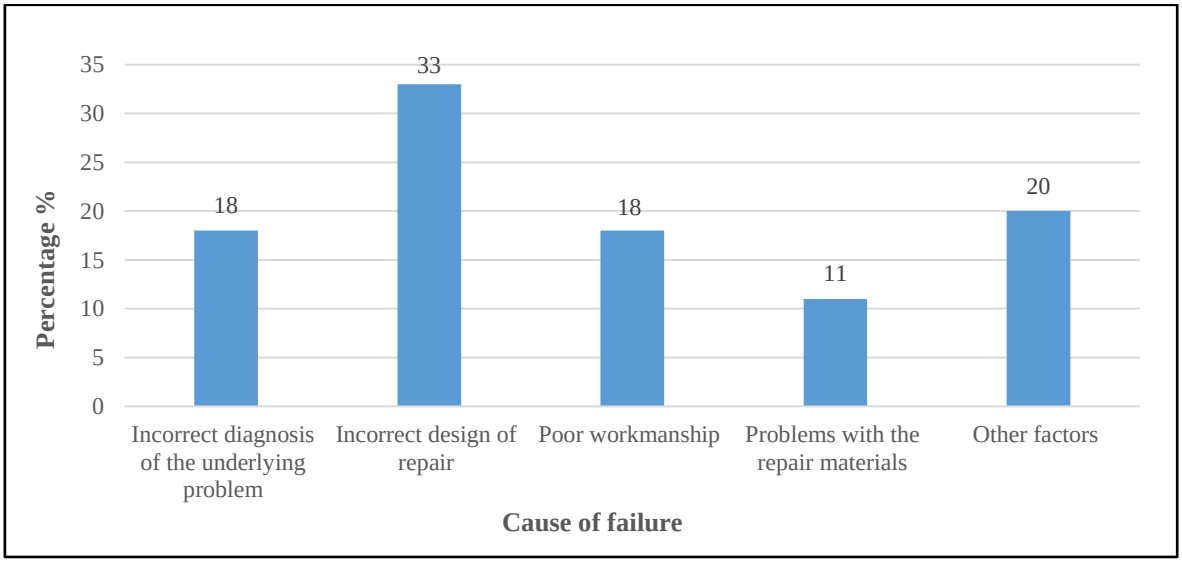

Figure 2-2: Main cause of repair failure (Matthews *et al.*, 2003)

2.2.1.2 Age at failure

The ConRepNet investigations also determined the age of repairs at failure and this data is summarised in Figure 2-3. It is apparent that most failures occur within the first 10 years, with nearly 38% of repairs failing within five years. This is an important finding that clearly identifies the issue of poor concrete repair durability in the construction industry.

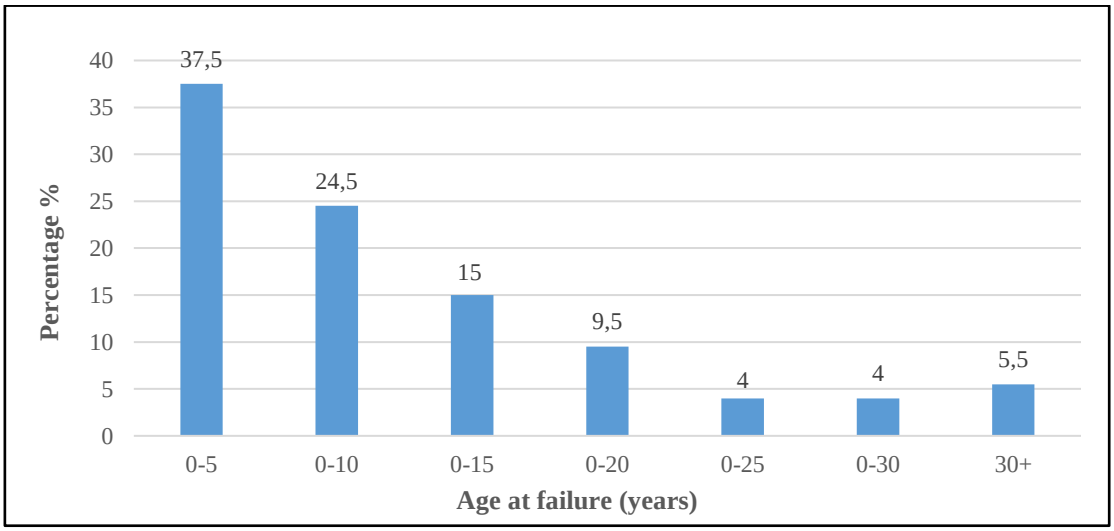

Figure 2-3: Age of concrete repair at failure (Matthews *et al.*, 2003)

2.2.1.3 Mode of failure

The key modes of concrete repair failure as identified by Matthews *et al*. (2003) are summarised in Figure 2-4. It is clear that continued corrosion, which is responsible for 37% of repair failures in this particular study, is the most important mode of failure. This is a consequence of incipient anode formation and not addressing the root cause of corrosion in the substrate concrete. Cracking of concrete was also identified to be a very significant mode of failure with 36%. Cracking is fundamentally caused by drying shrinkage and expansive corrosion products.

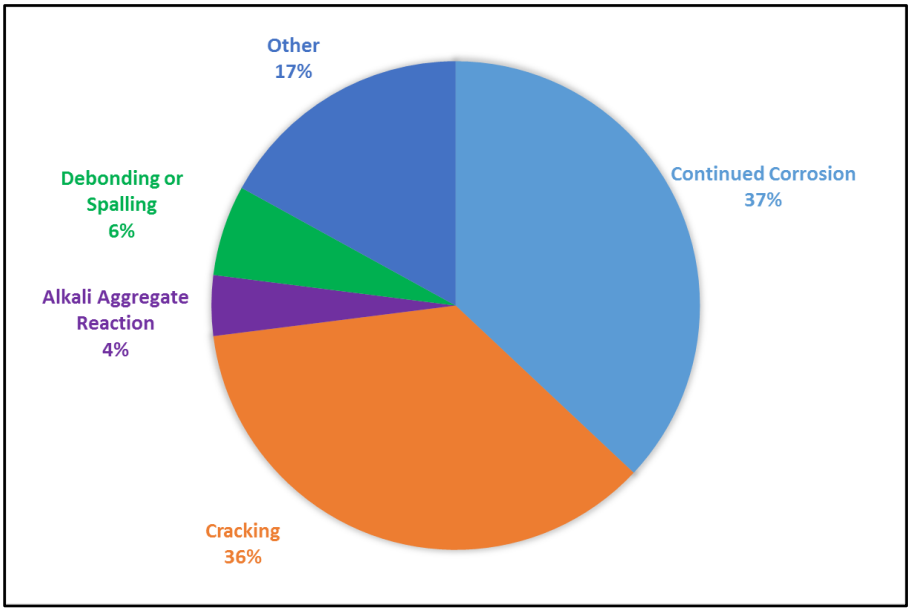

Figure 2-4: Mode of concrete repair failure (Matthews *et al*., 2003)

2.3 Understanding steel reinforcement corrosion

Refined metals such as steel are naturally unstable and therefore have a tendency to return back to a stable state in the form of as an oxide or hydroxide. As a consequence of this the iron present in the steel is susceptible to corrosion. Corrosion is the destruction of materials due to reactions with substances in the environment as they revert back to their naturally occurring forms. It is an electrochemical process that, with respect to steel, results in the oxidation of the iron present in the reinforcement. For corrosion to occur the following conditions are necessary (Bentur *et al*., 1997):

- Presence of a metal which can oxidise and breakdown anodically to release free ions.
- Presence of a metal that is reducible and can supply ions for the cathodic reaction.
- An electrolyte that facilitates the movement of free ions between the corroding material and the environment.

With steel embedded in concrete, the first two conditions are met. In the presence of moisture, the third condition is also met. The moisture behaves as an electrolyte and transports hydroxyl and oxygen ions to the steel, which causes corrosion. Essentially, corrosion of steel in concrete is initiated by the mechanism of either carbonation or chloride ion ingress.

Steel will only corrode when exposed to moisture, oxygen and aggressive ions such as chloride ions or an alkaline environment. The rate and severity of corrosion will depend on the ambient conditions within which steel is embedded in concrete. Although the corrosion of steel is a major cause for premature degradation of RC structures around the world, it must be understood that fundamentally this is not as a result of the intrinsic properties of concrete. In fact, uncontaminated concrete provides great protection to steel both physically and chemically. Physically this is done by concrete cover which provides a barrier against the external environment and chemically by developing a "passivating" layer on the steel bars (Owens, 2012). Concrete is inherently highly alkaline and generally has a pH within the range of 12 to 13. This is fundamentally due to the $Ca(OH)_2$ present in the concrete as a consequence of the hydration of Portland cement. Under the alkaline conditions a thin layer of gamma ferric oxide chemically develops on the steel's surface. This passivating oxide layer protects the steel from rusting by limiting the exchange of ions on the steel surface. This protection occurs even in the presence of water and oxygen (Owens. 2012).

Corrosion of steel is principally initiated by the breakdown of the passivating layer which mainly occurs in one of two ways. Firstly, the passivating layer can be disrupted by a reduction in the alkalinity of the concrete which in service, mainly results from carbonation. In carbonated concrete the availability of hydroxyl ions needed to repair pits in the passive film is reduced thereby, leading to depassivation of the protective layer and hence initiating corrosion. Secondly, the protective layer is damaged in the presence of aggressive media containing harmful ions. Chloride and sulphate ions are most destructive to steel embedded in concrete. This is especially evident for RC structures in coastal environments and those structures that are exposed to de-icing salts. RC structures that are exposed to salts containing chloride ions undergo extensive pitting corrosion since the chloride ions easily destroy the passivating layer and promote the dissolution of iron. It must be noted that the depassivation of steel does not necessarily point to a high probability of corrosion. This is because the rate and severity of corrosion is dependent on other factors such as oxygen concentrations, moisture content and amount of exposure to aggressive media. For RC, four states of corrosion can be identified which are highly dependent on the environmental conditions. These are (Arup, 1985):

- The passive state where small amounts of corrosion sustain the ferric oxide protective film.
- The pitting corrosion state which causes the local destruction of the passive film resulting in severe localised corrosion.
- General corrosion which results from an overall loss of passivity and results in corrosion occurring at multiple locations along the steel reinforcement.
- Active, low potential corrosion which is a slow corrosion process resulting from the limited availability of oxygen that is otherwise used to sustain the passive film.

Pitting and general corrosion are the most important states that result in the most significant corrosion of reinforcement. The severity of corrosion will depend on different internal and external factors (Bentur *et al*., 1997). Examples of some internal factors include the microstructure in the concrete matrix, cover depth and moisture conditions. External factors include stray currents, cyclic wetting and drying and impact damage.

2.4 Corrosion process

Corrosion in steel is initiated once the passive layer is disrupted. This layer is predominantly destroyed by concrete carbonation and chloride attack. However, the chemical reactions leading to the breakdown of the steel are similar whether corrosion occurs as a result of carbonation or chloride attack. The corrosion of steel reinforcement in concrete occurs in the presence of moisture and oxygen through the following steps (Bentur *et al*., 1997):

- At the anode section of the steel bar, the iron oxidises to the more stable ferrous state and discharges electrons. This reaction results in the dissolution of iron and the release of electrons. It occurs once the passive layer has been disrupted.

$$Fe \rightarrow Fe^{2+} + 2e^{-} \qquad \text{Equation 1}$$

- These electrons travel to the cathode section of the steel bar and react with water and oxygen to produce hydroxyl ions.

$$2e^{-} + H_2O + \frac{1}{2}O_2 \rightarrow 2OH^{-} \qquad \text{Equation 2}$$

These first two reactions are important in the corrosion process since they initiate the electrochemical corrosion in the steel. However, the negative effect of steel simply dissolving into the pore water solution without any further oxidation is minimal. In RC further oxidation stages occur that produce expansive products which have a volume of up to three to six times greater than the original steel (Smith & Virmani, 2000). These expansive products are essentially responsible for the cracking and spalling of the concrete matrix. The following reactions describe the oxidation stages that form the iron oxide compounds making up the expansive rust. A diagram illustrating the process of corrosion in steel is shown in Figure 2-5.

- The hydroxyl ions travel to the anode and react with the ferrous ions to produce ferrous hydroxide.

$$Fe^{2+} + 2\,OH^{-} \rightarrow Fe(OH)_2\ Ferrous\ hydroxide \qquad \text{Equation 3}$$

- The ferrous hydroxide is further oxidised to produce hydrated ferric oxide in the presence of oxygen and water.

$$4Fe(OH)_2 + O_2 + 2\,H_2O \rightarrow 4Fe(OH)_3\ Ferric\ hydroxide \qquad \text{Equation 4}$$

$$2Fe(OH)_3 \rightarrow Fe_2O_3{\cdot}H_2O + 2H_2O\ Hydrated\ ferric\ oxide\ (i.e.\ rust) \qquad \text{Equation 5}$$

The products of corrosion are expansive because the hydrated oxides have a tendency to swell in volume. Depending on the environmental conditions, this swelling usually varies between two to six times the actual volume of corrosion free steel (Broomfield 1997; Beeby 1983; Hansen & Saouma 1999). However, in extreme cases this value can be up to ten times the actual value (Mackechnie & Alexander, 2001). The result of this swelling is that due to pressure build up, tensile stresses are induced on the surrounding concrete ultimately resulting in cracking due to the limitations of concrete strength under tensile forces (Oh *et al*., 2009). Figure 2-6 displays the different compounds that can form during corrosion and their respective volumes.

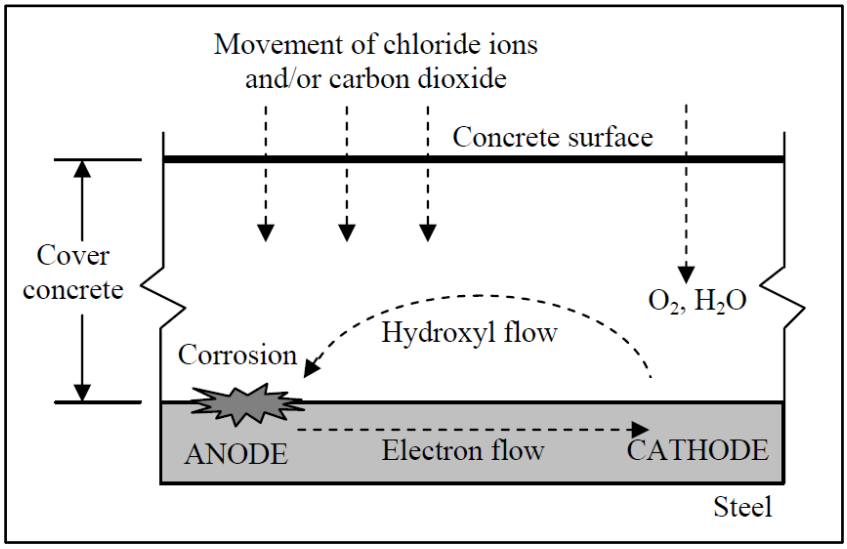

Figure 2-5: An illustration of the corrosion process in reinforced concrete (Mackechnie & Alexander, 2001)

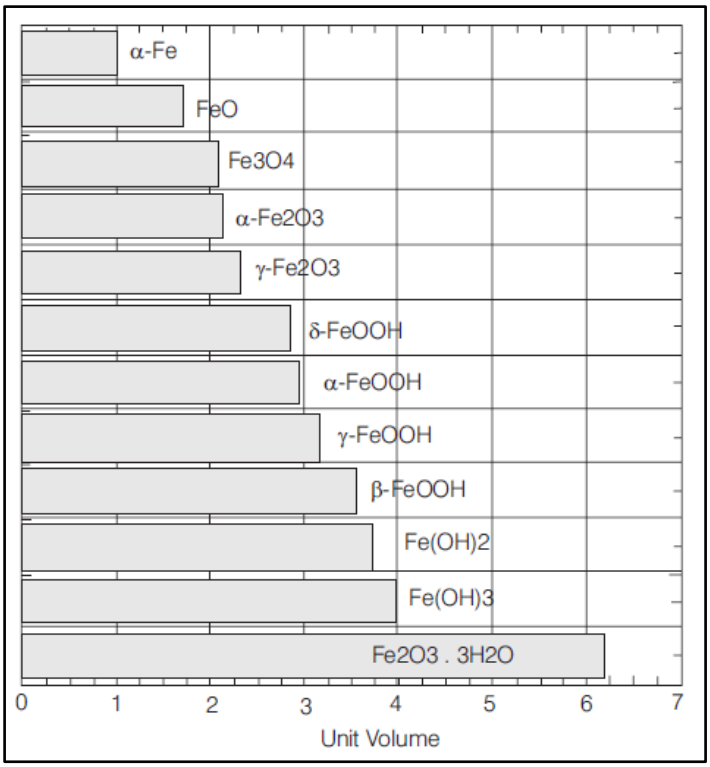

Figure 2-6: Volumes of the corrosion products of iron (Nielsen, 1985)

A three-stage damage model as illustrated in Figure 2-7 can be used to describe the loss of serviceability in RC structures damaged by corrosion. There are mainly two types of corrosion products formed from the corrosion of steel and these depend on the surrounding conditions:

- Red or brown rust is usually produced in the presence of high oxygen concentrations. This type of rust is flaky. Additionally, it is easily dislodged from the rebar.
- Black rust forms in the presence of low oxygen concentrations. It forms a dense and hard layer compared to red rust. This layer is not easily dislodged from the parent steel.

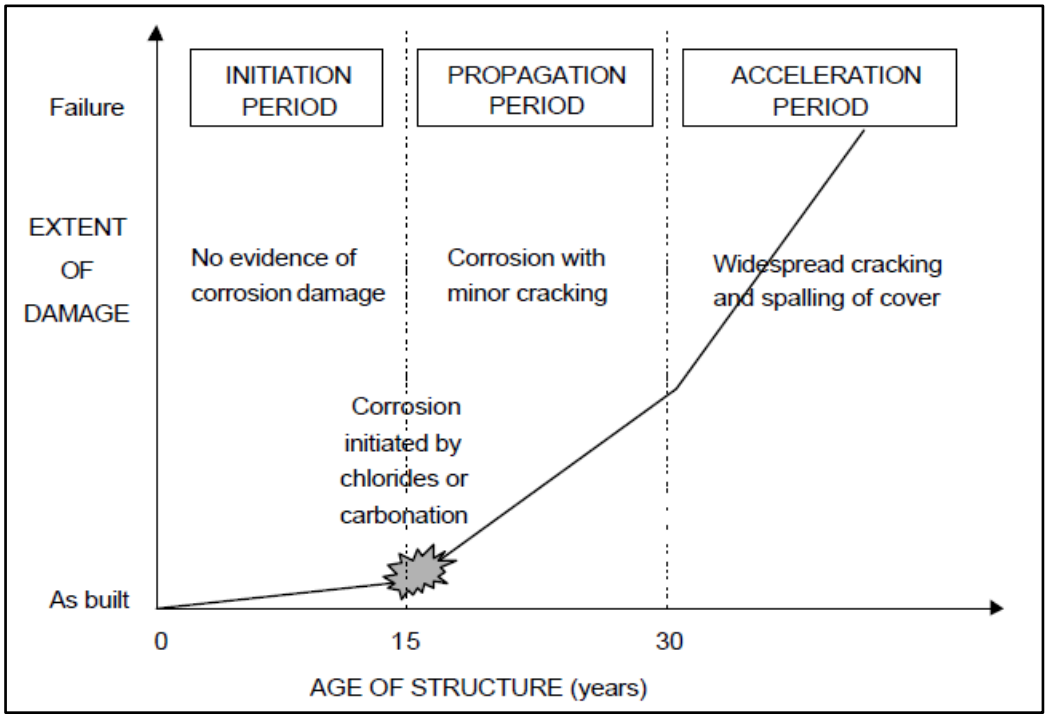

Figure 2-7: Three-phase reinforcement corrosion damage model (Miyagawa, 1991)

In the first initiation stage there is minimal corrosion present. This is the phase where the steel is still in the passive state and the passive layer is yet to be destroyed by carbonation or chloride attack. In the second propagation phase, the passive layer on the steel is disrupted. Corrosion begins ultimately leading to the cracking of the concrete matrix as a consequence of the formation of expansive rust compounds on the steel surface. In the final acceleration phase, the corrosion rate increases as a result of easy access to water and oxygen through the cracks in the concrete matrix. This is the phase where spalling of concrete occurs. Where spalling due to corrosion is observed, most RC structures will have gone beyond the point where an economic repair can be adopted to restore the serviceability and durability of the concrete.

2.5 Transport mechanisms in concrete

Reinforcement steel corrosion mechanisms in concrete are largely influenced by the ease with which aggressive media can penetrate through the concrete matrix up to the embedded steel level Bertolini *et al*. (2013). Aggressive ions and molecules in the aqueous, liquid or gaseous state are able to travel through concrete via a range of transport processes, which facilitate the movement of these species through concrete. Ingress of harmful substances into a concrete element is chiefly governed by the penetrability property of concrete. “Penetrability is the degree to which a material permits the transport through it of gases, liquids, or ionic species” Bertolini *et al*. (2013). Penetrability is an umbrella term that encompasses all the transports processes in concrete including migration, convection, diffusion, sorption and permeability (Alexander & Mindess, 2005). The microstructure of concrete is such that the matrix has many minute voids and cracks, and as a consequence concrete is inherently porous which paves the way for deleterious media ingress.

A vast amount of prior research has been conducted with respect to concrete durability, and harmful substance transport mechanisms in concrete form the foundation of these studies. Understanding transport mechanisms in concrete is fundamental in developing models to predict the serviceability and durability of RC structures, governing the rate of harmful media ingress, explaining and quantifying the effects of deleterious species ingress and in developing mitigation strategies.

Furthermore, steel corrosion is essentially caused by the ingress of water, chloride ions and carbon dioxide gas into the concrete matrix. It is therefore important to understand the different transport processes and mechanisms by which these corrosion initiating species are able to penetrate the concrete matrix. Additionally, it must be noted that the movement of aggressive media through concrete is accelerated in the presence of cracks and cavities created, for example, from debonding and shrinkage cracking phenomenon in failed patch repairs. The key transport processes in concrete are outlined in the following sections.

2.5.1 Permeation

Permeability is the measure of the ability of concrete to allow the movement of a fluid through its pore structure under an externally applied pressure whilst the pores are saturated with that fluid. It is also used to describe the speed with which fluid can flow through concrete. The mechanism of movement of liquids or gases through the concrete microstructure is facilitated by a pressure gradient. An example where permeation takes place is in concrete water-retaining structures, dams and tunnel linings. High permeability has serious detrimental effects on the durability of concrete. Furthermore, it is typical that other more harmful substances such as chloride ions are dissolved in water. These contaminants are transported into the concrete together with the water and ultimately results in concrete deterioration including initiation of reinforcement corrosion (Claisse, 2005). To model the rate of fluid ingress and the average velocity of flow, Darcy's law is applied:

$$v = \left(\frac{k}{n}\right)\left(-\frac{dh}{dx}\right) \quad \text{(m/s)} \qquad \text{Equation 6}$$

Where:

v = velocity of the fluid

k = permeability coefficient

n = porosity of the concrete

h = hydraulic head

x = distance parameter

2.5.2 Sorption

Sorption involves the movement of liquid into unsaturated or partially saturated concrete through the mechanism of capillary suction. The bulk absorption or sorptivity parameters are used to quantify sorption. The movement of a wetting front in dry or partially saturated concrete is principally sorptivity (Alexander & Mindess, 2005).

Sorptivity is largely affected by the concrete pore structure particularly, the capillary pores. These pores facilitate capillary suction and their degree of continuity will influence the extent of liquid uptake. Sorptivity is very sensitive to the degree of hydration of the outer concrete layer and therefore, highly dependent on curing. Furthermore, compaction, aggregate layout, aggregate distribution and mix design also influence sorptivity since these factors will determine the percentage of voids and capillaries that are allowed to form within the concrete matrix. Sorptivity is modelled using the following relationship:

$$\frac{V}{A}/t^{0.5} = S \ \text{(mm/hr}^{0.5}\text{)} \qquad \text{Equation 7}$$

Where:

V= volume of liquid absorbed

A= cross-sectional area of sample in contact with liquid

S= sorptivity

t= time

2.5.3 Convection

Convection, which is also known as advection, is the process of transportation of a solute as a consequence of the bulk movement of water in concrete. Along with diffusion, this mechanism of transport is one of the most important ones responsible for the ingress of chloride ions particularly in cracked concrete (Paulsson & Johan, 2002). Furthermore, convection plays a pivotal role in the deterioration of coastal infrastructure as a result of the exposure to constant wetting-drying conditions. The process of convection is modelled via the following relationship:

$$\left(\frac{\partial c}{\partial t}\right) = -v\left(\frac{\partial^2 c}{\partial x^2}\right) \ \text{(mol/m}^3\text{s)} \qquad \text{Equation 8}$$

Where:

v = average velocity vector of fluid flow

C = concentration of solute at depth x after time t

2.5.4 Diffusion

Diffusion is defined as the random movement of gasses, ions or molecules from a place of higher concentration to a place of lower concentration, i.e. under a concentration gradient. It is driven by the principle that a substance will move from a highly concentrated region to other surrounding regions until all the regions have the same concentration. In unsaturated concrete gaseous diffusion takes place including moisture diffusion, whereas in saturated concrete (or partially saturated) ionic diffusion is facilitated. If the concrete microstructure is such that the pores are relatively large then molecular diffusion can also take place (Sharif *et al*., 1999). Diffusion is particularly responsible for the ingress of deleterious carbon dioxide gas, oxygen gas and chloride ions into concrete structures.

Concrete infrastructure that is fully submerged in water is highly susceptible to ionic diffusion which facilitates the movement of contaminants to assume a similar concentration throughout the saturated concrete (Claisse, 2005). Gaseous diffusion of substances into concrete is typically modelled using Fick's first law of diffusion that applies for steady state diffusion:

$$J = -D\left(\frac{dc}{dx}\right) \text{ (mol/m}^2\text{s)} \qquad \text{Equation 9}$$

Where:

J = mass transport rate

D = diffusion coefficient

C = concentration of fluid

x = distance

dC/dx = concentration gradient

This relationship is commonly used to model carbon dioxide gas ingress in concrete. Ionic diffusion in concrete is represented by Fick's second law of diffusion which applies for non-steady state diffusion:

$$\left(\frac{\partial c}{\partial t}\right) = -D\left(\frac{\partial^2 c}{\partial x^2}\right) \text{ (mol/m}^3\text{s)} \qquad \text{Equation 10}$$

D = effective diffusion coefficient

C = Concentration of fluid (ion or gas)

x = distance

t = time

dC/dx = concentration gradient

This equation is usually used to model chloride ion ingress in concrete with respect to depth and concentration at a given time.

2.5.5 Migration

Migration is the accelerated movement of ions in solution under an electrical potential gradient. It is also known as electro-diffusion, conduction or accelerated diffusion. Movement occurs due to voltage difference that attracts ions which have a specific charge. The electric field is commonly applied externally in laboratory tests to accelerate the rate of ion ingress into concrete. This is especially used for accelerated chloride ion tests. However, in practice a natural electric potential can be initiated by pitting corrosion on reinforcing steel that induces variable charges on the steel bar (Claisse, 2005). Migration is modelled via the Nernst-Planck equation:

$$V = D\left(\frac{zF}{RT}\right)\left(\frac{dU}{dx}\right) \text{ (m/s)} \qquad \text{Equation 11}$$

Where:

V = velocity of the ionic species

D = diffusion coefficient of the ionic species

z = electrical charge (ionic valence)

T = temperature in kelvins

F = Faraday's constant (96485.33 C/mol)

U = potential difference across the sample

X = distance variable

R = universal gas constant (8.314 J/molK)

2.5.6 Thermal migration

Water and other liquids will move from warmer regions to colder regions in solids and this movement is principally dependant on the permeability of the solid. This process is not dependent on the drying process that takes place as a consequence of evaporation on the surface of the solid. In saturated concrete it is observed that ions in warmer pore water will migrate to colder areas. An example where thermal migration takes in concrete is when concrete contaminated with de-icing salt warms up under sunlight. The heating of the surface of the concrete enables salt in the saturated concrete pores to move rapidly into the cooler parts of the concrete. This mechanism causes severe chloride ion contamination in structures exposed to de-icing salts and chloride ions and as a consequence reinforcement corrosion is a common occurrence (Claisse, 2005).

2.5.7 Wick action

The movement of water along with its contaminants from a wet face of concrete exposed to water-salt solutions to the dry face is known as wick action. This process is fundamentally facilitated by capillary suction and concrete penetrability. Wick action commonly occurs in structures exposed to wetting and drying cycles, such as those in coastal regions (Buenfeld *et al*., 1997). Concrete left in a solution of salt over a few months will be observed to have crystalline salt filled up in the near surface pores of the dry face. This is because the salt solution is drawn up into concrete until it reaches the dry face after which water evaporates leaving behind the salt crystals. Eventually, with a build-up of these crystals severe concrete deterioration due to spalling will take place. This mechanism is common in climates with poor rains (Claisse, 2005). An illustration of wick action in concrete is presented in Figure 2-8.

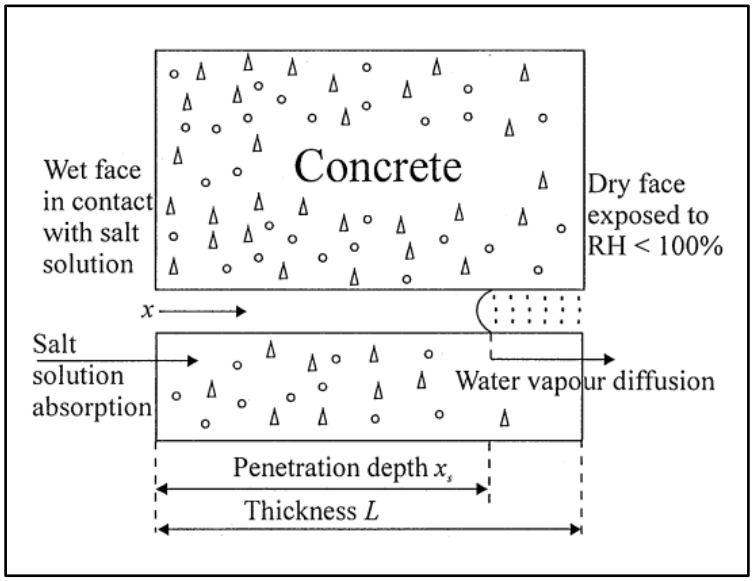

Figure 2-8: Wick action in concrete (Puyate & Lawrence, 1999)

2.6 Reinforcement corrosion initiation

2.6.1 Carbonation-induced corrosion

Concrete naturally provides good protection to steel due to its high alkalinity that passivates steel, developing a protective layer against corrosion. However, if the pH of the concrete drops below 10.5, this layer essentially breaks down and paves the way for corrosion to initiate (Bentur et al., 1997). In practice, carbonation is the most common mechanism responsible for the reduction in pH of RC structures. Carbonation induced corrosion due to a reduction of the pH in RC occurs through the following process:

- Carbon dioxide (CO_2) from the atmosphere chemically reacts with water (H_2O) present in the concrete pores to produce carbonic acid (H_2CO_3). This acid effectively lowers the pH of the concrete from above 12 to below 9 thereby, disrupting the protective passivating layer:

$$H_2O + CO_2 \rightarrow H_2CO_3 \qquad \text{Equation 12}$$

- This carbonic acid then reacts with the alkaline calcium hydroxide ($Ca(OH)_2$) and other hydroxides of silica and alumina in the concrete matrix to form calcium carbonate ($CaCO_3$) and compounds of silica and alumina gels in the following reaction:

$$H_2CO_3 + Ca(OH)_2 \rightarrow CaCO_3 + 2H_2O \qquad \text{Equation 13}$$

  The introduction of $CaCO_3$ further destabilises the passivation layer due to its low pH of about 8.5 (Owens, 2012). The water liberated from the second reaction sets up a series of these reactions that sustains both the formation of carbonic acid and the continuation of the carbonation process. Therefore, the carbonation process is almost self-sustaining due to the release of water in the reactions that follow. The reactions depicted in equation 12 and equation 13 work together to drastically lower the pH of the surrounding concrete.

The progression of carbonation into a RC structure is limited since it is increasingly difficult for carbonation to penetrate the concrete. However, once it reaches the embedded steel, reinforcement corrosion is initiated. It must be noted that carbonation is a slow process that does not result in visible change. Carbonation in concrete principally occurs due to carbon dioxide diffusion through the concrete matrix. The depth of the carbonation front therefore progresses following the square-root of time law:

$$x = k_{CO_2}\sqrt{t} \text{ (m)} \qquad \text{Equation 14}$$

Where:

x = carbonation depth after time t

k_{CO_2} = carbonation coefficient for a specific RC structure

t = time of exposure

This relationship indicates that if the concrete cover depth is doubled, the time of protection of steel increases by a factor of four. Therefore, the extent and severity of carbonation is significantly dependant on concrete cover. The more cover there is, the longer it takes for carbonation to affect the embedded steel and therefore, the more durable the concrete. The rate of carbonation is dependent on a number of factors (Bentur *et al*., 1997):

- Moisture content of the concrete.
  Carbonation cannot take place if the pores in the concrete are saturated or completely dry. This is because carbon dioxide is not readily dissolved in water and because moisture (H_2O) is a requirement for the formation of carbonic acid that reacts with the calcium hydroxide. These factors result in the most rapid carbonation to take place in the relative humidity range of between 50-70% as shown in Figure 2-9.

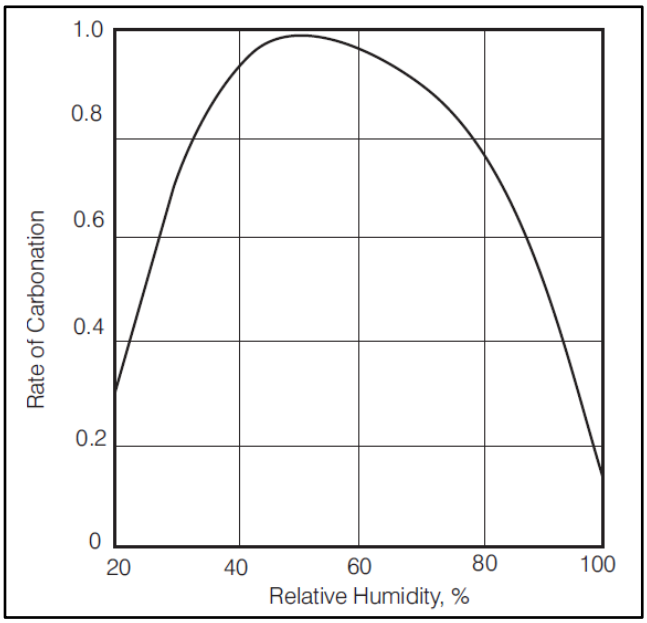

Figure 2-9: The influence of relative humidity on the rate of carbonation of concrete (Hansson *et al*., 2007)

- Gas permeability of the concrete.
  The denser a RC specimen is, the less permeable it is. This means a slower rate of gas (carbon dioxide and oxygen) diffusion into the concrete matrix and consequently a slower rate of carbonation. It must be noted that a higher concentration of carbon dioxide will result in a greater rate of diffusion. This is evident for example, in underground parkades. Factors that would reduce the penetrability of RC are low w/b ratios, sufficient compaction, proper curing and the use of FA or slag as cement extenders.

- Calcium hydroxide content of the concrete.
  $Ca(OH)_2$ has a counteracting effect on carbon dioxide due to its alkalinity. A high $Ca(OH)_2$ content will result in a slower carbonation rate. $Ca(OH)_2$ content can be increased by using more cement in the concrete mix design. Pozzolanic concrete such as concrete made of FA or slag is less resistant to carbonation than Portland cements owing to its lower $Ca(OH)_2$ content (Sisomphon *et al*., 2007).

2.6.2 Chloride ion-induced corrosion

Chloride ions are responsible for some of the most severe cases of steel reinforcement corrosion in RC structures. Sufficient concentration of chloride ions act as a catalyst to steel corrosion as they locally breakdown the protective passive layer on the steel thereby, initiating corrosion. Once the chloride ions reach the level of the embedded steel in concrete, corrosion takes place through the following process:

- At the anode, chloride ions attack the iron in the steel to form a soluble iron-chloride complex (Fraczek, 1987)

$$Fe + 2Cl^- \rightarrow (Fe^{2+} + 2Cl^-) + 2e^- \quad \text{Equation 15}$$

- This iron-chloride complex diffuses away from the steel surface. If this complex diffuses to an area of higher oxygen concentration and pH, then in the presence of water it will react with hydroxyl ions to form ferrous hydroxide (Dillard *et al*., 1993):

$$(Fe^{2+} + 2Cl^-) + 2H_2O \rightarrow Fe(OH)_2 + 2H^+ + 2Cl^- \quad \text{Equation 16}$$

- The liberated hydrogen ions from reaction two above then combines with excess electrons to form hydrogen gas:

$$2H^+ + 2e^- \rightarrow H_2 \quad \text{Equation 17}$$

- The ferrous hydroxide formed from reaction two further reacts with water and oxygen to form hydrated ferric oxide. This reaction is similar to the oxidation of ferrous hydroxide that occurs in the corrosion of steel without chloride ions.

$$4Fe(OH)_2 + O_2 + 2H_2O \rightarrow 4Fe(OH)_3 \ Ferric\ hydroxide \quad \text{Equation 18}$$

$$2Fe(OH)_3 \rightarrow Fe_2O_3 \cdot H_2O + 2H_2O \ Hydrated\ ferric\ oxide\ (i.e.\ rust) \quad \text{Equation 19}$$

Corrosion initiated due to chloride ion ingress leads to excessive pitting corrosion at a localised section of the steel reinforcement unlike carbonation that causes general corrosion with pitting occurring at multiple locations along the length of the steel bar as illustrated in Figure 2-10. Figure 2-11 illustrates the breakdown of the passive layer on steel due to chloride ion attack.

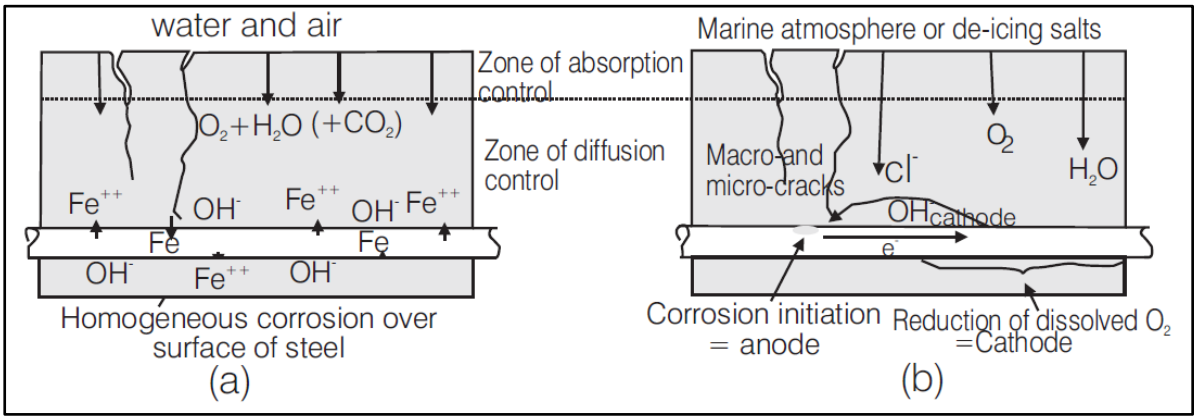

Figure 2-10: Schematic representation of (a) passive corrosion and (b) chloride-induced active corrosion of steel in concrete (Hansson *et al*., 2007)

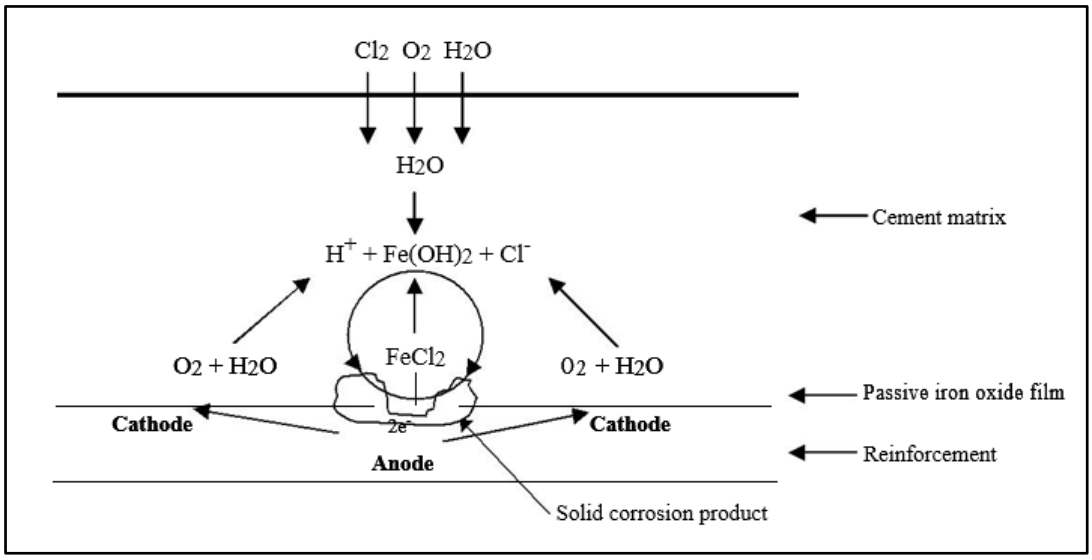

Figure 2-11: Reinforcement corrosion in concrete exposed to chloride ions (Broomfield, 1997)

Chloride ions can be introduced into RC in a number of ways during the different stages of concrete preparation and service. Specifically, during the concrete mixing stage chlorides can be introduced as a contaminant. Contaminate usually originates from aggregates containing chloride compounds, from the use of seawater or from admixtures that contain chloride ions as an ingredient particularly accelerators. Contamination of steel reinforcing can also take place during the concrete placing stage where chloride ions can be introduced on the steel surface. Chloride ions in solution form can also ingress/diffuse into hardened RC already in service. This is the most common form of chloride contamination in practice and is a very serious issue affecting concrete structures that are located close to the sea and those structures that are exposed to de-icing salts.

The precise mechanism by which the passive layer on steel is broken down as a consequence of chloride ion attack is not fully understood. This is because this passive film is too thin for any meaningful examination and because it forms whilst embedded within the concrete thereby, limiting access (Rosenberg *et al*., 1989). However, researchers such as Foley (1970), Shreir (1979) and Leek & Poole (1990) have developed hypothesis on how chloride ions could actually depassivate steel. One explanation for the weakening of the passive film is that chloride ions merge into the film and reduces its corrosion resisting capability. Another hypothesis is that chloride ions compete with the hydroxide ions to react with iron cations (Hansson *et al*., 2007).

The result of this is that the passive film is not formed as the iron cations are diffused away with the chloride ions since the iron-chloride complex is soluble. Ultimately the consequence of these propositions is that due to chloride ion-induced local pitting corrosion, the reinforcement cross-section and its structural integrity is compromised. It must be noted that the passivity of steel does not ensure complete protection against corrosion but acts as limiting value for the initiation of corrosion. The presence of hydroxide ions and other anions have corrosion counteracting properties whereas chloride ions facilitate the destabilisation of the passive layer thereby, encouraging corrosion. The result of this is that there is a minimum chloride ion concentration level, known as the threshold level, needed to initiate steel corrosion (Bockris *et al*., 1981).

2.6.2.1 Chloride threshold level

The chloride threshold level is the critical concentration of chloride ions required to disrupt the protective passive film on the steel surface thereby, initiating corrosion. It is the minimum amount of chloride presence needed on the steel surface for corrosion to initiate. A substantial amount of previous research (Tuutti 1982; Hansson & Sørensen 1990; Gouda 1970; Gouda & Halaka 1970) has been conducted with the aim of determining the threshold value of chloride concentration above which active corrosion will occur in RC.

There are essentially two important reasons for knowing the critical chloride concentration value needed for chloride-induced corrosion in concrete. Firstly, it is important to establish the limits of chloride contamination allowable from aggregates and water used in concrete preparation and secondly, it is important to enable the prediction of the incubation period between initial chloride attack and the beginning of active corrosion (Hansson *et al*., 1990). This is important to ensure that maintenance and rehabilitation can be scheduled appropriately. The chloride threshold value is a vital parameter that is used in service life design and prediction models. However, the idea of a universal threshold value applicable to all structures is not possible due to the multitude of varying factors affecting chloride threshold values in concrete which includes the following (Hansson *et al*. 2007; Nilsson *et al*. 1996):

- concrete mix design (proportions of materials used),
- amount and type of binder used,
- use of supplementary cementitious materials,
- w/c ratio,

- sulphate content,
- curing procedures and concrete age,
- presence of carbonation, defects or cracks,
- cover thickness,
- electrical potential of the reinforced concrete,
- binder chemistry,
- humidity and temperature of the surrounding environment and
- condition of the reinforcement used.

Chloride ions in concrete can be free (water soluble) or bound within the concrete. The free ions are mobile and therefore they are readily diffused into the concrete up to the embedded steel level. On the other hand, the bound chlorides are chemically bound to the aluminate phases within the concrete matrix or physically trapped in pores and as such are not readily available for chloride-induced corrosion. Previous studies suggested that only free chlorides are responsible for chloride-induced corrosion in concrete but these studies have since been challenged. Numerous new approaches have been established to determine a more fitting critical chloride concentration level that includes the following:

- Free (water soluble) chloride level.
- Total (acid soluble) chloride.
- Cl^-/OH^- ratio.

The use of the total chloride content in the determination of a critical threshold level is most widely adopted however, there still exists some controversy since only free chlorides are able to reach the steel. As a consequence of this, a large distribution of values is specified by different authors. This scatter is attributed to the above listed variables and due to the extent of these variables, many national standards specify different chloride threshold limits but a conservative value of 0.4% chloride ions by weight of dry binder content is most commonly adopted (Hansson *et al*., 2007). The increasing use of substituting cementitious materials and extenders in the preparation of concrete is adding to the difficulty in determining suitable chloride threshold values. This is because these extenders can contaminate the concrete with chloride ions, permit chloride binding or reduce the diffusion rate of free chlorides within the concrete matrix. This means that chloride threshold values need to be specific for a certain concrete mix design.

2.7 Concrete repair according to EN 1504

The market for the repair of RC structures around the world is ever-expanding due to the increasing age of structures and the lack of implementation of proper management plans to maintain and extend the expected service life of these assets. As a consequence, a significant amount of research has been conducted to develop materials and methods for the repair of deteriorated concrete structures. Many of these repair materials are commercially available. However, the lack of consistency in procedure and application recommended by different suppliers has necessitated the need to develop specific standards for such works and products (Raupach, 2005).

An extensive amount of work has gone into developing a European standard for the correct implementation of RC repair strategies and techniques. The European standard EN 1504 "Products and systems for the repair and protection of concrete structures – definitions, requirements, quality control and evaluation of conformity" outlines in detail the procedures and properties of materials needed to repair, maintain and protect RC infrastructure (Mapei, 2011). The primary aim of the standard is to optimise repair strategies and assist in overcoming the common approach of applying simplistic solutions to concrete repairs without addressing the underlying cause of deterioration (Raupach, 2005). EN 1504 has been in development for more than a decade and outlines comprehensive specifications and principles for RC condition assessment, repair, rehabilitation and structural strengthening. EN 1504 consists of a 10 part standard with up to 65 standards for test methods. Part 1 of the standard outlines definitions, parts 2 to 7 specify the key principles for repair strategies, part 8 regulates product quality, part 9 outlines the principles for product use and part 10 provides a guide for site application and workmanship. The EN 1504 standard is of paramount importance in the repair industry and has a significant influence on repair strategies in other non-European countries. EN 1504 outlines repair principles with respect to either damage to concrete or reinforcement corrosion induced damage. These principles are summarised in Table 2-1 and Table 2-2.

Table 2-1: Deterioration processes and remedial actions according to EN 1504

	Observation	Cause of defects	Principal of remedial actions (see Table 2-2)
Defects in concrete	Cracks. Spalling. Delamination. Disintegration of the matrix.	1. Mechanical: Impact. Overload. Movement (settlement). Explosion. Vibration. Seismic.	Concrete restoration (CR). Structural strengthening (SS).
		2. Chemical: Alkali-aggregate reaction. Aggressive agents (sulphates, soft water, acids, salts). Biological activities.	Protection against ingress (PI). Moisture control (MC). Increasing resistance to chemicals (RC).
		3. Physical: Freeze - thaw. Thermal - fire. Salt crystallisation. Shrinkage. Erosion. Wear.	Protection against ingress (PI). Moisture control (MC). Increasing physical resistance (PR). Structural strengthening (SS).
Reinforcement corrosion	Uniform corrosion. Pitting corrosion. Stress corrosion. Cracking.	Carbonation of concrete.	Preserving or restoring passivity (RP). Control of anodic areas (CA).
		Corrosive contaminants: Sodium chloride, calcium chloride, others.	Cathodic control (CC). Cathodic protection (CP). Control of anodic areas (CA). Preserving or restoring passivity (RP).
		Stray currents.	Increasing resistivity (IR).

Table 2-2: Principles and remedial actions according to EN 1504

	Principle (see Table 2-1)	Methods based on the principle (examples)
Surface protection	Protection against ingress (PI): reducing or preventing the ingress of adverse agents, e.g. water, other liquids, vapour, gas, chemicals, and biological agents.	Surface impregnation. Surface coating. Bandaging cracks. Filling cracks. Converting cracks to joints. Erecting external panels. Applying membranes.
	Physical resistance (PR): increasing resistance to physical or mechanical attack.	Overlays. Coatings. Impregnation.
	Resistance to chemicals (RC): increasing resistance of the concrete surface to deteriorations by chemical attack.	
	Moisture control (MC): adjusting and maintaining the moisture content in the concrete within a specified range of values.	Hydrophobic impregnation. Surface coating. Sheltering or overcladding.
Repair	Concrete restoration (CR): restoring to the originally designed shape and function.	Hand-applied mortar. Recasting with concrete. Spraying concrete or mortar. Replacing elements.
	Cathodic control (CC): creating conditions in which potentially cathodic areas of reinforcement are unable to drive an anodic reaction.	Reducing oxygen supply at the cathode by saturation or surface coating.
	Preserving or restoring passivity (RP): creating chemical conditions in which the surface of the reinforcement is maintained in, or is returned to, a passive condition.	Increasing cover with additional concrete or mortar. Replacing contaminated or carbonated concrete. Electrochemical realkalisation of carbonated concrete. Realkalisation of carbonated concrete by diffusion. Electrochemical chloride extraction.
	Cathodic protection (CP).	Applying electrical potential.
	Control of anodic areas (CA): creating conditions in which potentially anodic areas of reinforcement are unable to participate in corrosion reaction.	Painting reinforcement with coatings containing active pigments (e.g. zinc). Painting reinforcement with barrier coatings. Applying penetrating corrosion inhibitors to the concrete surface.
Structural strengthening	Structural strengthening (SS): increasing or restoring the structural load bearing capacity of an element of the concrete structure.	Adding or replacing embedded or external reinforcing steel bars. Installing bonded rebars in preformed or drilled holes in the concrete. Plate bonding. Adding mortar or concrete. Injecting cracks or voids. Filling cracks or voids. Prestressing - post- tensioning.

Furthermore, EN 1504 outlines the following listed alternatives to be considered for any concrete protection or repair programme:

- Do nothing.
- Assessing structural capacity and possible downgrading of use of structure.

- Prevention and minimising further deterioration, without improvement of the concrete element.
- Improvement, strengthening or refurbishment.
- Reconstruction.
- Demolition.

Additionally, the EN 1504-3 standard specifies performance characteristics required of structural and non-structural repair materials under repair principles 3 (concrete restoration), 4 (structural strengthening) and 7 (preserving or restoring passivity). These performance requirements are outlined in Table 2-3.

Table 2-3: Performance requirements of repair mortars under EN 1504-3

<table>
<tr><th rowspan="3">Item</th><th colspan="4">Requirement</th></tr>
<tr><th colspan="2">Structural</th><th colspan="2">Non-Structural</th></tr>
<tr><th>Class R4</th><th>Class R3</th><th>Class R2</th><th>Class R1</th></tr>
<tr><td>Compressive Strength</td><td>≥ 45 MPa</td><td>≥ 25 MPa</td><td>≥ 15 MPa</td><td>≥ 10 MPa</td></tr>
<tr><td>Chloride Ion Content</td><td colspan="2">≤ 0,05%</td><td colspan="2">≤ 0,05%</td></tr>
<tr><td>Adhesive Bond</td><td>≥ 2,0 MPa</td><td>≥ 1,5 MPa</td><td colspan="2">≥ 0,8 MPa</td></tr>
<tr><td rowspan="2">Restrained shrinkage
Expansion</td><td colspan="3">Max average crack width <0.05mm
No crack width >0.1mm
No delamination</td><td rowspan="2">No requirement</td></tr>
<tr><td>≥ 2,0 MPa</td><td>≥ 1,5 MPa</td><td>≥ 0,8 MPa</td></tr>
<tr><td>DURABILITY
Carbonation Resistance
(not required if coated)</td><td colspan="3">d_K ≤ Control concrete C(0,45)</td><td>Not required</td></tr>
<tr><td>Elastic Modulus</td><td>≥ 20 GPa</td><td>≥ 15 GPa</td><td colspan="2">Not required</td></tr>
</table>

Notes:

= For structural strengthening Principle 4 only

2.8 Patch repair systems

2.8.1 Repair process

2.8.1.1 Overview

The aging of concrete infrastructure and the associated effects of concrete cracking, contamination and spalling is of great concern in civil engineering. In multiple circumstances, the serviceability and structural integrity of the concrete structure is compromised. Bonded concrete overlays are typically applied to rehabilitate damaged structures. The term “patch repair” is used for bonded overlays of relatively small surface area (Owens, 2009). The patch repair method is the leading and most cost-effective solution applied for the repair of deteriorated RC (Courard *et al*., 2014). In the patch repair the new repaired concrete section is called the “patch” whereas the adjacent original concrete is called the “substrate”.

This repair method is commonly applied to concrete structures for addressing localised corrosion induced damage such as spalling. A proper and complete patch repair process involves the following steps:

- Removal of defective concrete that has been affected by cracking, spalling or debonding, to completely expose the embedded corroded steel.
- This is followed by addressing the corrosion on the steel surface. The steel is cleaned of all corrosion products and loose materials. An anti-corrosion epoxy coating or zinc rich primer coat is then applied to inhibit the occurrence of any future corrosion. If the corrosion is severe then the steel is typically replaced completely. Furthermore, sacrificial anodes may also be employed to protect the repair area from future corrosion.
- The removed concrete is then replaced with patching materials. These are usually commercially available, specialised repair mortars, many of which contain polymers.
- Finally, the finished surface of the repaired concrete including the adjacent areas is coated with a hydrophobic sealant to minimise the ingress of moisture into the repaired section. Figure 2-12 illustrates a characteristic patch repair system.

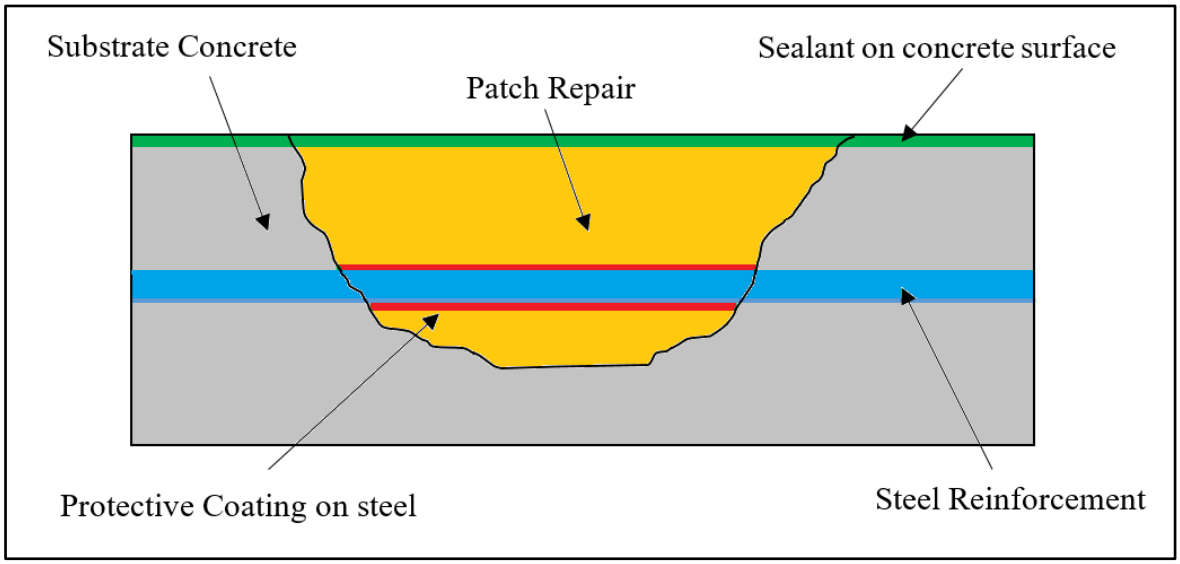

Figure 2-12: Illustration of the patch repair system

The lack of durability and premature failure of repairs is a common occurrence with patch repairs. In practice, the continuation of corrosion damage in the adjacent substrate concrete, cracking and subsequent debonding of the patch is evidently widespread. There are a multitude of underlying reasons for these failures including poor substrate preparation, wrong selection of repair materials, curing method used, time-dependent material properties and environmental conditions. However, poor workmanship and differential shrinkage between the substrate and patch are identified as the chief inhibiting factors for the durability and service life performance of patch repair systems with respect to crack resistance and bond strength (Beushausen & Alexander, 2009). A number of importance factors have to be considered in the application and design of patch repairs and a summary of these are presented in Figure 2-13.

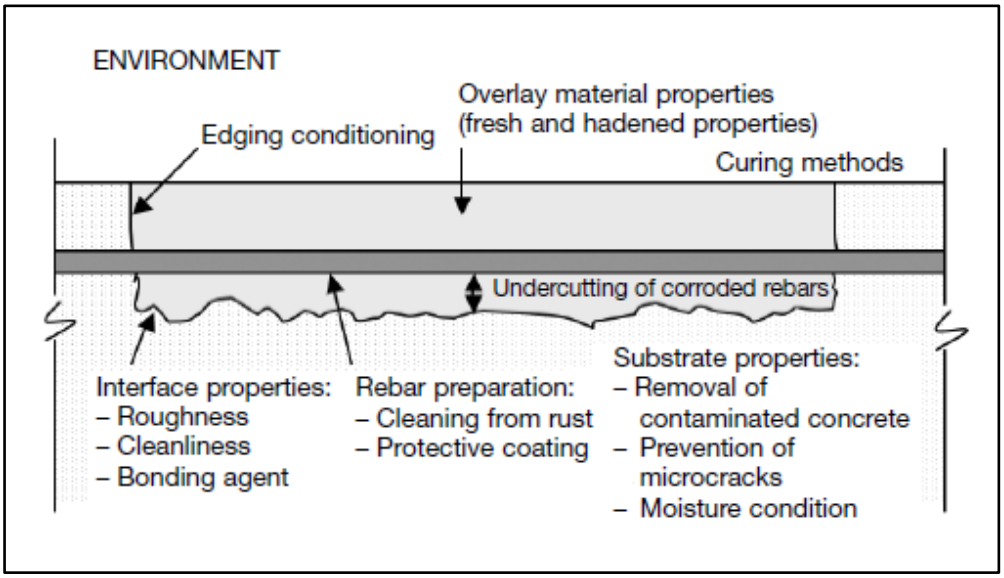

Figure 2-13: Factors to be considered in the design and application of patch repairs (Beushausen & Alexander, 2009)

2.8.1.2 Substrate preparation

Substrate preparation is generally accepted to be one of the most important steps in patch repairs. According to EN 1504 (2003), substrate preparation is a fundamental requirement which is considered for all concrete repair principles specified in the standard. To achieve a durable bond between the substrate and the repair material, the substrate would typically need to be prepared prior to any repair mortar application. Poor quality and deteriorated substrate has to be removed and the remaining substrate has to be cleaned of any contaminants or loose materials. Particularly, carbonated or chloride contaminated substrate needs to be treated by for example, completely removing the contaminated concrete. To facilitate monolithic behaviour between the patch and substrate it is essential to ensure that all remaining substrate in the locality of the patch application is of good sound quality. A poorly prepared substrate will always introduce a limiting weakness to the overall patch repair system independent of whether or not a good repair material is applied in a thorough procedure. Therefore, to ensure any long-term durability of the repair, substrate preparation is critical.

The process of substrate surface cleaning or removal in substrate preparation needs to be distinguished. Surface cleaning involves the removal or any loose contaminants whereas, surface removal involves taking away deteriorated parts of the substrate and any previously applied coatings. To ensure proper substrate preparation including the removal of all loose and contaminated material, adequate surface roughening and creation of a clean and sound interface, good workmanship and site supervision is necessary (Holl & O'Connor, 1997). Removal of deteriorated concrete and substrate surface roughening is typically completed via mechanical, water jetting or sandblasting techniques. However, many authors including Garbacz *et al*. (2005), Courard *et al*. (2014) and Silfwerbrand & Beushausen (2005) have emphasised that an important aspect to consider whilst removing deteriorated concrete is the creation of surface microcracks.

Microcracks in the substrate have the potential to greatly reduce the durability of a patch repair system and this is why EN 1504 (2003) identifies that:

''microcracked or delaminated concrete including that caused by the techniques of cleaning, roughening or removal which reduces bond or structural integrity, shall be subsequently removed or remedied''.

After the removal of contaminated concrete, the surface of the substrate needs to be analysed for the presence of microcracks since these cracks will otherwise introduce a zone of weakness that will ultimately lead to premature repair failure (Garbacz *et al*., 2005). The severity of microcracks will largely depend on the particular substrate removal method adopted. Prior to the application of any removal method, it is imperative to determine the strength of the substrate material in relation to the aggressiveness of the removal process adopted. Specifically, improvement in the roughness profile and the decrease in surface tensile strength due to substrate surface roughening must be monitored (Courard *et al*., 2014). Substrate surface roughening will promote mechanical interlocking and good contact between the substrate and patch repair material (Santos & Julio, 2007) which is the basic mechanism of adhesion. Therefore, good surface roughening will ensure good bond strength (Courard *et al*., 2014).

A comprehensive study by Moghtadaei *et al*. (2015) on the influence of different surface roughness types on the bond strength of repairs concluded that an increase in the roughness and contact area of the substrate surface will most definitely develop the highest bond strength. According to Silfwerbrand & Beushausen (2005), microcracking, absence of the laitance layer and cleanliness of the bond interface are the most significant substrate preparation factors affecting the quality and durability of the patch repair bond. Proper substrate testament can eliminate these factors and therefore ensure patch repair durability.

Principally, mechanical methods such as jackhammers will typically cause microcracking whereas water jetting and sandblasting procedures are less aggressive and have been shown to produce sound substrate surfaces (Silfwerbrand & Beushausen, 2005). Mechanical methods are usually necessary to remove concrete to a sufficient depth behind the corroded steel however, research has identified that treating the substrate via a water jetting technique after a mechanical treatment will ensure that microcracked concrete on the substrate surface is eliminated (Silfwerbrand & Petersson, 1993).

The moisture condition of the substrate concrete may have a significant effect on the durability of the substrate-patch bond. Adequate substrate surface saturation is essential for durability of repairs (Courard *et al*., 2011). A dry substrate surface can suck water away from the newly applied patch repair material which could result in a weak bond interface and therefore, poor bond strength. On the other hand, a very moist or wet surface will dilute the repair mortar at the bond interface thereby, increasing the water content in the mortar and as a consequence leading to poor material strength development, increased drying shrinkage and poor bonding. Furthermore, water contained in pores limits substrate-patch interlocking and therefore, the substrate should be saturated but dry on the surface (Owens, 2009).

It has been identified that different repair materials respond uniquely to different substrate moisture conditions. Therefore, specific material moisture condition requirements cannot be met by simply following generic standards such as those stipulated in EN 1504. In practice, it is difficult to determine an optimum moisture condition for a given combination of repair materials and substrate concrete. This is because no practical test method exists that could accurately determine optimum substrate moisture condition (Courard *et al*., 2011). However, Courard *et al*. (2011) suggested a quantitative test to establish the saturation level required in concrete repairs and recommended that a saturation level of between 50% and 90% be attempted for plain cement concrete systems.

In certain repair systems it may be necessary to pre-wet the substrate surface to allow it to successfully bond to the repair material. However, there is some controversy in literature with respect to pre-wetting. Common practice in the repair industry usually recommends that the substrate should be in a "saturated surface dry state" prior to conducting repairs (Courard *et al*., 2011). However, Zhu (1992), Silfwerbrand (2003) and Beushausen (2010) disagree with this and argue that a dry substrate would probably ensure better mechanical interlock between the substrate and repair material. Silfwerbrand & Beushausen (2005) summarised the results of previous studies with respect to substrate moisture conditioning as illustrated in Figure 2-14. The graph clearly indicates that there is no significant improvement in bond strength with pre-wetting however and free surface water dramatically reduces bond strength. The effect of pre-wetting surface conditioning on the differential shrinkage potential between the substrate and repair material may also be of concern (Talotti, 2014).

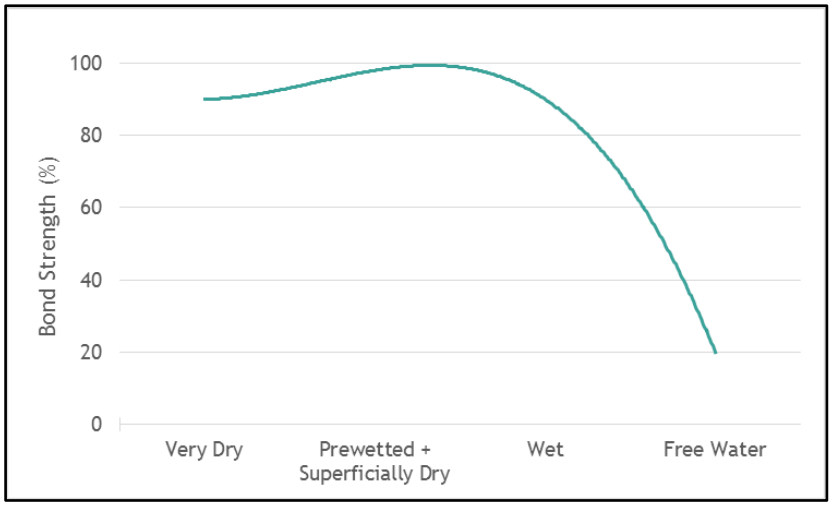

Figure 2-14: Effect of moisture condition on bond strength (Silfwerbrand & Beushausen, 2005)

2.8.1.3 Steel preparation

Prior to the application of the repair system it is vital to clean the steel surface of all corrosion products. Additionally, depending on the extent of the corrosion it may be necessary to replace a section of the steel reinforcement. Furthermore, it is recommended to coat the steel surface with a corrosion inhibitor to prolong and limit the occurrence of any future corrosion in the repaired section.

It is also essential to remove all deteriorated or contaminated concrete from the vicinity of the steel reinforcement. Particularly, corroded reinforcement steel needs to be undercut, typically by 20 mm and replaced with sound repair material (Owens, 2009). The patch repair system is typically applied to a localised deteriorated area and as such only the steel exposed by spalling or delamination is treated. Adjacent substrate concrete and embedded steel is usually left untreated. As a consequence, corrosion of adjacent steel is free to continue and this is frequently responsible for the early failure of patch repairs. It is therefore imperative to provide sacrificial anodic protection at the corners of a patch repair to prevent the occurrence of incipient anodes that would otherwise accelerate the corrosion of the adjacent steel. This theme is discussed in the following section.

2.8.1.4 Sacrificial anodes

Upon completion of a patch repair it is common for corrosion to continue in the repair area as well as in the adjacent substrate. The underlying reason for this is not addressing the root cause of corrosion. One way of protecting RC from post patch repair corrosion is by adopting a cathodic protection system. This system has an excellent track record with respect to long-term steel corrosion control (Owens, 2009). The principle of cathodic protection relies on the application of a voltage to steel reinforcement. To generate the voltage required to drive cathodic protection an external power supply or a metal that preferentially corrodes instead of the reinforcing steel is necessary. Systems that utilise a power supply are known as impressed current cathodic protection systems whereas, systems that utilise a metal are known as sacrificial (or passive or galvanic) anode cathodic protection (SACP) systems. Figure 2-15 illustrates the SACP system.

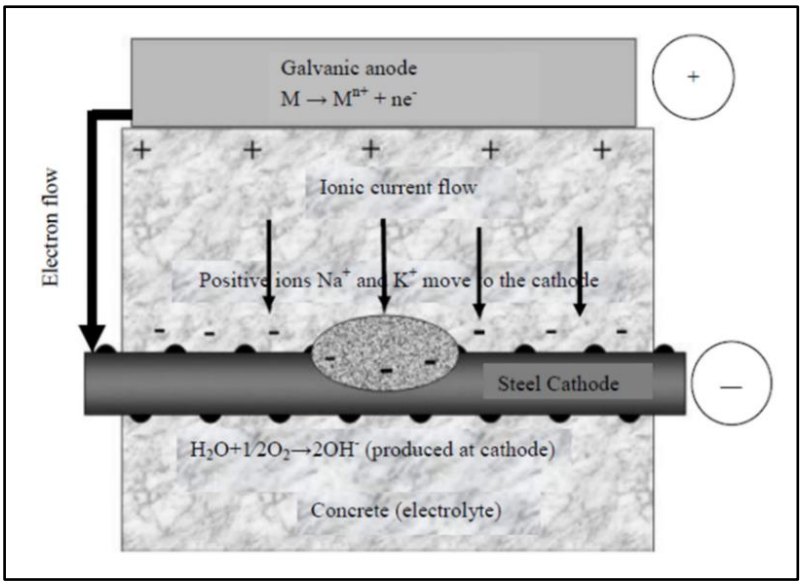

Figure 2-15: Illustration of an SACP system (Roberge, 2008)

An alkaline environment, relatively unrestricted cathodic reaction kinetics and minimum ion contamination are the chief parameters that promote and maintain the passivity of reinforcement steel (Glass *et al.*, 2001). Steel corrosion is an electrochemical process that is dependent on the electric potential of the reinforcement.

A negative shift in this potential will reduce the rate of corrosion by suppressing the anodic reaction. SACP is dependent on the cathodic polarisation of reinforcement. Polarisation moves the steel potential into the passive range or reduces the macrocouple process on its surface. This effectively hinders anodic dissolution of reinforcement (Bruns & Raupach, 2009). Furthermore, polarisation increases the pH at the cathode which enhances the reduction of oxygen i.e. the cathodic reaction (Montoya *et al*., 2009). Figure 2-16 compares the service life of RC structures with SACP systems relative to those without. SACP systems are expected to increase the service life of structures by:

- Increasing the corrosion initiation phase through cathodic prevention.
- Reducing corrosion rate during the propagation phase.
- Halting the corrosion process.

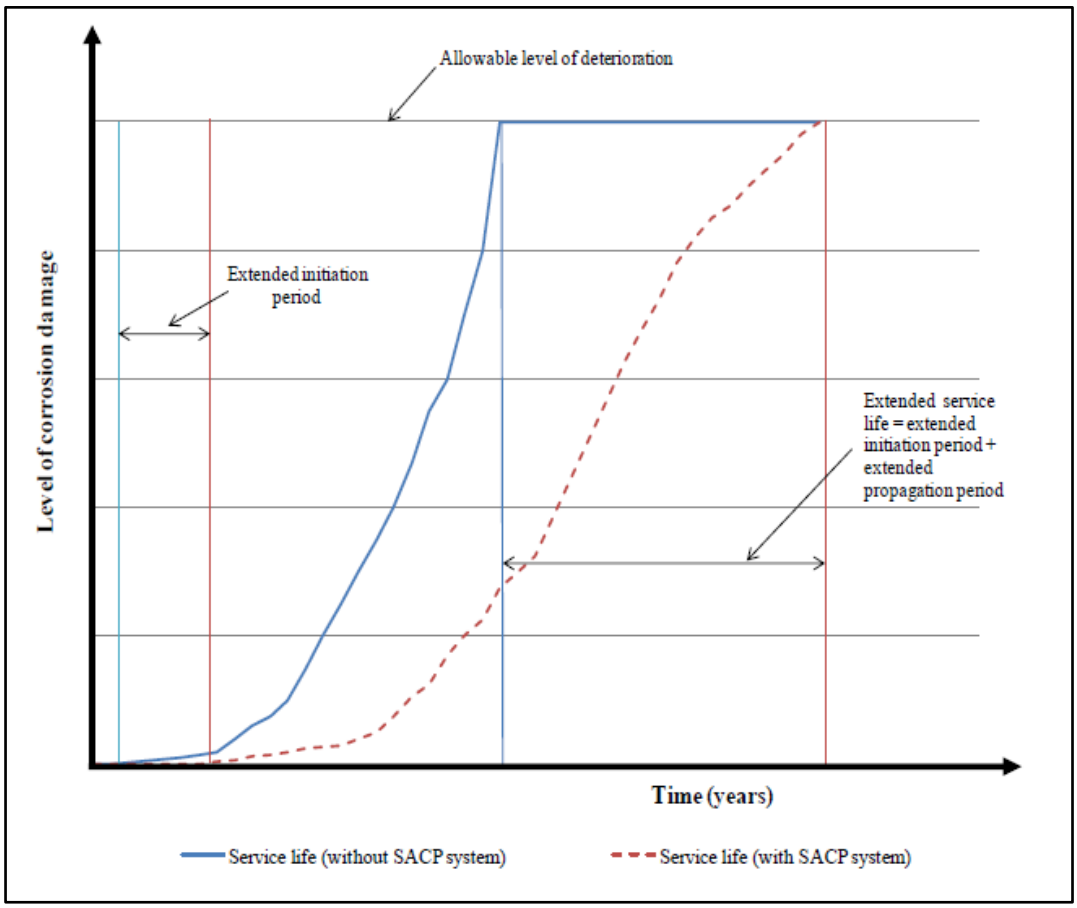

Figure 2-16: Service life model of RC structures with and without SACP (Arito, 2012)

The common materials used as sacrificial anodes in SACP systems are zinc, aluminium, magnesium and conductive polymers. Magnesium, zinc and aluminium are effective due to their higher negative electric potential relative to steel therefore, are more widely adopted. However, although less common, materials such as inert graphite, high-silicon cast iron, platinum coated titanium and alloys of magnesium, zinc aluminium and nickel are also used. The correct configuration and selection of a particular sacrificial anode material will ultimately determine the success of the SACP system (USDoT, 2001). SACP systems can be configured as single or multiple anodes that can be used to distribute the current from the cathode.

Furthermore, galvanic cathodic protection systems can be used as surface-applied systems or embedded into the concrete. They can also be encapsulated or non-encapsulated systems (Sohanghpurwala, 2009). The most widely adopted SACP system configurations used to protect RC from corrosion are (Arito, 2012):

- Thermal sprayed zinc systems.
- Thermal sprayed aluminium/zinc/indium systems.
- Zinc sheets.
- Expanded zinc mesh.
- Compact discrete zinc disks and probe anodes.
- Bulk anodes, wires, ribbons and strips.
- Conductive electro-active mesh and overlay systems.

Most patch repairs restore the short-term serviceability of deteriorating concrete structures however, many do not address long-term durability with respect to preventing future corrosion. With patch repairs, corrosion may in fact be more likely to occur in the adjacent steel due to an increase in the driving voltage of the new concrete composite. This increased voltage is due to the differences in moisture, chloride ion concentration, electrical conductivity and pH between the old substrate concrete and the new patch repair material. This is an important issue especially in chloride contaminated concrete because, unless all concrete containing chloride ions is removed, corrosion may reappear in the repaired area, the unrepaired area or in the interface between the two. The formation of incipient anodes at the interface between the substrate and patch is likely to occur without any cathodic protection system. Employing sacrificial anodes in a patch repair procedure is paramount in ensuring that the underlying cause of corrosion is also addressed rather than simply addressing visible concrete damage (Sergi & Page, 1999). In patch repairs the sacrificial anode elements are typically installed into substrate concrete around the corners of a patch repair close to the bond interface, as illustrated in Figure 2-17.

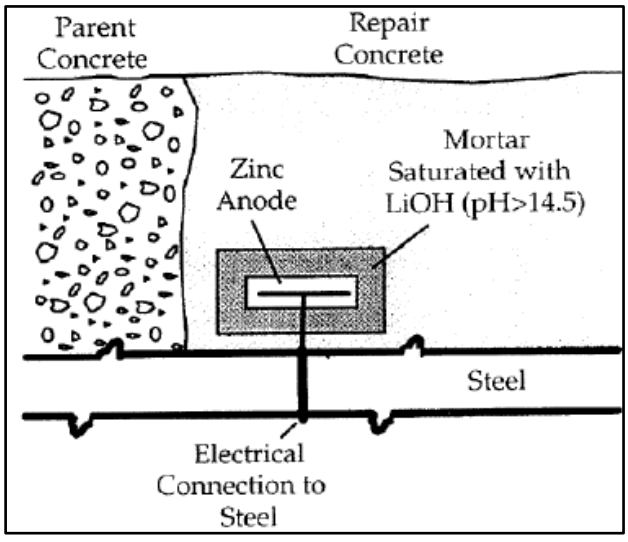

Figure 2-17: Sacrificial anode contained in mortar and connected to the steel reinforcement in a patch repair (Sergi & Page, 1999)

The anode metal is usually pre-wetted and connected directly to the steel bar (Ball & Whitmore, 2009). It must be noted that SACP systems in patch repairs do not prevent the formation of anodes further away from the patch repair. They only prevent corrosion in the vicinity of a patch repair (Owens, 2009). SACP systems are typically most effective in submerged elements where the concrete is saturated and the resistivity is low. They are also effective in regions of warm temperatures, above 20^{o}C (Owens, 2009). The key advantages and disadvantages of SACP systems are discussed in Table 2-4 (Arito, 2012):

Table 2-4: Advantages and disadvantages of sacrificial anode cathodic protection systems:

Advantages	Disadvantages
Relatively inexpensive and easy to install in contrast to impressed current systems.	Current capacity can be limited and is dependent on the mass of the anode.
Low monitoring requirement since they do not need electrical equipment for operation.	Ineffective in high resistivity concrete.
Low driving voltage enables application to prestressed structures and epoxy coated reinforcement.	Passage of current results in the accumulation of hydroxides at the metal cathode which can then react with the concrete resulting in softening.
Lower service life cost relative to other corrosion mitigation systems due to lower maintenance requirements.	Reactions at the reinforcement surface result in reduced bond strength and durability.
Save costs in repair procedures since contaminated concrete that is mechanically sound can be left in place.	Electrochemical reactions at the anode surface can generate acid and chlorine gas which results in concrete softening and failure of the anode system.
Anode types have been developed that can support loads and can be modelled into different shapes.	Cathodic polarisation increases the probability of ASR.
SACP systems can help increase the service life of structures. They can help preserve heritage and cultural structures.	The throwing power of common anode materials is very limited except in saline conditions.
No external power source is required.	Areas remote from the sacrificial anode may remain unprotected particularly in large structures.
Probability of stray currents is low.	Service life is highly dependent on the amount of sacrificial anode provided and the current density. Replacement of anodes is necessary at intervals that cannot be easily defined.
Provide localised protection to steel section that needs it the most even in large structures.	SACP systems do not work in dry concrete.
Current is self-regulated from the anode therefore, SACP systems can be directly connected to the cathode without any complex wiring which also minimises short-circuiting.	High initial capital cost relative to other methods such as corrosion inhibitors.

2.8.1.5 Placement, compaction and curing

The placement, compaction and curing procedures adopted for a repair programme will greatly influence the long-term performance of concrete repairs (Silfwerbrand & Beushausen, 2005). Adopting the correct repair process will ensure good early bond strength development and long-term durability. Workability of a fresh repair material will determine the ease with which it can be placed into substrate cavities. A workable and more fluid repair material allows for capillary suction within the substrate concrete matrix and thus improves bonding between the patch and substrate.

Concrete with high workability is commonly used for repairs on large application zones. For example, shotcrete or gunite is often used for the repair of vertical and inclined surfaces. The energy involved in the use of sprayed concrete enables the mixture to be forced into the pores on the surface of the substrate thereby, enabling the formation of bonds with high strength and durability (Lacombe *et al*., 1999). However, the patch repair of concrete sections over a small surface area is commonly done through the use of stiff concrete mixes. In effect, this reduces capillary suction in the concrete adjacent to the patch and hence limiting bond strength. Bonding mechanisms can be used to enhance adhesion in such cases.

Once placed, good compaction of the repair material will ensure that minute cavities in the substrate are filled thereby, increasing the overall contact between the substrate and the patch. A well compacted repair material will be denser and therefore exhibit good strength. Furthermore, repair material compaction will remove excess voids thereby, reducing penetrability. Low penetrability will ultimately improve durability by limiting the ingress of deleterious substances that would otherwise cause reinforcement corrosion. Early-age plastic and autogenous shrinkage of patch repairs need to be considered to prevent crack development and premature failure. Early-age shrinkage and subsequent cracking and/or debonding of the repair material will restore a repaired element back to a deteriorated state by providing new pathways for aggressive media to enter the substrate. Therefore, the curing process used for patch repairs needs to be carefully monitored and applied as per standard concrete curing procedures. Proper curing will minimise rapid moisture loss thereby ensuring good strength development and more importantly, minimum shrinkage (Beushausen & Alexander, 2009).

A thorough investigation conducted by Beushausen & Bester (2016) identified the importance of curing regimes on repaired concrete elements (overlays), by studying the effect of curing on the restrained shrinkage cracking behaviour of repaired concrete. The study recognised that curing regimes influence all of the concrete material parameters governing cracking due to restrained shrinkage. The study identified that prolonged or more effective curing methods would have a positive influence on crack resistance by either delaying or decreasing the rate of shrinkage respectively; which was directly dependant on the curing process adopted. Furthermore, proper curing was also shown to increase tensile strength and elastic modulus and decrease tensile relaxation. Beushausen & Bester (2016) concluded that 7 days curing using wet cloth or curing compound will present the best results with respect to crack resistance of concrete repairs.

2.8.2 Patch repair on carbonation damaged concrete

Carbonation causes general corrosion to steel in concrete with localised pitting occurring at multiple locations along the length of the steel bar. Concrete affected by carbonation usually has a high resistivity that discourages the formation of macro-cells. This allows only moderate corrosion rates and steel exposed to such conditions will show clear signs of corrosion such as stains, cracking and spalling. Carbonation-induced corrosion damage is usually not as severe compared to chloride ion-induced damage (Mackechnie & Alexander, 2001). Due to this, the application of the patch repair for the restoration of carbonation damaged concrete is generally successful. This is provided that all of the corroded reinforced steel is properly treated, or replaced in extreme cases, and that the patch repair is designed and applied properly. In order to economically restore carbonation damaged concrete, patch repairs are commonly applied to sections of RC structures that show visible and detectable signs of corrosion damage. The localised application of patch repairs is sometimes not sufficient to extend the durability and service life of a complete RC section or structure.

This is because the areas adjacent to the patch repair may typically also be affected by carbonation. These areas may not show clearly visible signs of corrosion damage and as such would not be repaired through the patch repair system. For the patch repair to be durable with respect to these adjacent areas, they will need to be protected against further deterioration due to carbonation. This can be done by applying a surface coating or utilising corrosion inhibitors. This process is principally aimed at slowing down carbonation-induced corrosion rates and thus, preventing defects from materialising in these regions. It must be ensured that workmanship is up to standard and performance monitoring is essential to establish the effectiveness of the repair patch. It is essential to ensure that the repair material bonds securely to the boundaries surrounding the patch. Debonding and cracking of the patch repair needs to be prevented at all costs as these defects would effectively restore the RC back to a deteriorated state. This is because these defects expose new pathways for aggressive media to attack the embedded reinforcement steel and therefore, initiating new corrosion sites. This process ultimately renders the patch repair unsuccessful (Beushausen & Alexander, 2009).

2.8.3 Patch repair on chloride ion damaged concrete

Corrosion induced by chloride ions is characterised by severe pitting with distinctive cathodic and anodic sites. The chloride ions encourage the formation of large cathodic sites driving intense contained anodes. As a consequence macro-cell corrosion is initiated and severe pitting corrosion is sustained in these conditions. With chloride ion contamination, a large extent of steel reinforcement may be at risk of corrosion, without any visible signs of damage on the surface of the concrete. The localised application of a patch repair only to areas that show visible signs of corrosion damage is not very effective against chloride-induced corrosion. This is because the adjacent substrate is usually also contaminated with chloride ions and hence the reinforcement is still exposed to corrosion. Furthermore, the patch repair often results in the formation of new anodic sites adjacent to the restored section as illustrated in Figure 2-18. The formation of these new corrosion sites leads to the continuation of corrosion damage to the structure and hence renders the patch repair ineffective (Mackechnie & Alexander, 2001).

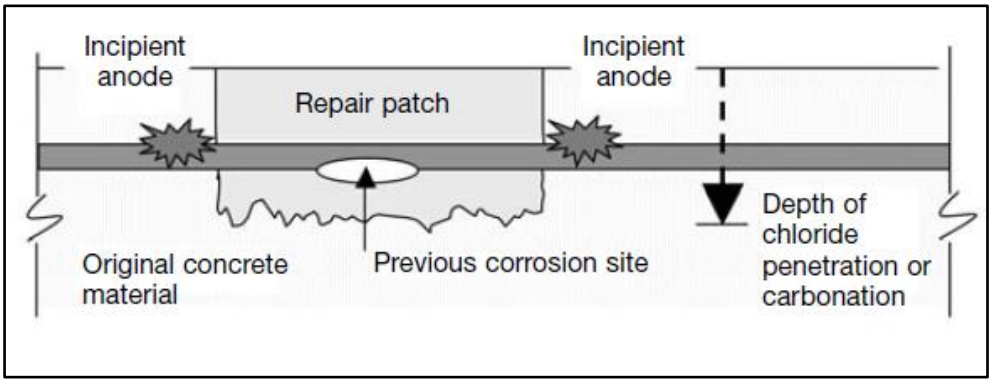

Figure 2-18: Incipient anode formation after patch repairs (Beushausen & Alexander, 2009)

For the patch repair to be successful in rehabilitating chloride ion-induced corrosion, it is imperative that all chloride contaminated concrete is removed from the surrounding areas of the corrosion damaged reinforcement. This would ensure that the passive conditions in the concrete are restored and as a result, corrosion is effectively halted. The application of the patch repair to concrete damaged due to chloride ion-induced corrosion is only effective in cases where low levels of penetration have occurred. The repair of concrete where chloride ions have penetrated deep into the matrix and has caused widespread corrosion is uneconomic and physically difficult. In such cases the use of electrochemical repair methods including cathodic protection and the use of penetrating corrosion inhibitors should be considered (Beushausen & Alexander, 2009).

2.8.4 Conventional patch repair materials

Most patch repair materials are commercially available in pre-packaged form. They are commonly available in premixed, standard 25 kg bags. Prepacked repair mortars are usually specialised and typically exhibit more “superior” properties, particularly mechanical properties such as high compressive strength, relative to ordinary cement based mortars. The most common repair materials contain sand, cement, polymers and fibres. Proprietary repair mortars are commonly accepted to provide enhanced performance and consistency than site-batched mortars due to quality assurance from suppliers (Owens, 2009).

The concrete repair industry is saturated with a multitude of commercially available repair materials many of which are supplied by different manufacturers. As a consequence engineers are conflicted in selecting appropriate materials for a particular repair programme (Cusson & Mailvaganam, 1996). This issue is exacerbated by the lack of universal standards available to characterise and select proper repair materials for specific environmental and substrate concrete conditions. Particularly, the relative shrinkage, bonding and penetrability properties of different proprietary repair materials is not well-known. The most common concrete repair materials can be grouped into either cementitious mortars, polymer-modified cementitious mortars or resinous mortars. There are numerous types of repair products that fall under each of these categories as summarised in Table 2-5. The characteristic mechanical properties exhibited by the different categories of repair materials are identified in Table 2-6.

As shown in Table 2-6, different repair materials exhibit unique mechanical properties and the large variations in these make it difficult to select repair materials for specific service conditions. Portland cement based mortars are usually adopted for most general concrete repair works and particularly, for deep sections where the use of proprietary materials would be uneconomic. However, the durability of plain cement materials can be an issue nevertheless, this may be improved by the use of cement extenders and/or admixtures (Owens, 2009). Polymer mortars are applied in unusual repair cases where for example, good chemical resistance is required or where only thin coatings are needed.

Table 2-5: Common concrete repair materials (Emberson & Mays, 1990)

Cementitious mortars	Polymer-modified cementitious mortars	Resinous mortars
Portland cement (PC)	Styrene-butadiene rubber	Epoxy
High alumina cement (HAC)	Vinyl acetate	Polyester
PC/HAC mixtures	Magnesium phosphate	Acrylic
Expansion producing grouts	Acrylic	Polyurethane
	Engineered cementitious mortar	

Table 2-6: Typical repair material mechanical properties (Mays & Wilkinson, 1987)

Mechanical properties	Cementitious mortars	Polymer-modified cementitious mortars	Resinous mortars
Compressive strength (MPa)	20-50	30-60	50-100
Tensile strength (MPa)	2-5	5-10	10-15
Elastic modulus in compression (GPA)	20-30	15-25	10-20
Coefficient of thermal expansion ($^oC^{-1}$ x 10^{-6})	10	10-20	25-30
Water absorption (percentage by weight)	5-15	0.1-0.5	1-2
Maximum service temperature (^oC)	>300	100-300	40-80

2.8.5 Issues with patch repairs

2.8.5.1 Shrinkage induced cracking

Any long-term performance of patch repairs fundamentally depends on their resistance to cracking. The failure mechanisms leading to cracking are a consequence of deformation due to differential volume changes between a fresh patch repair and relatively mature substrate. Early age repair material volume change is caused by heat development through the hydration process however, with age the effect of shrinkage on the dimensional stability of patch repair systems is more important.

Plastic, autogenous, carbonation, thermal and drying shrinkage are known to be the different types of shrinkage affecting concrete structures. Plastic shrinkage is the reduction in volume of concrete due to rapid loss of concrete surface moisture. It occurs within the first few hours of casting. Concrete elements with high surface area to volume ratios such as thin overlays and patch repairs are particularly vulnerable to early age plastic shrinkage induced cracking. Autogenous shrinkage is the decrease in volume of concrete as a consequence of water consumption by the cement hydration process. Autogenous shrinkage occurs immediately after setting after which the rate drops rapidly (Alexander & Beushausen, 2009). The hydration reactions develop products that have smaller volumes than the reactants which ultimately results in autogenous shrinkage.

Carbonation shrinkage is the reduction in volume of concrete as a consequence of the reaction of cement constituents with carbon dioxide in the atmosphere (Alexander & Beushausen, 2009). The carbonation process results in the rearrangement of the concrete microstructure, reduction in porosity and reduction in total volume resulting in differential shrinkage between the concrete surface and the inner matrix. Carbonation shrinkage is a slow process and occurs over a long time period.Large concrete structures, particularly those exposed to hot climates, are subjected to significant heating within the first few days of casting as a consequence of the cement hydration process and poor heat dissipation. When the concrete contracts during the cooling phase, thermal shrinkage results and can eventually cause cracking (Mehta & Monteiro, 2006a). Thermal shrinkage needs to be accounted for in designing repair systems, but essentially only in service conditions where the rate of temperature fluctuation is large such that cyclic thermal expansion and subsequent contraction on cooling takes place (Holt, 2001).

Drying shrinkage occurs due to the loss of moisture from the exposed surface of a cementitious based repair material, which results in moisture gradients along the cross section of the repair. Tensile stresses occur in the exposed repair surface where moisture loss is greatest and over time these stresses develop with progressing drying shrinkage. In patch repair systems, the patch material being fresher is subject to more shrinkage than the substrate material, which would typically have undergone most of its shrinkage. This results in differential shrinkage between the patch and the substrate materials (Momayez *et al*., 2005). Furthermore, drying shrinkage in patch repairs is substrate restrained.

As a consequence tensile stresses developed in the repaired layer may ultimately lead to cracking, if the tensile capacity of the repair material is exceeded (Banthia & Gupta, 2009). Cracks may develop at the surface of the repair which then propagate along the cross section. With crack propagation surface crack width will widen thereby, affecting the durability of the repair. The initiation of cracking will fundamentally depend on the material properties and severity of moisture loss. There are numerous factors influencing the extent of drying shrinkage in concrete structures and these are identified in Figure 2-19. Tensile forces developed within a patch repair due to deformations, including free and restrained shrinkage and volume changes, are typically accepted to be the chief parameters responsible for cracking in repairs (Mauroux, 2012). Cracking is of major concern in patch repairs, especially with chloride ion affected structures, since it dramatically alters the movement of deleterious substances into concrete. This facilitates rapid deterioration of concrete and premature repair failure.

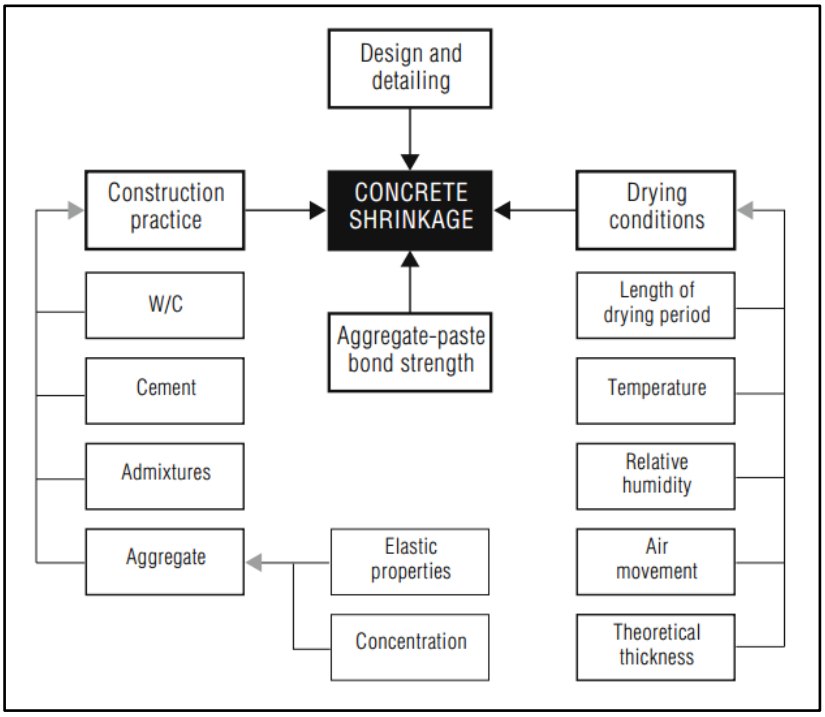

Figure 2-19: Factors influencing drying shrinkage (CCAA, 2002)

The extent to which a repair material can withstand restrained volume change and resist cracking will largely depend on the dimensional stability of the patch repair material. The relative drying shrinkage of a repair material is considered to be the most critical factor affecting the dimensional stability of repair systems. However, in practice it is impossible to control shrinkage since it always takes place in new repairs soon after application (Li & Mo, 2009). Nevertheless, it must be understood that high shrinkage in repairs does not necessarily relate to high cracking potential. Research by Chilwesa (2012) has shown that shrinkage does not necessarily have to be limited to ensure good performance in terms of resistance to cracking and/or delamination.

Chilwesa's research recognised that repair mortars with the highest shrinkage performed best with respect to crack resistance. Therefore, in patch repairs shrinkage would not necessarily be detrimental, provided it does not cause delamination. The underlying reason for this is that patch repair mortars made of cement based material are viscoelastic. Consequently, the stresses developed in patch repairs as a consequence of restrained drying shrinkage are influenced by a number of factors which are difficult to evaluate individually. Cracking and debonding is caused by intricate mechanisms which depend particularly on time-dependent material properties, degree of restraint, service conditions, structural properties and workmanship (Beushausen & Alexander, 2006). The performance of repair systems is a function of both the material components and synergistic effect of the interaction of the repair system with the environment. Therefore, although restrained shrinkage is the driving force for cracking in patch repairs, the aforementioned factors will determine whether shrinkage will actually lead to cracking (Bentur & Kovler, 2003). Particularly, the combined effect of the time-dependant properties of the repair material will influence its overall resistance to cracking and crack propagation.

Extensive repair material research has established that substrate-patch dimensional stability is a time-dependant process. The critical time-dependant material properties governing the mechanisms of crack development are identified to be the synergetic interactions between elastic modulus, tensile strength, drying shrinkage, bond strength, free shrinkage, tensile relaxation, creep and viscoelastic properties (Beushausen & Chilwesa, 2013). The time-dependant parameters that influence repair material resistance to cracking can be modelled via the following relationship (Chilwesa, 2012):

$$\sigma\,(t) = \mu\, x\, E\, x\, \xi\, x\, \varepsilon \quad (\mathrm{N/m^2}) \qquad \text{Equation 20}$$

Where:

σ (t)= stress at time t

μ = the degree of restraint

E = modulus of elasticity

ξ = tensile relaxation

ε = strain.

From the above relationship it is clear that stress is dependent on the degree of restraint, strain and stiffness. Additionally, stiffness is influenced by the modulus of elasticity, creep and tensile relaxation. A detailed analysis of stress distribution and failure mechanisms in repair systems affected by drying shrinkage is outlined by Wittmann & Martinola (2003). Drying shrinkage should be one of the most important considerations in patch repair designs since restrained drying shrinkage is the fundamental cause for cracking in repairs (Kristiawan 2013; Zhou 2010; Li 2009; Aly & Sanjayan 2008; Beushausen & Alexander 2006; Abbasnia *et al*. 2005; Martinola *et al*. 2001).

Tensile stress in repair systems is partially relieved with relaxation. This process leads to stress redistribution to ensure tension-compression equilibrium. Stress relaxation of a repair material therefore affects the strain at the substrate-patch interface. This occurs indirectly with the decrease in the actual shrinkage force exerted on the repair system (Beushausen & Alexander, 2007). Tensile relaxation has the potential to relive a significant amount of repair material stresses for example Gutsch & Rostásy (1994) identified relaxation to be in the range of 35-50% of the initial stress and Beushausen & Alexander (2007) found relaxation to be around 40-50%. Therefore, the tensile relaxation characteristics of a repair system is an important factor affecting stress development of repairs subjected to restrained shrinkage (Beushausen *et al*., 2012).

The elastic modulus and compressive strength properties of patch repairs may not necessarily have to be high for enhanced durability. In fact high compressive strength has been shown to increase the risk of cracking due to increased brittleness, high elastic modulus and small creep deformation (Beushausen & Bester 2016; Chilwesa 2012). Beushausen & Chilwesa (2013) have noted that generally cracking risk is greater with increasing shrinkage and elastic modulus. Cracking risk also increases with lower tensile relaxation and tensile strength.

If the elastic modulus is high with constant tensile relaxation then the stress will be high leading to greater cracking risk and vice versa. Small elastic moduli will thus imply a lower stiffness in concrete and as a consequence this will relate to smaller stress development due to restrained shrinkage (Beushausen & Chilwesa, 2013). Therefore, to resist drying shrinkage cracking, any new material developed for non-structural patch repairs would ideally have a small elastic modulus. Conversely, if the material adopted does not undergo a significant amount of shrinkage then the elastic modulus will not be an important design parameter.

Understanding restrained shrinkage in cementitious repair systems is a critical step in preventing crack development. However, it must be noted that deformation in repair materials is a complex process that is affected by many interdependent factors as mentioned earlier. These factors have a synergetic effect which makes modelling the deformation of repair materials difficult. Furthermore, in practice there is a misconception that high-performance concrete with high stiffness, rapid early strength development and high compressive strength will perform well with respect to shrinkage and crack resistance in patch repairs. However, standard concrete with lower stiffness properties usually outperforms high mechanical strength concrete since such concrete has much more cracking resistance (Aysburd & Emmons, 2006). The underlying issue is that these materials do not address the inherent brittleness of cement based materials. Preventing crack development in cementitious repair materials is therefore unreliable.

2.8.5.2 Debonding

The European Standard (EN 1504-10: 2004) defines bond strength as the adhesion of a repair system to a substrate. One of the most common failure mechanisms of repair systems is the separation of the repair material from the substrate i.e. debonding. Debonding of patch repair materials creates new pathways for aggressive media to penetrate concrete. Similarly to the effects of cracking, debonding radically alters the movement of aggressive media into concrete thereby exacerbating further deterioration. Bond strength and adhesion quality between the substrate and patch is a critical parameter that will ultimately determine the durability and effectiveness of a repair system (Courard *et al*. 2014; Czarnecki & Emmons 2000). Therefore, adhesion of a patch repair material to the substrate is a critical issue concerning the durability of repaired concrete structures (Czarnecki, 2008). There are a large number of interrelated factors that affect bond strength and its durability between substrate and patch materials. Figure 2-20 outlines some of these factors with an estimation of the level of importance. It must be noted that the early traffic and fatigue factors as outlined in Figure 2-20 are not applicable to non-structural patch repairs.

The mechanism of bonding between the substrate and patch repair materials can be explained in terms of specific and mechanical adhesion. Specific adhesion can be determined by analysing the interfacial and surface forces at the bonding surface particularly, the conditions for good wettability and spreading. Good wettability will allow for better fulfilling of the substrate concrete surface profile by the repair material. Mechanical adhesion is influenced by surface preparation of the substrate concrete, in particular, surface roughness (Courard, 2000).

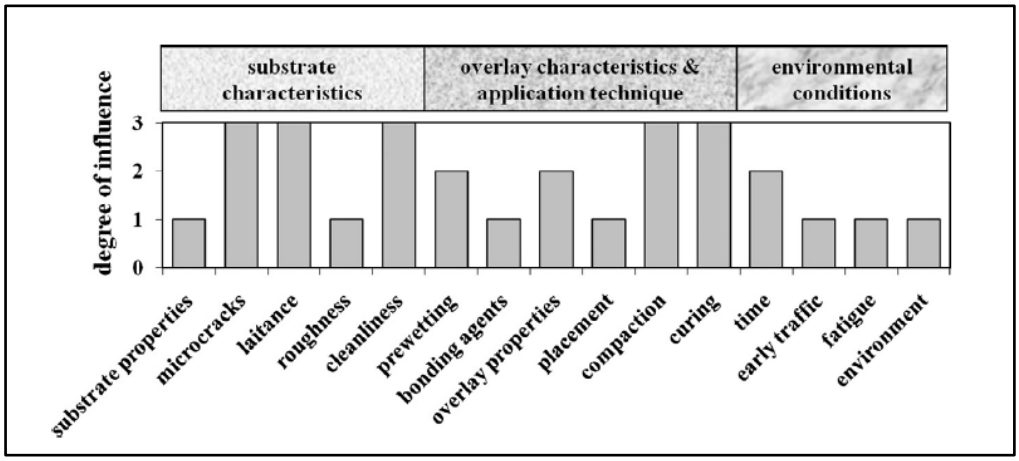

Figure 2-20: Factors influencing bond strength between substrate and overlays (Silfwerbrand & Beushausen, 2005)

A rough substrate increases mechanical interlocking which is one of the basic mechanisms of adhesion (Courard, 2014). Therefore, repair material wettability and substrate surface preparation can be identified to be key parameters influencing substrate-patch bond quality. Furthermore, increasing surface roughness also increases contact surface area and modifies the contact angle both of which improve bond durability (Zhou, 2010). However, it has been suggested that surface roughness does not necessarily increase bond strength but rather decreases the probability of debonding (Perez *et al*., 2008). Research by Bissonnette *et al*. (2011) has shown that bond strength is similar in both rough and smooth substrate surfaces however, interface failure is more frequent in smoother surfaces. As detailed in Section 2.8.1.2, it must be ensured that an appropriate surface roughening procedure is used relative to the strength of the substrate concrete to ensure that micro cracking at the substrate surface does not occur which would otherwise outweigh any benefits of increased roughness (Bissonnette *et al*. 2008; Courard 2014).

As outlined in Figure 2-20, adhesion and therefore, integrity and strength of the substrate-patch bond depends not only on the physical and chemical properties but also on environmental exposure conditions. Temperature and relative humidity influence the initial saturation level of a substrate element and therefore, can influence bonding (Lukovic *et al*., 2012). Prewetting (detailed discussion in Section 2.8.1.2) of substrate surface may undermine proper bonding and there is general agreement that a saturated surface dry substrate condition is required for achieving a good bond (Bissonnette *et al*., 2011). One important aspect that needs special attention is the curing method and duration adopted for a repair programme. Curing is more often than not neglected however, it is important to achieve good substrate-patch adhesion. Curing has been suggested to be at least 3 days for non-structural applications (Behfarnia *et al*., 2005) and at least 5 days wet curing for structural applications (Silfwerbrand & Paulsson, 1998). The use of bonding agents is sometimes adopted to enhance adhesion of substrate-patch systems. Bonding agents such as epoxy resins, latex modified Portland cement grout, and Portland cement grout are typically used as a bonding agents. Pretorius & Kruger (2001) have shown that the use of bonding agents can significantly improve adhesion.

However, it is recommended that the use bonding agents should normally be avoided due to the creation of another plane of weakness (Bissonnette *et al*. 2011; Silfwerbrand & Paulsson 1998). Furthermore, it should be emphasised that bonding agents should not be used as a substitute for adopting incorrect repair procedures/materials and poor workmanship (Lukovic *et al*., 2012). Depending on the combined properties of a substrate-patch repair and their mutual interaction, stress can be differently distributed, in the end leading to cracking and/or debonding of the repair system as illustrated in Figure 2-21. Increased mechanical strength of repair material increases the probability of interfacial debonding as a consequence of increased stress build-up at the interface, which would have otherwise been relieved through crack development. Conversely, accelerating bond strength development may postpone debonding but exposes the repair to cracking. Debonding can reduce constraints and has the capability to partially relieve tensile stresses and therefore, debonding can limit and reduce the time to crack development in repair systems (Lukovic *et al*., 2012).

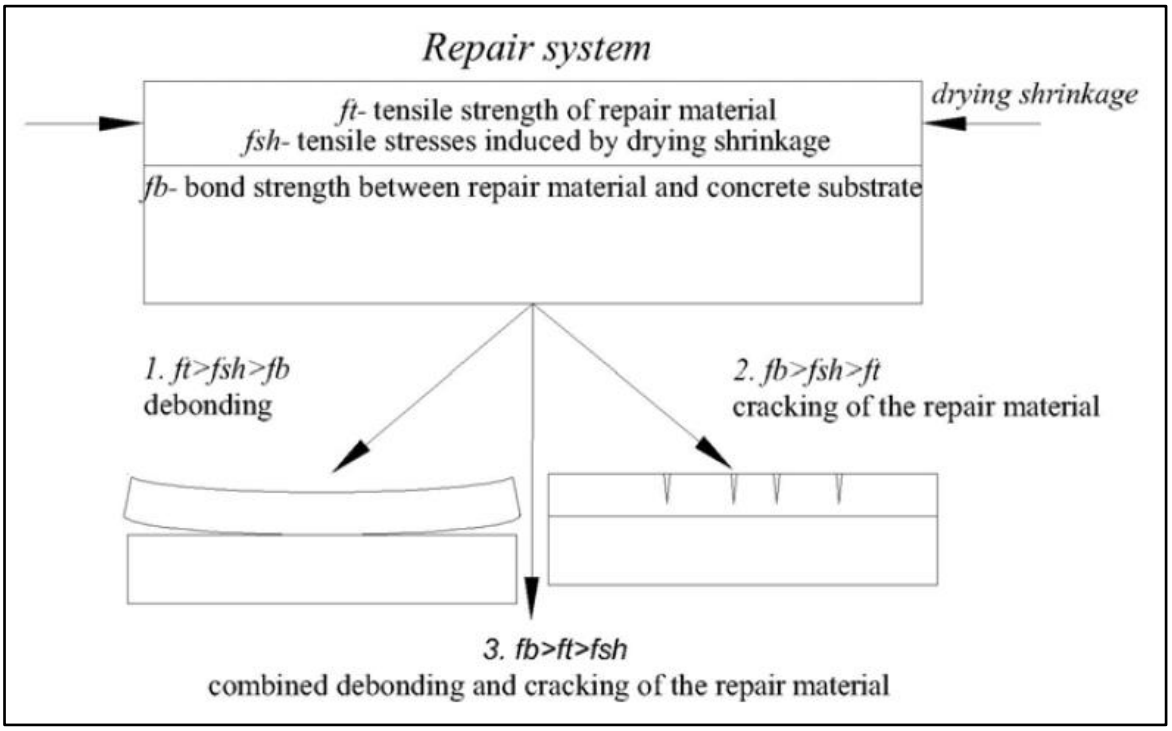

Figure 2-21: Damage mechanisms in repair systems

2.8.5.3 Post-repair corrosion

Electrochemically, a patch repair is principally aimed at eliminating the anodic reaction on the steel reinforcement that existed before any repairs. It is also meant to prevent the anodic reaction from occurring in the future by passivating the patch repair area. However, the addition of a patch repair to RC changes the corrosion state in the reinforcement steel that usually results in new corrosion risks in the adjacent areas of the patch repair. These risks are further exacerbated in severe environments which ultimately results in the impairment of the newly applied repair material (Kim *et al*., 2016). The patch and the substrate inevitably expose the steel reinforcement to varying electrochemical conditions as shown in Figure 2-22.

The repaired section protects the steel by providing good alkaline pH conditions for the passivating layer to form as would normally happen with sound concrete. If the repaired concrete had deteriorated due to carbonation or chloride attack then active corrosion would typically continue in the non-repaired substrate section of the concrete. In patch repair systems, the same reinforcing steel bar is covered by both the patched section and the adjacent substrate section. Therefore, the active and passive sections of the reinforcement are effectively connected electrically. This condition encourages macrocell corrosion in which the active section is polarised anodically and the passive section is consequently polarised cathodically (Qian *et al*., 2006).

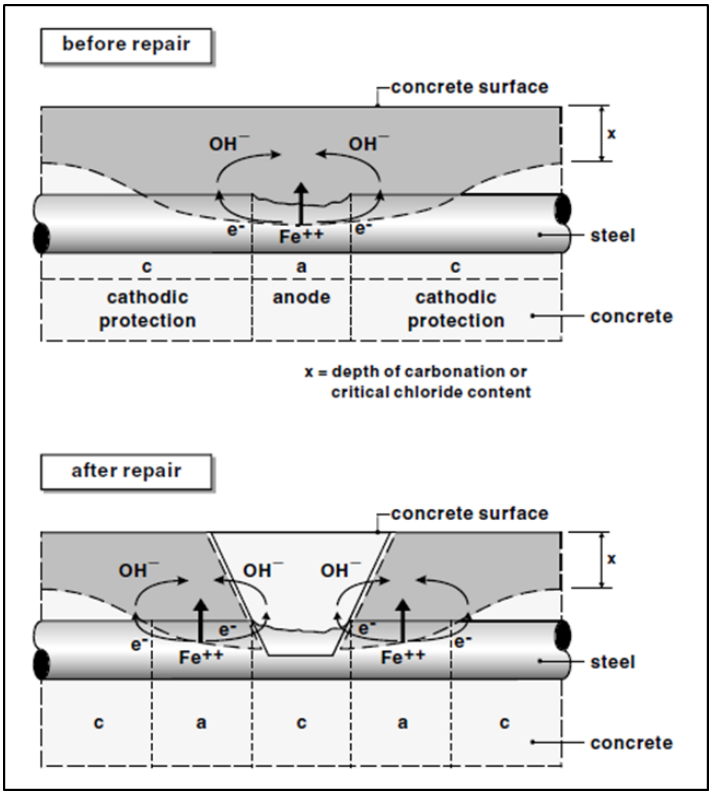

Figure 2-22: Mechanisms of corrosion before and after a patch repair (Raupach, 2006)

Countless patch repairs on RC structures have evidently failed due to prevalent cases of new corrosion thereby, limiting the durability of patch repair systems. Furthermore, corrosion often continues to take place along the border of the substrate-patch repair. This is recognised as the incipient corrosion or ring-anode effect, since the substrate provides a more corrosive environment for steel compared to the new patch (Qian *et al*., 2006). Consecutively, the principle corrosion deterioration mechanism recognised in patch repairs is macrocell corrosion. However, in certain chemical conditions microcell corrosion is also initiated in the repaired RC structure. Before repairs, the damaged section would have been more corrosive to steel and would serve as the anodic site whilst the surrounding substrate would cathodically be protected. Repairs would eliminate corrosion conditions and subsequently, the cathodic protection on the reinforcing steel in the substrate. Therefore, microcell corrosion is also encouraged in the substrate after repairs (Castro *et al*. 2003; Raupach 1996).

2.8.5.4 Local application of patch repairs

One important aspect that needs consideration with the patch repair system is the local application of the repair in isolation to the deterioration and integrity of the substrate concrete. Patch repairs are frequently applied only in areas where corrosion damage is evidently visible. Furthermore, many repairs only serve to provide cosmetic relief rather than addressing the underlying cause of deterioration. This is a common practice and is favoured due to the low cost and quick aesthetic relief (Mackechnie & Alexander, 2001). As a consequence of this, RC damaged due to carbonation or chloride attack is not removed completely. Therefore, even after the application of the patch repair, other areas of the reinforcement typically exhibit corrosion damage not long after a repair. With localised patch repairs there is no guarantee of protection to adjacent concrete and a high risk of corrosion damage still remains in these zones. Additionally, the nature of the patch repair applied to address localised corrosion damage on the steel reinforcement may even accelerate corrosion in the adjacent areas that have not been repaired. This is due to the formation of incipient anodes that promote corrosion in adjacent, untreated steel reinforcement. A holistic approach to the design of patch repairs is needed to address this issue (Raupach, 2006).

2.8.5.5 Deficient patch repair standards

With the patch repair system a critical inadequacy is the lack of detailed specifications in standards for the engineering design of patch repairs exposed to unique environmental and service conditions. Many standards that specify repair materials are established on limited quantitative knowledge of the substrate-patch system (Mangat & O'Flaherty, 2000). Furthermore, standards are deficient in scope and detail and as a consequence engineers are left to specify appropriate materials and procedures on an ad-hoc basis (Owens, 2009). Moreover, variations in international systems lead to further inconsistencies in implementing proper repair strategies. Commonly, shear resistance between patch and substrate is used to define the limitations for repair designs (Lukovic *et al*., 2012). Concrete repair design standards thus use bond strength as a limiting factor for design acceptance criteria. To test the in situ bond strength of repairs, the most common method applied is the pull-off test (Beushausen & Alexander, 2009).

However, parameters such as the pull-off and compressive strengths are determined in laboratory conditions that do not relate to actual service conditions. Moreover, standards do not specify shrinkage and crack resistance requirements which are effectively more important since most patch repairs fail through the mechanism of drying shrinkage induced cracking and debonding. Furthermore, there are a multitude of commercially available patch repair mortars, each exhibiting a range of different properties. The amount of research into the long term performance and durability of these is limited (Lee *et al*., 2007). As a result, engineers are left to specify suitable materials and methods without the required technical knowledge more often than not, leading to defective designs (Morgan, 1996). Additionally, the limited availability of scientific models makes it more difficult to select appropriate materials and procedures for specific repair programmes (Taffesea & Sistonen, 2013).

2.8.6 Compatibility of repair materials

The term "compatibility" is frequently mentioned in concrete repair literature. However, there is considerable controversy regarding its meaning and application in repair programmes. The issue of repair material compatibility has been widely discussed by numerous authors including Lukovic *et al*. (2012), Li (2009), Vaysburd *et al*. (2004), Cusson & Mailvaganam (1996), Morgan (1995) and Emberson & Mays (1990). Emmons *et al*. (1993) define compatibility as:

"A balance of physical, chemical and electrochemical properties and dimensions between a repair material and the existing substrate that will ensure that the repair can withstand all the stresses induced by volume changes and chemical and electrochemical effects without distress and deterioration over a designated period of time."

Dimensional, mechanical, chemical, permeability, electrochemical and aesthetic parameters are the key compatibility aspects identified in literature as summarised in Figure 2-23.

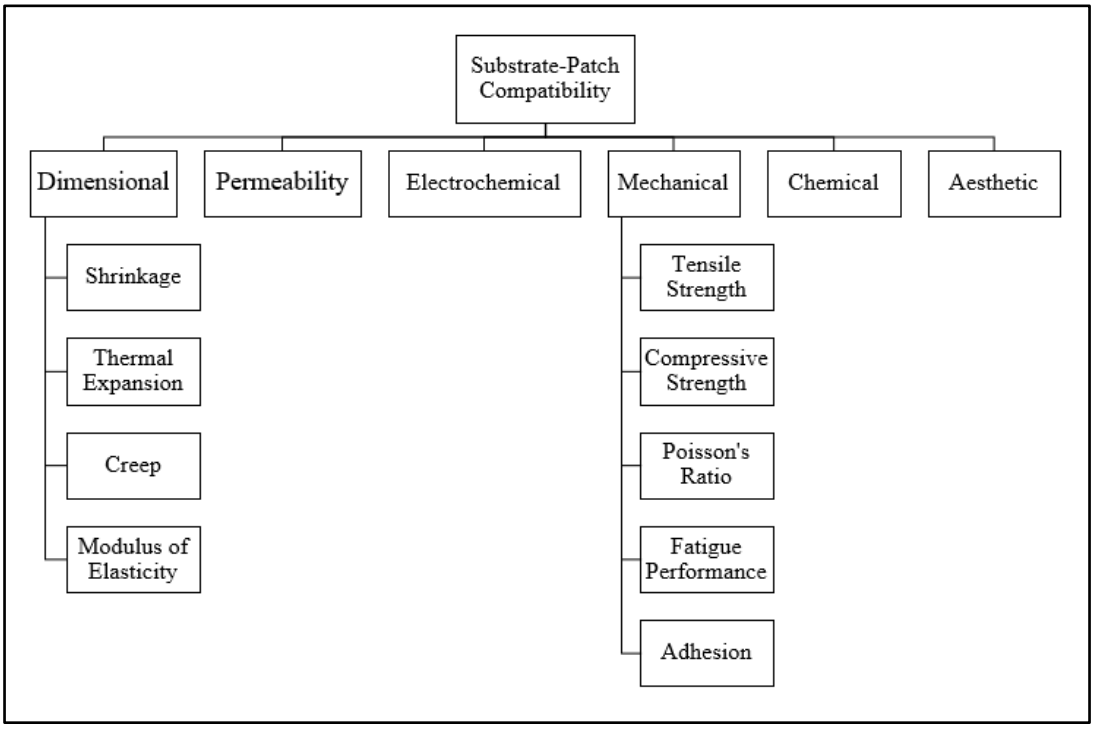

Figure 2-23: Compatibility factors considered for repair materials (Vaysburd, 2006)

Literature on compatibility points out that a repair system is a multi-layered, composite system. For any long-term performance of this system, compatibility between the repair material and substrate concrete needs to be considered. Essentially, it is believed that proper compatibility would enable the composite repair system to behave monolithically. This would circumvent durability issues arising as a consequence of volumetric changes and uneven stress distribution. An extensive amount of prior research has been conducted considering the compatibility of repair materials with substrate concrete. However, such research has been of little significance since 50% of concrete repairs still fail prematurely and 75% fail within the first 10 years as identified in the ConRepNet study conducted by Matthews *et al*. (2003).

2.8.6.1 Critical evaluation of compatibility requirements

Merely adopting substrate-patch compatibility as the basis for repair material selection is the wrong approach for durable concrete repairs, as clearly evidenced by the large failure rate. The theme of compatibility of repair materials with substrate concrete is essentially theoretical. To achieve a "balance of properties" between substrate and patch repair material is practically impossible. A concrete repair system is a complex system of materials exposed to differing environments internally in the repair structure and externally, to service conditions. Therefore, a repair material cannot be made to "match" the properties of the substrate. Reliable quantification of the parameters required for compatibility is highly lacking (Mangat & O'Flaherty, 2000). Furthermore, literature identifies specific properties required of repair materials for compatibility, such as high compressive strength, low elastic modulus and low shrinkage. However, specifying such particular properties cannot be made in isolation to the synergetic effects of the different properties of concrete. This is because concrete is a viscoelastic material which exhibits a range of interdependent properties. Therefore, without considering the combined effects of different concrete repair material properties exposed to in service conditions, following compatibility recommendations specified in literature is misleading.

Moreover, research by Beushausen & Bester (2016) and Chilwesa (2012) has shown that high compressive strength and elastic modulus in concrete repair materials actually increases the risk of cracking. This may seem counter-intuitive but can be explained by considering the combined effect of concrete repair material properties that influence cracking including elastic modulus, tensile strength, tensile relaxation and shrinkage strain. In low strength concrete the tensile strength is lower and consequently resistance to cracking decreases. However, low strength concrete also exhibits lower elastic modulus. Therefore, it undergoes reduced stress development and increased stress relaxation under restrained shrinkage conditions. Due to this, lower strength concrete has less cracking potential (Beushausen & Bester, 2016). These findings further support the argument that high strength concrete is not a critical design factor when considering the durability of patch repairs.

There is a common misconception in the concrete repair industry that repairing "like with like" is an ideal solution for monolithic substrate-patch material behaviour. This belief is a direct consequence of the widespread use of the term compatibility in literature and it is fundamentally flawed. The result of this is that engineers are compelled to select repair materials solely based on similarity to the substrate material without considering the underlying causes of concrete deterioration and service conditions. Furthermore, it is believed that repairing concrete with specialised commercially available repair mixes will guarantee durability. However, this is a serious misconception verified by the widespread premature failure of such repair materials. According to Lukovic *et al*. (2012), substandard concrete must not be repaired with similar substandard repair materials. However, this view may not be entirely true particularly for non-structural patch repairs. For non-structural applications, the repair material does not need to exhibit high mechanical strength properties. If the underlying cause of concrete deterioration is addressed and the reinforcing steel properly treated, then it may be possible to utilise seemingly substandard repair materials for patching.

The lack of comprehensive engineering standards supporting the requirements of compatibility mentioned in literature is limited. Standards typically identify mechanical strength parameters such as minimum compressive strength, as guides for repair material selection. However, such specifications are misleading particular for non-structural repairs where compressive strength is not a design requirement. The lack of suitable standards and the availability of a variety of proprietary repair materials has made it greatly difficult for engineers to select appropriate repair materials based on the principles of compatibility. Therefore in practice many repair materials are selected on an ad hoc basis (Mangat & O'Flaherty, 2000).

2.9 Literature review into alternative materials

The objective of this research project is to identify new, non-structural patch repair materials. A non-structural repair implies that the materials selected do not necessarily need to exhibit high mechanical strength properties such as compressive strength and/or elastic modulus. Therefore, theoretically ordinary Portland cement (OPC) can be partially or fully replaced in the development of a new patch repair material since mechanical strength is not a limiting factor. In order to provide a framework for the selection of new non-structural patch repair materials, literature is reviewed in the following sections that specifically looks into large volume OPC replacement (60-100%) and the use of polymers as the sole binder in concrete production.

2.9.1 Large volume OPC replacement

The underlying cause of shrinkage cracking and debonding in concrete patch repairs is attributed to the limiting properties of repair materials composed of OPC, which is used in most patch repair systems. OPC repair mortar requires water for the hydration process and as a consequence has considerable potential for drying shrinkage. This consequently results in cracking if the shrinkage occurs under restrained conditions. Additionally, the use of OPC in repair mortar results in the formation of a matrix that has significant imperfection particularly micro-cracks which emanate from surplus water, bleeding, settlement, thermal strains, concentration of stress imposed by external restraints and more importantly, shrinkage strains.

Under service conditions these cracks can propagate to eventually form macro-cracks which exposes the repaired element to aggressive media attack and reinforcement corrosion (Banthia *et al*., 2014). The production of OPC is also not an environmentally sustainable process as it leads to massive amounts of carbon dioxide pollution and energy consumption. Furthermore, OPC is relatively expensive and this is exacerbated by the use of specialised proprietary repair mixes. These mixes develop mortars with high mechanical strength properties such as compressive strength, which is effectively wasteful since compressive strength is not a design factor for non-structural patch repairs. Theoretically, replacing OPC in concrete with a suitable alternative binder could possibly eliminate these limitations, provided the new binder forms a concrete/mortar matrix that has good crack resistance and adhesion properties. In the theme of identifying suitable alternative materials for durable patch repairs, literature review into large volume OPC replacement in concrete was conducted and this is discussed in the following sections.

2.9.1.1 Lime kiln dust concrete

Lime kiln dust (LKD) is a by-product produced during the manufacturing of quick lime. LKD is mostly disposed off into landfills creating a host of environmental problems which can be partially addressed by reusing LKD in the production of concrete. Latif *et al*. (2015) investigated into the use of LKD as a cementitious material for use in the production of mortar. This research focused on the sustainable use of LKD whilst possibly developing mortar with strength properties comparable to 100% OPC based mortar. In the study, LKD was used to replace OPC by up to 60% (by weight) in the production of mortar. The mix designs adopted in the different formulations are summarised in Table 2-7.

Table 2-7: Mix proportions adopted by Latif *et al*. (2015)

Mix ID	LKD Replacement (%)	OPC (kg/m^3)	LKD (kg/m^3)	Water (kg/m^3)	Manufactured Silica Sand (kg/m^3)	SP (Sika VS2199) (%)
LKD0	0	550	0	220.1	1100	0
LKD5%	5	522.5	27.5	220.1	1100	0
LKD10%	10	495.0	55.0	220.1	1100	0
LKD15%	15	467.5	82.5	220.1	1100	0
LKD20%	20	440.0	110.0	220.1	1100	0
LKD30%	30	385.0	165.0	220.1	1100	0.145
LKD40%	40	330.0	220.0	220.1	1100	0.257
LKD50%	50	275.0	275.0	220.1	1100	0.419
LKD60%	60	220.0	330.0	220.1	1100	0.568

Experimental tests were conducted on LKD concrete specimens, with respect to physical, mechanical and engineering properties. The results of this study concluded that the inclusion of LKD in mortar production reduces its density and compressive strength relative to 100% PC mortar. Latif *et al*. (2015) established that LKD can effectively be used as OPC replacement to develop fast setting, green mortar. LKD could possibly be used in non-structural patch repair systems where compressive strength is not important. The fast setting times of LKD based mortars can be useful for patch repair programmes where there is a need for quick restoration. Furthermore, low density LKD mortars can be handled and applied to patch repairs relatively easily. However, more research into the durability of LKD mortar is necessary. Particularly, this study did not investigate into the penetrability properties of LKD mortars which is especially important for patch repairs exposed to chloride ions.

2.9.1.2 80% fly ash concrete

FA resembles OPC both physically and chemically and as a result there has been significant effort in developing its use as OPC replacement in concrete production. FA is sourced from coal-fired power plants as a by-product of the combustion process. The properties of FA vary considerably as a consequence of factors such as the nature of coal used and the extent of combustion. Consequently, the use of FA in replacing OPC in the concrete industry has been conservatively limited.

Rivera *et al*. (2015) investigated into the use of up to 80% FA replacing both OPC and aggregate in concrete. The mix formulations adopted in the study are summarised in Table 2-8. The research was aimed at maximising FA content in concrete production to promote the theme of sustainability rather than improving mechanical properties. Concrete with a composition of as much as 728 kg/m^3 of FA aggregate (cold-bonding) was developed with compressive strengths greater than 30 MPa, a low chloride ion permeability and improved electrical resistivity.

Table 2-8: Mix proportions adopted by Rivera *et al*. (2015)

Mixture ID	Cement (kg/m^3)	Fly ash %	Fly ash (kg/m^3)	Water (kg/m^3)
OPC	1359.7	0	0.0	571.1
BC	1307.5	0	0.0	549.1
40-C	865.7	40	431.5	544.8
60-C	595.4	60	667.7	530.4
80-C	307.4	80	919.2	515.2
40-F	864.4	40	434.5	545.5
60-F	594.0	60	671.7	531.6
80-F	306.4	80	924.0	516.7
C & F: type of fly ash C:blended cement OPC: ordinary Portland cement				

The study concluded that the use of large volume FA (65 – 85%) in concrete would result in some improved concrete durability characteristics compared to OPC concrete. This study establishes the basis for further studies into the use of FA to completely replace OPC in concrete production. In addition to the environmental benefits of using FA in concrete production, prior research has shown that FA concrete has improved workability, less drying shrinkage and reduced steel reinforcement corrosion (Malhotra & Ramezanianpour 1994; Mehta 2004; Corral *et al*. 2013).

A concrete mix based on FA could be used in non-structural patch repairs. However, the use of up to 728 kg/m^3 of FA as investigated by Rivera *et al*. (2015) is not economical since such a high FA content will increase the cost of concrete production. Although, for non-structural patch repairs this amount can be largely reduced since mechanical strength would not be required. Furthermore, the improved penetrability properties of FA based concrete would be beneficial particularly for patch repairs exposed to chloride ions.

2.9.1.3 65% fly ash concrete with 10% lime

Naidu & Pandey (2014) looked into the replacement of OPC in concrete by using up to 65% FA and 10% lime as cementitious material in concrete production. The study was aimed at determining the feasibility of replacing large amounts of OPC in concrete whilst improving the pozzolanic and binding properties of high volume FA concrete with limestone inclusion. The mix designs of the different formulations adopted in the study are summarised in Table 2-9.

Table 2-9: Mix design of different formulations as adopted by Naidu & Pandey (2014)

Material	For 1m^3 (kg)			
	0% w/c - 0.30	65% w/c - 0.25	70% w/c - 0.25	75% w/c - 0.25
Cement	440	146.3	132	110
Fly ash	0	271.7	286	286
Lime	0	22	22	44
C-Sand	805	805	805	805
10 mm	392	392	392	392
20 mm	705	705	705	705
Water	167	110	110	110
Admixture	4.20	4.50	4.50	4.50
Strength (MPa)				
7 Days	53.11	30.07	28.54	17.92
28 Days	71.11	55.40	45.36	39.12
56 Days	-	58.22	54.67	48.73

The investigations carried out concluded that FA can be practically used to develop environmentally sensitive and cost efficient concrete. The use of FA in high volume also improves workability and concrete microstructure which leads to improved resistance to ingress of aggressive media. Therefore, this mix design of FA concrete could be applied to improve the durability of non-structural patch repairs exposed to chloride ions. Furthermore, due to less OPC content, less water is required for hydration and the remaining cement content is able to achieve complete hydration. Reduced water content could limit the relative amount of drying shrinkage however, experimental studies would be necessary to confirm the extent of shrinkage reduction and the effect of this on crack resistance. A FA concrete mix with relatively good crack resistance will improve the durability of patch repairs since most repairs fail due to the effects of long-term drying shrinkage. Additionally, the study found that the use of lime leads to improved binding within the concrete matrix (Naidu & Pandey, 2014). Improved binding will ensure the development of an improved matrix that would reduce concrete penetrability. Furthermore, such concrete could bond well to patch repair materials thereby, limiting the possibility of debonding.

2.9.1.4 100% fly ash concrete with glass aggregate

Over ten years of research conducted by Berry *et al*. (2009), Cross & Stephens (2005) and Cross *et al*. (2005) at the Montana State University (MSU) extensively investigated into the use of 100% FA concrete with glass aggregate. The typical mix designs adopted in manufacturing 100% FA concrete with pulverised glass aggregate are summarised in Table 2-10.

Table 2-10: Mix formulations adopted for 1m^3 of concrete (Berry *et al*., 2009)

Concrete	Water (kg)	Fly ash (kg)	Fine aggregate (kg)	Coarse aggregate (kg)	Borax (kg)
Traditional Aggregate	91.77	382.99	315.57	631.14	4.77
Glass Aggregate	120.23	601.27	274.83	274.83	7.49

To determine the engineering properties of this new concrete, a multitude of experimental programs were setup at MSU. The researchers concluded that 100% FA has exceptional potential for use in the concrete industry. The main obstacles to its widespread use were associated with not following the correct batch preparation procedures as stipulated specifically for 100% FA concrete. In field applications, it was identified that FA concrete was prepared without following good concrete practice, which is a common occurrence even with OPC concrete production. Furthermore, applying the same OPC concrete batch preparation procedures to 100% FA concrete is detrimental to the quality of 100% FA concrete produced. This is because FA concrete is more sensitive to batch preparation procedures relative to OPC concrete.

Research efforts at MSU have obtained very promising results and clearly validated that 100% FA concrete with pulverised glass aggregate can be effectively used for both structural and non-structural applications. The 100% FA concrete mix developed at MSU could be applied to non-structural patch repairs. The relatively fast setting times of the FA concrete can be applied to patch repair programmes that have quick turn-around times. Furthermore, the FA mix was found to exhibit good workability without the use of sophisticated admixtures.

2.9.1.5 100% fly ash based geopolymer concrete

With the advancement of research into concrete technology, multiple novel concretes have been developed, particularly to address the underlying issues of concrete durability, cost-efficiency and sustainability. One of these is an inorganic, green polymer concrete known as geopolymer concrete which is made by the replacement of OPC in concrete with a pozzolanic material after a geopolymerisation process. The term geopolymerization was coined by Davidovits (1988) describing the reaction that results when aluminosilicates are alkali activated at low temperatures. Geopolymers are inorganic materials which have three-dimensional silico-aluminate structures as a consequence of polycondensation.

Lohani *et al*. (2012) explained that a geopolymerisation process involves the combination of an alkali material, usually NaOH, with FA. The mix is dried in an oven at 60°C to 80°C for 6-12 hours. It is then left in an open atmosphere for 24 hours which essentially converts the mix to an alkali activated FA geopolymer. This forms a binder for effective OPC replacement in manufacturing concrete. Generally, geopolymer binders are developed through the reaction of an aluminosilicate powder with an alkaline silicate mixture. The most common source for making geopolymers is fly ash (Somna *et al*., 2011). Numerous studies have researched into the use of alkali activated fly ash concrete however, these are very limited with reference to South African fly ash (Shekhovstova, 2015).

The development of an alkali activated fly ash geopolymer with good properties is dependent on many factors. The geopolymerization process is greatly dependant on the chemical and mineralogical composition of the fly ash material (Shekhovstova, 2015). According to Xu and Van Deventer (2000) the percentage of CaO, K_2O, molar Si-Al ratio in the material and type of alkali used for activation has a significant effect on the compressive strength of the alkali activated material.

Komljenović *et al*. (2010) has shown that NaOH and $Ca(OH)_2$ have considerable activation potential however the most common activators used are NaOH and KOH (Davidovits, 1999). Arjunan, Silsbee & Roy (2001) have mentioned that the chemical and mineralogical composition of low calcium fly ash does not affect alkali activation. Furthermore, Fernandez-Jimenez & Palomo (2003) have identified that CaO content in alkali activated fly ashes should actually be low. Nevertheless, research by Diaz *et al*. (2003) has recommended that a 5-15% content of CaO in fly ash is desirable. These findings are particularly relevant to South African fly ash which have low calcium oxide contents.

The curing regime adopted in developing geopolymers is also important. Katz (1998) found that the reactivity of fly ash increases with increasing activator concentration and curing temperature. Katz (1998) has established that no significant reaction will take place at ambient temperature and higher temperature curing is needed for activating fly ash. Numerous other researchers including Bakharev (2005), Winnenfield *et al*. (2010), Criado *et al*. (2010) and Kovalchuck *et al*. (2007) have agreed with this. In these studies, curing temperatures ranging from ambient to 90^{o}C have been researched in producing alkali activated concrete. It has been established that heat curing greatly accelerates the development of strength in alkali activated fly ash. With respect to South African fly ash Shekhovstova (2015) recommended curing at 60°C for 16 hours with the alkali content (Na_2O) not exceeding 12%. This is because with higher alkali concentrations, high standard deviation of compressive strength as well as efflorescence formation would occur.

Contrary to this, Somna *et al*. (2011) produced ground fly ash paste cured at room temperature with compressive strengths between 20-23 MPa (28 days). The results of the study identified that the strength development of alkali activated fly ash was similar to that of Portland cement. The study used 9.5-14.0 M NaOH as activator and established that the compressive strength and microstructure of the geopolymer was greatly dependant on the concentration of the activator. Strength was generally shown to increase with an increase in activator concentration. In line with these findings, Hole (2009) also established that curing of alkali-activated fly ash at room temperatures is possible but strength gain is slow. Additionally, Bakharev (2005) and Rangan (2005) have established that long pre-curing at room temperature is beneficial for compressive strength development of alkali activated fly ash.

With reference to this thesis, the development of an alkali activated fly ash material for use in industry should preferably require ambient curing. This is particularly important in developing a practical patch repair material for effective industry application. Additionally, the studies by Lohani *et al*. (2012) and Somna *et al*. (2011) have obtained promising results in developing concrete with some properties comparable to OPC concrete, whilst reducing its cost and promoting the theme of sustainability. Applying such materials to non-structural patch repairs could be feasible however, much research into the bonding, shrinkage and subsequent crack resistance properties would be necessary.

2.9.1.6 Calcium sulfoaluminate cement system

Calcium sulfoaluminate cement (CSA) is a cementitious material manufactured by calcining limestone, bauxite and clay. Gypsum or anhydrite is then added to activate it into a cementitious material. CSA cement clinker is manufactured at a temperature of between 1250-1350°C. Processing the raw materials produces calcium sulfoaluminate, upon which calcium sulphate in the form of gypsum or anhydrite is added. CSA has a range of advantages over OPC and as a consequence it is attracting a significant amount of interest worldwide (Quillin, 2001). The advantages of CSA relative to OPC include the following (Zhou *et al*., 2006):

- CSA clinker is processed at a temperature of 1250-1350°C. Although this is a high temperature, it is lower than that used for OPC production. This reduces the energy consumption in its production and hence reduces its cost.
- There is less use of limestone in the CSA cement system and therefore, the CO_2 emissions are considerably lower.
- The hydration chemistry of CSA is different and consequently results in a lower pH of the pore solution.
- Excellent durability properties even in marine construction.

Zhou *et al*. (2006) concluded that CSA cement has good potential for use in the construction industry. It is compatible with other construction materials and its main hydration product, ettringite, is able to bind and immobilise ions and water. This enhances its durability against aggressive media attack. This material could therefore be applied to improve the durability of non-structural patch repairs exposed to chloride ions and other aggressive media. Furthermore, the formation of ettringite during the hydration of CSA results in volume expansion. This is an important finding that could be used for shrinkage compensation in concrete elements and possibly limiting the amount of shrinkage induced cracking in patch repairs. Therefore, incorporating CSA in the production of a repair material could ensure the durability of patch repairs which frequently fail as a consequence of shrinkage induced cracking and/or debonding.

2.9.2 Polymer based concrete

There are numerous classes of polymer based concretes namely polymer concrete, polymer-cement concrete and polymer impregnated concrete. Polymer concrete is a composite material which consists of aggregates and a polymer binder, typically a resinous compound that sets to form a continuous polymer matrix (Saribiyik *et al*., 2013). Polymer concrete is made by utilising a thermoset resin as the sole binder for natural or artificial aggregates thereby, replacing cement and water which is otherwise required in conventional hydraulic concretes (Nóvoa *et al*., 2004). Polymer-cement concrete (also known as polymer-modified concrete) consists of ordinary Portland cement based concrete with a polymer modifier added such as polyvinyl acetate and ethylene vinyl acetate. Polymer impregnated concrete is hydrated Portland cement concrete that has been infiltrated with a polymer material which is polymerised in situ. There are a multitude of polymer compounds used in concrete production and the most common ones are resins which comprise of unsaturated epoxies, urethane, polyesters, furan, acrylics and vinyl ester. Such concrete was initially used in cladding applications in the late 1950s.

However, ever since the 1950s and particularly in the 1970s, the excellent properties exhibited by polymer based concrete led to the rapid increase in its use for a variety of different construction applications. A variety of coarse aggregates are used as filler in polymer based concrete including granite, crushed stone, calcareous gravel, limestone, quartz, silicates and clay. Consequently, a range of fine aggregates are also utilised to improve the properties of polymer based concrete such as glass fibre, fly ash, silica fume and carbon fibre (Aggarwal *et al*., 2007).

Polymer based concretes exhibit many superior properties relative to OPC concrete including: high strength, rapid curing, excellent chemical resistance against chlorides and sulphates, long-term durability, low water penetrability and greater freeze-thaw damage resistance (Blaga & Beaudoin 1985; Fowler 1999). However, the excellent adhesion property of polymer based concrete is identified to be the most important. Moreover, polymer based concrete does not require the addition of water and hence it is not exposed to drying shrinkage induced cracking. Countless OPC based repair materials have failed prematurely as a consequence of drying shrinkage induced cracking and/or debonding. Therefore, the use concrete consisting of polymer for concrete repair applications provides a viable alternative for durable patch repairs (Saribiyik *et al*., 2013). The use of polymer based repair mortars is therefore widespread in the concrete repair industry.

However, polymer based concrete is more expensive than OPC concrete. As a consequence, it is typically only used for special cases and avoided in cases where large volumes of concrete are required (Nóvoa *et al*., 2004). Moreover, this is exacerbated by the use of specialised proprietary repair mixes. These mixes develop mortars with enhanced mechanical properties such as high compressive strength and elastic modulus. However, the use of such specialised repair mortars is highly inefficient particularly for non-structural patch repairs where properties such as high compressive strength are not required.

For non-structural patch repairs it may be possible to use significantly less polymer material as binder in developing a suitable repair mortar. Furthermore, it is not necessary to utilise conventional aggregates that exhibit good mechanical strength in developing non-structural patch repair mixes. Therefore, in identifying new materials for non-structural patch repairs, it is interesting to research into polymer concrete developed by using unconventional aggregates such as those sourced from waste materials. In line with this, the following sections review select studies that have successfully developed polymer concrete mixes by incorporating unconventional materials as aggregate/filler.

2.9.2.1 Epoxy polymer concrete with rubber inclusions

The bonding characteristics of polymer concrete is exceptional however, this mechanism is adversely affected by repetitive temperature changes. Extensive temperature fluctuations lead to cyclic expansion and contraction of the polymer concrete and this can result in bond failure, particularly at the substrate-patch interface. Polymer concrete has between three to four times higher coefficients of thermal expansion relative to cement based concrete (Roh *et al*., 2015). This results in differential deformation between the polymer repair system and the substrate.

Differential deformation is particularly evident with airport runway repairs that are exposed to a range of temperatures combined with enormous impact loads. There is a need to minimise the development of large stresses within the substrate-repair patch interface in harsh environmental conditions. Interlinked research conducted by Jung *et al*. (2015) and Roh *et al*. (2015) has been focused at enhancing the performance of polymer concrete in runway repairs, by looking into the use of ductile materials as inclusions in polymer concrete.

Investigations by Roh *et al*. (2015) looked into the incorporation of silicone and tire waste rubber in an epoxy-based polymer concrete. The control polymer concrete was made-up of aggregate and epoxy resin in the ratio of 80:20 by weight. Mechanical, ductility, shrinkage and bond tests were then performed on specimens containing 3, 5, 8 or 10% by weight of either silicone or tire waste rubber, used to replace coarse aggregate. The mix formulations adopted are summarised in Table 2-11.

From the results of the study the new polymer composites exhibited improved ductility and bond strength. Jung *et al*. (2015) and Roh *et al*. (2015) concluded that rubber can be effectively used in polymer repair mortars for improved compliance in outdoor environment applications such as runways. Such a material could be applied to patch repairs, particularly those exposed to fluctuating temperatures. However, it must be noted that epoxy polymer concrete is expensive and has a higher risk of cracking and debonding.

Table 2-11: Mix formulations of aggregate: epoxy resin: silicone (S) /tyre rubber (T) Roh *et al*. (2015)

Mixing ratio	Density (kg/m^3)
80:17:03 S	1968
80:15:05 S	1940
80:15:05 T	1839
75:20:05 T	1948
72:20:08 T	1958
70:20:10 T	1925
80:20	2004
Cement concrete	2108

2.9.2.2 Polyester resin polymer mortar with GFRP inclusions

A study by Ribeiro *et al*. (2013) investigated into the use of mechanically recycled glass fibre reinforced plastic (GFRP) wastes in the development of polymer mortars. GFRP was added to a siliceous sand mixed with 20% (by weight) content of polyester resin binder. Including GFRP in a polymer mortar and its influence on the compressive, mechanical and flexural properties of the polymer mortar was investigated.

Two size grades of GFRP were used as fillers in the polyester polymer mortar namely, coarse fibrous and fine powdered mixture. In order to establish the optimum content of GFRP additions, amounts (by weight) of 0, 4, 8 and 12% were used. A 1% (by weight) content of silane coupling agent was also used to determine its effect on adherence of the GFRP in the polymer mortar. The polymer to aggregate mix proportions used in this study are summarised in Table 2-12, where FW and CW denote fibrous and coarse waste respectively.

Based on the results of the study it was concluded that the inclusion of GFRP in polymer mortar significantly improves its flexural and compressive strengths. This was irrespective of the amount or size of waste content added and whether the silane coupling agent was used or not. The compressive strength was observed to improve by about 14% from the control strength whereas the flexural strength was observed to improve by about 10%.

Although properties such as compressive and flexural strength are principally not important for non-structural patch repairs, this study advances the possibility of utilising waste materials to successfully develop polymer mortars with improved properties whilst adding to the theme of sustainable material use. Such a polymer mortar could be applied to non-structural patch repairs however, research into the shrinkage, bonding and crack resistance of this material would be necessary.

Table 2-12: Mix formulations adopted by Ribeiro *et al.* (2013)

Trial formulations	GFRP waste type	GFRP waste content[a]	Silane content[b]	Sand content[a]	Resin content[a]
FW0	FW	0%	0%	80%	20%
FW4	FW	4%	0%	76%	20%
FW8	FW	8%	0%	72%	20%
FW12	FW	12%	0%	68%	20%
CW0	CW	0%	0%	80%	20%
CW4	CW	4%	0%	76%	20%
CW8	CW	8%	0%	72%	20%
CW12	CW	12%	0%	68%	20%
FWS0	FW	0%	1%	80%	20%
FWS4	FW	4%	1%	76%	20%
FWS8	FW	8%	1%	72%	20%
FWS12	FW	12%	1%	68%	20%
CWS0	CW	0%	1%	80%	20%
CWS4	CW	4%	1%	76%	20%
CWS8	CW	8%	1%	72%	20%
CWS12	CW	12%	1%	68%	20%

[a] Weight content of total mass.
[b] Weight content of resin mass.

2.9.2.3 Epoxy resin polymer mortar with granulated cork inclusions

Nóvoa *et al*. (2004) looked into the use of cork granules as a filler in a polymer mortar. The study focused on developing a polymer mortar with epoxy resin, a siliceous sand and granulated cork. The binder to total filler/aggregate weight ratio (sand plus cork) was kept constant. The mix formulations used in the study are summarised in Table 2-13. Cork has a significantly low density and stiffness relative to conventional aggregate.

As a result of this Nóvoa *et al*. (2004) expected the inclusion of cork granules in polymer concrete to reduce the material weight and more importantly brittleness. Based on this, the authors aimed to develop a lightweight polymer concrete mix with improved ductility and reduced brittleness.

Table 2-13: Mix proportions of mortar formulations (Nóvoa *et al*., 2004)

Test series		Resin:sand (m/m)	Cork:sand (v/v)	Resin:sand:cork (v/v/v)
A	A-0	20:80	0:100	36.0:64.0:0.0
	A-25		25:75	29.8:52.9:17.3
	A-35		35:65	26.8:47.7:25.5
	A-45		45:55	23.8:42.3:33.9
B	B-0	25:75	0:100	42.8:57.2:0.0
	B-25		25:75	36.1:48.2:15.7
	B-35		35:65	32.8:43.8:23.4
	B-45		45:55	29.4:39.2:31.4

Flexural and compressive tests were performed on specimens containing up to 45% of the aggregate volume as cork content. The study concluded that cork-modified polymer concrete formulations adversely affect the strength and elastic modulus of the composite. However, the inclusion of cork results in a change in mechanical behaviour such that material becomes more ductile with increasing cork content, particularly in compression. This results in less brittle failure of material. Such a material has potential in developing lightweight polymer concrete with improved ductility. The use of cork granules as identified in this study could be adopted in developing a new polymer mortar for non-structural patch repair applications, where any reduction in compressive strength would not be an issue and where a reduction in elastic modulus could actually promote crack resistance.

2.9.2.4 Rubberised bitumen

Bitumen compounds are frequently used for the waterproofing of building features, particularly roofs and joints. Rubberised bitumen emulsions are used as the basis to manufacture such compounds. The viscous bitumen compound is directly applied to the treatment surface, which usually sets within a few hours of application. There are a multitude of proprietary waterproofing bitumen compounds which are usually available in single-pack containers. An important advantage of such materials is that they are typically all-in-one elastic rubberised bitumen systems which do not require separate primers for adhesion. Furthermore, rubberised bitumen compounds have exceptional adhesion and waterproofing properties. Additionally, they have good environmental resilience, application flexibility and they are non-toxic.

Rubberised bitumen compounds could be used for the patch repair of corrosion damaged concrete. It may be possible to mix such a compound with aggregate to develop a repair material that can be effectively used in concrete patch repairs. The polymer nature and excellent bonding characteristics of bitumen will be fundamental in developing a practical repair material. The bitumen compound would serve as the sole binder in the development of a new repair material.

However, research effort is necessary to validate the possibility of utilising bitumen as a patch repair material. Particularly, experimental investigations are crucial to establish the practicality and effectiveness of bitumen use as a binder in patch repair systems. Specifically, it will be important to establish the shrinkage, bonding and crack resistance properties of this material. Furthermore, bitumen compounds are designed to set quickly and hence any mix developed with such a compound may exhibit rapid setting times.

The most important issue to consider with bitumen compounds is its cost relative to cementitious based repair materials. Rubberised bitumen emulsions are specialised waterproofing compounds and as such are expensive relative to typical cementitious based repair materials. Therefore, if bitumen is used as the sole binder in concrete production, it would have to be optimised to minimise its content when designing a bitumen-aggregate mix. Additionally, it must be noted that rubberised bitumen is a messy black compound which cannot be easily removed from skin or clothing. As a consequence of this, supplementary protective clothing would be necessary when handling this material. Furthermore, surface coating would be required to restore the aesthetics of the repaired element.

2.9.3 Alternative material performance requirements

The ConRepNet report has recognised that continued corrosion, cracking and debonding are chiefly responsible for the poor durability performance of concrete repairs. As explained in the literature review, the use of cementitious repair materials are fundamentally responsible for the aforementioned failure modes. Dimensional changes in cementitious materials caused primarily by restrained drying shrinkage leads to crack development and debonding. Subsequently, the chemical composition of cementitious materials develops the risk of steel corrosion such as in carbonated concrete. Furthermore, the cost of specialised cementitious repair mortars is relatively high, especially when such materials are also used for non-structural applications.

In line with the theme of this study the use of alternative materials, including non-cementitious materials that may not be subjected to the same failure mechanisms as cementitious repair materials, may provide a solution to concrete repair durability. However, any new material developed for concrete repairs needs to meet certain basic performance criteria to be practically applied to non-structural patch repairs and provide meaningful durability improvement. The following sections identify specifications that detail what critical characteristics and properties an alternative patch repair material would ideally need to exhibit for effective application to non-structural patch repairs. The specifications identified are aimed at providing a framework upon which appropriate materials can be selected and investigated for use in non-structural patch repair systems.

2.9.3.1 Crack resistance

An ideal repair material developed for non-structural patch repairs primarily needs to resist cracking caused by drying shrinkage. Restrained drying shrinkage is generally accepted to be the most important factor determining long-term durability of patch repair composite members (Beushausen & Alexander, 2006).

Excessive shrinkage has resulted in the premature failure of countless repaired structures around the world and hence, it is being increasingly recognised to be an important design parameter in patch repair systems. The appearance of cracks in patch repairs principally returns the concrete element back to a deteriorated state. This is because cracks cause a range of durability problems including: increasing the penetrability of concrete and therefore, increasing the likelihood of aggressive media ingress, subsequent reinforcement corrosion and alkali silica reaction (Hossain & Weiss, 2004). These durability issues result in increased maintenance costs and ultimately reduces the serviceability lifespan of the structure. Therefore, patch repair resistance to cracking directly relates to their durability and service life performance (Beushausen & Alexander, 2007).

2.9.3.2 Bonding

An ideal repair material needs to adequately bond to the substrate concrete, without the need for additional bonding agents. A good substrate-patch bond will ensure the uniform transfer of stresses and would assist in achieving monolithic behaviour. However, it must be noted that the patch repair material does not need to have a very high bond strength. Bond strength can be low as long as debonding does not occur, since poor bond strength is not necessarily related to the risk of debonding. Numerous conventional patch repairs fail due to stress induced debonding at the substrate-patch interface. Debonding allows aggressive media to easily penetrate into concrete through the new pathways created thereby, restoring it back to a deteriorated state (Lukovic et al. 2012; Beushausen & Alexander 2007).

2.9.3.3 Penetrability

The repair material adopted should ideally provide resistance to the ingress of aggressive media. This is important because if aggressive media can easily flow through the material then the embedded steel is at risk of undergoing reinforcement corrosion. Principally, the repair material should be able to provide protective cover to the steel against the environment and corrosion reactants. This is important to ensure the durability of a repair system, since durability is highly dependent on concrete penetrability and the movement of deleterious substances through a concrete matrix. However, it must be noted that crack resistance of the repair is fundamentally more important than penetrability. This is because cracks in concrete massively outweigh the movement of aggressive media relative to penetrability.

Patch repair materials used for rehabilitating chloride ion damaged concrete would need to exhibit different penetrability requirements relative to carbonation damaged concrete. Carbonation induced corrosion in RC is caused by the reduction in pH of the surrounding concrete due to the reaction of carbonic acid with calcium hydroxide and other hydroxides of silica and alumina present in the concrete matrix. The presence of these hydroxides is an issue associated specifically with cementitious based concrete. Steel that is exposed to carbonation and not embedded in concrete will not necessarily corrode. Therefore, adopting a repair material with sub-standard penetrability properties may probably be applicable for the non-structural patch repair of carbonation damaged concrete. However, steel exposed to chloride ions is prone to corrosion whether embedded in concrete or not.

Therefore, any patch repair material exposed to chlorides certainly needs to fulfil the added function of chloride protection. A repair material with a low penetrability would inhibit the penetration of chloride ions into the concrete thus, prolonging its service-life (Beushausen & Alexander, 2009). This is particularly important for RC structures located in a marine environment or those frequently exposed to de-icing salts.

2.9.3.4 Workability

In order to ensure good contact and proper adhesion between the repair mortar and the substrate concrete, it is important for the repair material to have good workability. Additionally, the material used should be viscous enough to easily fill the exposed cavity created by the removal of deteriorated concrete in the patch repair process. This is essential to ensure that all voids are filled in by the repair material. However, the material must not be too fluid and should be able to bond to a vertical substrate without slumping. Furthermore, it should be practically possible to apply the material on vertical and ideally, overhead surfaces.

2.9.3.5 Setting time

The material selected should not set within a short time-frame nor should it take days to completely set. There must be ample time available to apply the repair patch adequately before any irreversible setting of the material occurs.

2.9.3.6 Aesthetics

A patch repair is typically required to restore the serviceability (aesthetics) of a structure. Therefore, any material selected for a patch repair should not diminish the aesthetics of the structure once applied. However, in cases where the substrate concrete is protected on the surface by paint or cladding then the repair material can also be treated with paint or cladding thereby, allowing it to blend in with the surrounding substrate.

2.10 Summary of literature review

Reinforcement steel corrosion is of great concern with respect to the durability and service life of concrete structures. Steel is naturally protected in sound concrete due to the alkaline nature of the concrete environment that passivates the steel thereby, creating a protective layer against corrosion. However, due to the effects of carbonation and chloride ion attack, the protective layer is damaged eventually leading to corrosion. Corrosion results in the formation of hydrated oxide by-products which have a tendency to swell in volume and result in pressure build up that exerts significant tensile forces within the concrete matrix. If swelling continues and the tensile strength of concrete is exceeded, cracking, delamination and/or spalling occurs.

Steel corrosion in concrete is fundamentally influenced by the ease with which aggressive media can penetrate through concrete up to the embedded steel. The microstructure of concrete is such that the matrix has minute voids and cracks and as a consequence concrete is inherently porous, which paves the way for deleterious media ingress. Additionally, the aforementioned defects caused by corrosion dramatically alter the movement of deleterious substances into a concrete structure which exacerbates ongoing deterioration processes.

Through the mechanisms of permeation, sorption, convection, diffusion, migration and wick action, harmful substances are able to penetrate concrete. The penetrability of concrete is directly related to its durability and service life performance particularly in marine environments and those exposed to de-icing salts where the effects of chloride ion exposure can be severe.

The world's infrastructure in continually aging and as a consequence the market for the repair of corrosion damaged concrete is ever increasing. A significant amount of research has been conducted to develop materials and methods for the repair of deteriorated concrete structures However, the lack of consistency in procedure and application recommended by different suppliers has necessitated the need to develop specific standards for such works and products. The EN 1504 standard has been developed to this end. EN 1504 has been in development for more than a decade and outlines comprehensive specifications and principles for RC condition assessment, repair, rehabilitation and structural strengthening. The EN 1504 standard is of paramount importance in the repair industry and has a significant influence on repair strategies in other non-European countries. One of the most common methods recommended to rehabilitate corrosion damaged concrete is the patch repair procedure. A successful, non-structural patch repair would be one where:

- The repair material does not delaminate from the substrate concrete.
- Cracking is limited and any cracking of the repair material does not impair repair performance with respect to delamination and corrosion.
- Corrosion is prevented in areas around the patch repair.
- Application of the repair material is easy and practical.
- The repair material is aesthetically acceptable.

It must be understood that a patch repair material will only exhibit good long-term durability if a complete repair procedure is implemented correctly. To achieve the above performance requirements, a complete repair process must include the following:

- Treatment of corrosion damaged steel in the patch repair area by cleaning and coating or replacement in severe corrosion cases.
- Substrate surface preparation by thorough cleaning and surface roughening.
- Installation of sacrificial anodes to prevent future corrosion, particularly in the case of chloride contaminated concrete.
- Applying a surface coating once the patch repair has been completed to provide further protection and restore the aesthetics of the structure.

In practice, patch repair systems have very limited performance with respect to long-term durability. The ConRepNet report concluded that up to 50% of all repaired structures assessed had failed prematurely, with 75% failing within the first 10 years of service (Matthews *et al*., 2003). Restrained drying shrinkage induced cracking and/or debonding and post-repair corrosion are the key causes of poor patch repair durability performance. Furthermore, standards typically outline properties required of patch repair materials such as minimum bond and compressive strengths.

However, these are determined in laboratory conditions and therefore, do not relate to those obtained in actual service conditions. Moreover, standards do not specify shrinkage and crack resistance requirements which are effectively more important. One of the major causes of poor concrete repair durability is attributed to the lack of technical understanding of the substrate-patch system. The theme of "compatibility" is frequently mentioned in concrete repair literature and there is significant controversy regarding its meaning and application to concrete repair programmes. Compatibility refers to the balance of material properties between the substrate concrete and a repair material. However, compatibility is impossible to achieve in practice since a relatively fresh patch repair material cannot be made to match the properties of older substrate concrete. Furthermore, there are a vast range of different commercially available repair materials which often exhibit varying properties. This makes it difficult for engineers to select appropriate materials for a patch repair procedure, particularly when suitable standards based on the principles of compatibility are very limited.

Most common concrete repair materials are cementitious based which are inherently brittle. As a consequence such materials are subject to drying shrinkage and under restrained conditions cracking will occur. Furthermore, typical proprietary repair materials boast high performance properties such as high compressive strength and elastic modulus. However such properties are fundamentally not required for non-structural patch repairs and in fact high compressive strength has been shown to increase the risk of cracking (Beushausen & Bester 2016; Chilwesa 2012). Therefore, it is interesting to research into the development of new and unconventional materials for use in non-structural patch repairs with the aim of improving long-term service life performance of patch repaired concrete structures. The use of alternative non-cementitious materials that may not be subjected to the same failure mechanisms as cementitious based repair materials may provide a solution to the widespread failure of concrete repairs.

3 Experimental methods

3.1 Introduction

This chapter details the methods and procedures that were followed to investigate the research topic. The chapter identifies the different materials that were required for the laboratory investigations as well as their properties. All tests were carried out in the civil engineering laboratory at UCT.

3.2 Overview

An overview of the different phases and experimental investigations conducted in this research project are summarised in Figure 3-1. The research presented in this thesis was divided into a number of phases. In phase one a literature review was conducted to develop a framework to understand the underlying principles and issues concerning the research topic. Phase two was directed towards identifying alternative materials for non-structural patch repairs by specifying the performance properties required of such materials and reviewing literature that looked into the development of new concrete materials including non-cementitious ones. Phase three delved into the development and optimisation of the mix designs for the FA, bitumen and polymer materials selected for use in non-structural patch repairs. This was necessary since there was no existing literature (at the time of this study) on the use of these materials for patch repairs particularly, for the bitumen and polymer materials. Phase four of the research project was concentrated on experimentally determining the performance of the FA, bitumen and polymer materials in non-structural patch repairs relative to a control. Lastly, phase 4 and 5 of the research project looked into the analysis of the experimental results in order to draw out conclusions and make recommendations for future studies based on the theme of this research.

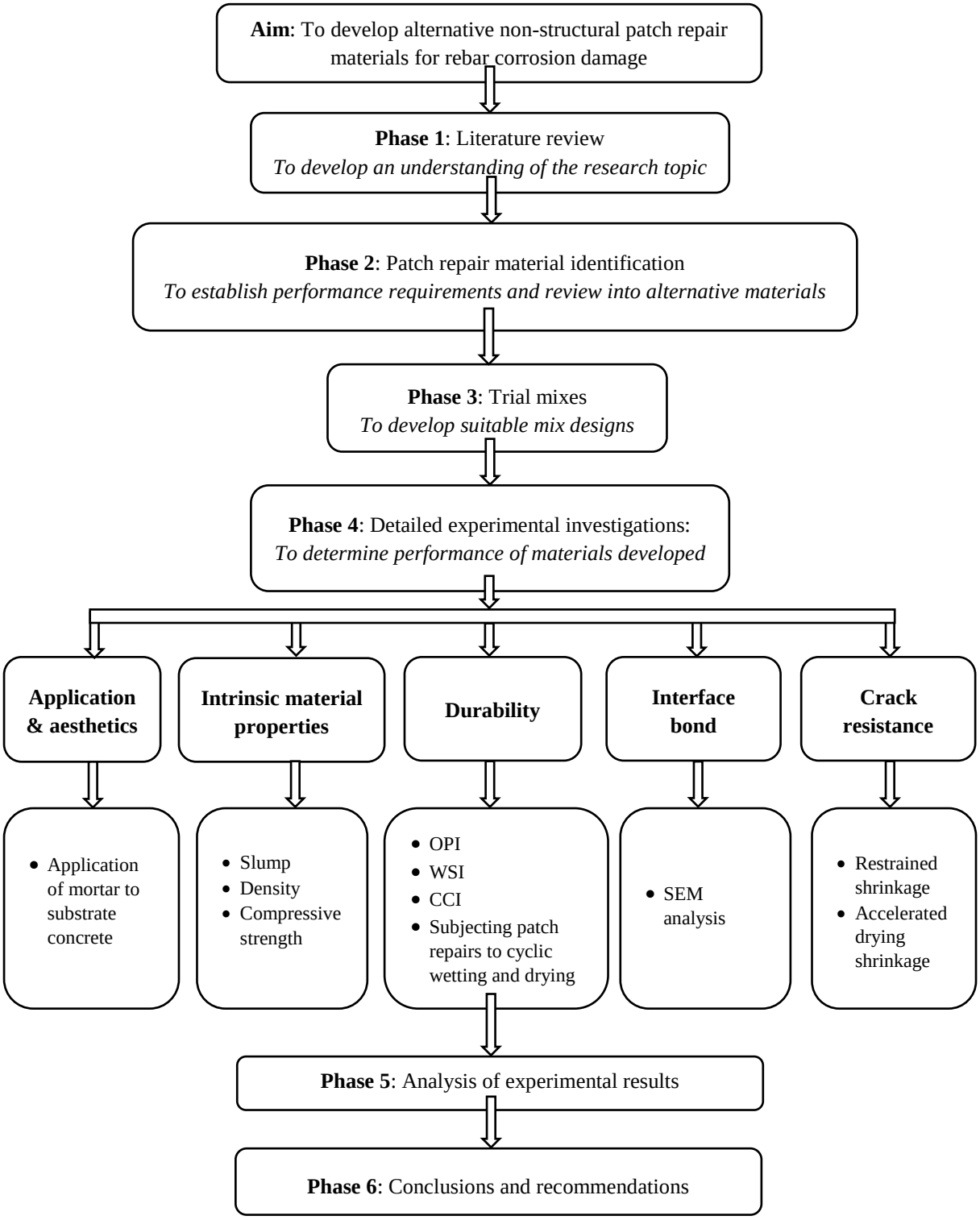

Figure 3-1: Flow chart illustrating structure of research

3.3 Research materials

In order to investigate into the research topic, a number of different materials were required. These were cement, polymer, FA, bitumen, alkaline compound, fine aggregate, coarse aggregate, plasticiser and substrate moulds needed for patching. The materials selected for investigation were based on local availability and the details of the specific materials adopted in this project are outlined in the following sections.

3.3.1 Bitumen

Rubberised bitumen compounds exhibit good adhesion and flexibility properties. Furthermore, these compounds are impermeable and highly resistant to varying temperature conditions (a.b.e.® Construction Chemicals, 2014). They are widely applied to restore waterproofing of roof systems. Rubberised bitumen is an all in one material that comes in ready to use liquid form. Moreover, it is relatively easy to apply and has very fast setting times (a.b.e.® Construction Chemicals 2014; Dalven Products n.d.). A rubberised bitumen compound was selected for study in this dissertation with the aim of incorporating these properties in developing a more durable patch repair material. Particularly, bitumen was selected for its excellent waterproofing and adhesion characteristics in the hope that such a material will limit patch repair debonding and aggressive media ingress.

The bitumen compound used in this study was WaterBloc rubberised waterproofing bitumen compound (RWBC) with a relative density of 1.05. The material was sourced from Dalven Products. RWBC is a mineral filled emulsion of a refined grade of bitumen which contains a high percentage of rubber latex. This compound is specifically used for waterproofing and sealing. Furthermore, the compound is water based that requires no heating or additional processing before use. The compound has the consistency of a soft paste and is thixotropic. RWBC gives a highly elastic bituminous film which is impervious to water after drying. The drying time is between 2-3 hours in a warm outdoor environment. A detailed product sheet of this bitumen is attached under Appendix B1.

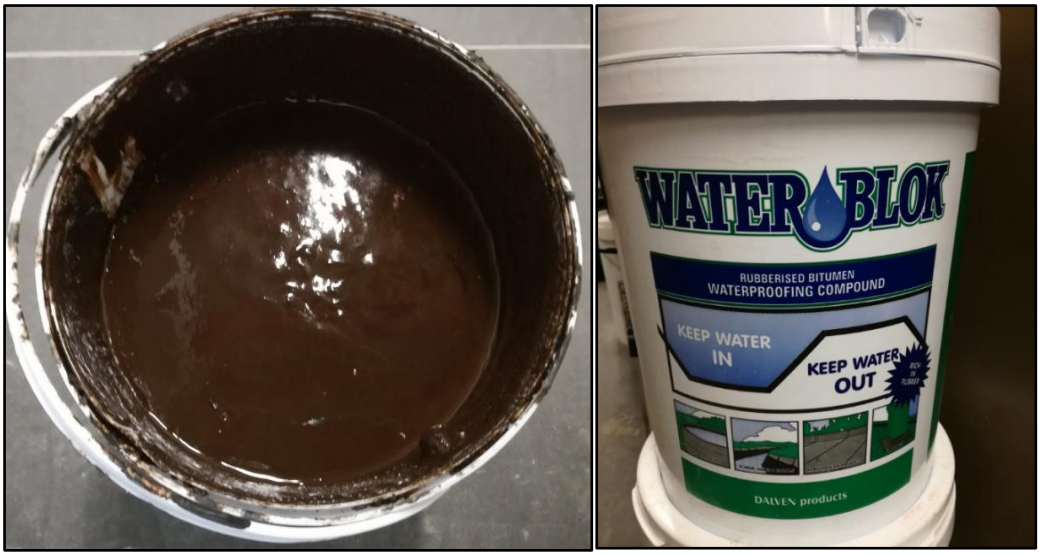

Figure 3-2: Bitumen used for the investigations

3.3.2 Fly ash

High volume FA mixes typically exhibit much lower mechanical strength compared to OPC concrete. However, the development of mechanical strength of FA mixes is slow which could prevent cracking and/or debonding in patch repairs since lower mechanical strength in repair materials has been shown to limit cracking (Beushausen & Bester 2016; Chilwesa 2012). Furthermore numerous studies have successfully developed high volume FA materials with improved properties relative to OPC concrete for example:

- Aloji (2015) identified research on FA that successfully produced a 50% FA concrete with good durability and mechanical properties.
- Cross *et al*. (2008) studied 100% FA mixes and concluded that the material exhibits acceptable durability properties compared to OPC concrete.
- Rivera *et al*. (2015) investigated into the use of up to 80% FA mixes and concluded that high volume FA mixes can exhibit lower penetrability and electrical resistivity compared to OPC concrete.

These studies among many others, have produced promising results with high volume FA materials. Therefore, it is interesting to investigate into the use of high volume FA mixes for the development of non-structural patch repair materials. To this end, FA was selected for study in this dissertation. Class F FA sourced from Lafarge, with a relative density of 2.30 was used in this research project. This class of FA has a very low calcium content (0-6%) and is a pozzolanic material therefore, it will react in the presence of water and calcium hydroxide to form cementitious properties. The class F FA was used to develop the 60%, 80% and 100% FA mixes.

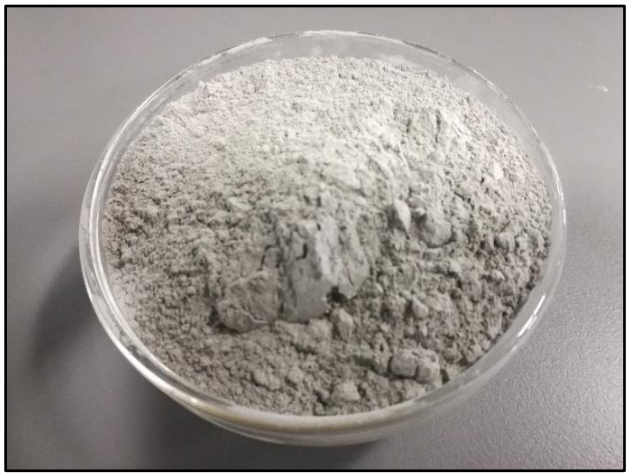

Figure 3-3: Class F fly ash

3.3.3 Polymer

In an effort to develop alternative non-cementitious materials for patch repairs, a polymer was selected for study. Countless polymer based repair materials have been developed and many exhibit a range of properties that can be tailored for specific uses. Polymers are typically used as additives in the production of polymer-cement concrete and as a sole binder in the production of polymer concrete.

Research has identified such concrete to exhibit excellent durability, chemical resistance, fast curing, low penetrability, high strength and bonding properties compared to OPC (Bedi *et al*., 2014). Developing a patch repair material that could exhibit such properties would significantly improve repair durability. Therefore, a polymer was studied in this dissertation with the aim of developing a new repair material with improved bonding and low penetrability.

The polymer used in this research project was a redispersible polymer powder based on a copolymer of vinyl acetate and ethylene as shown in Figure 3-4. The relative density of the material was 0.65. The polymer was sourced from ELOTEX® with the specific product code FX2320. This polymer is a flexible binder that is used for the modification of mortar and plaster systems based on cement with or without hydrated lime. A detailed product sheet of this polymer is attached under Appendix B2. The polymer is mainly used as an admixture where it is used to develop a concrete/mortar with:

- Increased adhesion, especially on expanded polystyrene and extruded polystyrene.
- Increased flexibility and impact resistance.
- Increased cohesion.
- Increased surface abrasion resistance.
- Avoids crack formation.
- Increased long-term performance.

Figure 3-4: Polymer used in the investigations

3.3.4 Coarse aggregate

13 mm Greywacke coarse aggregate was used for all mixes except the substrate mix where 9 mm Greywake was used. Smaller size aggregate was used for the substrate moulds to allow the concrete to properly fill the substrate moulds since they were only 30 mm in thickness. The relative density of the material was 2.75. The compacted bulk density and K factor used in the thesis was 1700 kg/m^3 and 0.8 respectively.

Figure 3-5: Coarse aggregate

3.3.5 Fine aggregate

Cape Flats dune sand and crusher sand was used as fine aggregate in this research project. The crusher sand was only used in the substrate concrete mixes. The relative density of the crusher sand was 2.75, where as that of the dune sand was 2.50. The fineness moduli for the crusher and dune sand were 3.2 and 2.0 respectively. The sands were of good quality.

Figure 3-6: Dune sand

3.3.6 Cement

Surebuild CEM II/B 42.5 N PPC cement with a relative density of 3.14 was used to develop concrete mixes for the substrate moulds, control repair mortars and as an admixture to the polymer-cement concrete mixes. This cement conforms to the 42.5 N strength class of SANS 50197 and is a Portland composite cement with an extender content between 20 and 35%. CEM I 52.5 N OPC cement from PPC was used in the 80% and 60% FA mixes. CEM I contains between 0 and 5% extender content.

Figure 3-7: PPC 42.5 N CEM II cement (left) and CEM I cement (right)

3.3.7 Plasticiser

To obtain the necessary consistency of the different concrete/mortar mixes, CHRYSO Fluid Premia 310 superplasticizer was used. The superplasticizer was added in 5 mL increments using a marked syringe, until good workability was achieved. If a particular mix already had good workability, superplasticizer was not used.

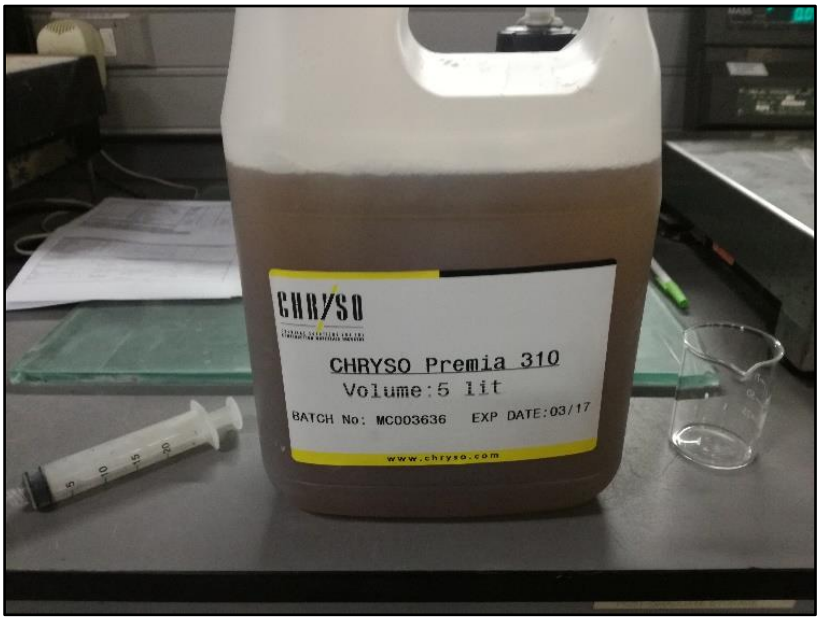

Figure 3-8: Superplasticizer

3.3.8 Calcium hydroxide and sodium hydroxide

Calcium hydroxide and sodium hydroxide was used in the 100% FA mix only, to enable the pozzolanic FA to form calcium silicate hydrate (CSH) compounds.

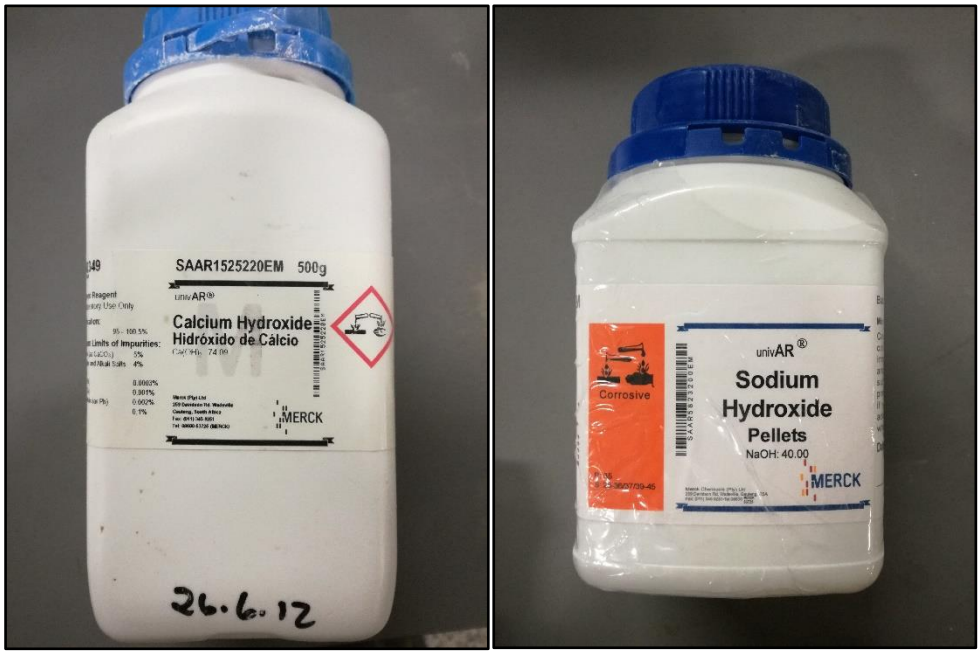

Figure 3-9: Calcium hydroxide and sodium hydroxide

3.3.9 Water

Clean tap water at room temperature (20-25°C) was used in this research project. All containers and measuring cylinders used were cleaned before use to avoid contamination.

3.4 Repair material mix design

3.4.1 Trial mixes

The bitumen, FA and polymer utilised in this research project had not been previously used for non-structural patch repairs and therefore, no prior literature existed with respect to mix design and concrete/mortar preparation procedure. As a consequence, a series of trial mixes were performed with these materials to identify an appropriate mix design that could be practically applied to patch repairs. The objective of performing the trial mixes was to:

- Determine what proportions of fine and coarse aggregate would be required to develop a FA, polymer or bitumen concrete mix for application to patch repairs.
- Determine what w/b ratio would be needed for the mixes.
- Optimize the bitumen and polymer mixes to minimise the amount of binder required.

3.4.1.1 Bitumen

In order to determine a suitable mix design for the bitumen mixes firstly, trial mixes were performed to determine the percentage of binder required to develop a suitable mortar. The bitumen binder content relative to the total mass of repair material required was varied. The different mixes trialled are outlined in Table 3-1. From these trial mixes it was found that 30% (by total mass) bitumen content developed a mortar mix with good workability and sufficient material binding. The mixes with 20% and 25% binder content were found to be very brittle since there was not enough bitumen content for adequate binding.

Table 3-1: Bitumen mortar trial mixes

Binder mass (g)	Binder %	Fine aggregate mass (g)	Fine aggregate %	Total mass (g)
100	50	100	50	200
100	40	150	60	250
100	30	233	70	333
100	25	300	75	400
100	20	400	80	500
100	18	450	82	550

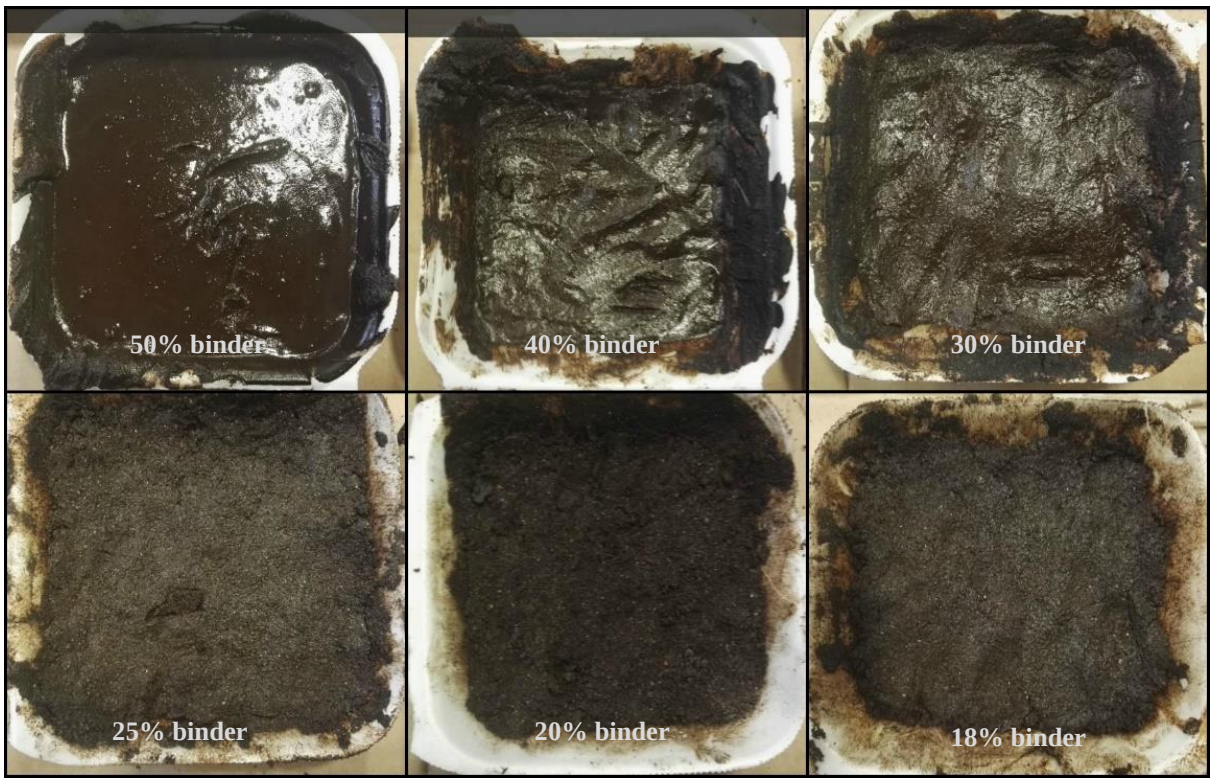

Figure 3-10: Bitumen mortar trial mixes

Next a series of trial mixes were conducted by developing different concrete mixes including fine and coarse aggregate. The mixes were developed using a constant bitumen content of 30% as determined from the first series of trial mixes. The fine aggregate and coarse aggregate contents were varied and the different mixes trialled are outlined in Table 3-2. From these samples it was found that a concrete mix developed using 30% (by total mass) of fine aggregate and 40% (by total mass) of coarse aggregate developed a mix with good workability and sufficient material binding.

Table 3-2: Bitumen concrete trial mixes

Binder mass (g)	Binder %	Fine aggregate mass (g)	Fine aggregate %	Coarse aggregate mass (g)	Coarse aggregate %	Total mass (g)
100	30	233	70	0	0	333
100	30	200	60	33	10	333
100	30	167	50	67	20	333
100	30	133	40	100	30	333
100	30	100	30	133	40	333
100	30	67	20	167	50	333
100	30	0	0	233	70	333

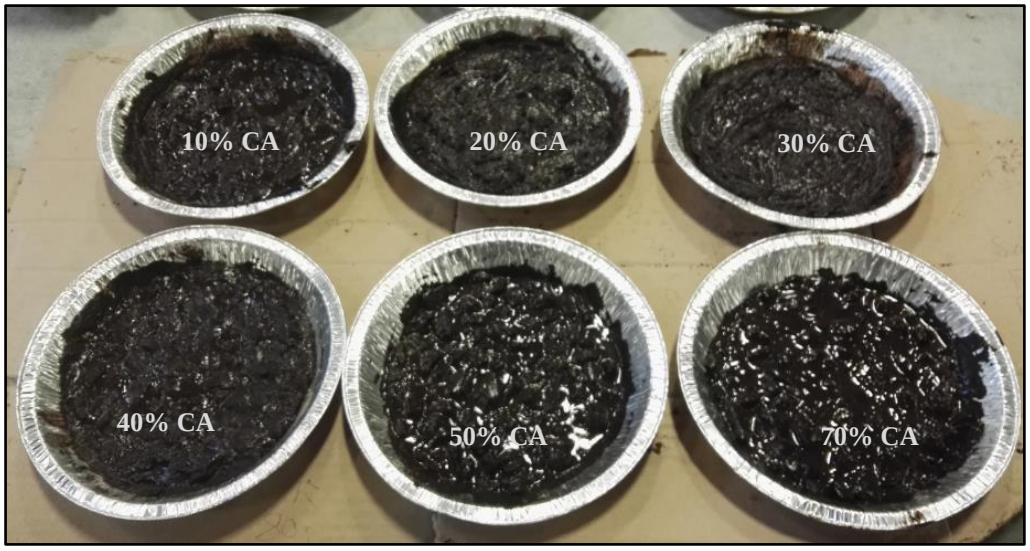

Figure 3-11: Bitumen concrete trial mixes (CA = coarse aggregate)

Based on the bitumen concrete trial mixes, a series of further mixes were lastly conducted to optimise the amount of bitumen used as binder material. This was possible for the bitumen concrete mixes since it was found that these mixes required less binder content relative to the mortar mixes. The different trial mixes conducted to optimise the bitumen content are summarised in Table 3-3. Based on these it was found that a bitumen content of below 16% (by total mass) would not be sufficient to allow for adequate material binding in developing a suitable concrete mix. The minimum binder content required to develop an appropriate bitumen concrete mix was therefore determined to be 18% (by total mass).

Table 3-3: Trial mixes optimising bitumen concrete

Binder mass (g)	Binder %	Fine aggregate mass (g)	Fine aggregate %	Coarse aggregate mass (g)	Coarse aggregate %	Total mass (g)
100	30	100	30	133	40	333
90	28	100	31	133	41	323
82	26	100	32	133	42	315
74	24	100	33	133	43	307
66	22	100	33	133	44	299
58	20	100	34	133	46	291
50	18	100	35	133	47	283
43	16	100	36	133	48	276

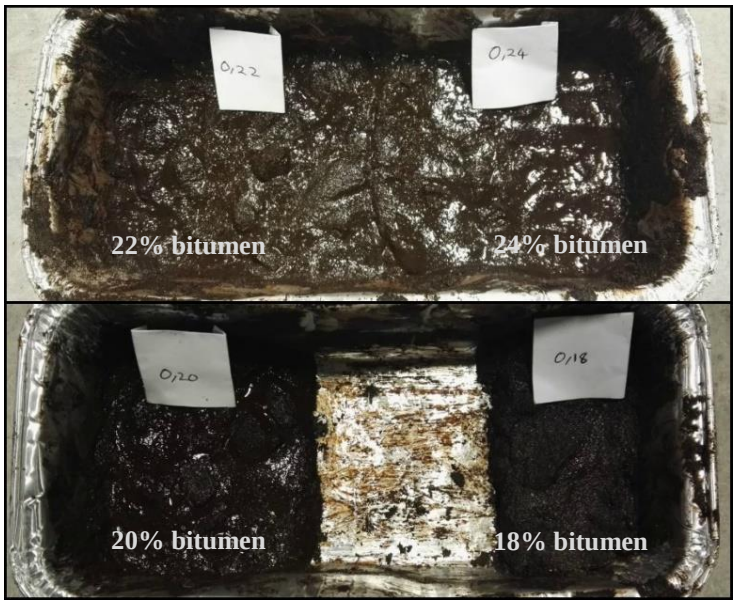

Figure 3-12: Trial mixes optimising bitumen concrete

3.4.1.2 Fly ash

Existing research on the use of class F FA in developing high volume FA mortar (such as 100% FA) is limited. Furthermore, FA sourced from different suppliers around the world would vary considerably, even between different batches from the same supplier. As a consequence, FA trial mixes were conducted to determine what w/b ratio, binder content and aggregate content would be appropriate to develop a suitable FA repair mortar mix. With reference to the control mix design, a total binder content of 550 kg/m^3 was selected and kept constant for all the FA mixes. It was anticipated that this content of FA would be high enough to allow for the production of a mix design with sufficient binder content and therefore, strength. To determine a suitable w/b ratio a series of trial mixes were conducted as summarised in Table 3-4.

The volumetric mix design method was used to determine the fine aggregate content. From these trial mixes a w/b ratio of between 0.40 and 0.50 was found to be suitable to develop a patch repair mortar. Note the class F FA used in the experimental program is a pozzolan. Therefore, this FA possesses little cementitious value on its own. However, in the presence of water and calcium hydroxide it will chemically react to form cementitious compounds. Furthermore, for the 100% FA mix an alkaline activator was needed and therefore, sodium hydroxide was used.

Trial mixes were conducted to establish the proportions of calcium hydroxide and sodium hydroxide needed for the 100% FA mixes as summarised in Table 3-5. Initially a trial mix with 5% (by mass of FA) of both calcium hydroxide and sodium hydroxide was added to the mix design. After setting of this mix, it was found that there was substantial white precipitation on the surface of the material. This was likely excess calcium hydroxide and therefore, another trial mix with 2.5% (by mass of FA) of calcium hydroxide and sodium hydroxide was considered. Finally, to develop a 60% and 80% FA mix, the 100% FA mix design was altered to replace FA content with cement whilst keeping the w/b ratio constant as summarised in Table 3-4. Note no calcium hydroxide or sodium hydroxide was added to the 60% and 80% FA mixes since it was expected that the cement content in these mixes would facilitate a pozzolanic reaction to occur. The final fine aggregate content for the 60% and 80% FA mixes was reduced to 1650 kg/m^3 since a content of 1969 kg/m^3 was identified to be too high as it resulted in very dry mortar mix.

Table 3-4: 100% FA trial mixes to determine w/b ratio

Binder mass (g)	Water mass (g)	w/b	Fine aggregate mass (g)
550	220	0.40	1969
550	250	0.45	1969
550	275	0.50	1969
550	330	0.60	1969

Table 3-5: 100% FA trial mixes to determine content of calcium hydroxide and sodium hydroxide

Binder mass (g)	Water mass (g)	w/b ratio	Fine aggregate mass (g)	Calcium hydroxide mass (g)	Calcium hydroxide %	Sodium hydroxide mass (g)	Sodium hydroxide %	Binder mass (g)
550	250	0.45	1969	0	0	0	0	550
550	250	0.45	1969	27.5	5.0	27.5	5.0	550
550	250	0.45	1969	13.8	2.5	13.8	2.5	550

Table 3-6: 60% and 80% FA trial mixes

FA mix	FA mass (g)	Cement mass (g)	Water mass (g)	w/b	Fine aggregate mass (g)	Calcium hydroxide mass (g)	Calcium hydroxide %	Sodium hydroxide mass (g)	Sodium hydroxide %
100% FA	550	0	250	0.45	1969	13.8	2.5	13.8	2.5
80% FA	440	110	250	0.45	1650	0	0	0	0
60% FA	330	220	250	0.45	1650	0	0	0	0

Figure 3-13: FA trial mixes

3.4.1.3 Polymer and polymer-cement concrete

In order to develop a suitable mix design for the polymer material, as series of trial mixes were firstly conducted to determine the amount of binder content (by percentage of total mass) required to develop a suitable mortar mix. From the initial trials it was found that the w/b ratio of one was very high. Therefore, further trials were performed using the same binder and filler contents as outlined in Table 3-7 but by using w/b ratios of 0.5, 0.6 and 0.8. From these trials it was found that a w/b ratio of 0.5 and 0.6 was the optimum amount required to develop a suitable polymer mortar mix.

Table 3-7: Polymer mortar trial mixes

Water mass (g)	Water %	w/b ratio	Binder mass (g)	Binder %	Fine aggregate mass (g)	Filler %	Total mass (g)
100	33.3	1	100	33.3	100	33.3	300
100	25.0	1	100	25.0	200	50.0	400
100	20.0	1	100	20.0	300	60.0	500
100	14.3	1	100	14.3	500	71.4	700
100	12.5	1	100	12.5	600	75.0	800
100	11.1	1	100	11.1	700	77.8	900
100	10.0	1	100	10.0	800	80.0	1000
100	9.1	1	100	9.1	900	81.8	1100
100	8.3	1	100	8.3	1000	83.3	1200

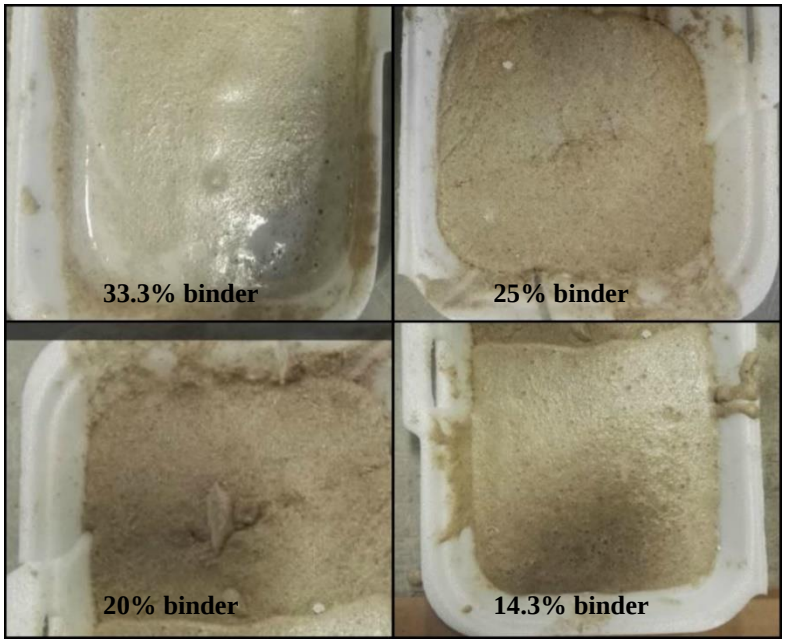

Figure 3-14: Polymer mortar trial mixes

Next a series of trial mixes as outlined in Table 3-8 were performed to determine the proportions of fine and coarse aggregate required to develop a suitable polymer concrete mix. Based on the results of these trials is was established that a fine aggregate content of 30.3% (by total mass) and a coarse aggregate content of 45.5% (by total mass) developed a concrete mix with good workability and adequate binding of the filler materials. Therefore, this mix was selected for further analysis.

Table 3-8: Polymer concrete trial mixes

Water mass (g)	Water %	w/b ratio	Binder mass (g)	Binder %	Fine aggregate mass (g)	Fine aggregate %	Coarse aggregate mass (g)	Coarse aggregate %	Total mass (g)
60	9.1	0.6	100	15.2	500	75.8	0	0.0	660
60	9.1	0.6	100	15.2	400	60.6	100	15.2	660
60	9.1	0.6	100	15.2	300	45.5	200	30.3	660
60	9.1	0.6	100	15.2	200	30.3	300	45.5	660
60	9.1	0.6	100	15.2	100	15.2	400	60.6	660
60	9.1	0.6	100	15.2	0	0	500	75.8	660

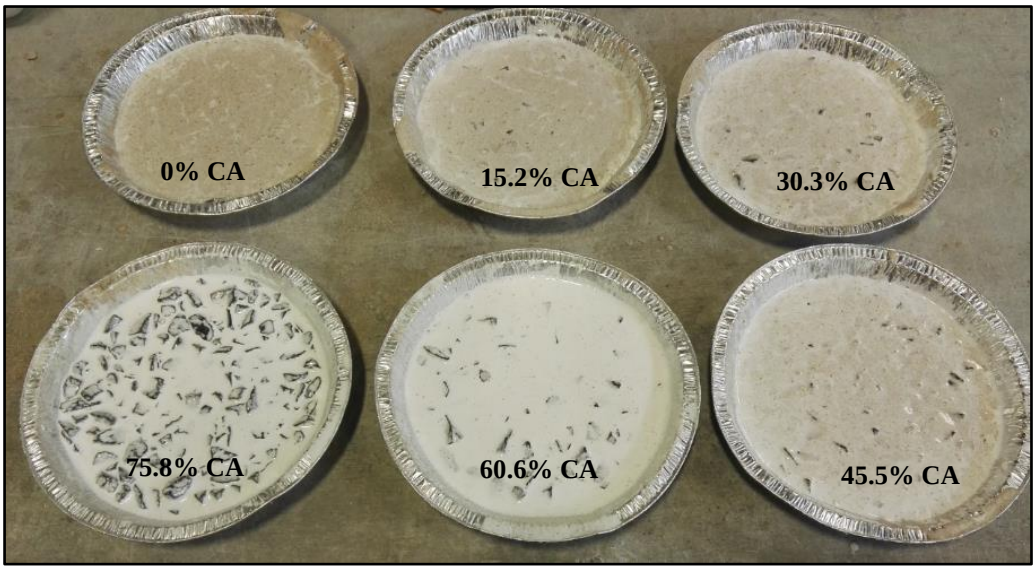

Figure 3-15: Polymer concrete trial mixes (CA = coarse aggregate)

Based on the results of the polymer concrete trial mixes, further trials were conducted to optimise the water content. This was done to minimise the amount of water required in the mixes since the polymer concrete mixes were found to take a considerable amount of time to fully set. Varying w/b ratios of 0.3, 0.4, 0.5 and 0.6 were used. It was found that to develop a polymer concrete mix with good workability, a w/b ratio of 0.5 or 0.6 was needed. Lastly, a series of trials were performed to optimise the amount of binder content in the polymer concrete mixes. This was necessary to minimise the quantity of polymer used as binder. The different optimising trial mixes developed are outlined in Table 3-9. From these trials it was identified that a binder content below 7% (by total mass) was too low to allow for adequate binding of the filler materials.

Table 3-9: Trial mixes optimising polymer concrete

Water mass (g)	Water %	w/b ratio	Binder mass (g)	Binder %	Fine aggregate mass (g)	Fine aggregate %	Coarse aggregate mass (g)	Coarse aggregate %	Total mass (g)
30	9.1	0.6	50	15.2	100	30.3	150	45.5	330
24	7.6	0.6	40	12.7	100	31.8	150	47.8	314
18	6.0	0.6	30	10.1	100	33.6	150	50.3	298
12	4.3	0.6	20	7.1	100	35.5	150	53.2	282
9	3.3	0.6	15	5.5	100	36.5	150	54.7	274
6	2.3	0.6	10	3.8	100	37.6	150	56.4	266

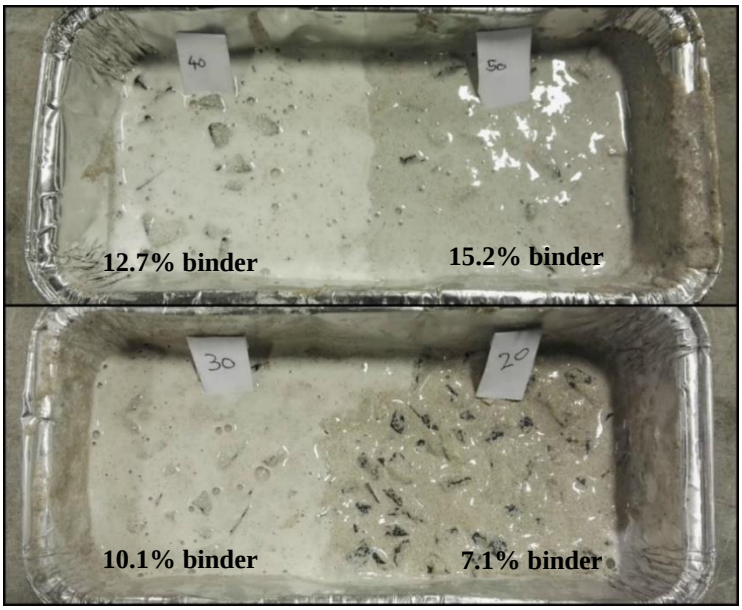

Figure 3-16: Trial mixes optimising polymer concrete

The polymer concrete mixes developed in this research project were all found to have very long setting times. Concrete cubes cast with 8% (by total mass) polymer were found to be still wet internally when demoulded after 28 days. After 28 days, the polymer concrete cubes had set only to a depth of about 2 cm from the face exposed to the atmosphere. The underlying reason behind this was that the polymer used in this research project did not chemically react with the water in the mix, unlike cement. Therefore, for the polymer concrete mixes to set, water had to be completely removed through evaporation. However, water could not effectively evaporate from the standard 100 x 100 x 100 mm cube moulds as they are designed to hold in water, which is otherwise needed for OPC concrete. As a consequence, the polymer concrete mixes could not be effectively analysed following the standards developed for OPC based concrete, particularly with respect to compressive strength testing. In order to develop a polymer concrete mix with a reasonable setting time, further trial mixes were performed by replacing an 8% polymer concrete mix with some OPC cement as an extender effectively creating a polymer-cement concrete.

Cement chemically reacts with water and therefore would effectively remove some of the water from the polymer concrete mixes. The different trial mixes performed for the polymer-cement concrete mixes are outlined in Table 3-10. A constant 8% polymer concrete mix was used for the analysis. Cement was added to the different mixes in replacement amounts of between 0-25% by mass of total binder. The polymer-cement concrete mixes all exhibited much shorter setting times as expected.

Table 3-10: Polymer-cement concrete trial mixes

w/b	Total binder mass (g)	Total binder %	Polymer mass (g)	Cement mass (g)	Cement %	Sand mass (g)	Stone mass (g)	Total mass (g)
0,6	192	8	192	0	0	840	1253	2400
0,6	192	8	182.4	9.6	5	840	1253	2400
0,6	192	8	172.8	19.2	10	840	1253	2400
0,6	192	8	163.2	28.8	15	840	1253	2400
0,6	192	8	153.6	38.4	20	840	1253	2400
0,6	192	8	144	48	25	840	1253	2400

Figure 3-17: Polymer-cement concrete trial cubes (100 mm cubes)

3.4.2 Mix designs developed

The following sections outline the mix designs selected for the FA, bitumen and polymer-cement concrete materials based on the results of the trial mixes. These mixes were adopted for further detailed experimental investigations.

3.4.2.1 Bitumen

The mix designs selected for the bitumen mixes are outlined in Table 3-11.

Table 3-11: Mix design used for the bitumen repair mix

Material	18% bitumen mix	20% bitumen mix	22% bitumen mix
Bitumen binder (kg/m^3)	373	404	437
Fine aggregate - dune sand (kg/m^3)	729	696	661
Coarse aggregate – 13 mm greywacke (kg/m^3)	971	927	881

3.4.2.2 Fly ash

The mix design developed for the 100%, 80% and 60% FA repair mortar is outlined in Table 3-12.

Table 3-12: Fly ash repair mortar mix designs

Material	100% FA mix	80% FA mix	60% FA mix
Fly ash (kg/m^3)	432	388	299
Cement - CEM I 52.5 N (kg/m^3)	0	97	200
Calcium hydroxide (by mass of fly ash)	2.5%	0	0
Sodium hydroxide (by mass of fly ash)	2.5%	0	0
Water (kg/m^3)	194	218	225
Fine aggregate - dune sand (kg/m^3)	1545	1455	1455
Superplasticizer (ml/m^3)	238	0	0
w/b ratio	0.45	0.45	0.45
Average density (kg/m^3)	1901	2106	2121
28 day compressive strength (MPa)	1.5	8.0	17.4

3.4.2.3 Polymer and polymer-cement concrete

The mix designs developed for the polymer concrete and polymer-cement concrete mixes are outlined in Table 3-13.

Table 3-13: Polymer and polymer-cement concrete mix designs

Material (kg/m^3)	8% Polymer concrete mix	9% Polymer concrete mix	10% Polymer concrete mix	8% Polymer-cement concrete mix (5% cement)
Polymer binder (kg/m^3)	160	174	188	153
Cement - CEM II 42.5N (kg/m^3)	0	0	0	8
Fine aggregate - dune sand (kg/m^3)	696	664	632	703
Coarse aggregate – 13 mm greywacke (kg/m^3)	1044	996	948	1055
Water (kg/m^3)	96	105	113	97
w/b ratio	0.60	0.60	0.60	0.60
28 day compressive strength (MPa)	N/A	N/A	N/A	1.4

3.4.2.4 Control

The mix design adopted for the control repair mortar is outlined in Table 3-14. The mix design was selected with reference to the works of Beushausen & Chilwesa (2013).

Table 3-14: Control mortar mix design

Material	Quantity
Cement - CEM II 42.5 N (kg/m^3)	540
Water (kg/m^3)	243
Fine aggregate - dune sand (kg/m^3)	1462
Superplasticizer (ml/m^3)	66
w/b ratio	0.45
Density (kg/m^3)	2132
28 day compressive strength (average MPa)	45.1

3.5 Repair material mixing procedure

3.5.1 Bitumen

The mixing procedure adopted for the bitumen repair concrete was as follows:

- The coarse and fine aggregate was thoroughly mixed by hand in a bucket. A mechanical mixer was not used to avoid contamination of the mixer.
- After the dry mixing, the bitumen was added and mixed further.

3.5.2 Fly ash

The mixing procedure adopted for the 100% FA repair mortar was as follows:

- FA was mixed mechanically with the calcium hydroxide powder.
- The sodium hydroxide pellets were dissolved in the required water content.
- The fine aggregate was mixed with FA containing calcium hydroxide powder (dry mix).
- Water with dissolved sodium hydroxide was added and all the constituents thoroughly mixed.

The mixing procedure adopted for the 60% and 80% FA repair mortar was as follows:

- FA was mixed with the fine aggregate (dry mix).
- Cement replacement was added and dry mixed.
- The required amount of water was then added and further mixed mechanically.

3.5.3 Polymer and polymer-cement concrete

The mixing procedure adopted for the polymer and polymer-cement repair concrete was as follows:

- The polymer powder was first added to the mechanical mixer.

- The required water content was added next.
- The polymer and water was thoroughly mixed until a uniform paste with minimum lumps formed.

Figure 3-18: Mechanically mixing polymer with water

- Cement was then added to the paste for the polymer-cement concrete mix only.
- After a well-mixed polymer paste formed, the coarse and fine aggregate was added and further mixed in the mechanical mixer.

Figure 3-19: Polymer-cement concrete repair material after mixing

3.6 Experimental tests

3.6.1 Ease of application and aesthetics

3.6.1.1 Substrate moulds

With respect to the theme of this research project it was paramount to experimentally investigate into the ease and process of application of the selected repair materials to non-structural patch repairs as well as the aesthetics of a repaired element. These tests were essential to determine the practicality of using the repair materials developed. To test the application of the new repair materials on patch repairs, custom concrete moulds were manufactured to mimic a typical substrate. A characteristic substrate requiring a patch repair would have all deteriorated concrete removed from the vicinity of the corroded steel, creating a cavity with exposed steel. Therefore, to manufacture concrete elements representative of such substrates, special wooden moulds were developed to make concrete slabs as shown in Figure 3-20.

Figure 3-20: Wooden mould used to cast substrate concrete slabs (with styrofoam insert to create the cavity for mortar application)

The dimensions (in mm) of the concrete mould developed are outlined in Figure 3-21. To develop the cavity that would resemble a characteristic substrate with exposed reinforcing steel bars, styrofoam was used. As shown in Figure 3-22, steel bars were embedded into the styrofoam which was then placed in the wooden moulds.

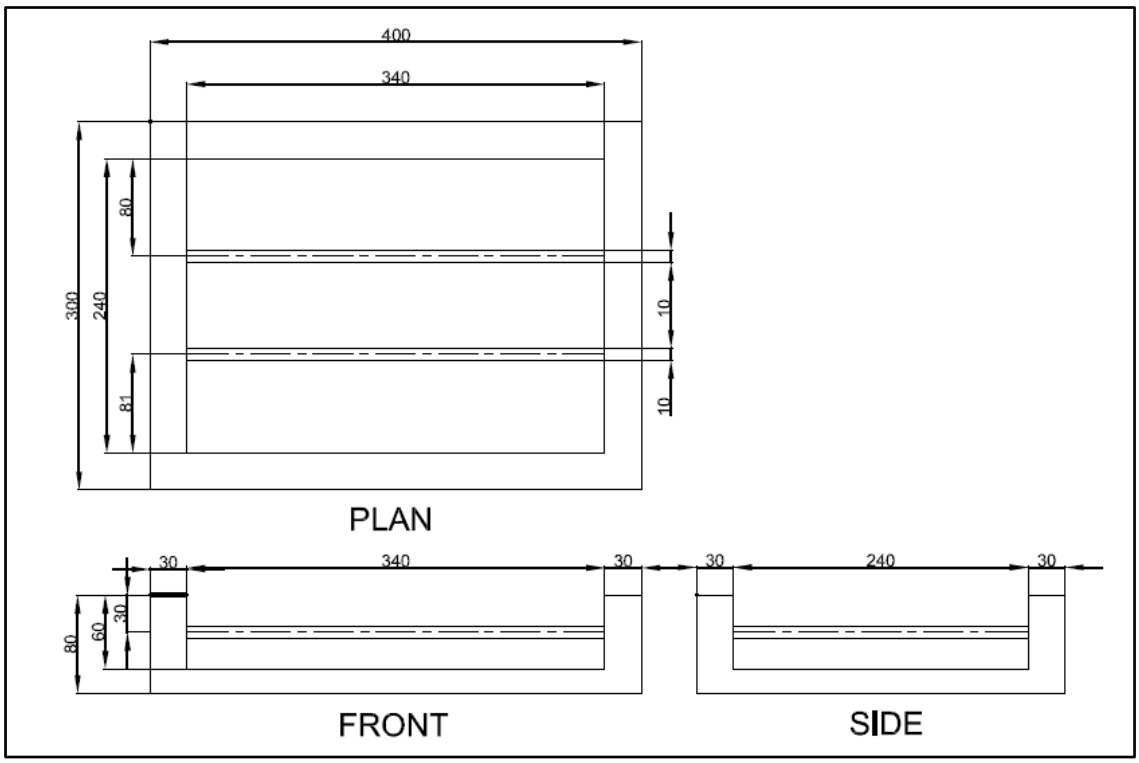

Figure 3-21: Dimensions (in mm) of the concrete mould developed

Figure 3-22: Styrofoam with embedded 10 mm diameter steel bars

The styrofoam was removed after the concrete set thereby exposing the steel bars. It must be noted that the steel bars used to develop the concrete substrate moulds were new and corrosion-free. This was because the scope of the research conducted was focused on developing new patch repair materials without considering their effect on the embedded steel reinforcement with respect to corrosion. The steps followed in developing the substrate concrete moulds prior to patch repair is outlined as follows:

- The wooden moulds were prepared by securing all the bolts and coating the moulds with oil to allow the easy removal of the concrete after setting.
- Styrofoam blocks with embedded steel were inserted into the wooden moulds using spacers to ensure the correct positioning of the styrofoam. The styrofoam was secured in position with the help of four nails which were driven into the base of the wooden moulds.
- Concrete with a mix design outlined in Table 3-15 was then poured into the mould. The method used in developing the mix design was the volumetric mix design method, typically used in South Africa, as recommended by the Cement and Concrete Institute (C&CI). A high strength mix design was used to ensure that the exposed steel bars would remain intact and that substrate moulds would not damage with handling whilst conducting the experimental investigations.

Table 3-15: Substrate concrete mix design

Material	Quantity (kg/m^3)
Cement (CEM II 42.5N)	543
Water	217
Fine aggregate (crusher sand and dune sand)	702
Coarse aggregate (9.2 mm Greywacke)	906
w/b ratio	0.40
Average density (kg/m^3)	2422
28 Day Compressive strength (MPa)	62.6

- The mould filled with concrete was placed on a mechanical vibrator to allow for good compaction and to remove excess air voids. However, it must be noted that the moulds were vibrated for up to 30 seconds only to ensure that the styrofoam would not rise up, which would otherwise allow concrete to flow underneath.
- The moulds were covered with a plastic sheet and allowed to set under normal room conditions; i.e. 21 ± 1°C and 59 ± 5% RH (Beushausen & Bester, 2016) for 24 hours.
- The concrete samples were demoulded after 24 hours and the styrofoam was manually removed with a scraper thereby, exposing the embedded steel bars.
- The first batch of moulds used for the cyclic testing were cured under room conditions. However, the second batch used for the patch repairs under room condition analysis were cured in a water bath for 7 days.
- All moulds were then placed in an oven at 50°C for 7 days, to allow for accelerated drying shrinkage.
- The moulds were sandblasted to roughen the substrate and increase its bonding surface area. In order to develop uniform surface roughness on each mould, it was ensured that the height of the machine from the substrate and time of sandblasting was kept constant.
- The concrete substrate moulds were thoroughly cleaned with water and pressurised air to remove any loose sand and debris left behind from the sandblasting. The moulds were then left to dry prior to applying the patch repair material.

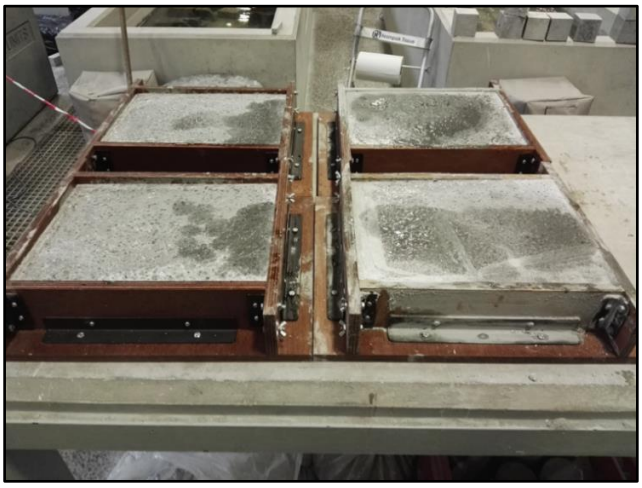

Figure 3-23: Cast substrate moulds

Figure 3-24: Sandblasted substrates

3.6.1.2 Patch repairs

Two patch repair substrates were cast for each of the five different repair materials. One was left for observation under room conditions and the other was used for cyclic wetting and drying conditioning. Whilst applying the patch repair material to the substrate moulds, the process and ease of application of the repair material was determined. The procedure adopted in applying the repair material to the substrate mould was as follows:

- The substrate moulds were thoroughly cleaned with a brush and pressurised air to remove any dust and loose material. The substrate moulds were not saturated before casting the repair mixes.
- The substrate mould was placed horizontally on a level surface.
- The patch repair material was mixed and manually applied to the substrate mould until the repair material was flush with the upper face of the mould. Note, the substrate mould was not subjected to mechanical compaction as this would not be done on site.
- The patch repair material was levelled off at the surface with a trowel.

3.6.2 Material properties

3.6.2.1 Workability

In order to determine the workability and consistency of the repair materials selected, the slump test was conducted. The test was conducted on the different repair materials in accordance to SANS 5862-1.

3.6.2.2 Compressive strength

Compressive strength tests were conducted to characterise the different repair materials developed. Compressive strength tests for all the repair materials was conducted on 100 x 100 x 100 mm standard cubes. The cubes were cast and covered with plastic for 24 hours. Three cubes were tested for each repair material at 7, 14, 28 and 60 days to monitor the strength development of the different materials. The testing was done with reference to SANS 5863 (2006) using an Amsler compression test machine.

The dimensions and weight of all cubes were measured prior to testing. For the control repair mix, the cubes were demoulded after 24 hours and then inserted into a water bath at 22 ± 2.0°C for wet curing prior to testing. The polymer-cement concrete cubes were demoulded after two days because these cubes had not yet set sufficiently after one day. They were then left to set under normal room conditions prior to testing. The polymer-cement concrete cubes were not subjected to any further curing. This was because unlike ordinary concrete, the polymer-cement concrete mix required water to completely evaporate for the repair material to achieve full strength. For the 60% and 80% FA mixes, the cubes were demoulded after 24 hours and left to set under normal room conditions for one day. This was necessary because these FA mixes had not completely set after 24 hours. Followed by this, the 60% and 80% FA cubes were allowed to cure in a water bath at 22 ± 2.0°C prior to testing. Lastly, the 100% FA repair cubes were demoulded after two days since they had not fully set after 24 hours however, even after two days the 100% FA samples were still slightly wet.

These cubes were then left under room conditions prior to compressive strength testing and no wet curing was adopted. The 100% FA mixes were observed to be very soft and brittle after demoulding. As a result of this, they were not subjected to wet curing in a water bath since these cubes would likely disintegrate if submerged in water.

3.6.2.3 Density

In order to establish the density of the different repair materials developed, 100 x 100 x 100 mm cubes were cast. The dimensions and weight of these cubes were measured and used to calculate the density of the repair materials. The average density of the 12 cubes used for the compressive strength testing (7, 14, 28 and 60 days) were used to determine the density of the repair materials.

3.6.3 Durability

3.6.3.1 Cyclic wetting and drying

One patch repaired substrate mould for each of the five different repair materials was left for observation under normal room conditions. The development of any debonding and/or surface cracking on the moulds was observed for 56 days (8 weeks). Additionally, one repaired substrate mould for each of the five different repair materials was subjected to cyclic wetting and drying conditions. Cyclic testing was done to identify the effect of cyclic conditioning on the repaired element with respect to cracking and/or debonding (i.e. durability). The substrate moulds were left for 24 hours in a controlled environmental room at 30 ± 2.0°C and a relative humidity of 30 ± 4% for the drying cycle as shown in Figure 3-25. The moulds were then removed and placed for 24 hours in a water bath at 22 ± 2.0°C for the wetting cycle. After 24 hours, the moulds were removed from the water bath and surface dried with a paper towel. The drying cycle was then repeated. The wetting and drying cycles were conducted for 56 days i.e. 28 cycles.

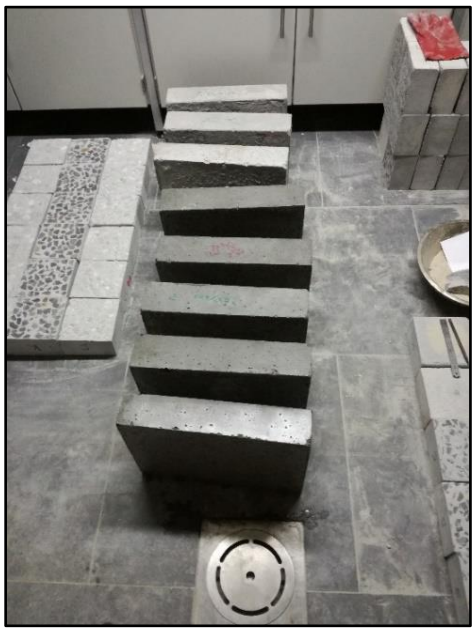

Figure 3-25: Substrate moulds left for drying in the control room

3.6.3.2 Oxygen permeability index (OPI) test

In order to establish the permeability of the different repair materials, which can be related to the resistance against ingress of deleterious substances, OPI tests were conducted. OPI tests measure the pressure decay of oxygen passed through a test specimen placed in a falling head permeameter. OPI values usually range from 8.5 to 10.5 and a higher value points to improved durability due to a higher impermeability. It must be noted that OPI is measured on a log scale and therefore, the difference between 8.5 and 10.5 is significant (Alexander & Beushausen, 2008). The tests were conducted as specified in the Durability Index Testing Procedure Manual (2010) developed at UCT.

It must be noted that the OPI test was specifically developed for concrete. Therefore, OPI testing of the polymer-cement concrete may not provide a true measure of the actual permeability of this material. Nevertheless, the OPI test was conducted on the polymer-cement concrete to provide a permeability reference relative to the control. Coring of the polymer-cement concrete cube samples was found to be difficult since this mix was still soft inside the cube even after 28 days.

As a consequence, the coring equipment combined with the running water was found to be too aggressive to core the polymer-cement concrete cubes since they would completely disintegrate as shown in Figure 3-26 (a). Therefore, the cubes were first cut into 25 mm thick sections and these were then allowed to dry in an oven at 50 ± 2°C for 7 days. After 7 days drying coring was done and intact samples were produced as shown in Figure 3-26 (b). These were then dried for a further 7 days prior to durability index testing. The coring equipment utilised in the research is depicted in Figure 3-27. The setup of a test specimen within the OPI test equipment is illustrated in Figure 3-28.

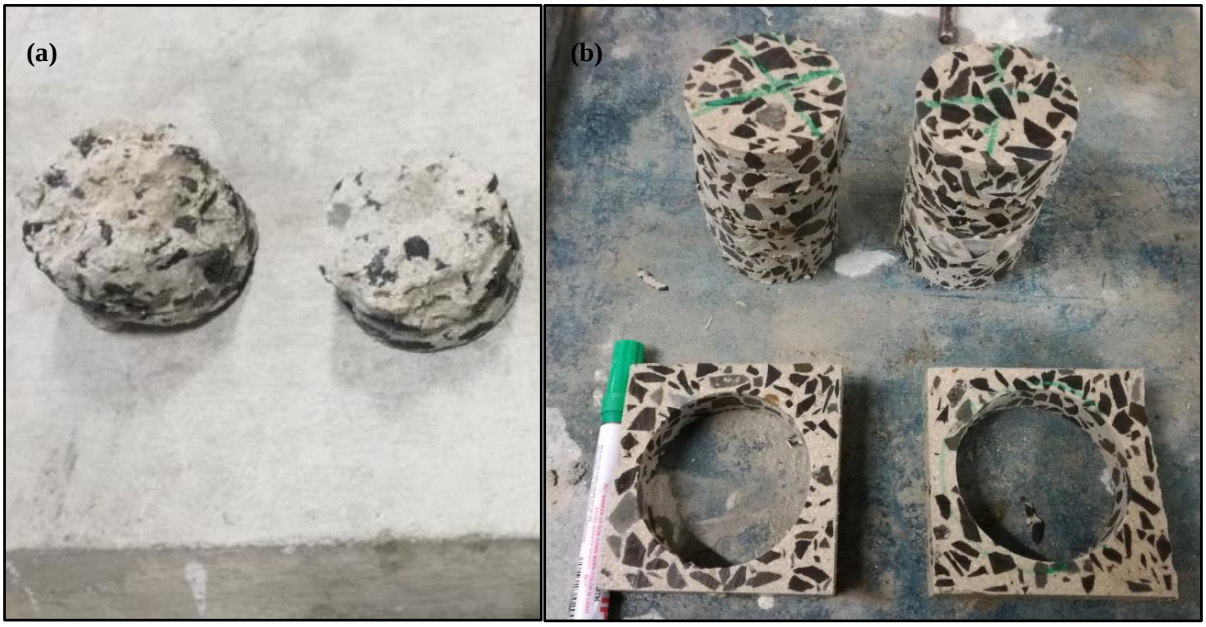

Figure 3-26: (a) Disintegrated polymer-cement concrete cores and (b) cores from 25 mm sections

Figure 3-27: Coring equipment

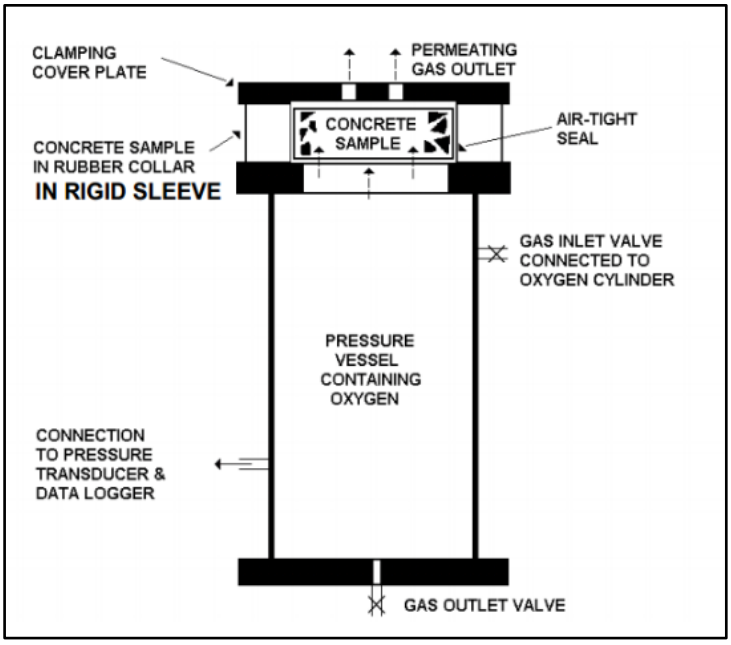

Figure 3-28: Oxygen permeability test specimen setup

3.6.3.3 Water sorptivity (WSI) test

In order to establish the durability of the different repair materials with respect to the rate at which they absorb water, water sorptivity tests were conducted. The water sorptivity tests were conducted as specified in the Durability Index Testing Procedure Manual (2010). The same test specimens from the OPI tests were used for the sorptivity test immediately after removing the test specimens from the OPI apparatus. It must be noted that the WSI test was specifically developed for concrete. Therefore, WSI testing of the polymer-cement concrete may not provide a true measure of the actual sorptivity of this material. Nevertheless, the WSI test was conducted on the polymer-cement concrete to provide a sorptivity reference relative to the control. The test equipment utilised for the WSI tests is displayed in Figure 3-29 and Figure 3-30.

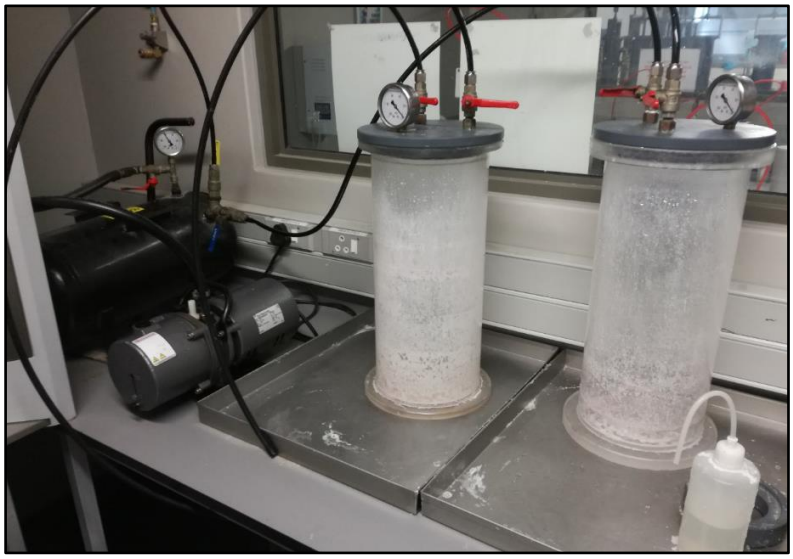

Figure 3-29: Vacuum saturation facility

Figure 3-30: Water sorptivity test apparatus

3.6.3.4 Chloride conductivity (CCI) test

In order to determine durability with respect to resistance to chloride ingress of the different repair materials developed, chloride conductivity tests were conducted. The tests were carried out in accordance to the Durability Index Testing Manual (2010) developed at UCT. However, it must be noted that the CCI test was specifically developed for concrete and therefore, it is unsuitable for testing polymer-cement concrete as there is no known relationship between conductivity of a polymer-cement concrete matrix and chloride ingress. OPI and sorptivity tests, in contrast, measure a physical property related to porosity and pore connectivity, which arguably can be used to characterise the polymer-cement concrete. Figure 3-31 displays the chloride conductivity test apparatus. A schematic illustration of the chloride conductivity test setup is illustrated in Figure 3-32.

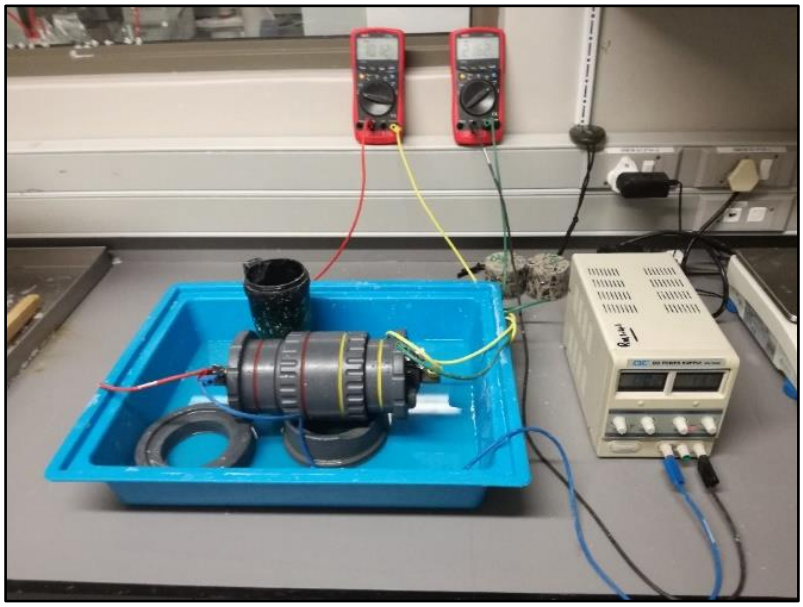

Figure 3-31: Chloride conductivity test apparatus

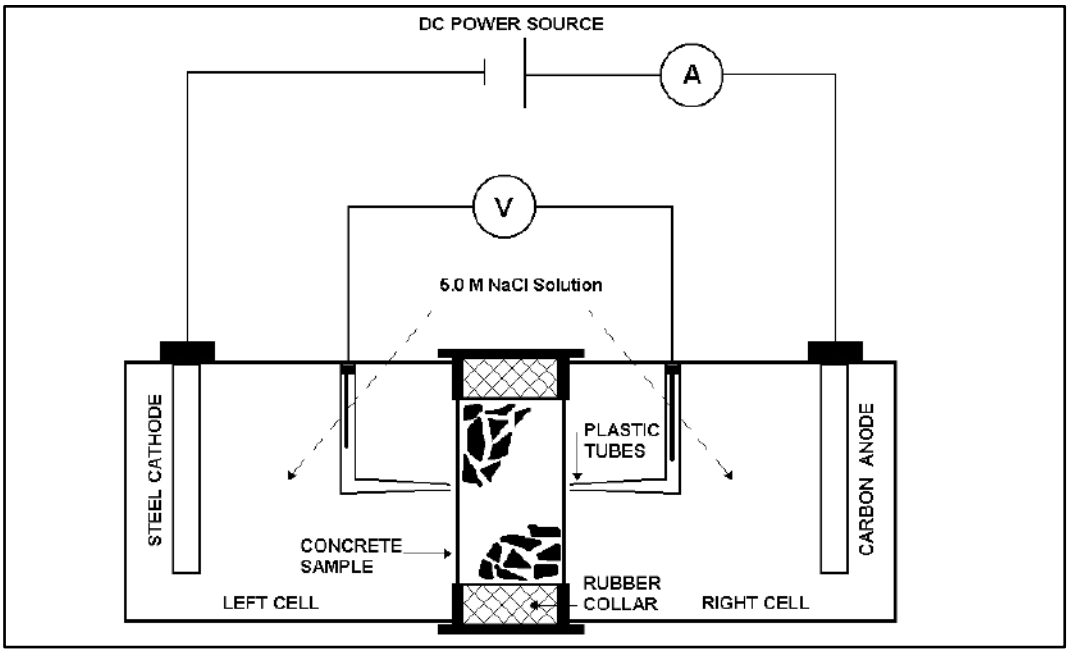

Figure 3-32: Schematic of chloride conductivity test apparatus

3.6.4 Crack resistance

3.6.4.1 Restrained shrinkage - ring test

The ring test was conducted to determine the cracking potential of the different repair materials studied in this dissertation. The ASTM C1581 standard was followed in conducting the ring tests however, a crack meter was used for measuring crack width instead of the recommended strain gauge. The dimensions of the mould used for developing the test samples for restrained shrinkage analysis is outlined in Table 3-16 and Figure 3-33. The dimensions of the mould used varied slightly from that stipulated in the ASTM C1581 standard due to the availability of the laboratory equipment.

Table 3-16: Dimensions of ring test mould (Bester, 2015)

Dimension	Symbol	Value (mm)
Inner diameter of mortar annulus	D_{IM}	323.8
Outer diameter of mortar annulus	D_{OM}	400
Thickness of inner steel ring	T_{IS}	12.7
Thickness of outer steel ring	T_{OS}	3.0
Height of inner/outer steel rings	h	155

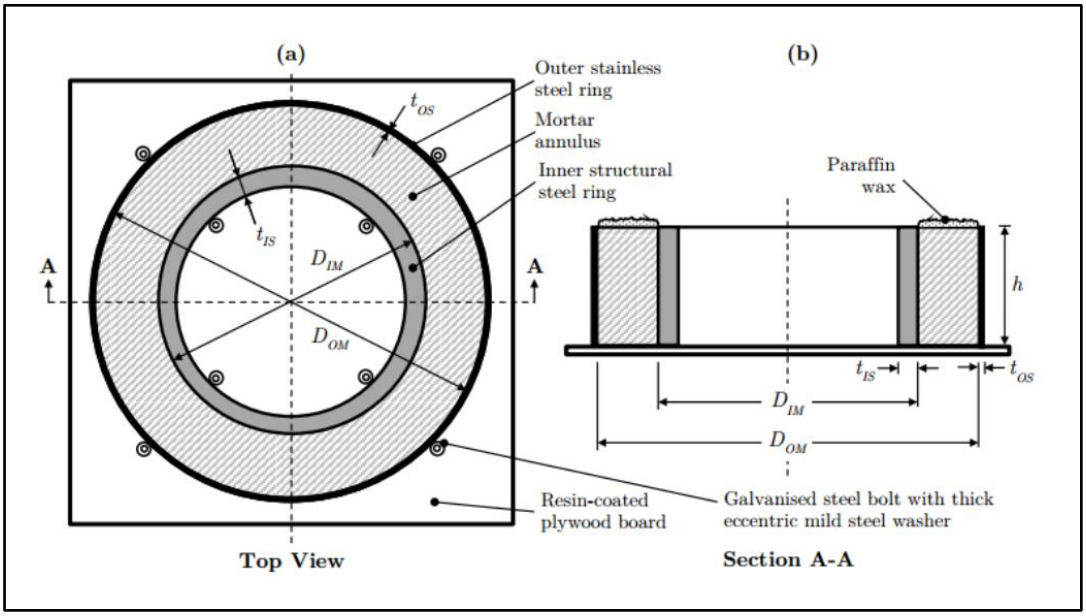

Figure 3-33: Dimensions of ring test mould (Bester, 2015)

The mould was assembled as shown in Figure 3-34. Spacers were used to ensure that a uniform diameter was maintained and that the inner and outer rings of the mould were properly aligned. Silicon glue was applied on the outer perimeters of the inner and outer rings to minimise bleeding. The silicon was allowed to dry for at least 24 hours prior to casting. The outer ring was coated with oil prior to casting to allow for easy demoulding. This was particularly important for the polymer-cement concrete as this mix was very sticky.

Figure 3-34: Assembled ring test mould

The control test specimens were demoulded after 24 hours. They were then marked and placed in a control room at 23.0 ± 2.0°C and a relative humidity of 50 ± 4%. The control specimens were subjected to moist curing for 7 days using wet hessian as shown in Figure 3-35 (a). After the curing period, the samples were coated on the top surface with paraffin wax as shown in Figure 3-35 (b). This was done to minimise moisture loss and to ensure that only circumferential drying took place.

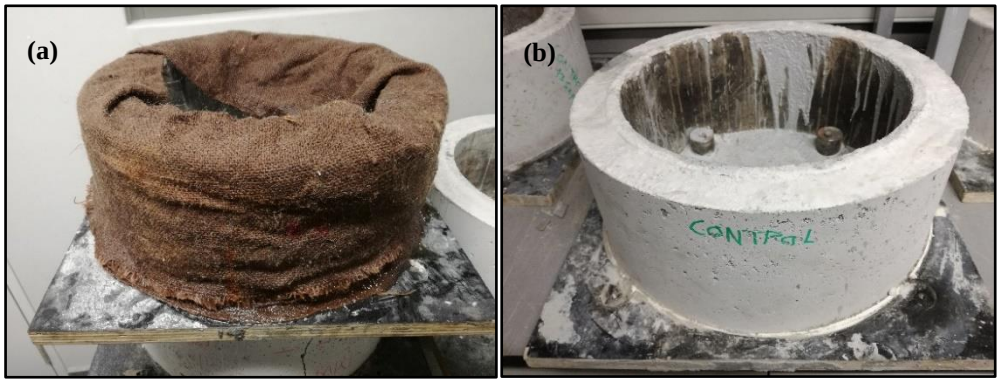

Figure 3-35: (a) Wet hessian moist curing and (b) waxed test specimen

The 60% and 80% FA mixes were demoulded after 24 hours and allowed to set for a further 24 hours under normal room conditions. This was necessary since these mixes were found to be still wet with demoulding after 24 hours. The specimens were then placed in the control room as for the control and allowed to cure for 7 days using wet hessian. The specimens were finally coated with paraffin wax and left for observation. All ring specimens were observed daily for the appearance of any cracks. Observations were further continued for up to 28 days after the first cracks appeared before recording the number of cracks and crack widths.

The 100% FA specimens were demoulded after one day and allowed to set for a further 24 hours. They were then placed in the control room and allowed to set. A wet curing regime was not adopted for the 100% FA specimens since these specimens were found to be very soft and brittle. Hence any moist curing would likely cause disintegration of the matrix. The polymer-cement concrete ring specimens were demoulded after 7 days. This was necessary to allow ample time for the matrix to set. However, after 7 days the samples were still found to be wet since the mould would not allow water to sufficiently evaporate which is required for the polymer-cement concrete to gain strength. The samples were then coated with paraffin wax and left for observation. Wet curing was not adopted for this repair material because unlike ordinary cement based concrete, polymer-cement concrete required water to be completely lost to gain strength rather than be retained.

3.6.4.2 Accelerated drying shrinkage test

In order to determine the shrinkage potential of the different repair materials, accelerated drying shrinkage tests were conducted on 100 x 100 x 200 mm prisms in accordance to SANS 6085 (2006). The equipment used in measuring the strains is depicted in Figure 3-36. Three samples were tested for each repair material and were prepared as shown in Figure 3-37.

Figure 3-36: Strain extensometer

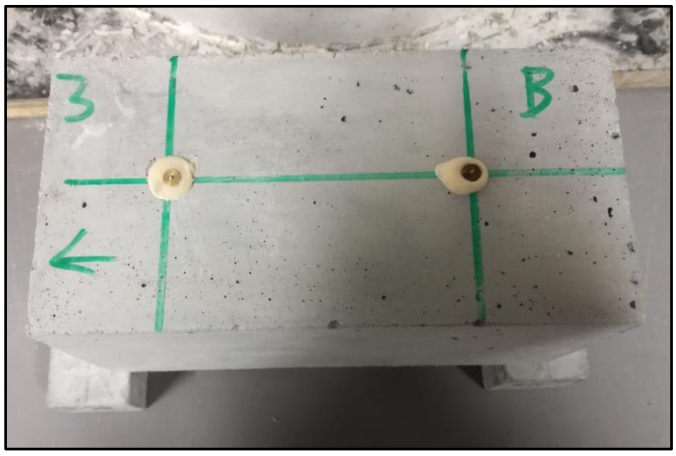

Figure 3-37: Accelerated drying shrinkage test prism

It must be noted that the accelerated drying shrinkage test was specifically developed for concrete. Therefore, accelerated drying shrinkage testing of the polymer-cement concrete may not provide a true measure of the actual shrinkage potential of this material. Nevertheless, the test was conducted on the polymer-cement concrete to provide a shrinkage reference relative to the control.

The control specimens were prepared and cured with reference to SANS 6085 (2006). They were demoulded after 24 hours and allowed to cure in a water bath at 22 ± 2.0°C prior to testing. The polymer-cement concrete specimens were demoulded after two days and allowed to set under normal room conditions for 7 days prior to testing. The 60% and 80% FA prisms were demoulded after 24 hours and allowed to set for one day under normal room conditions. They were then allowed to cure in a water bath at 22 ± 2.0°C prior to testing. The 100% FA prisms were demoulded after two days and allowed to set under normal room conditions. No wet curing was adopted for the 100% FA prior to testing. No formal standards exist to characterise shrinkage values and therefore the guidelines outlined in Table 3-17, which are based on typical shrinkage results, were used (CoMSIRU, 2016).

Table 3-17: Characterisation of accelerated drying shrinkage results

Shrinkage value (m)	Characterisation
< 350 x 10^{-6}	Low shrinkage
350 – 550 x 10^{-6}	Moderate shrinkage
>550 x 10^{-6}	High shrinkage

3.6.5 Interface bond - microscopic (SEM) test

Microscopic analysis was conducted on the different repair materials to investigate into the bond characteristics between the patch repair material and the substrate concrete. Material specimens were cored from the patch repair moulds. 70 ± 2 mm diameter cores were taken and these were cut into 8 ± 2 mm discs. The cores were taken from a corner of the patch repair mould as shown in Figure 3-38.

Figure 3-38: Core for SEM taken from corner of substrate mould

The prepared discs were then sent to the Centre for Minerals Research at the chemical engineering department of UCT for SEM sample preparation. The samples were prepared through the following process (Nkemba, 2016):

- The material specimens were further cored from the 70 ± 2 mm diameter and 8 ± 2 mm thickness discs and cut to fit into 30 mm diameter moulds. It was ensured that the samples were less than 20 mm in height. Sawing was done to achieve this.
- The moulds were labelled and lubricated. The material specimens were then inserted into the moulds.
- The moulds were placed under vacuum for 5 minutes before adding resin to cover the samples and a further 5 minutes after.
- The samples were then placed in an oven to cure overnight at 30ºC.

- Polishing was done in a series of grinding and polishing steps until a 1 µm polish was achieved. The samples were carefully rinsed and lightly soaped between each grinding and polishing step.
- Next, the samples were placed in an ultrasonic bath for about 10 minutes and cleaned after with ethanol.
- The samples were finally allowed to dry in an oven at 30ºC for a minimum of 1 hr. The specimens were then ready for SEM analysis as depicted in Figure 3-39.

Figure 3-39: Prepared samples for SEM analysis

The prepared samples were taken to the Centre for Imaging and Analysis at UCT for SEM imaging. The samples were coated with a thin film of carbon and a strip of silver for conductivity. Carbon tape was used to fasten the samples to the equipment. Multiple microscopic images were then taken along the bond interface of the different repair materials. These images were analysed for bond integrity, debonding and bond failure characteristics. The SEM test equipment used for imaging is depicted in Figure 3-40.

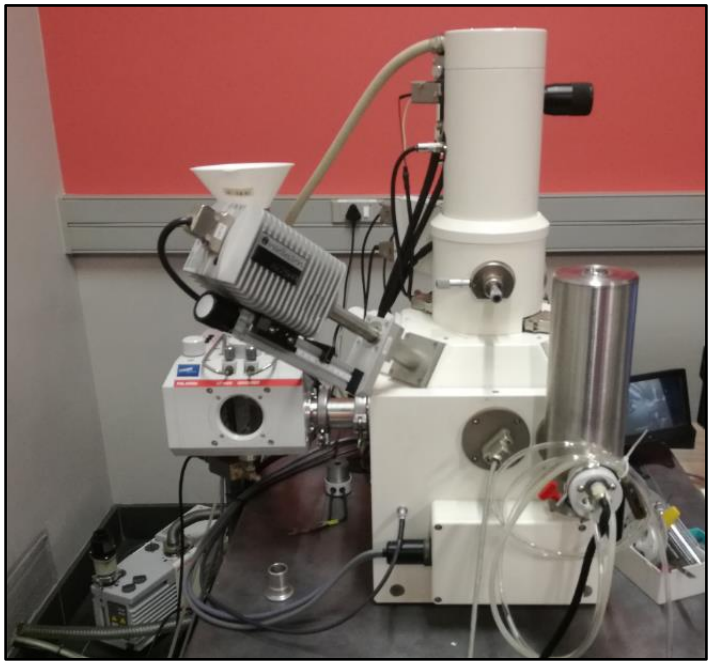

Figure 3-40: SEM test equipment

4 Results and discussions

This chapter presents the results from the laboratory investigations, accompanied by an analysis and on the key findings. The analysis is supplemented by critical discussions that look into the validation of the results obtained and considering the possible reasons for the trends and relationships developed.

4.1 Ease of application and aesthetics

4.1.1 Bitumen

Three substrate moulds were patched with the 18%, 20% and 22% bitumen mixes developed. Application of the bitumen repair material to the substrate mould was fairly easy however, it must be noted that the bitumen repair material is very messy and proper protective clothing including gloves is necessary when handling this material. Furthermore, cleaning of hands and equipment after application of the bitumen material was problematic and a cleaning solvent was required. The nature and dark brown colour of the bitumen material as shown in Figure 4-1 meant that contamination of the repaired structure would be unavoidable. Therefore, special treatment including the application of surface paint would be necessary to restore the aesthetics of a structure repaired with this material.

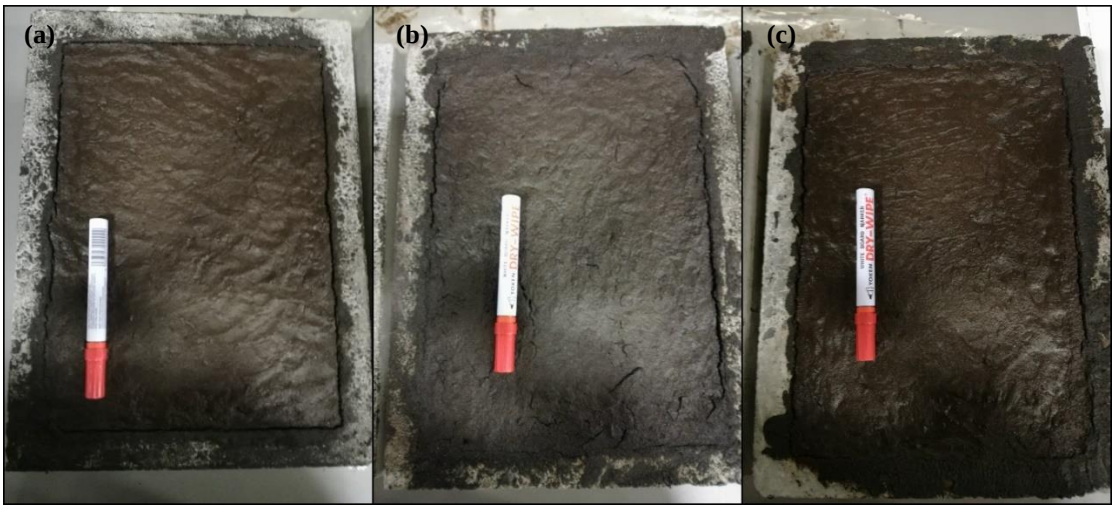

Figure 4-1: (a) 18%, (b) 20% and (c) 22% bitumen patch repairs

After application of the bitumen patch repair, the substrate moulds were left under normal room conditions for observation. The moulds were not subjected to any curing process such as covering with plastic because unlike concrete, bitumen requires water to fully evaporate to achieve full strength. The moulds were inspected after a day and it was observed that the material had set well. However, as displayed in Figure 4-2, after only three days of observation there was excessive shrinkage cracking and debonding clearly visible on all three bitumen moulds. The cracks were more than 5 mm in width and as a consequence the bitumen material was concluded to be completely unsuitable for use as a practical patch repair material. Therefore, no further experimental investigations were conducted using the bitumen material developed.

Figure 4-2: Excessive cracking and debonding occurrence on bitumen patch repairs

4.1.2 FA

Application of the 100%, 80% and 60% FA patch repair mortars to the substrate moulds was straightforward since the mortars developed had good workability and had similar consistencies to OPC based mortar. Furthermore, the aesthetics of a finished FA patch repair was comparable to the appearance of the control as shown in Figure 4-3. This meant that no special treatment would be needed to restore the aesthetics of a structure repaired using the FA material. Handling of the FA repair material as well as the cleaning of equipment and hands was done with relative ease unlike the bitumen and polymer materials.

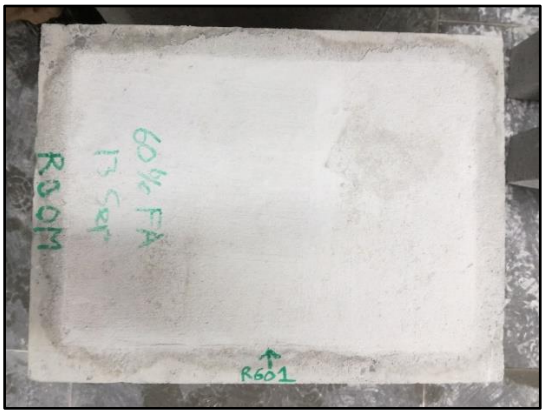

Figure 4-3: Appearance of FA patch repair

4.1.3 Polymer-cement concrete

Application of the polymer-cement concrete to the substrate moulds was problematic. The very sticky nature of this material made it difficult to work with. Particularly, it was difficult to properly finish off the surface of the patch repair since the material would easily stick to the trowel. Cleaning of hands and equipment after application of the polymer-cement concrete was done with relative ease since the polymer binder could be removed easily with water.

Similarly to the polymer-cement concrete, application of the polymer concrete repair material to the substrate moulds was also problematic due to the very sticky nature of the polymer binding material. The polymer-cement concrete repair material developed a good finished appearance with a smooth surface as shown in Figure 4-4. However, the unique light brown colour of the polymer-cement concrete material may necessitate the application of surface paint to restore prior aesthetics of a repaired element.

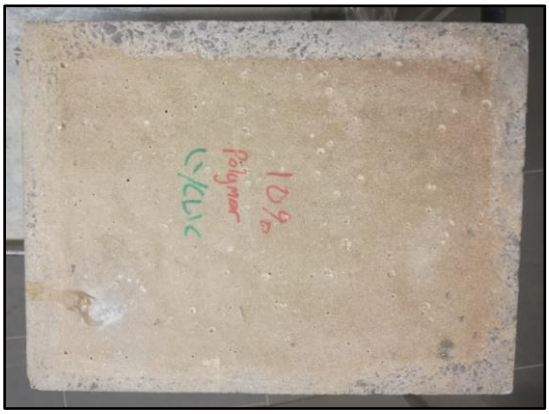

Figure 4-4: Appearance of polymer-cement concrete patch repair

4.2 Material properties

4.2.1 Workability

Slump tests were carried out on the different materials to give an indication of the workability of these materials, particularly for the polymer-cement concrete mix developed for which no prior studies exist. The results of the slump tests are summarised in Figure 4-5. The 60%, 80% and 100% FA mixes all had true slump shapes. The 60% FA mix had a slump of 25 mm which would have a very low workability. A slump of 25 mm is classified as a dry mix according to the EN 206-1 standard. A low slump would be favourable particularly in vertical and overhead patch repairs. The 80% and 100% FA mixes had slumps of 65 mm and 45 mm respectively. These are classified as standard slump values according to the EN 206-1 standard. The control repair mortar had a slump of 35 mm. This slump value indicates that the concrete mix was a dry mix and would have low a workability. The slump shape was observed to be a true slump with no collapse or shearing of the material.

The slump of the polymer-cement concrete was found to be 260 mm which was very high. The polymer-cement concrete slumped completely and therefore, the slump type was a collapse slump as seen in Figure 4-6. According to the EN 206-1 standard the slump is categorised as a self-levelling slump. This type of slump indicates that the mix was too wet and would have a high workability. A material with a high slump would usually be more workable however, the converse was observed with the polymer-cement concrete. Even though this mix had a high slump value, the material was not easy to work with. A considerable amount of effort was needed to scoop the material from the mixer and place it into the concrete substrates. This was likely due to the very adhesive nature of the fresh polymer-cement concrete and rapid evaporation of surface moisture that caused quick setting of the polymer-cement concrete on the surface.

This meant that more exertion was need to collect and place a sample of material from the mixer. Furthermore, the sticky nature of this material meant that a patch repair could not be levelled off using a trowel since the polymer-cement concrete material would stick to the underside and cause unevenness. However, self-levelling of this material was adequately achieved due to the high slump value.

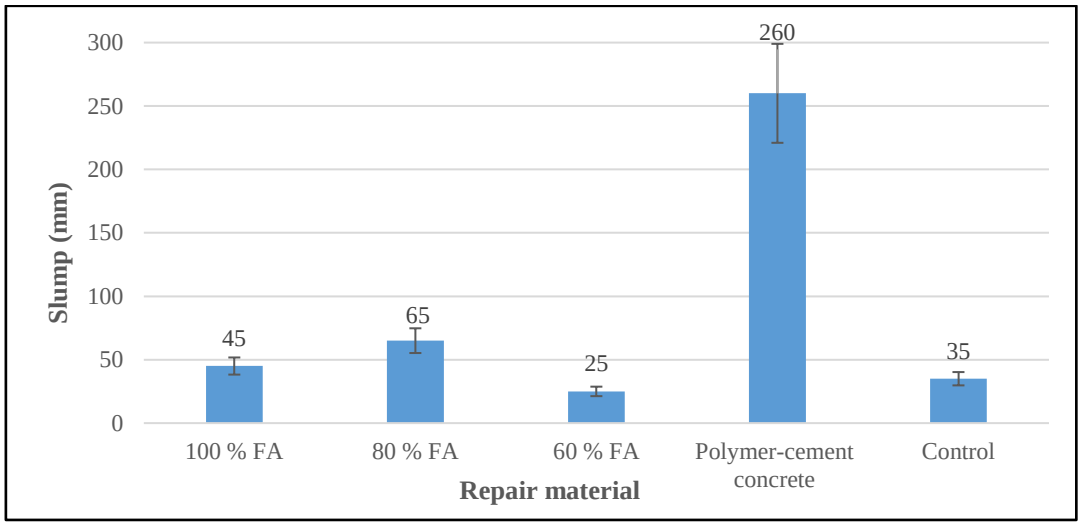

Figure 4-5: Slump test results

Figure 4-6: Repair material slumps

4.2.2 Compressive strength

Figure 4-7 summarises the results of the compressive strength tests carried out on the five different repair materials. All the materials tested had significantly lower compressive strengths relative to the control. The 60% FA material had a 28 day compressive strength of 17.4 MPa whereas the 80% FA and 100% FA specimens had low strengths of 8.0 MPa and 1.5 MPa respectively. Furthermore, the 60% FA and 80% FA specimens developed strength continuously over a 60 day period. After 60 days the 60% FA material had a compressive strength of 21.5 MPa, whereas the 80% FA material had a strength of 14.2 MPa. However, this trend was not observed with the 100% FA material. The difference between the 7 day compressive strength and 60 day compressive strength was only 0.4 MPa implying that there was effectively no strength gained.

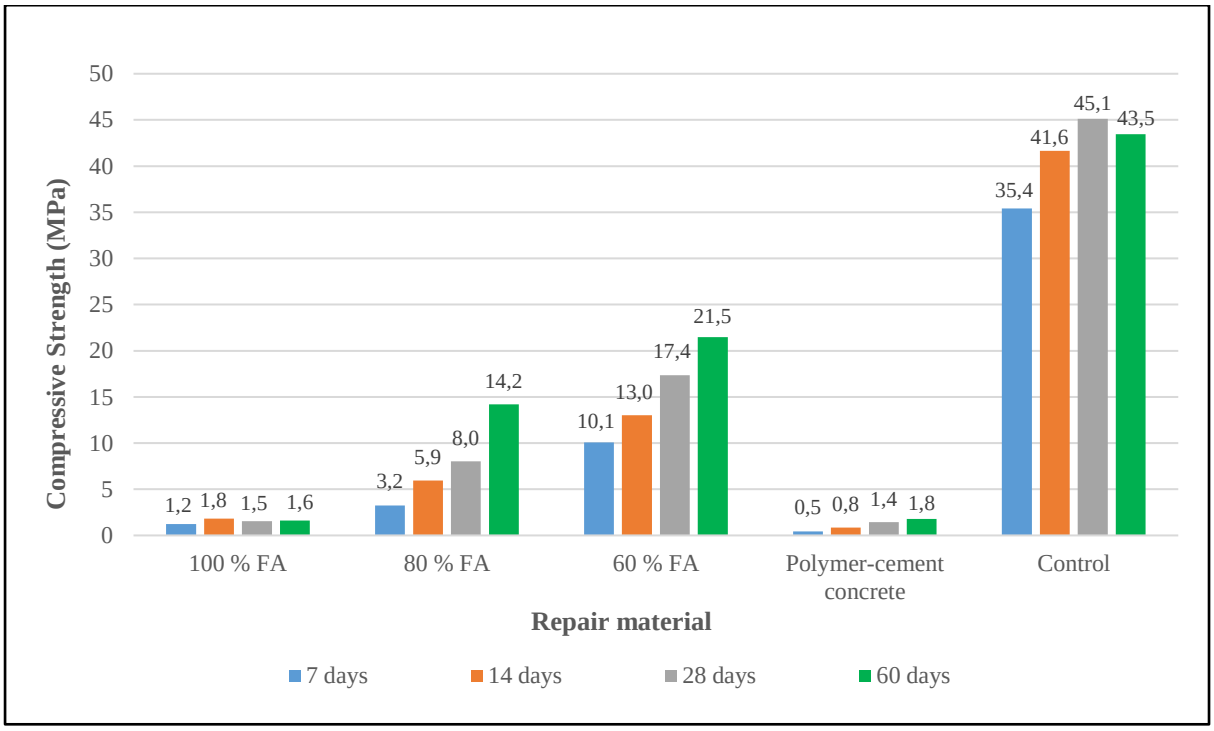

Figure 4-7: Compressive strength test results

It was found that as the FA content increased, the compressive strength decreased significantly. This trend can be explained by the quantity of cement used in the different FA mixes. A larger cement content would allow for more CSH compounds to form and thus allow for an improved matrix formation. A 100% FA mix would inherently have a lower compressive strength since FA is a pozzolanic material with little cementitious properties on its own. Furthermore, class F FA was used in the laboratory investigations which has a very low calcium content. This further allows for limited CSH compound formation. The polymer-cement concrete had a very low compressive strength of only 1.4 MPa after 28 days. This low strength was likely because the polymer-cement concrete matrix had not fully set after a 28 day period. This was evidenced by the fact that the cubes tested for compressive strength were still soft inside since excess water had not been removed either by evaporation or reaction with cement.

However, the 60 day compressive strength of the polymer-cement concrete was found to be 1.8 MPa, which was still very low. Furthermore, the polymer-cement concrete prisms used for the accelerated drying shrinkage tests were cut into two cubes (100 x 100 x 100 mm) and tested for compressive strength. This was done to determine the strength of the polymer-cement concrete after prolonged drying. The strength was found to be only 4.1 MPa. The cubes were tested after 50 days from the day of casting and a total drying period of 43 days at 50 ± 2°C. This result indicates that a polymer-cement concrete repair material with only 5% cement replacement is unlikely to gain compressive strengths above 5 MPa. It must be noted that compressive strength is not a design factor for non-structural patch repairs. Therefore, a low compressive strength would not necessarily mean a sub-standard repair material. However, the extremely low compressive strengths obtained for the 100% FA material would not allow for the development of a practical repair material. This is because the 100% FA material was very brittle and will be easily damaged in service by small contact forces.

The compressive strength of the polymer-cement concrete was found to be the lowest from all the repair materials tested. However, the outer surface of the polymer-cement concrete test cubes were significantly harder than the inside since water here had completely evaporated and/or reacted with cement. Therefore, even though the compressive strength was low, this material would not be easily damaged as the surface was hard enough to provide sufficient protection. The failure mode for the control, 60%, 80% and 100% FA cubes was observed to be typical crushing failure. However, the failure mode for the polymer-cement concrete was unique. The material was characterised by a gradual bulging failure as depicted in Figure 4-8. The material was still largely intact even after failure and this was likely due to the adhesion and ductility properties of the hardened polymer-cement concrete.

Figure 4-8: Failure mode for the polymer-cement concrete

4.2.3 Density

Density was determined using the average mass and volume of the 12 standard 100 x 100 x 100 mm cubes that were used for the compressive strength tests (i.e. 7, 14, 28 and 60 days). The average densities of the different repair materials developed in this thesis are summarised in Figure 4-9. All the materials had a density above 2100 kg/m^3 except the 100% FA repair material that had an average density of 1872 kg/m^3. The polymer-cement concrete repair material was the only material that included coarse aggregate in the mix design however, it did not have the highest density. This was likely due to the low density of the polymer powder used to develop the polymer-cement concrete material.

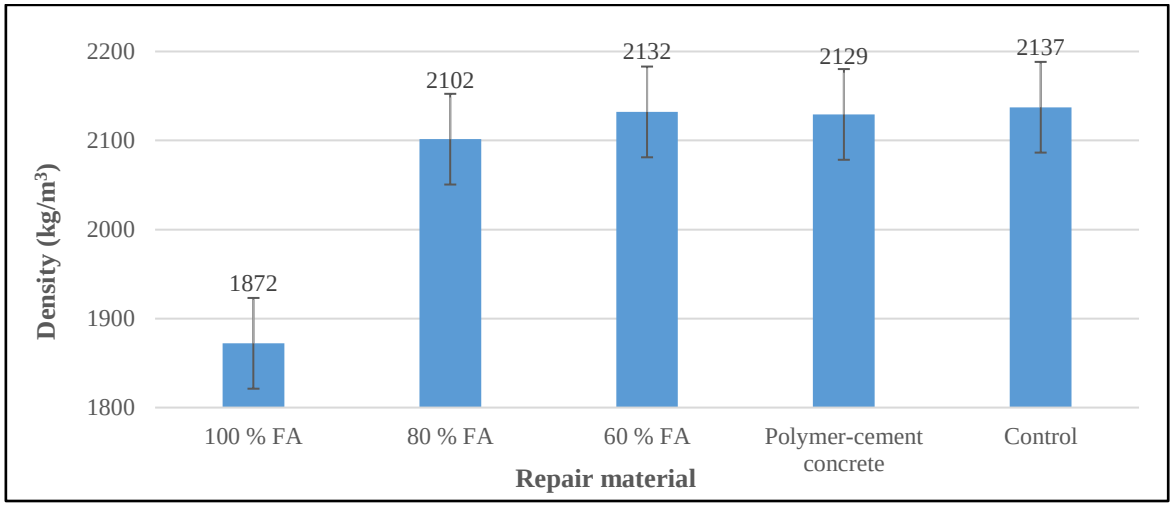

Figure 4-9: Density of different repair materials

4.3 Durability

4.3.1 Cyclic

The different patch repair materials developed were applied to substrate moulds and subjected to cyclic wetting and drying for 56 days (8 weeks). One substrate for each repair material was also left for observation under normal laboratory room conditions i.e. 21 ± 1°C and 59 ± 5% RH (Beushausen & Bester, 2016) in order to provide a reference for comparison with the moulds subjected to cyclic wetting and drying. Upon completion of the cyclic conditioning the moulds were cut through the centre to provide a sectional view of the repair material and the substrate concrete. This was particularly useful in analysing the substrate-patch bond interface.

4.3.1.1 100% FA

The 100% FA patch repair mould left for observation under room conditions is shown in Figure 4-10. There was some denting on the surface due to handling and this was a consequence of the very weak strength of the material. There was clearly visible debonding along the entire length of the substrate-patch interface. Furthermore, white precipitation was seen along the debonded interface as illustrated in Figure 4-10 and this was probably excess unreacted sodium hydroxide which leached from the 100% FA mix.

As seen in Figure 4-11 the extent of debonding along the cross-section of the 100% FA mould was very significant. Additionally, the bond strength of the 100% FA material was found to be very low. This was identified during the sample preparation process for the SEM test, where the 100% FA mortar had completely disintegrated from the substrate due to vibrations caused by the cutting/coring equipment.

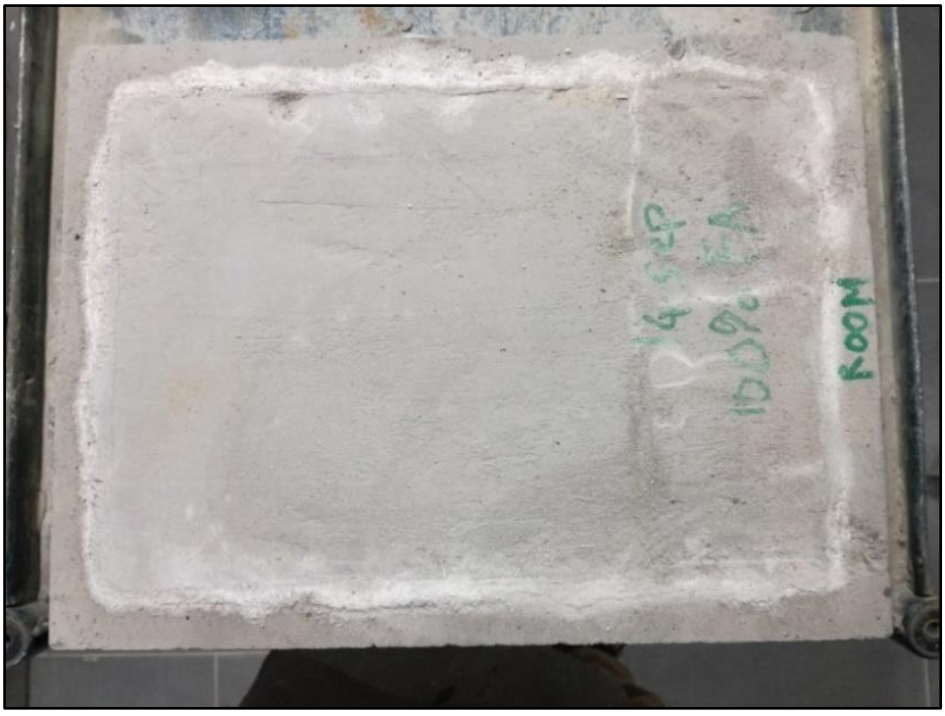

Figure 4-10: 100% FA patch repair left under room conditions

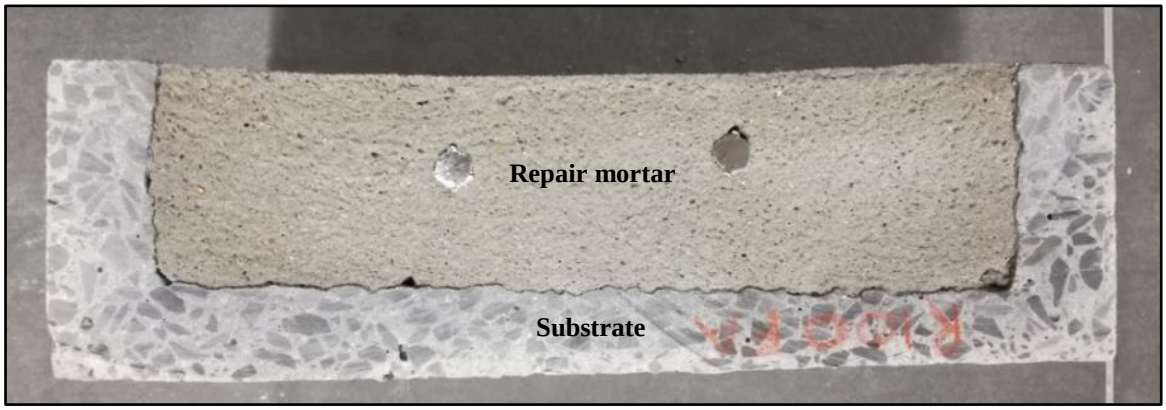

Figure 4-11: Cross-section of 100% FA patch repair

The 100% FA patch repair mould subjected to cyclic wetting and drying is shown in Figure 4-12. As seen in Figure 4-12 there was significant debonding along the entire length of the substrate-patch interface (at the perimeter of the patch). Furthermore, there was significant surface damage caused by both the wet cycles and handling due to the very low compressive strength of the 100% FA repair material. Debonding occurrence was very prominent along the cross-section as depicted in Figure 4-13. The bond strength of the 100% FA repair material subjected to cyclic conditioning was found to be very low as identified in the sample preparation process for the SEM tests. The 100% FA material had completely disintegrated from the substrate caused by vibrations from the coring and cutting process. Performance of the 100% FA repair material with respect to debonding was found to be very poor relative to all the other materials investigated.

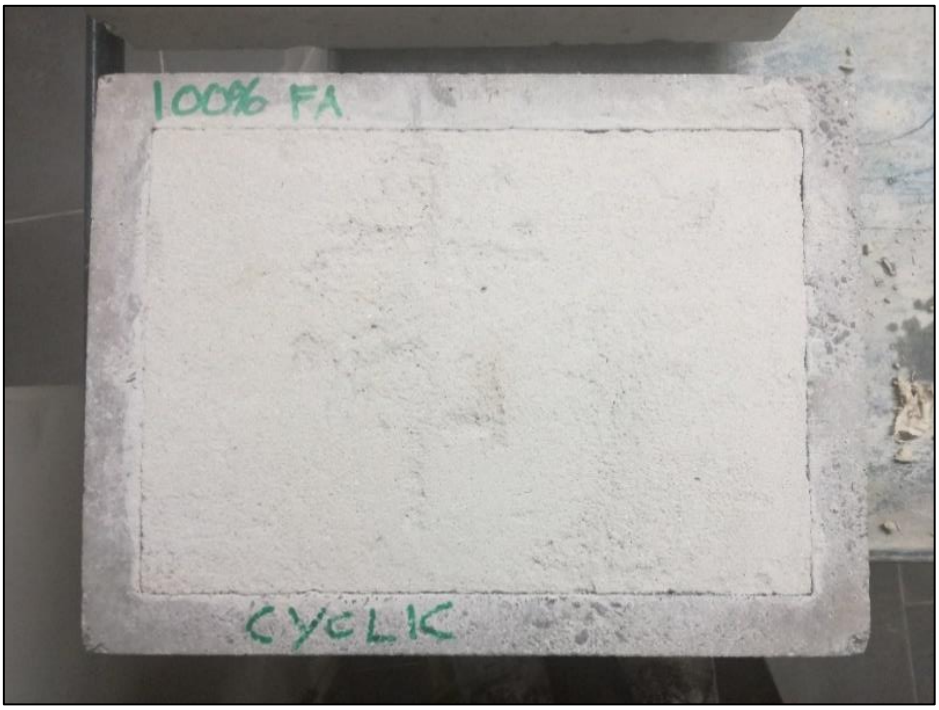

Figure 4-12: 100% FA patch repair after cyclic wetting and drying

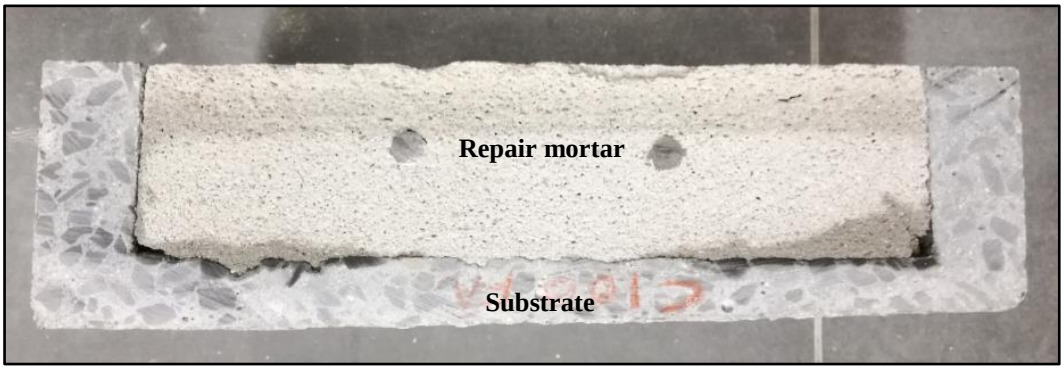

Figure 4-13: Cross-section of 100% FA patch repair after cyclic wetting and drying

4.3.1.2 80% FA

The 80% FA patch repair mould left for observation under room conditions is shown in Figure 4-14. There were cases of debonding along the entire length of the substrate-patch interface however, this was barely visible. The width of debonding was very small compared to both the control and the 100% FA samples; which is depicted in Figure 4-15.

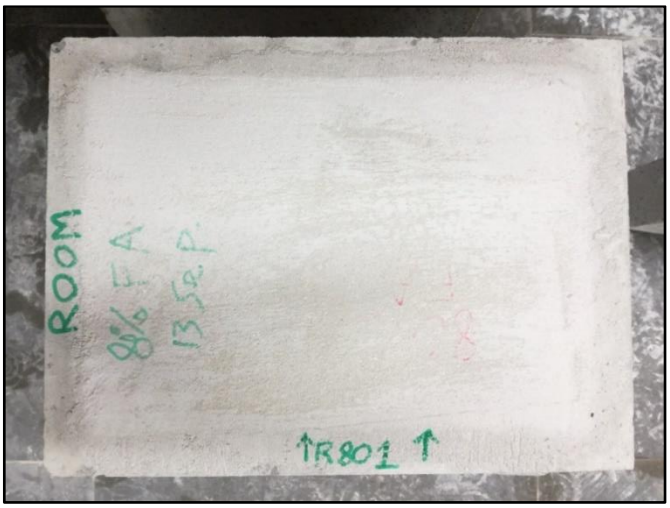

Figure 4-14: 80% FA patch repair left under room conditions

Figure 4-15: (a) Case of debonding and (b) cross-section of 80% FA patch repair

The 80% FA patch repair mould subjected to cyclic conditioning is illustrated in Figure 4-16. As seen in Figure 4-16, there were visible signs of debonding on the surface of the patch repair. However, it was observed that there were only two cases of debonding along the perimeter of the repair as depicted in Figure 4-17. Debonding was more prominent when observed along the cross-section of the substrate-patch mould as shown in Figure 4-17.

Figure 4-16: 80% FA patch repair after cyclic wetting and drying

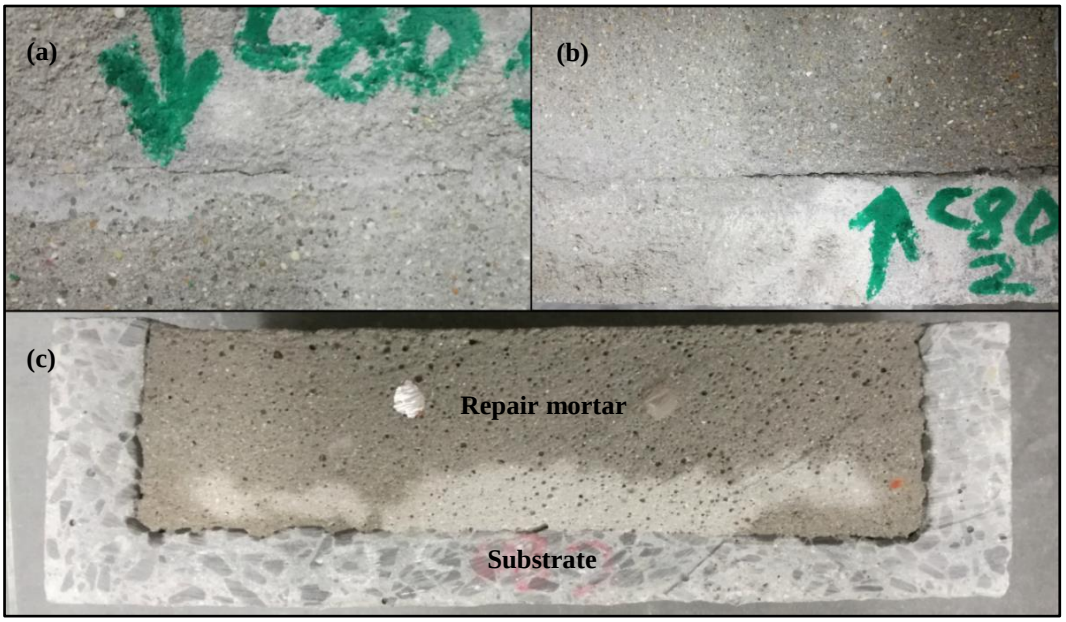

Figure 4-17: (a-b) Cases of debonding and (c) cross-section of 80% FA patch repair after cyclic wetting and drying

4.3.1.3 60% FA

The 60% FA patch repair mould left for observation under room conditions is shown in Figure 4-18. There was only one occurrence of visible debonding along the entire length of the substrate-patch interface. This case of debonding as depicted in Figure 4-19, was barely visible with very small width compared to the 100% FA, 80% FA and control samples. The debonding was more prominent when observed along the cross section of the mould as illustrated in Figure 4-19 however, this could be a consequence of vibrations caused by the cutting equipment. It was found that with decreasing content of FA there was less debonding on the substrate moulds and this was likely due to the increase in cement content in the 60% and 80% FA mixes which facilitated improved adherence.

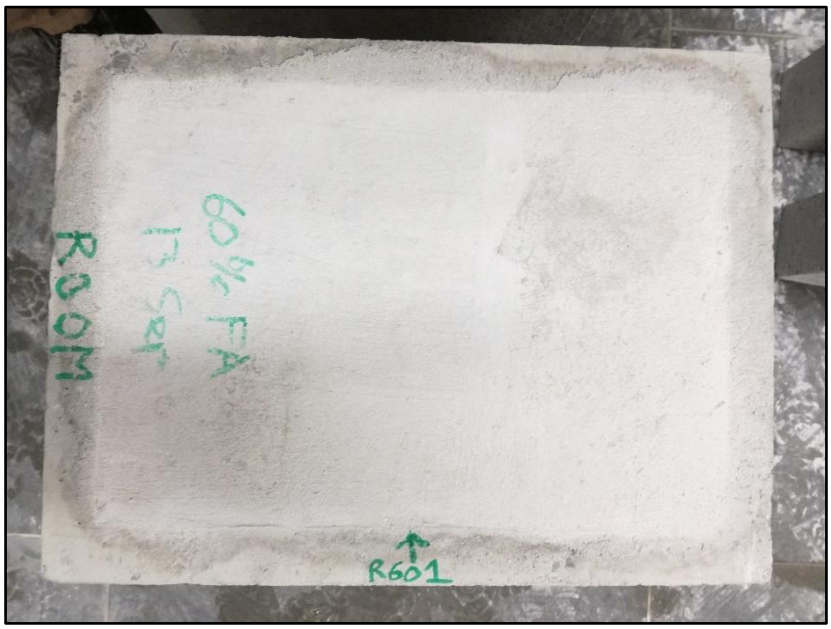

Figure 4-18: 60% FA patch repair left under room conditions

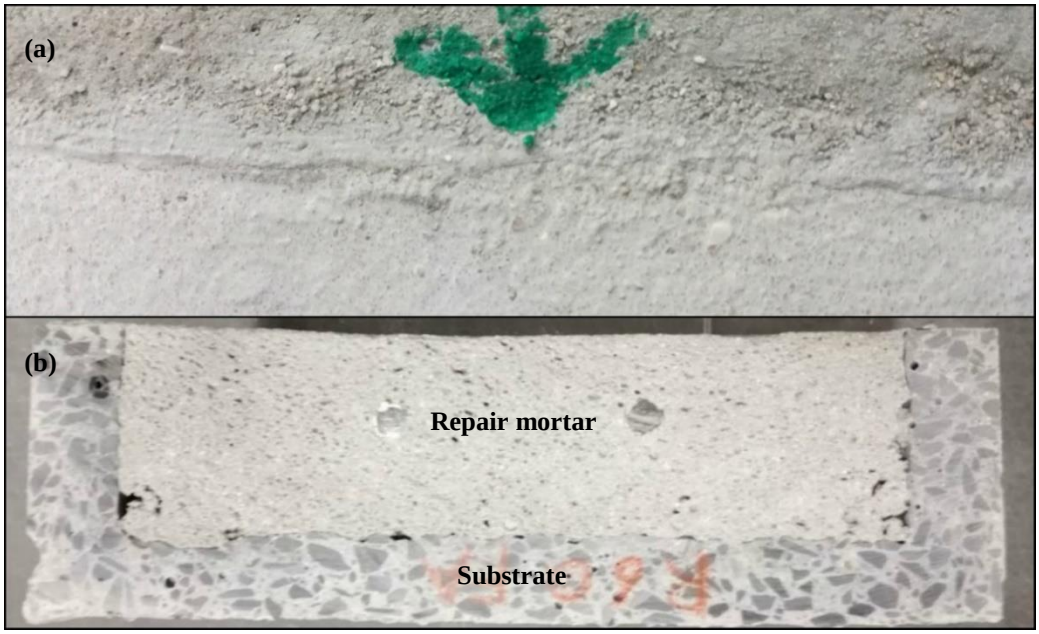

Figure 4-19: (a) Case of debonding and (b) cross-section of 60% FA patch repair

The 60% FA patch repair mould subjected to cyclic conditioning is shown in Figure 4-20. There were no visible signs of debonding along the surface of the mould. Furthermore, as seen in Figure 4-21, there were no clear signs of debonding along the cross-section of the patch repair material. With respect to debonding the 60% FA repair material displayed good performance, relative to the 80% and 100% FA patch repair materials.

Figure 4-20: 60% FA patch repair after cyclic wetting and drying

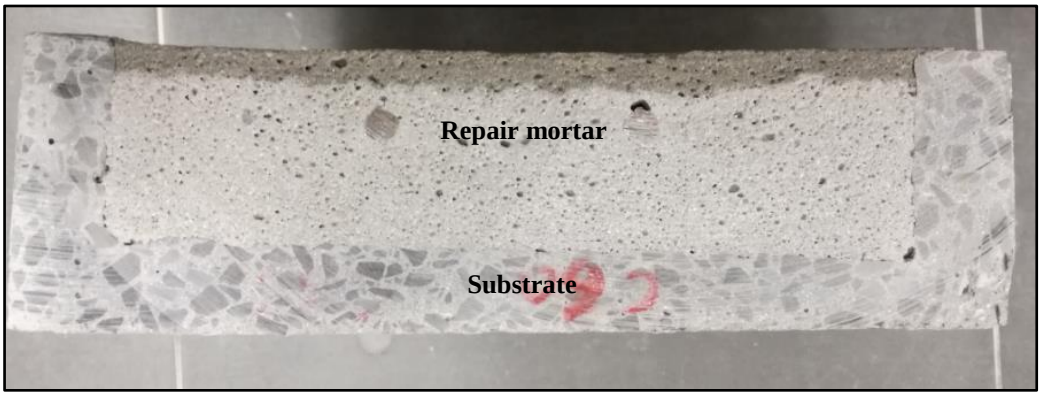

Figure 4-21: Cross-section of 60% FA patch repair after cyclic wetting and drying

4.3.1.4 Polymer and polymer-cement concrete

Three different polymer concrete patch repair moulds were subjected to cyclic wetting and drying. There was no visible debonding on the surface of either of the 8%, 9% or 10% polymer concrete moulds as seen in Figure 4-22, Figure 4-24 and Figure 4-26. However, all three polymer concrete specimens had significantly softened due to water ingress from the wetting cycles. Furthermore, all three polymer concrete mixes were considerably soft in the interior when the cross-section was analysed as illustrated in Figure 4-23, Figure 4-25 and Figure 4-27. Additionally, the polymer concrete was observed to take very long to fully set and this was impossible under the cyclic wetting and drying conditioning since the wet cycles would replenish any water lost from the polymer concrete matrices.

As a consequence of this, sections of the polymer concrete matrices had disintegrated during the cross-section cutting process as seen in Figure 4-23, Figure 4-25 and Figure 4-27. Also, since the material was still soft in the interior, coring and sample preparation for SEM analysis was difficult since the cores would completely disintegrate.

Figure 4-22: 8% polymer concrete patch repair after cyclic wetting and drying

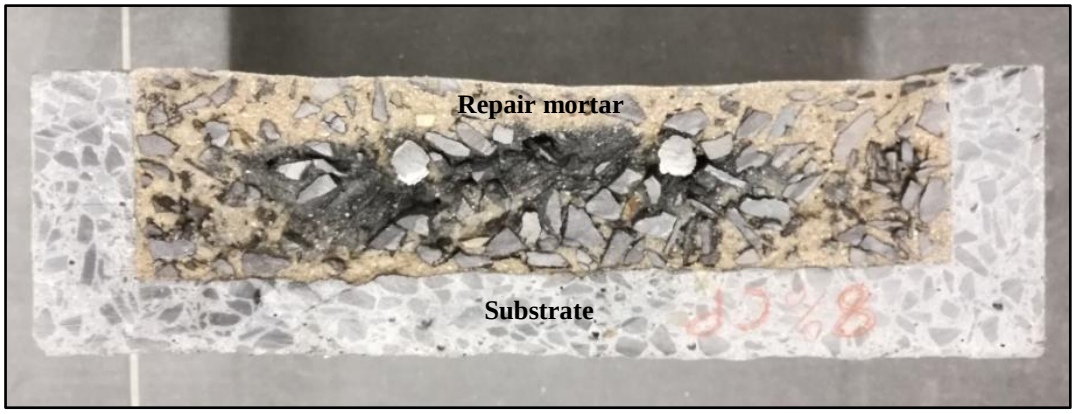

Figure 4-23: Cross-section of 8% polymer concrete patch repair after cyclic wetting and drying

Figure 4-24: 9% polymer concrete patch repair after cyclic wetting and drying

Figure 4-25: Cross-section of 9% polymer concrete patch repair after cyclic wetting and drying

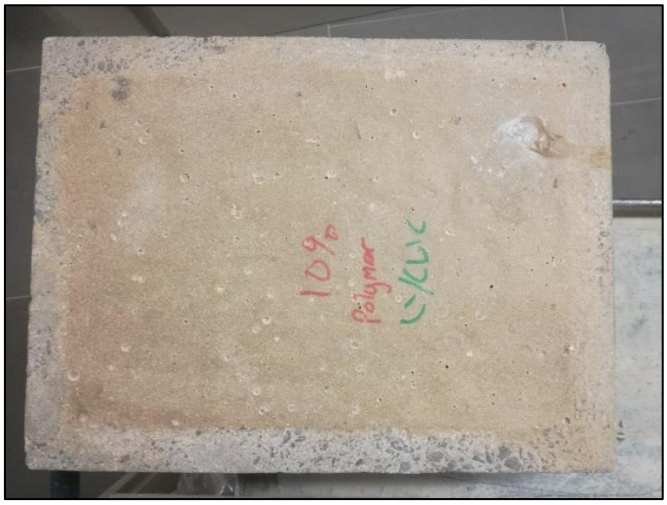

Figure 4-26: 10% polymer concrete patch repair after cyclic wetting and drying

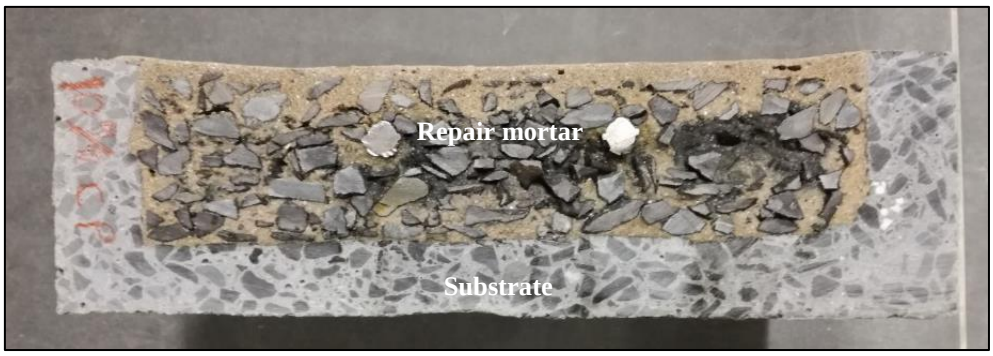

Figure 4-27: Cross-section of 10% polymer concrete patch repair after cyclic wetting and drying

The polymer-cement concrete (5% cement) patch repair mould left for observation under room conditions is shown in Figure 4-28. The polymer-cement concrete had set well on the surface after 24 hours. There were no signs of debonding on the surface of the mould as depicted in Figure 4-28. Furthermore, there were also no signs of debonding along the cross-section of the polymer-cement concrete mould as seen in Figure 4-29. Analysis of the cross section, revealed that the polymer-cement concrete had set to some extent in the interior however, it must be noted that the material was still wet and had not set completely.

Figure 4-28: Polymer-cement concrete FA patch repair left under room conditions

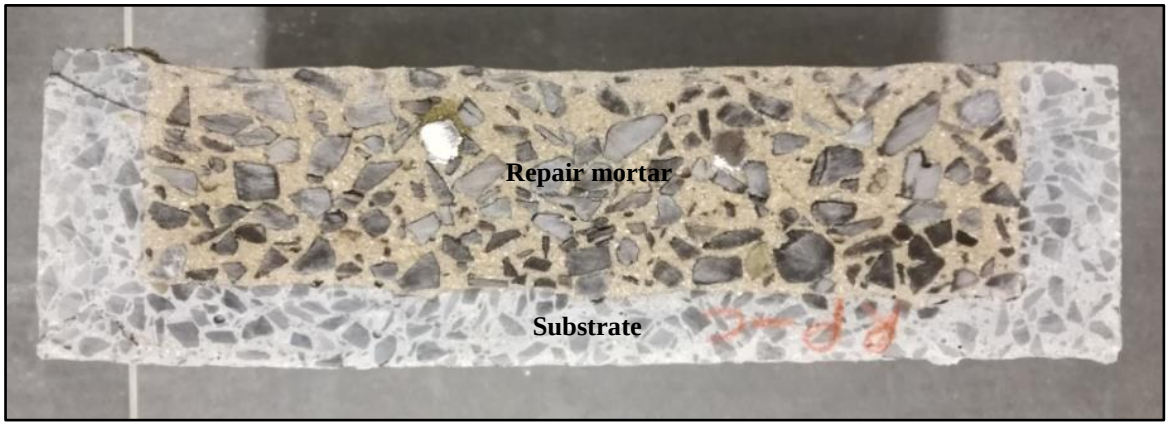

Figure 4-29: Cross-section of polymer-cement concrete patch repair

The polymer-cement concrete (5% cement) patch repair mould subjected to cyclic wetting and drying is shown in Figure 4-30. There was no visible debonding on the surface of the repair mould. The polymer-cement concrete patch repair material had set well on the surface and unlike the polymer concrete material, there was no evidence of water ingress into the interior of the patch repair. Analysis of the polymer-cement concrete cross section, depicted in Figure 4-31, revealed that the interior of the matrix was still soft. However, the material had set much more relative to the polymer concrete material. This indicated that the addition of cement significantly improves the setting properties of the polymer concrete material. As seen in Figure 4-31, there were no clear signs of debonding along the cross-section of the polymer-cement concrete material.

Figure 4-30: Polymer-cement concrete patch repair after cyclic wetting and drying

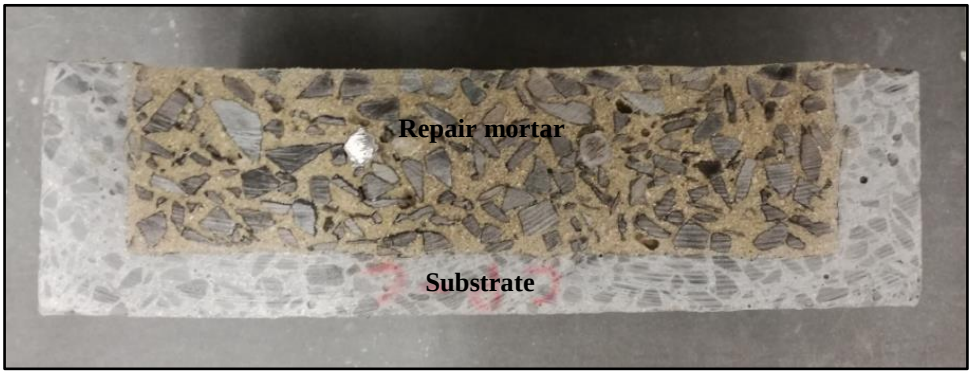

Figure 4-31: Cross-section of polymer-cement concrete patch repair after cyclic wetting and drying

4.3.1.5 Control

The control patch repair mould left for observation under room conditions is depicted in Figure 4-32. There were two visible cases of debonding on the surface of the repair as illustrated in Figure 4-33. However, it must be noted that the debonding was isolated and did not occur along the entire length of the substrate-patch interface. Furthermore, there was no visible debonding along the cross-section of the control mould as seen in Figure 4-33.

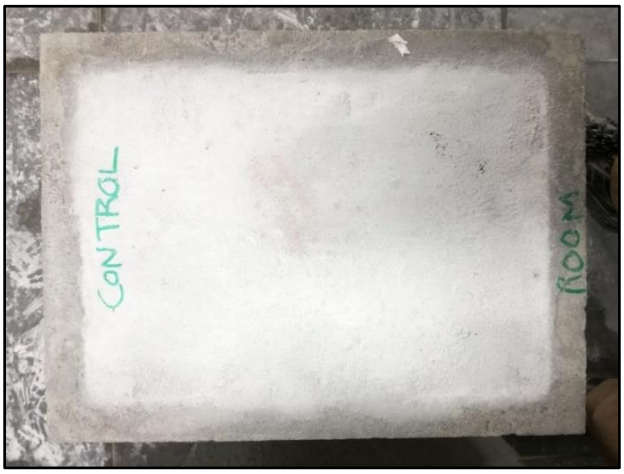

Figure 4-32: Control patch repair left under room conditions

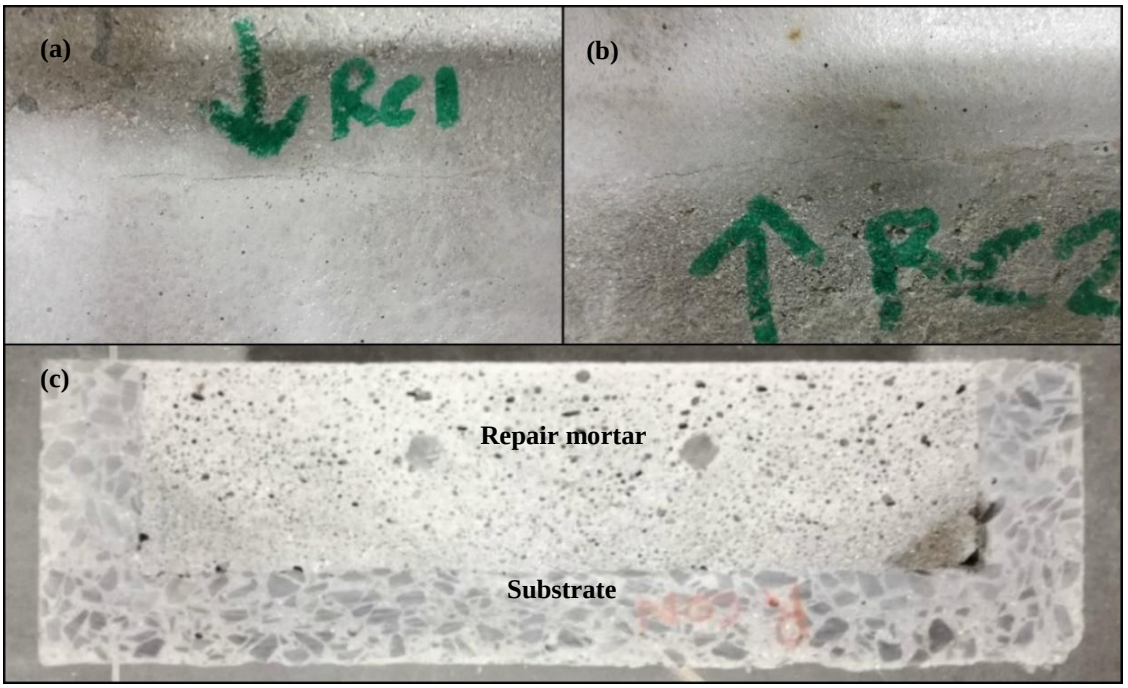

Figure 4-33: (a-b) Cases of debonding and (c) cross-section of control patch repair

The control patch repair mould subjected to cyclic wetting and drying is shown in Figure 4-34. There was no denting or cracking on the surface of the repair. White precipitation, as seen in Figure 4-35, was observed along the substrate-patch interface and this was likely lime leaching caused by the cyclic conditioning. Debonding was not clearly visible on the surface of the mould due to the precipitation however, it was visible observed along the cross-section. It must be noted that the cyclic conditioning greatly affected the bond strength between the substrate and patch repair material. This was identified when preparing samples for the SEM test. Coring and cutting of discs from this specimen led to complete separation of the patch repair material and substrate sections due to vibrations caused by the equipment.

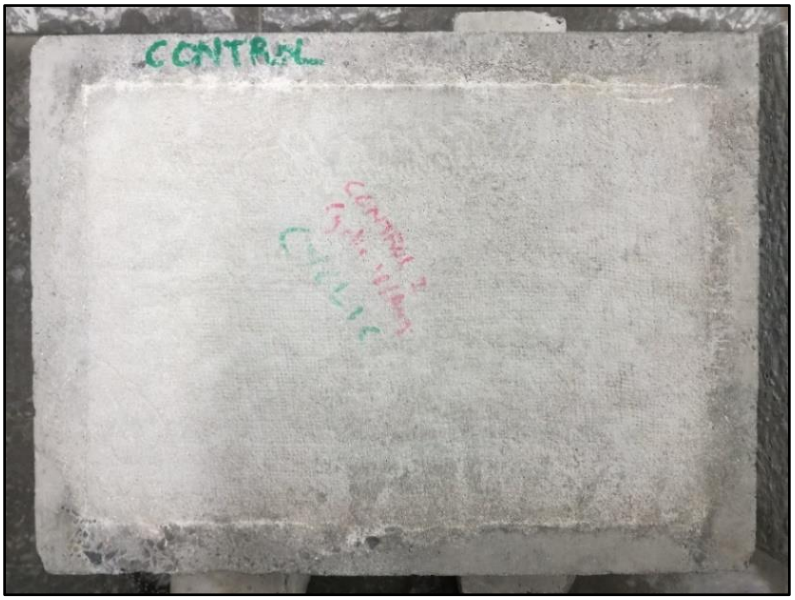

Figure 4-34: Control patch repair after cyclic wetting and drying

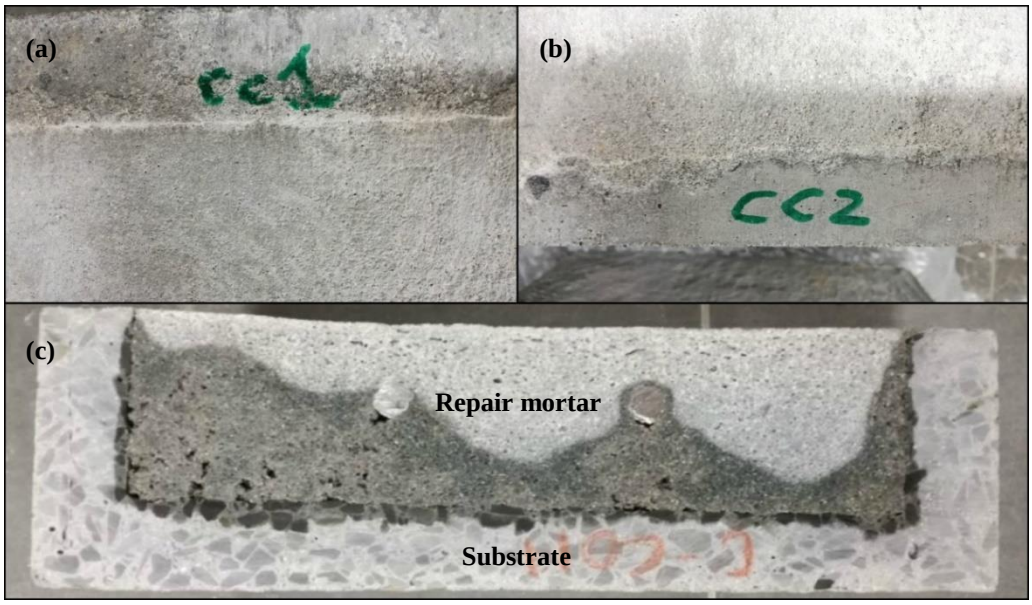

Figure 4-35: (a-b) Cases of debonding and (c) cross-section of control patch repair after cyclic wetting and drying

4.3.2 Oxygen permeability (OPI) test

The results of the OPI tests are summarised in Figure 4-36 and Figure 4-37. Figure 4-36 summarises the relative OPI values whereas Figure 4-37 summarises the relative permeability coefficients of the materials studied. The polymer-cement concrete repair material had the best OPI value with 10.15 corresponding to a permeability coefficient (k) of 7.07E-11 m/s. The process of sample preparation for the polymer-cement concrete OPI test samples involved oven drying at 50 ± 2°C for 7 days of 25 mm discs which were then cored. The cored samples were further dried at 50 ± 2°C for 7 days. This ensured that the polymer-cement concrete samples were well dry which allowed the material to fully set. The OPI results indicated that a fully set polymer-cement concrete sample will have excellent impermeability and hence enhanced durability properties.

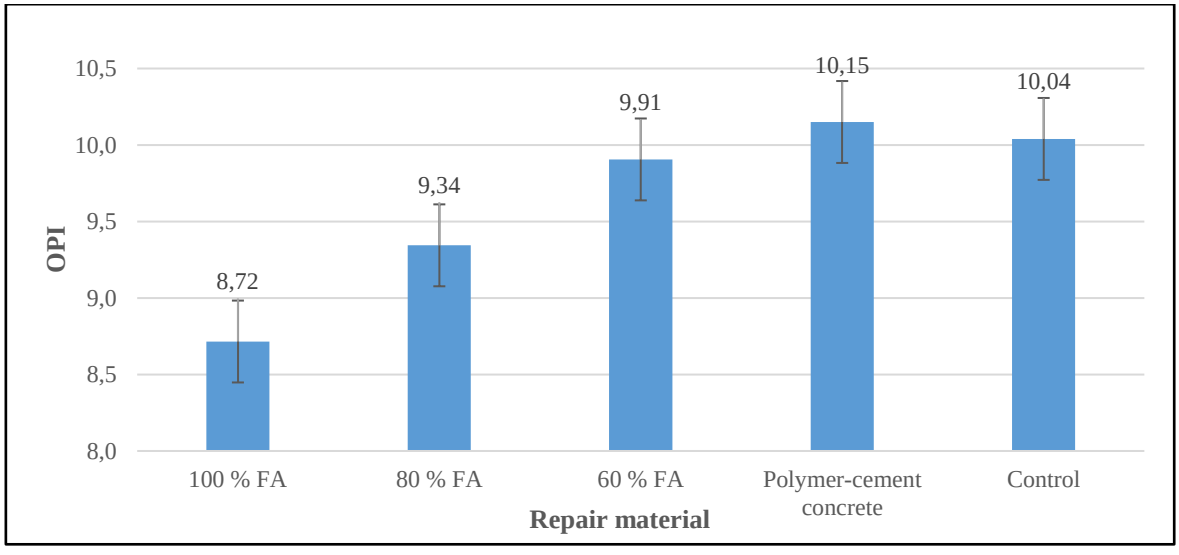

Figure 4-36: OPI results showing index values

The lowest OPI value was obtained by the 100% FA repair material with an index value of 8.72 corresponding to a permeability coefficient (k) of 1.93E-09 m/s. This was significantly lower than the control value which had an OPI of 10.04 corresponding to a permeability coefficient (k) of 9.12E-11 m/s. The results indicated that the 100% FA material has very low impermeability and as a consequence will have limited durability particularly when exposed to chloride ions and/or carbonation. The 60% FA and 80% FA repair materials had relatively good OPI penetrability coefficients (k) of 1.24E-10 m/s and 4.53E-10 m/s respectively. Furthermore, it was observed that increasing the FA content greatly reduced the OPI values. This meant that high volume FA repair materials would have much limited impermeability and therefore, durability.

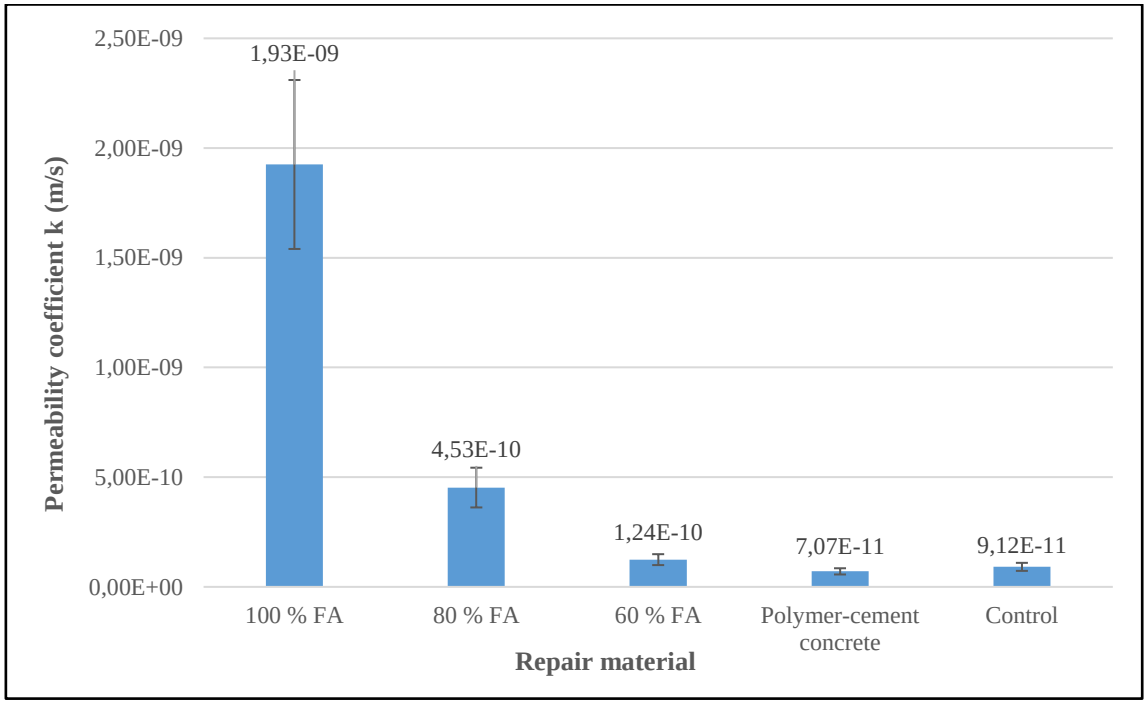

Figure 4-37: OPI results showing permeability coefficients

4.3.3 Water sorptivity (WSI) test

WSI tests were conducted on the repair materials developed to determine the permeability and porosity parameters. The sorptivity results of the different repair materials are summarised in Figure 4-39. The 100% FA repair material had the largest sorptivity with a value of 42.4 mm/hr$^{0.5}$ which was complemented by the low OPI value obtained. Upon completion of the WSI test for the 100% FA repair material, water was seen at the top surface of the samples as illustrated in Figure 4-38.

This indicated that the 100% FA repair material had very low impermeability and therefore, resistance to the ingress of deleterious substances. The 60% FA and 80% FA repair materials had sorptivity values of 10.0 mm/hr$^{0.5}$ and 13.2 mm/hr$^{0.5}$ respectively. It was hence identified that higher volume FA mixes increased the sorptivity of the repair material. The polymer-cement concrete had a sorptivity value of 11.4 mm/hr$^{0.5}$. This was higher than the control which had a value of 5.2 mm/hr$^{0.5}$.

Figure 4-38: 100% FA WSI test sample

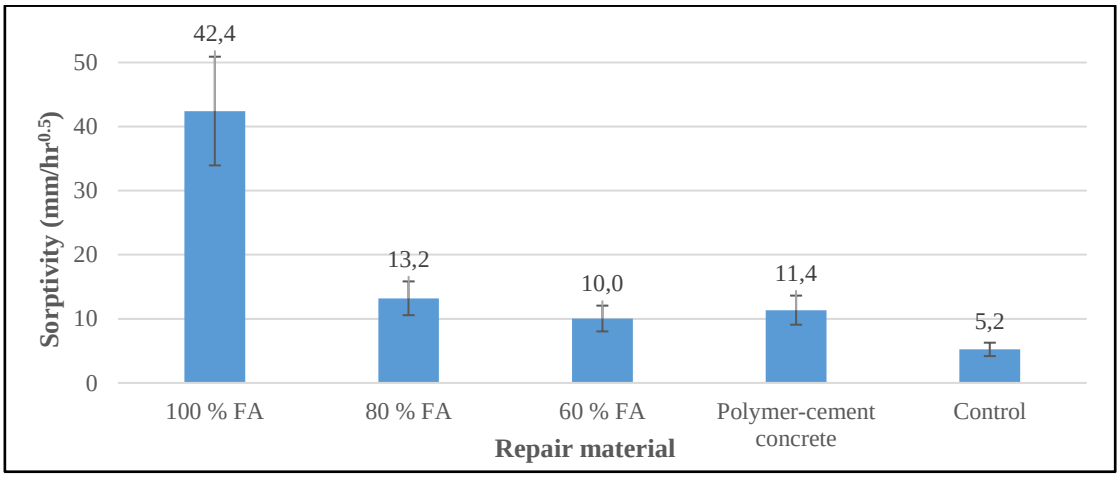

Figure 4-39: Sorptivity results

The results of the porosities of the different materials obtained via the WSI tests are summarised in Figure 4-40. The polymer-cement concrete had the lowest porosity with a value of 2.5%. The control specimen had a porosity value of 14.5%. The 80% FA repair material had the highest porosity value with 21.8%. There was no clear trend observed between FA content and the porosity.

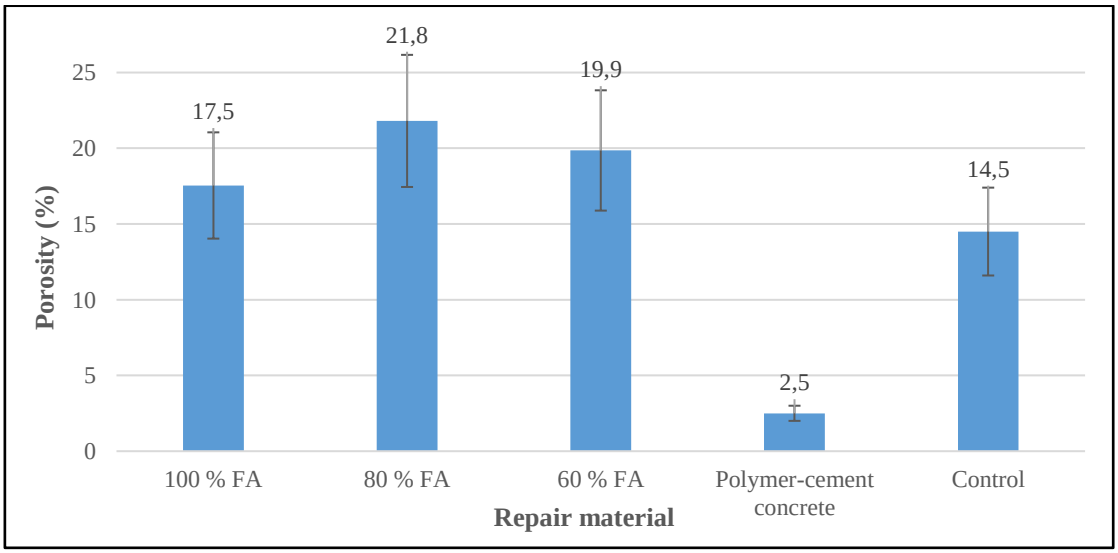

Figure 4-40: Porosity results from WSI tests

4.3.4 Chloride conductivity (CCI) test

CCI tests were conducted on the different repair materials to determine their resistance to chloride ingress. Figure 4-41 summarises the results of the CCI tests conducted. It must be noted that the current readings for the 100% FA specimens were taken at a voltage of 2 V which was different from the standard recommendation of 5 V. This was because the 100% FA material was found to have very high conductivity and therefore, caused the multimeters to short circuit when a higher voltage was applied. A voltage of 5 V was used for the 60% and 80% FA and a voltage of 10 V was used for the polymer-cement concrete and control specimens.

Note that the CCI test was developed for conventional concrete. The relationship between a CCI value and expected chloride ingress for a high volume FA mix and a polymer-cement concrete mix is not known, which makes it difficult to interpret the CCI test results for these materials. The test results indicate that further investigations into the chloride resistance of the high volume FA mixes as well as the polymer-cement concrete mix is required in future research. The control test specimen (conventional mortar) had a conductivity of 1.26 mS/cm which is rated as having good chloride resistance.

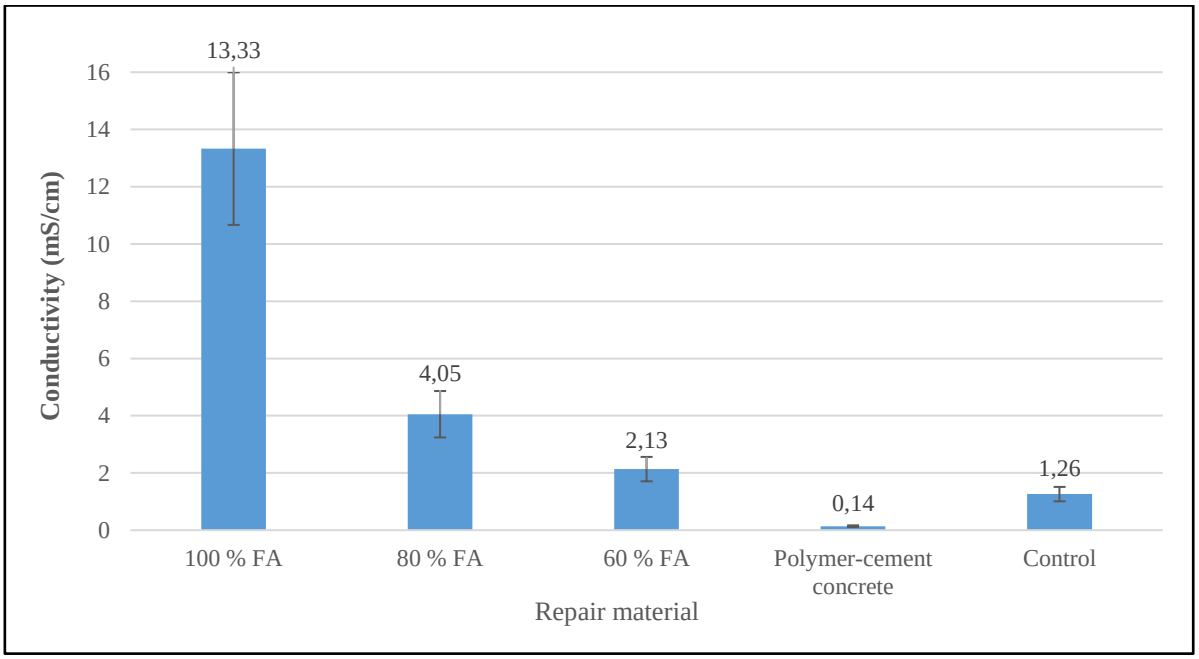

Figure 4-41: Chloride conductivity of different repair materials

4.3.5 Correlation between OPI, WSI and CCI

Table 4-1 summarises the results of the durability index test results obtained for the different repair materials investigated. It was observed in general that as the OPI values increased for the different repair materials, the CCI conductivity values were found to decrease. Furthermore, with the exception of the polymer-cement concrete material, the sorptivity results generally showed to decrease with increasing OPI values.

Table 4-1: Summary of durability index test results

Test	100% FA	80% FA	60% FA	Polymer-cement concrete	Control
OPI	8.72	9.34	9.91	10.15	10.04
Permeability coefficient k (m/s)	1.93E-09	4.53E-10	1.24E-10	7.07E-11	9.12E-11
Sorptivity (mm/hr$^{0.5}$)	42.4	13.2	10.0	11.4	5.2
Porosity (%)	17.5	21.8	19.9	2.5	14.5
CCI Conductivity (mS/cm)*	13.33	4.05	2.13	0.14	1.26

* Note the relationship between a CCI value and expected chloride ingress for a high volume FA mix or polymer-cement concrete mix is not known which makes it difficult to interpret and compare the results obtained.

However, the actual values of sorptivities of the different materials displayed no clear correlation relative to the OPI and CCI values. It has been established in literature that there is no direct relationship between WSI and deterioration mechanisms in concrete. However, WSI tests measure a physical property which is related to porosity. Therefore, WSI values can be used in durability specifications as a site quality control measure since the sorptivity value is more dependent on construction parameters such as curing and less reliant on concrete material composition. Similarly to the WSI results, there was no clear relationship between the porosity and the OPI or CCI values. It is possible to correlate the OPI and CCI values directly to the rate of ingress of deleterious substances into concrete. Durability index values can therefore be related to the deterioration of reinforced concrete and can be used in service life prediction and performance based design. Concrete deterioration processes are linked to transport mechanisms of deleterious substances into concrete. The durability index tests are therefore related to a particular transport mechanism of aggressive media that facilitates deterioration. OPI is related to concrete permeability, CCI is related to diffusion properties and WSI is related to concrete porosity. Given the durability index values determined for the different materials, service life and concrete design criteria for the South African context can be predicted based on models developed by Mackechnie & Alexander (2002).

4.4 Crack resistance

4.4.1 Ring test

In order to determine the crack resistance of the repair materials under restrained shrinkage conditions, shrinkage rings were cast. Three specimens were cast for each repair material and these were observed until cracks developed. The results of the age of cracking of the different repair materials are summarised in Figure 4-42. Upon removal of the hessian used for curing, it was found that the control specimens had already cracked. Therefore, cracking of the control specimens may have occurred earlier than 7 days. This was unusual since cracking is only expected on drying and not during the wet curing process. However, cracking most likely occurred because the hessian had completely dried during the curing period due to the low humidity settings in the controlled environmental room.

Increasing FA content resulted in an increase in resistance to cracking. The 100% FA specimens took 24 days to crack compared to the 60% FA specimens that took only 10 days. A direct linear trend between FA content and crack resistance was identified. This can be explained by the fact that with increasing FA content, mechanical strength reduced significantly. With a low mechanical strength (tensile and compressive) the elastic modulus decreases therefore, the material undergoes less stress development and increased stress relaxation under restrained shrinkage conditions. As a consequence, the lower strength FA mortar exhibited less cracking.

These results complement studies by Beushausen & Bester (2016) and Chilwesa (2012) which concluded that high compressive strength and elastic modulus in concrete repair materials actually increases the risk of cracking as evidenced by the early cracking of the control specimens. No cracks were observed on any of the three polymer-cement concrete ring specimens as shown in Figure 4-48, even after 70 days of observation. The polymer-cement concrete was found to take very long to completely set. The material was found to dry and set well on the outside however, the interior section would still be soft and was found to take a very considerable amount of time to completely set. As a consequence of this, any deformations occurring due to shrinkage on the polymer-cement concrete ring specimens were not restrained since the soft interior would easily accommodate any deformations. Therefore, no cracks developed on any of these specimens. This is an important finding that identifies the superior crack resistance potential of a polymer-cement concrete repair material.

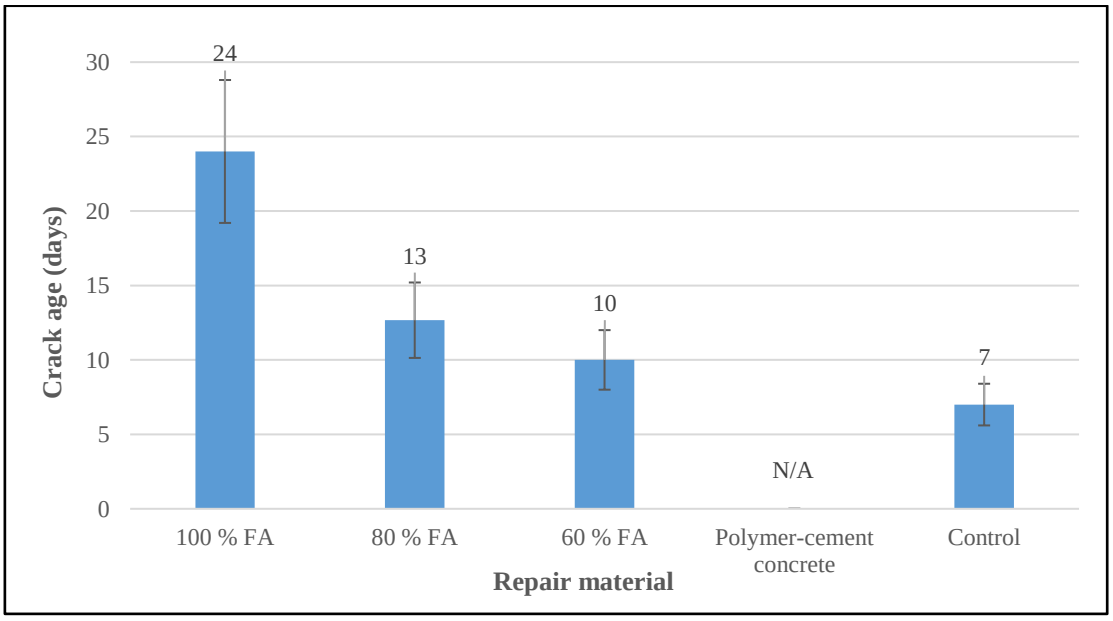

Figure 4-42: Average repair material crack age

Crack width on the restrained shrinkage ring specimens was determined using a crack meter. Crack width readings were taken on the first crack that appeared on each specimen and three readings were taken along the crack. An average crack width value using the three different specimens for each repair material was then determined. The results are outlined in Figure 4-43. The control specimens had the largest average crack width of 1.41 mm. The 100% FA repair material had the smallest average crack width of 0.24 mm.

Furthermore, it was identified that with increasing FA content, crack width decreased significantly. Similarly to the age of cracking, this finding supports the idea that low strength repair materials will undergo much less cracking compared to high strength materials.

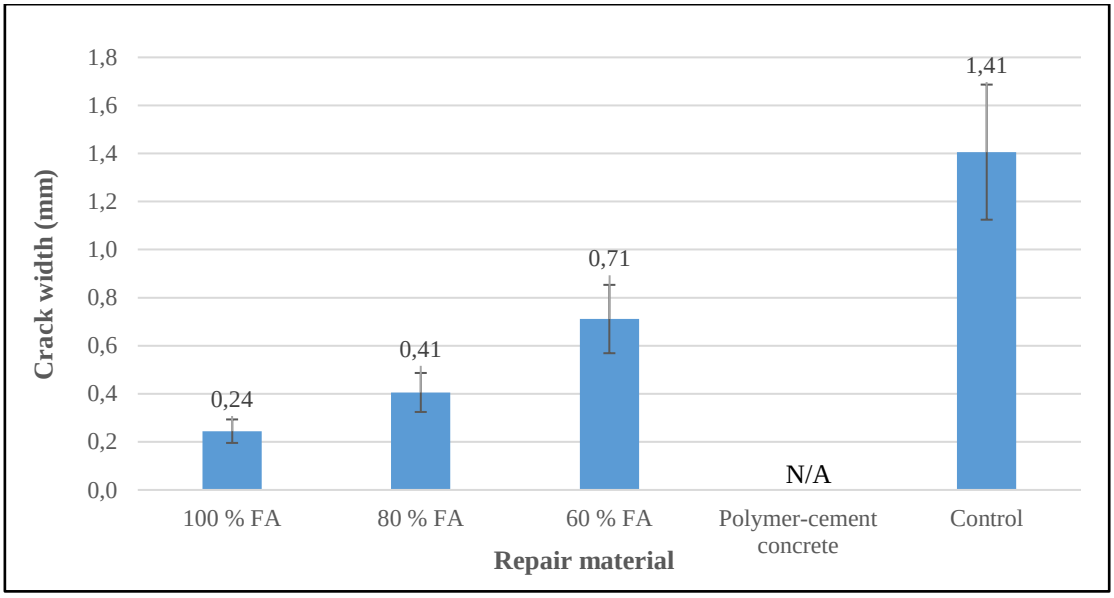

Figure 4-43: Average crack width of different repair materials

The number of cracks that developed on each specimen is summarised in Table 4-2. Excluding the 100% FA, two cracks had developed on all the other specimens except one 80% FA specimen that had only one visible crack. Two 100% FA specimens had only one visible crack and one specimen had three visible cracks. However, it must be noted that of these three cracks two did not run right down along the edge of the ring specimens. Images of the first cracks that appeared on each specimen were taken (i.e. those with the largest crack widths) and these are presented in Figure 4-44, Figure 4-45, Figure 4-46 and Figure 4-47.

Table 4-2: Number of cracks per ring specimen

Material	Specimen 1 No. of cracks	Specimen 2 No. of cracks	Specimen 3 No. of cracks
Control	2	2	2
60% FA	2	2	2
80% FA	2	1	2
100% FA	1	3	1
Polymer-cement concrete	N/A	N/A	N/A

Figure 4-44: Crack distribution on 100% FA rings

Figure 4-45: Crack distribution on 80% FA rings

Figure 4-46: Crack distribution on 60% FA rings

Figure 4-47: Crack distribution on control rings

Figure 4-48: No cracking on polymer-cement concrete rings

4.4.2 Accelerated drying shrinkage test

The shrinkage strain development of the repair materials tested are summarised graphically in Figure 4-49 and Figure 4-50. Detailed results of the accelerated drying shrinkage tests are attached under Appendix A6. The following results were obtained for the different materials:

- The shrinkage of the control specimen was determined to be 415 µ-ε (after 15 days) therefore, this material can be categorised as having moderate shrinkage.
- The shrinkage of the 100% FA specimen was determined to be 573 µ-ε (after 13 days) therefore, this material can be categorised as having high shrinkage.
- The shrinkage of the 80% FA specimen was determined to be 343 µ-ε (after 11 days) therefore, this material can be categorised as having low shrinkage.
- The shrinkage of the 60% FA specimen was determined to be 293 µ-ε (after 11 days) therefore, this material can be categorised as having low shrinkage. The 60% FA repair material was found to have the lowest shrinkage magnitude relative to all the repair materials. Furthermore, it was observed that with decreasing FA content, the accelerated drying shrinkage decreased indicating a direct relationship between FA content and shrinkage potential.
- The shrinkage of the polymer-cement concrete specimen was determined to be 1517 µ-ε which was abnormally high. Furthermore, the material continued to shrink for a long period of up to 45 days. This was likely due to the fact that this material took a considerable amount of time to completely set. As a consequence, the material underwent prolonged drying shrinkage as it slowly set by losing water and contracting in the process.

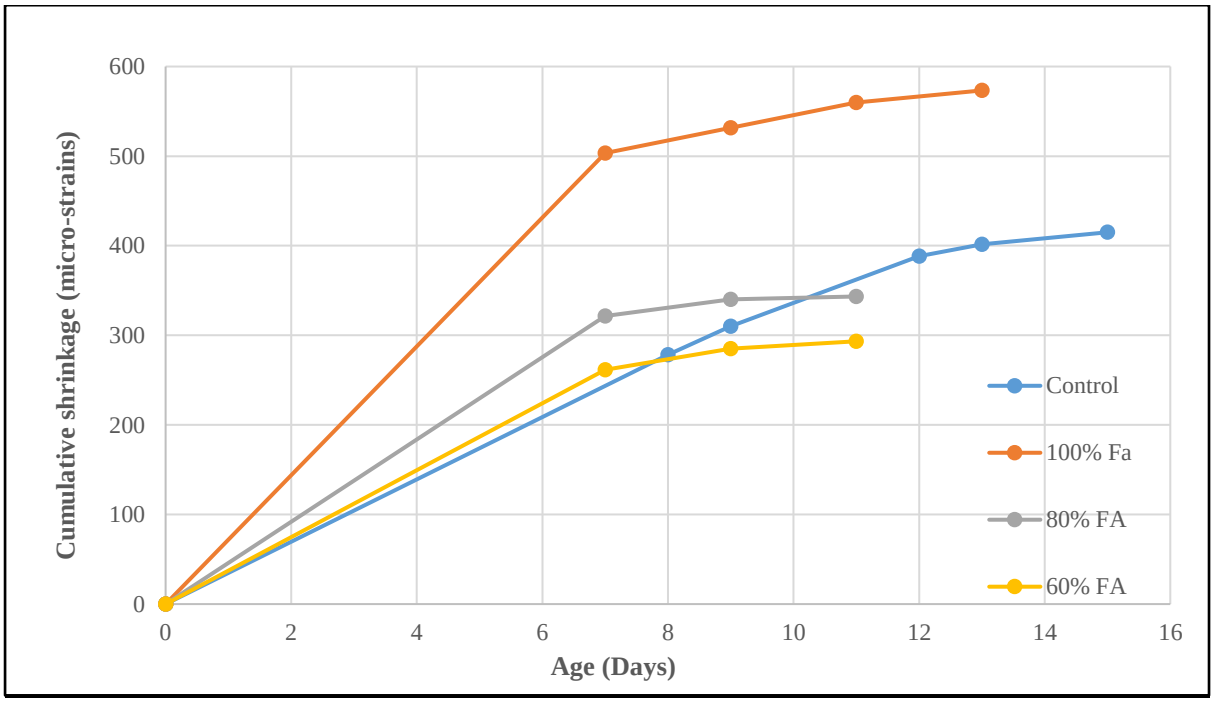

Figure 4-49: Accelerated drying shrinkage strain development graphs

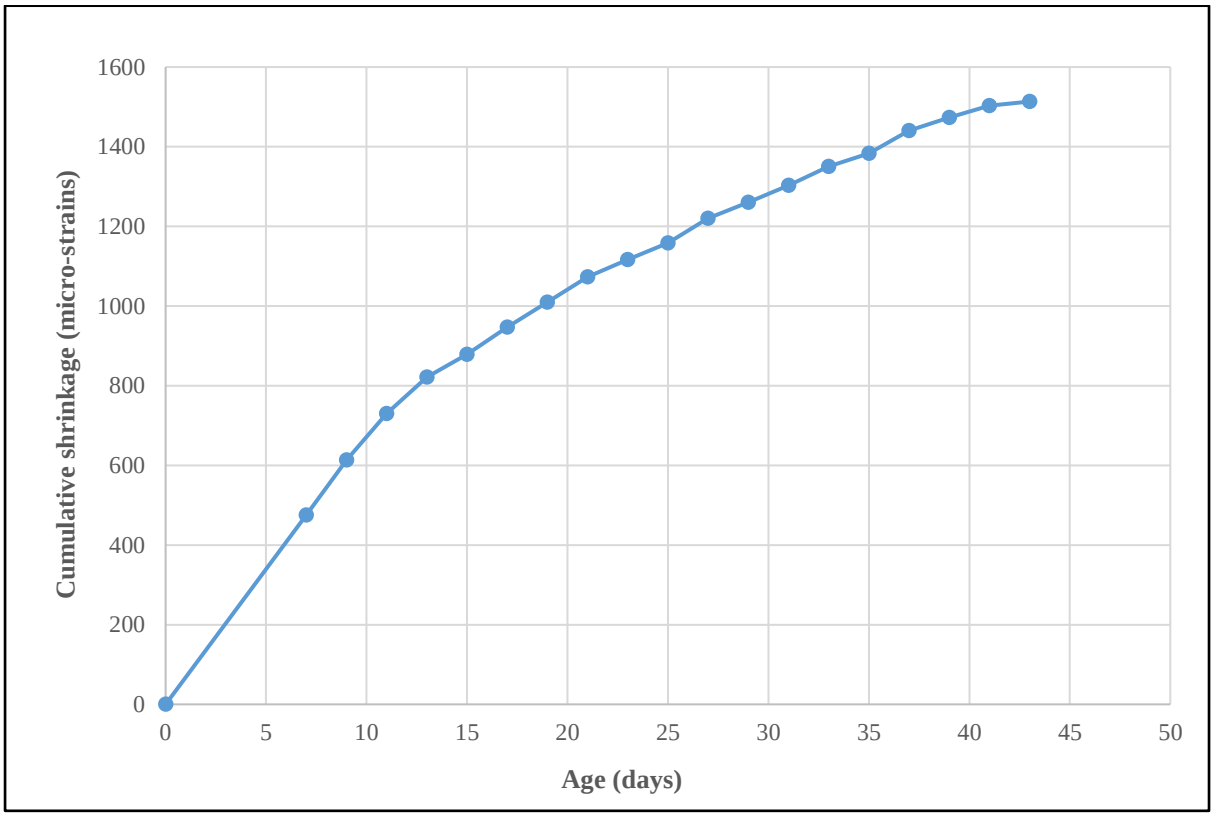

Figure 4-50: Polymer-cement concrete strain development graph

4.5 Interface bond - microscopic (SEM) test

SEM analysis was conducted on specially prepared samples to analyse the bond interface between the patch repair material and substrate concrete at a microscopic level. The results of the SEM imaging are presented in the next subsections. It must be noted that some material sample cores could not be prepared without causing complete separation of the patch repair material from the substrate concrete. This was a consequence of the poor bond strength in these specimens which resulted in easy bond failure due to vibrations caused by the coring/cutting equipment.

4.5.1 100% FA

SEM images taken on the 100% FA specimens are presented in Figure 4-51 and Figure 4-52. SEM sample preparation of the 100% FA specimens subjected to room conditions and cyclic conditioning resulted in complete separation of the patch repair material from the substrate concrete. This was a consequence of the very weak bond between the substrate and 100% FA patch repair material. However, as depicted in Figure 4-51, there were cases where some patch repair material was still attached to the substrate.

This result indicated that the bond may be stronger than the repair material with failure occurring in the repair material rather than the bond. Furthermore, Figure 4-51 and Figure 4-52 show that the matrix of the 100% FA repair material was of very poor strength as indicated by the complete separation of individual particles making up the material. There was clearly very weak adhesion between particles within the matrix of the 100% FA material. This was likely due to the lack of CSH compound formation due to the use of high volume class F FA, which is a pozzolanic material. This also explains the very low compressive strengths obtained for the 100% FA repair material.

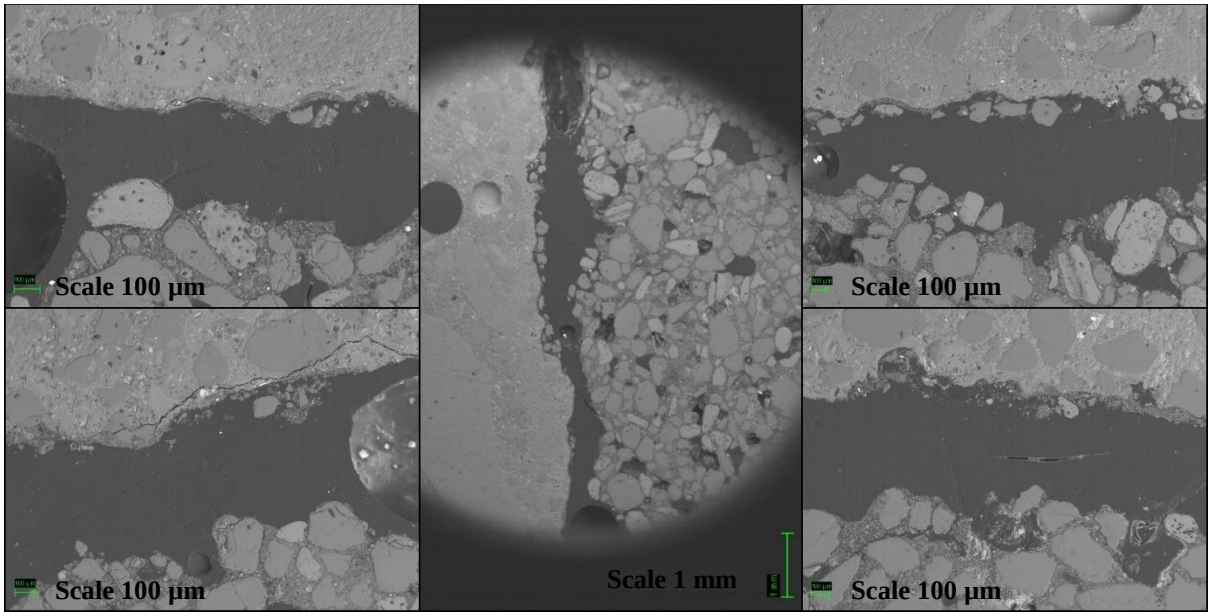

Figure 4-51: SEM images of 100% FA subjected to room conditions

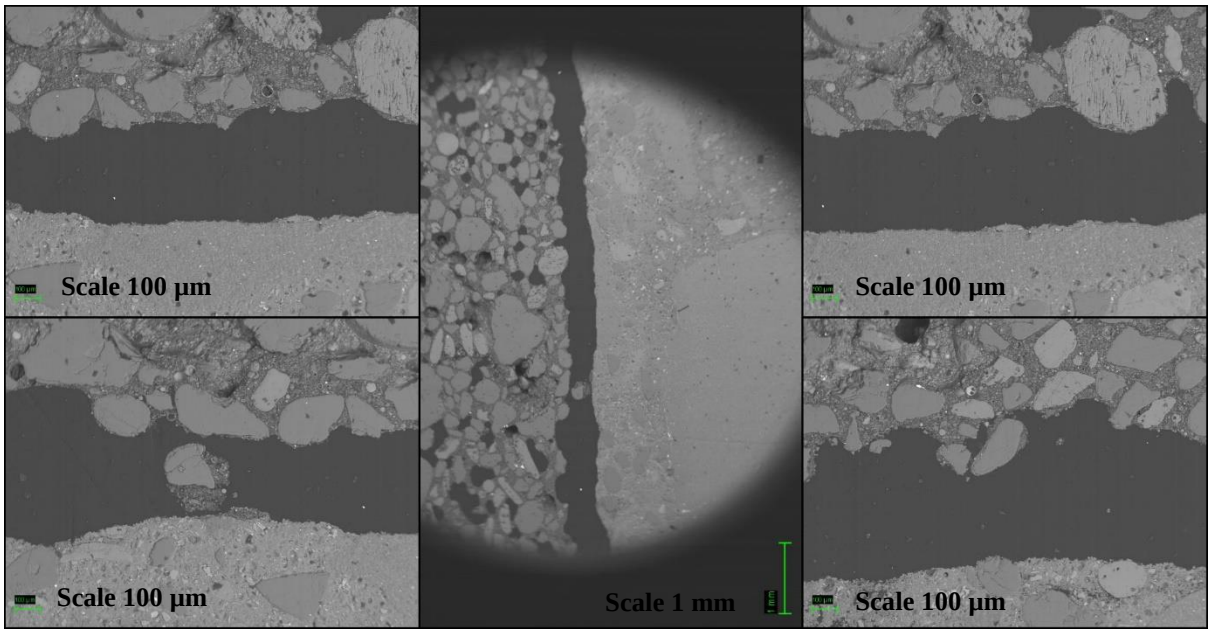

Figure 4-52: SEM images of 100% FA subjected to cyclic conditioning

4.5.2 80% FA

The SEM images taken on the 80% FA specimen subjected to room conditions are presented in Figure 4-53. As can be seen in these images, the patch repair material completely separated from substrate concrete. This indicated that the bond between the substrate and patch repair material was very weak and gave way during the SEM sample preparation process. Additionally, there were locations where the bond seemed intact but failure occurred in the patch repair material. This result indicated that the matrix of the 80% FA repair material was inherently very weak.

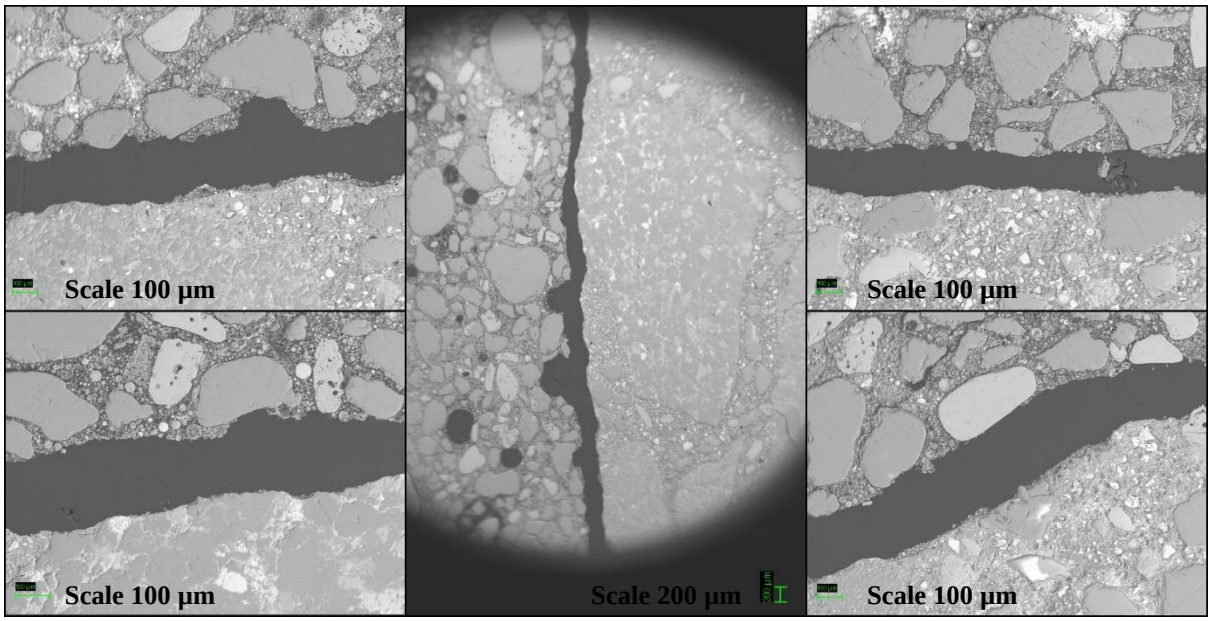

Figure 4-53: SEM images of 80% FA subjected to room conditions

The SEM images taken on the 80% FA specimen subjected to cyclic conditioning are presented in Figure 4-54. The bond interface was not intact and there was visible separation between the patch repair material and substrate concrete. However, the 80% FA repair material performed much better relative to the 100% FA repair material with respect to bonding. This was likely due to the cement content in the 80% FA repair material that resulted in improved adhesion.

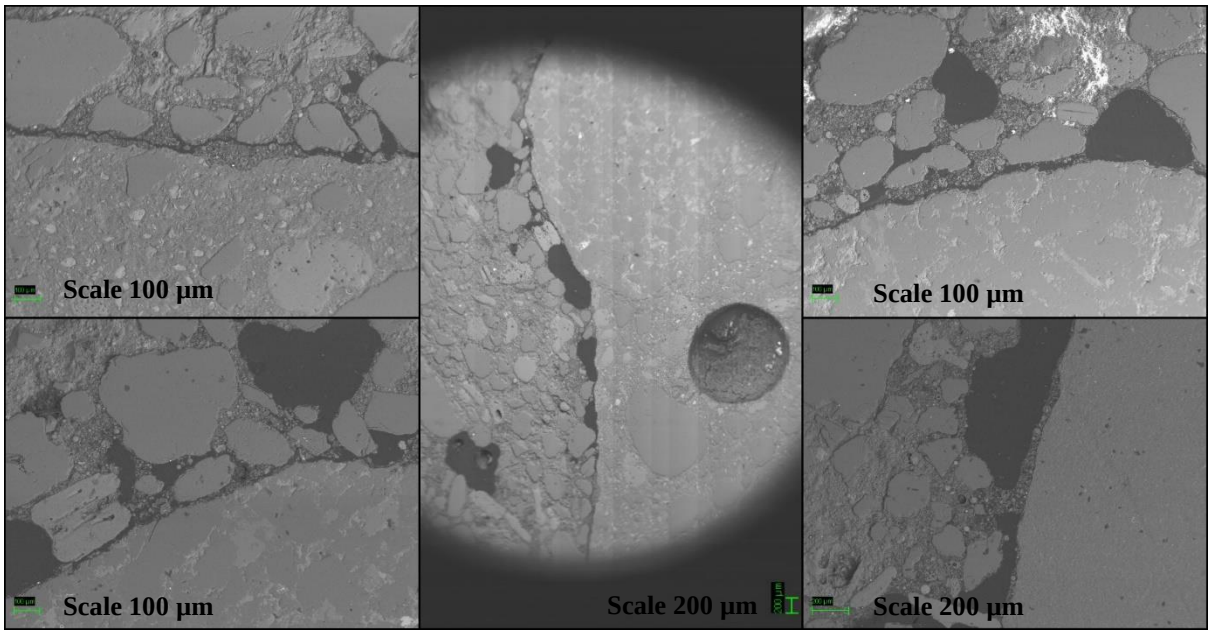

Figure 4-54: SEM images of 80% FA subjected to cyclic conditioning

4.5.3 60% FA

SEM images taken on the 60% FA specimens are presented in Figure 4-55 and Figure 4-56. The bond interface was found to be largely intact in the sample subjected to room conditions and the one subjected to cyclic conditioning. There were no cases of complete separation between the substrate and patch repair material indicating that the strength of the bond was acceptable even after exposure to the SEM sample preparation process. These results showed that the 60% FA repair material had good performance with respect to substrate-patch bonding. Furthermore, the 60% FA repair material had the best bond performance compared to the 80% and 100% FA repair materials. This was likely due to the higher cement content in the 60% FA material that allowed for improved adhesion and bonding properties.

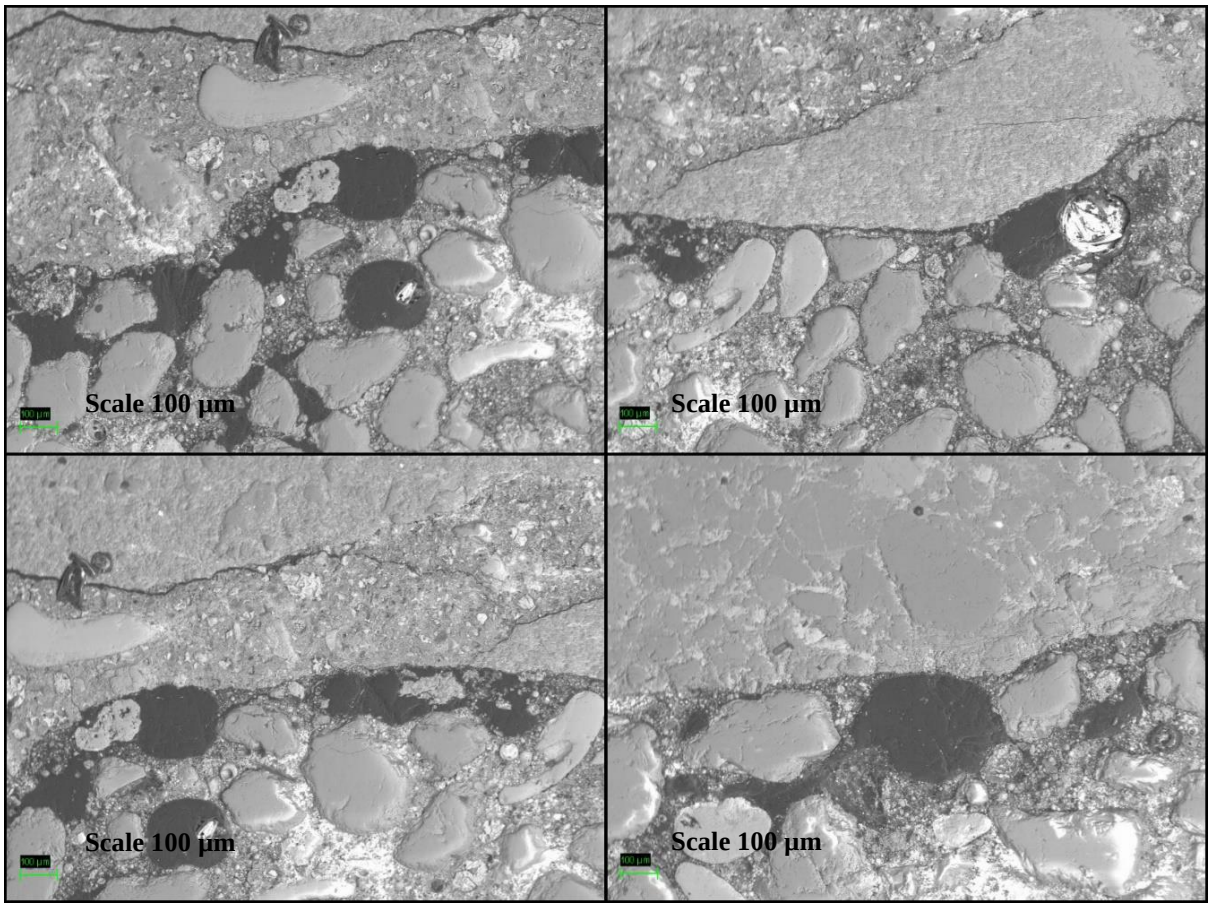

Figure 4-55: SEM images of 60% FA subjected to room conditions

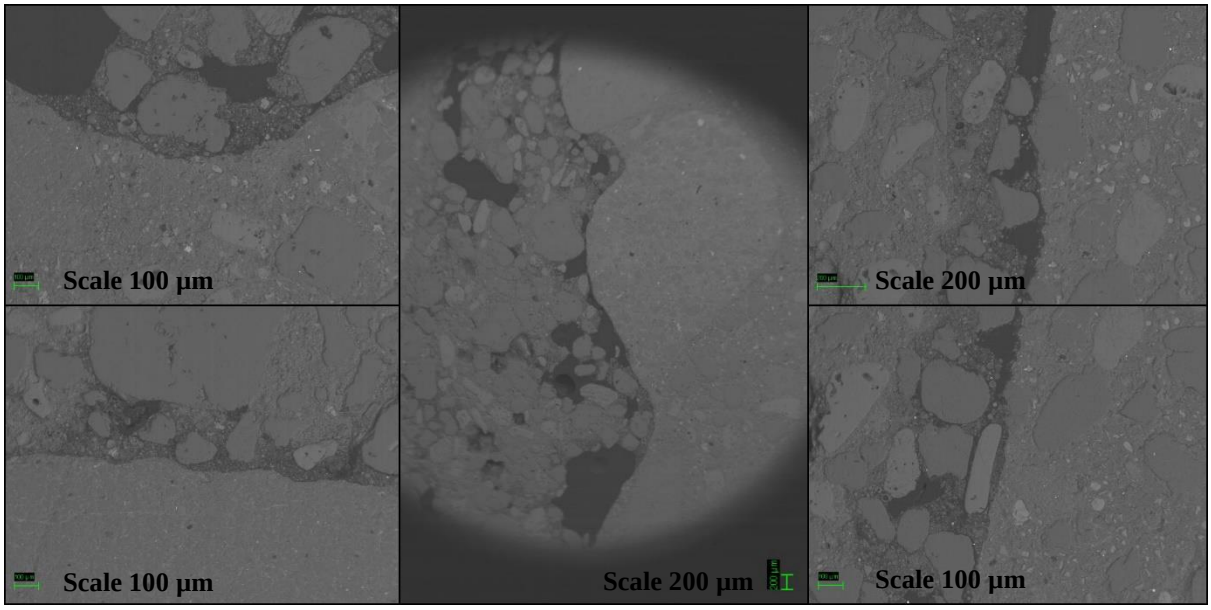

Figure 4-56: SEM images of 60% FA subjected to cyclic conditioning

4.5.4 Polymer and polymer-cement concrete

SEM images taken on the polymer concrete specimens are presented in Figure 4-57, Figure 4-58, Figure 4-59 and Figure 4-60. The bond integrity in all the polymer concrete specimens analysed was found to be exceptionally good relative to all the other repair materials. As depicted in the images there were virtually no cases of debonding in any of the specimens and this indicated that the bonding performance of the polymer concrete specimens was very good. The polymer-cement concrete specimen subjected to cyclic conditioning showed good bond integrity with no evidence of debonding as depicted in Figure 4-60. These results were anticipated since one of the key properties exhibited by the polymer material used in this study is good adhesion.

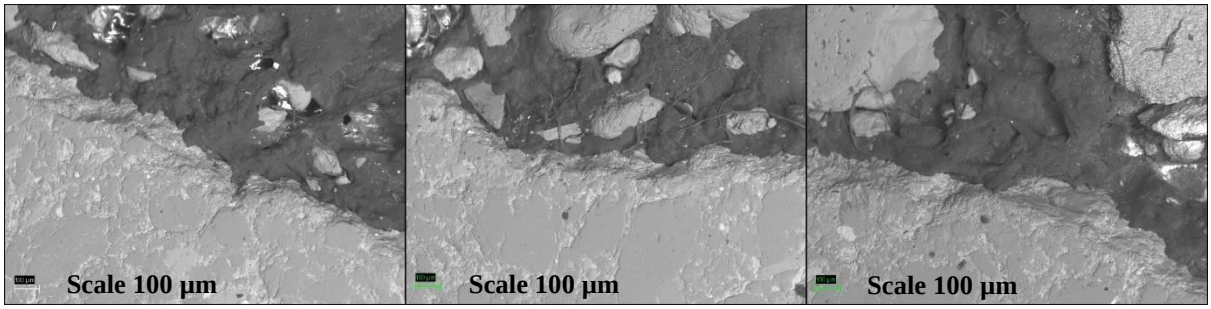

Figure 4-57: SEM images of 8% polymer concrete subjected to cyclic conditioning

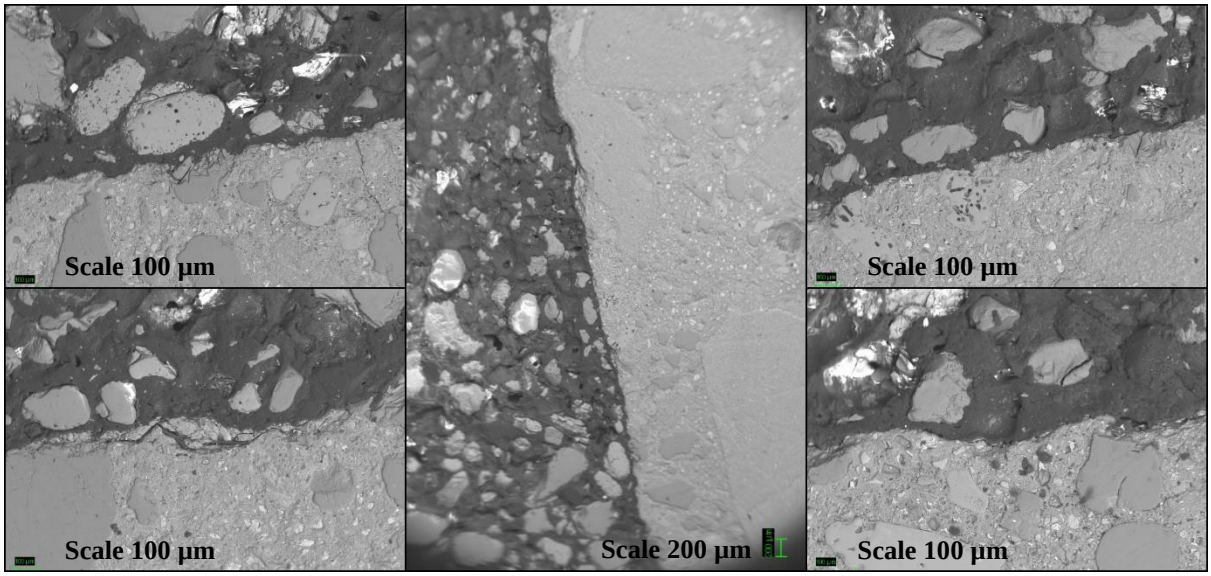

Figure 4-58: SEM images of 10% polymer concrete subjected to cyclic conditioning

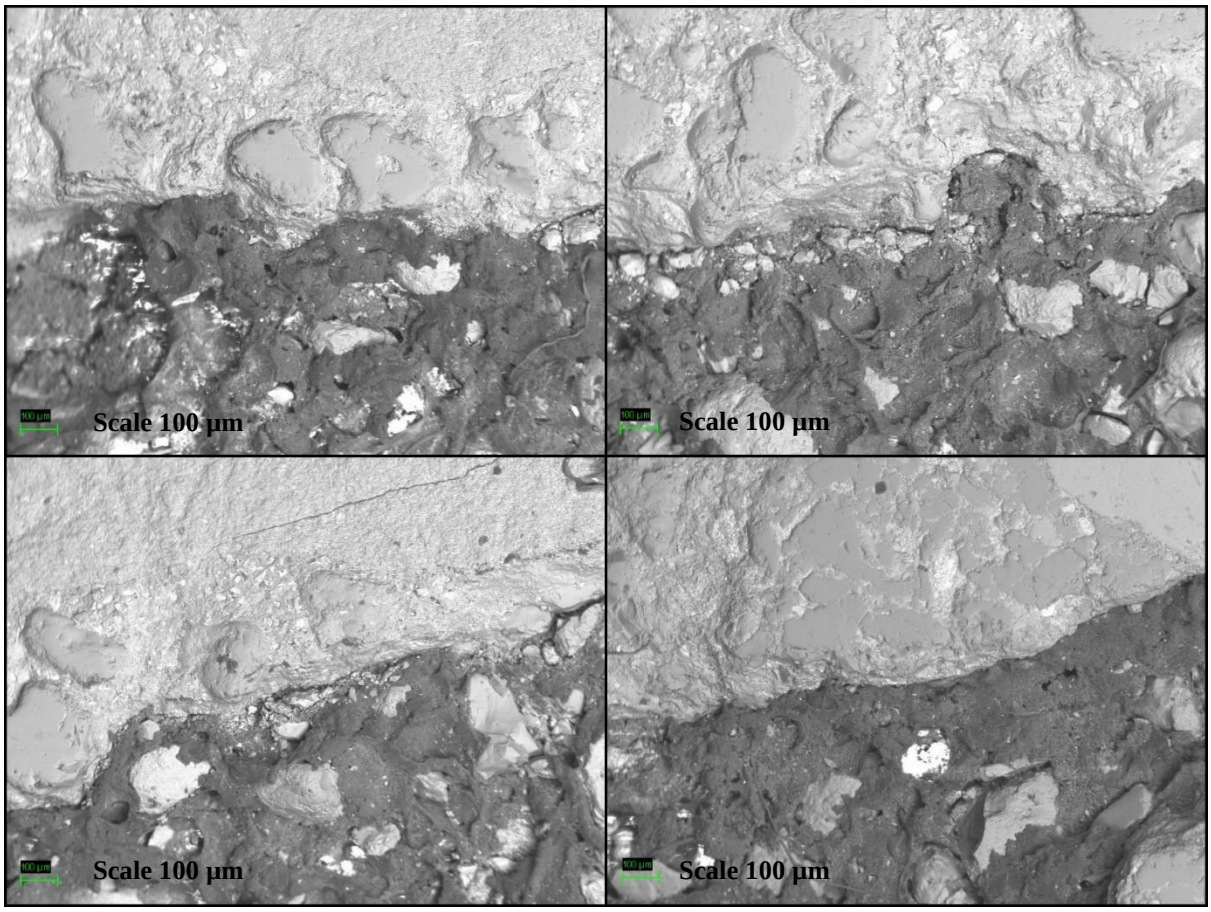

Figure 4-59: SEM images of polymer-cement concrete specimen subjected to room conditions

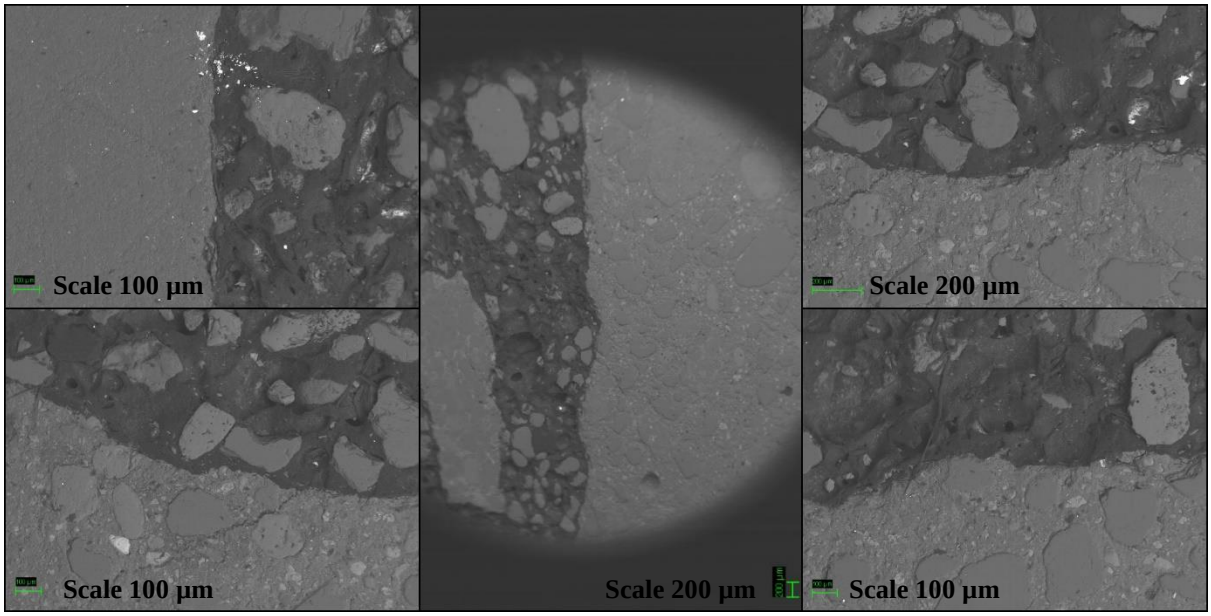

Figure 4-60: SEM images of polymer-cement concrete specimen subjected to cyclic conditioning

4.5.5 Control

SEM images taken on the control specimen subjected to room conditions are presented in Figure 4-61. As seen in the images, the bond interface in the control was largely intact. There was very limited debonding occurrence and no cases of complete separation of patch repair material from the substrate concrete. As expected, the bonding performance of the control repair material was found to be acceptable with the integrity of the bond still maintained.

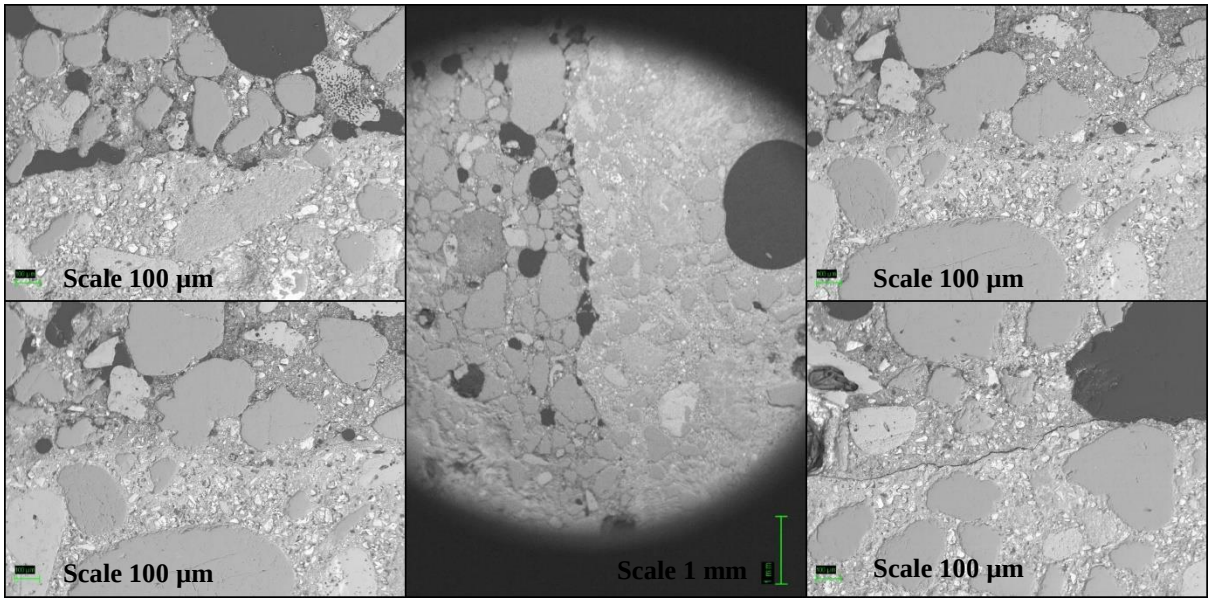

Figure 4-61: SEM images of control specimen subjected to room conditions

SEM images taken on the control specimen subjected to cyclic conditioning are presented in Figure 4-62. As seen in the images, the control repair material completely separated from the substrate due to the SEM sample preparation process (coring and cutting). This result indicated that the bond strength of the control specimen was greatly affected by cyclic conditioning.

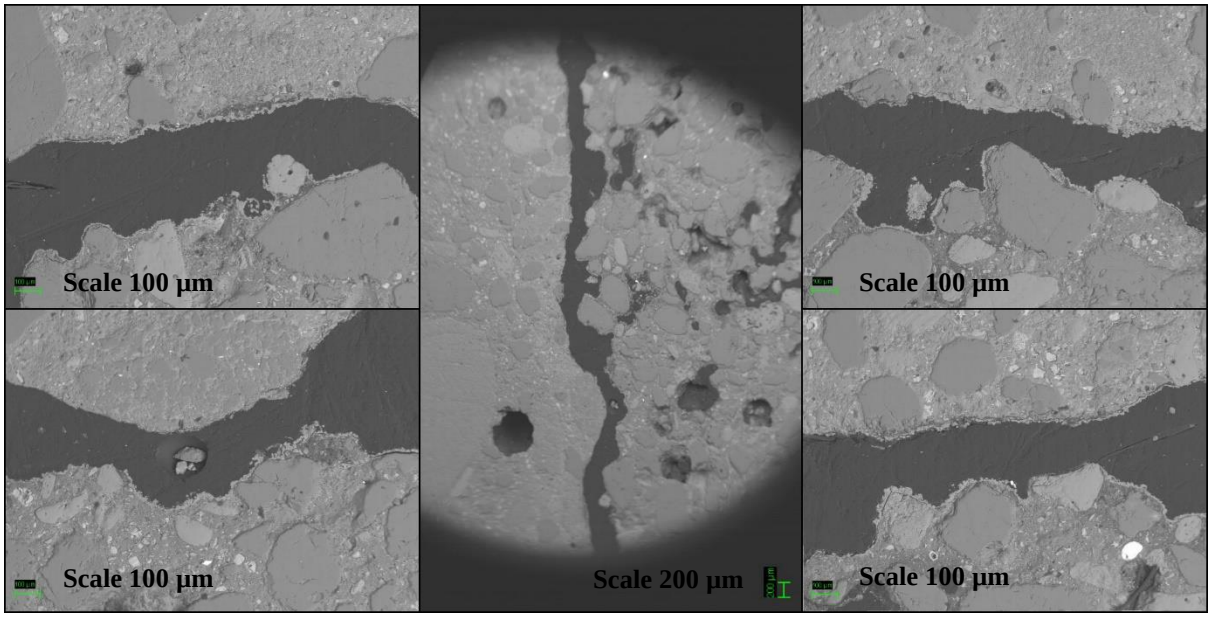

Figure 4-62: SEM images of control specimen subjected to cyclic conditioning

4.6 Summary of results

Table 4-3 summarises the key quantitative results of the experimental programme conducted in this dissertation.

Table 4-3: Summary of key quantitative experimental results

Test	100% FA	80% FA	60% FA	Polymer-cement concrete	Control
Slump (mm)	45	65	25	260	35
60 day compressive strength (MPa)	1.6	14.2	21.5	1.8	43.5
Density (kg/m^3)	1872	2102	2132	2137	2137
OPI	8.72	9.34	9.91	10.15	10.04
Permeability coefficient k (m/s)	1.93E-09	4.53E-10	1.24E-10	7.07E-11	9.12E-11
Sorptivity (mm/hr$^{0.5}$)	42.4	13.2	10.0	11.4	5.2
Porosity (%)	17.5	21.8	19.9	2.5	14.5
CCI Conductivity (mS/cm)*	13.33	4.05	2.13	0.14	1.26
Restrained shrinkage (ring) test crack age (days)	24	13	10	No cracks after 70 days	7
Accelerated drying shrinkage (μ-ε)	573	343	293	1517	415

* Note the relationship between a CCI value and expected chloride ingress for a high volume FA mix or polymer-cement concrete mix is not known which makes it difficult to interpret and compare the results obtained.

The bitumen concrete material developed in this thesis was found to exhibit extreme and abnormal shrinkage and subsequent cracking when applied to the substrate moulds. As a consequence the bitumen concrete material was found to be completely unsuitable for application to non-structural patch repairs. Therefore, experimental testing of this material was abandoned.

The FA repair material results generally show that a higher percentage of FA led to significant deterioration in the overall performance of the repair material. Furthermore, application of the FA mixes to substrate concrete was straight forward since the mixes had similar consistencies to the control repair mortar. Although innovative and resource sensitive, the 100% FA repair material exhibited poor durability and very low strength properties. This was likely due to the adoption of an unsuitable mix design and the ambient curing of the alkali activated fly ash rather than elevated temperature curing. However, a 100% FA mix would inherently have low strength since FA is a pozzolanic material with little cementitious properties on its own. The 100% FA material exhibited good crack resistance since deformations could be easily accommodated within the matrix due to the very low strength. However, the bonding performance of this material was very poor.

Upon analysis, the 100% FA specimens subjected to both room conditions and cyclic conditioning were found to completely separate from the substrate concrete. The 100% FA material developed in this study would thus not be suitable for any practical application to patch repairs due to its very low strength and poor bonding performance.

The 80% FA repair material displayed borderline performance properties. The restrained shrinkage performance of this material was good relative to the control. Restrained shrinkage rings cracked after 13 days which was almost double the time it took for the control rings to crack. Furthermore, the strength performance of this material was much better relative to the 100% FA repair material. The 80% FA material exhibited compressive strengths of up to 14 MPa after 60 days. However, the poor durability index test results meant that this material will not allow for any durable concrete repair application. Moreover, the 80% FA specimens subjected to cyclic conditioning showed clear signs of debonding and hence the bonding performance of this material was found to be unsatisfactory. It can be identified that both the 80% FA and 100% FA repair materials would fail to significantly improve the durability of non-structural patch repairs particularly in aggressive environments. The strength and bonding performance of the 80% FA and 100% FA materials could be improved by using certain admixtures (such as the polymer used in this study) which can be investigated in future studies.

In contrast, the 60% FA repair material exhibited satisfactory strength and durability performance. The compressive strength of this material was found to be up to 21 MPa after 60 days. This material exhibited the lowest accelerated drying shrinkage relative to all the other repair materials analysed. Furthermore, the 60% FA specimens subjected to cyclic conditioning exhibited good performance with respect to adhesion with no clear signs of debonding. The trend observed here was likely due to the cement content (40% by mass) that allowed for an improved matrix formation and thus improved penetrability and strength properties. It was found that the 60% FA repair material developed in this study has good potential to be effectively applied to non-structural patch repairs.

The polymer-cement concrete displayed very good performance with respect to crack resistance and durability (low penetrability and sorptivity). The polymer-cement concrete shrinkage rings showed no visible cracks even after 70 days of observation. This was despite the fact that the material exhibited high shrinkage (which is commonly perceived as bad) when tested under accelerated drying conditions. However, high shrinkage had no negative effect on crack resistance since the shrinkage was offset by the plastic nature of the polymer-cement concrete. Furthermore, bonding of the polymer-cement concrete was found to be very good even though the strength of the material was low. There was no evidence of debonding on any of the polymer-cement concrete specimens analysed under a microscope. These results show that such innovative materials cannot be assessed with the conventional testing philosophy that relates strength to performance. Application of the polymer-cement concrete material to substrate concrete was found to be difficult to some extent, relative to conventional repair mortars due to the very sticky nature of a freshly mixed polymer-cement concrete. However, the material could still be practically applied to patch repairs. The overall performance of the polymer-cement concrete was found to be good with potential to be effectively applied to patch repairs.

5 Conclusions and recommendations

5.1 Conclusions

The deterioration of RC structures due to steel corrosion is of great concern in civil engineering. The effects of steel corrosion including concrete cracking, delamination and spalling dramatically alter the movement of deleterious substances into concrete. Patch repairs are commonly applied to address spalling and corrosion induced damage on concrete structures. However, in practice patch repairs have been found to have very limited long-term performance. The ConRepNet report conducted by Matthews *et al*. (2003) has established that 50% of all concrete repairs fail prematurely with up to 75% of all repairs failing within the first 10 years of service. Patch repairs widely fail through the mechanisms of shrinkage induced cracking and debonding. These defects effectively restore a repaired concrete element back to a deteriorated state which facilitates the need to conduct repairs of repairs which is highly inefficient and has significant cost implications.

There are many reasons for the widespread failure of concrete patch repairs however, poor workmanship and differential shrinkage have been identified by Alexander & Beushausen (2009) to be the primary cause of poor performance of patch repairs. It has been identified that a correct and complete patch repair procedure will ensure a low failure rate. Provided that the underlying cause of steel corrosion is properly addressed and all the corroded steel is adequately treated or replaced, then the main requirement of a patch repair material on concrete affected by carbonation would be to simply fill in the cavity initially created by removing all defective concrete. For non-structural repairs on carbonation damaged concrete, the main purpose of the fill repair material would be to restore the aesthetics of the repaired element. This can fundamentally be achieved by any material that does not need to be a specialised repair mortar. However, in the case of chloride ion induced damage, any patch repair material also needs to provide adequate protection against the ingress of aggressive media into the repaired element. This is an important distinction between the repair requirements of carbonation and chloride ion induced corrosion.

The use of highly specialised commercially available repair materials for non-structural patch repairs is widespread in industry. These materials boast “superior” properties such as high elastic modulus and compressive strength gain. However, the use of such materials has shown no improvement in the durability of repaired elements. There is a common misconception that repairing corrosion damaged concrete with such high strength specialised materials will guarantee durability. However, this approach is principally incorrect and in many cases the use of such materials for non-structural repairs is probably not necessary. Moreover, research conducted at UCT by Beushausen & Bester (2016) and Chilwesa (2012) has established that high compressive strength materials may actually exhibit poor performance with respect to crack resistance. This is an important finding which identifies that structures repaired with high strength repair materials are unlikely to perform well with respect to long-term durability since they are exposed to cracking which dramatically accelerates the ingress of deleterious substances into concrete.

A major cause of the poor durability of concrete patch repairs can be attributed to the lack of technical understanding of the substrate-patch system. The theme of compatibility between substrate concrete and patch repair material is frequently mentioned in literature however, in practice compatibility is difficult to achieve. This is because a fresh patch repair material cannot be made to match the properties of older substrate concrete. Moreover, it is a challenge for engineers to select appropriate materials for patch repairs based on the theme of compatibility, particularly when standards based on the principles of compatibility are very limited. Additionally, the concrete repair industry is saturated with a range of commercially available repair materials which makes it further difficult to select an appropriate material. Also, the long-term durability performance of these materials is not well known. Furthermore, standards such as the EN 1504 typically specify prescriptive requirements of repair materials such as limiting compressive and bond strengths. However, these are usually determined in laboratory conditions and based on the widespread failure of concrete repairs is its clear that these do not relate to actual service conditions. It is important for the concrete repair industry to move towards performance based concrete repairs to ensure long-term durability and service life performance.

There is a need to have a fundamental understanding of the critical material properties actually required of patch-repair materials. An adequate substrate-patch bond and crack resistance are the core requirements of any repair material selected for a patch-repair programme. A seemingly substandard material that meets these principle requirements has the potential to outperform specialised repair materials in non-structural applications. In addition, any non-structural patch repair material also needs to exhibit good workability, low penetrability, quick setting time and good aesthetics. These performance parameters need to be met by any new repair material to be practically adopted for patch repairs. The development of an alternative and new patch repair material that may not be subjected to the same failure mechanisms as common cementitious based repair materials may provide a solution to the premature failure of concrete patch repairs.

The study presented in this thesis was therefore conducted in an effort to develop such new, unconventional and non-structural patch repair materials that could possibly be used to rehabilitate corrosion damaged concrete structures. Furthermore, the study aimed to provide an understanding of the fundamental reasons behind the poor performance of patch repairs. This study developed five new repair materials namely: 100% FA, 80% FA, 60% FA, bitumen and a polymer-cement concrete (5% cement replacement) repair materials. A broad experimental regime was conducted to establish the properties of these repair materials and determine whether they could be practically used for non-structural patch repairs. The experimental tests conducted included: the application of repair mortars to substrate concrete, analysing patch repairs under cyclic wetting and drying, microscopic analysis (SEM), oxygen permeability, water sorptivity, chloride ingress, restrained shrinkage (ring), accelerated drying shrinkage, slump, density and compressive strength tests. The results from these tests were analysed relative to a control and the following general conclusions were drawn out:

- The use of specialised and expensive commercially sourced repair materials is not required to ensure durability of non-structural patch repairs. The performance of the control repair mortar in this study has showed that high strength repair materials do not necessarily correlate to improved durability performance.
- With an increase in FA content from 60% to 100%, it was identified that there was a significant drop in overall performance with respect to durability and strength.
- The research complemented prior studies at UCT which identified that a high strength repair material directly correlates to increased risk of cracking as was evidenced by the early cracking of the high strength control ring specimens.

More specifically with respect to each repair material developed and investigated in this research project the following conclusions can be made:

- The bitumen repair material was found to exhibit extreme and abnormal shrinkage induced cracking and debonding on patch repairs after only three days. This material was therefore found to be unsuitable for application to patch repairs. Further testing of this material was therefore abandoned.
- With respect to crack resistance, the 100% FA repair material exhibited good performance with cracking of restrained ring specimens occurring after 24 days. Cyclic conditioning of the 100% FA patch repair revealed that the repair material had completely debonded throughout the perimeter of the substrate-patch interface. Furthermore, a very low compressive strength of 1.6 MPa (60 days), OPI of 8.72 and high sorptivity of 42.4 mm/hr$^{0.5}$ resulted in this material being very brittle and absorptive. Additionally, a high chloride conductivity of 13.33 mS/cm and accelerated drying shrinkage of 573 µ-ε was also obtained. Therefore, this material was found to exhibit very poor overall performance and it is concluded that the 100% FA repair material developed in this study is not suitable for any effective application to non-structural patch repairs. The principle reasons behind the poor performance of the 100% FA repair material can be attributed to the mix design and curing conditions adopted in the research. Particularly, it is known that ambient curing of alkali-activated FA is slow. It is expected that strength development will be accelerated at elevated temperature curing.
- The 80% FA restrained shrinkage rings cracked after 13 days, which was good relative to the control which cracked after only 7 days. 80% FA Patch repairs exhibited some debonding after cyclic conditioning. However, the debonding cases were isolated and much smaller in width compared to the 100% FA repair material. The compressive strength was determined to be 14.2 MPa (60 days). Durability index tests established an OPI of 9.34, chloride conductivity of 4.05 mS/cm and sorptivity of 13.2 mm/hr$^{0.5}$. A low accelerated drying shrinkage of 343 µ-ε was obtained for this material. The overall performance of this material was found to be borderline. It can be concluded that an 80% FA repair material is unlikely to significantly improve the durability of non-structural patch repairs and it will not provide sufficient long-term protection to reinforcement steel particularly, in aggressive environments.

- The 60% FA repair material exhibited low resistance to cracking with restrained shrinkage rings cracking after 10 days. However, 60% FA patch repairs subjected to cyclic conditioning exhibited good performance with no visible debonding identified. The compressive strength of the material was determined to be 21.5 MPa (60 days). An OPI of 9.91, chloride conductivity of 2.13 mS/cm and sorptivity of 10 mm/hr$^{0.5}$ was obtained. A low accelerated drying shrinkage value of 293 µ-ε was established. The overall performance of this material was found to be most promising relative to the other materials developed in this study. The results indicate that a 60% FA repair material could be applied to improve the durability of non-structural patch repairs. Though, supplementary research would be essential to optimise this material's performance as well as determine the field performance of this material, particularly in high carbon dioxide and chloride ion environments.
- The polymer concrete repair material investigated in this dissertation was found to exhibit very abnormal setting times. The surface of this repair material would quickly set, establishing an impermeable layer from which no water could easily evaporate from the interior of the material hence leading to slow setting. Therefore, it is concluded that the polymer concrete repair material developed in this study is not suitable for practical application to non-structural patch repairs, since this material will not set within a reasonable time frame. Furthermore, entrapped water within the patch repair may create aggressive conditions for corrosion to initiate.
- Shrinkage ring specimens of the polymer-cement concrete repair material exhibited no cracking since the material was not fully set and therefore, any deformations were not restrained. The polymer-cement concrete patch repair subjected to cyclic conditioning exhibited good performance with respect to debonding. A low compressive strength of 1.8 MPa was obtained after 60 days. An OPI of 10.15, chloride conductivity of 0.14 mS/cm and sorptivity of 11.4 mm/hr$^{0.5}$ was obtained. An extremely high accelerated drying shrinkage of 1517 µ-ε was exhibited by this material since it continuously contracted due to the slow setting and water loss process. The overall performance of the polymer-cement concrete material is concluded to be promising since when considered in isolation, strength does not really matter, neither does shrinkage. The excellent adhesion properties and crack resistance, as well as good durability index results indicate that this material can perform well when fully set.

5.2 Recommendations

This thesis has researched into the development of new and innovative non-structural patch repair materials with the aim of improving durability. However, the research conducted was by no means exhaustive and therefore the following recommendations are made for any future studies conducted in line with the theme of this research:

- This thesis was a feasibility study which was aimed at identifying alternative non-structural patch repair materials which in principle might be useful to study in future research. Costing of the different repair materials developed in this thesis was beyond the scope.

Therefore, it is recommended that future studies look into the optimisation of the 60% FA and polymer-cement concrete repair materials researched in this thesis in order to refine the knowledge to develop these materials into cost effective patch repair materials.

- It was identified that the 60% FA exhibited the best overall performance with 80% FA exhibiting borderline performance. Therefore, it is recommended that future studies investigate into a 70% FA mix (30% cement) which could also potentially exhibit promising performance.
- The polymer used in this thesis exhibited great adhesion and crack resistance properties. Therefore, future studies should look into the use of polymer as an admixture and possibly other admixtures, in the development of a 60% FA and 70% FA repair mortar mix in order to establish any improvements in performance with respect to strength, bonding and crack resistance.
- This thesis did not look into the long-term corrosion effects of the new materials developed. It is therefore recommended that future studies look into this particularly, with the 60% FA repair material since it exhibited good overall performance.
- The polymer-cement concrete developed in this thesis exhibited abnormal setting times yet, a fully set sample displayed good results with respect to durability performance. The amount of cement used in this study as polymer replacement was only 5% of the mass of total binder. It is therefore recommended that future studies investigate into polymer-cement concrete mixes with 10%, 15%, 20% and 25% cement replacements since a higher cement content will facilitate the removal of water from the polymer-cement concrete matrix thereby, allowing it to set within a reasonable time frame.
- The performance of the 60% FA repair material should be evaluated relative to widely used commercially available repair materials to determine its full potential as an effective patch repair material.
- It is recommended that future studies investigate into the development of a 100% FA repair material using a different mix design exposed to elevated temperature curing. The ambient cooling regime adopted in this thesis meant that strength development of the alkali-activated FA was very slow and this eliminated the material from any practical application. It is expected that strength development will be improved with elevated temperature curing which can be investigated in future studies. Furthermore, this study used only class F fly ash which has a low proportion of reactive calcium oxide that would otherwise facilitate the formation CSH compounds. It is therefore recommended that future studies look into the development of 100% FA repair material using class F fly ash. However, it must be noted that mostly class C FA is available in South Africa and hence the use of class F fly ash would not be applicable to the South African industry.

6 References

Abbasnia, R., Godossi, P. and Ahmadi, J., 2005. *Prediction of restrained shrinkage based on restraint factors in patching repair mortar*. Cement and concrete research, 35(10), pp. 1909-1913.

a.b.e.® Construction Chemicals, 2014. *Super Laykold Rubberised Bitumen Waterproofing Emulsion Technical Data Sheet*. Borsburg North, South Africa. Available at: http://abe.co.za/portfolio/super-laykold/ Accessed on the 23rd of March 2016 @ 12.56 p.m

Addis B J. & Owens G., 2009. *Fulton's Concrete Technology*. Chapter 27, Concrete repair by Hans Beushausen and Mark Alexander. Cement & Concrete Institute, South Africa.

Aggarwal, L.K., Thapliyal, P.C. and Karade, S.R., 2007. *Properties of polymer-modified mortars using epoxy and acrylic emulsions*. Construction and Building Materials, 21(2), pp. 379-383.

Alexander, M.G. & Beushausen, H.D., 2009. *Deformation and Volume Change of Hardened Concrete*. In Fulton's Concrete Technology. G. Owens, Ed. Ninth ed. South Africa: Cement and Concrete Institute. 111.

Alexander, M.G. and Beushausen, H., 2008. *Performance-based durability testing, design and specification in South Africa: latest developments*. Excellence in Concrete Construction through Innovation, pp.429-434.

Alexander, M. G. and Mindess, S., 2005. *Aggregates in Concrete*, published by Taylor and Francis.

Aloji, L., 2015. *Use of High Volume Fly Ash in Concrete*. International Journal of Scientific Research And Education, 3(07).

Aly, T. & Sanjayan, J.G., 2008. *Factors contributing to early age shrinkage cracking of slag concretes subjected to 7-days moist curing*. Materials and Structures, Vol. 41, pp. 633-642.

Andrade, C. and Alonso, C., 2001. *On-site measurements of corrosion rate of reinforcements*. Construction and building materials, 15(2), pp. 141-145.

Andrade, C., 1993. *Calculation of Chloride Diffusion Coefficients in Concrete from Ionic Migration Measurements*. Cement and Concrete Research, 23(3), pp. 724-742.

Arito P., 2012. *Discrete Sacrificial Anodes and Their Use in Service Life Extension of Chloride Contaminated Reinforced Concrete Structures*. MSc Dissertation, Department of Civil Engineering. University of Cape Town, South Africa.

Arjunan, P., Silsbee, M.R. and Roy, D.M., 2001. *Chemical activation of low calcium fly ash. Part 1: Identification of suitable activators and their dosage*. In 2001 International Ash Utilisation Symposium.

Arup, H., 1985. '*The mechanisms of the protection of steel by concrete', Corrosion of reinforcement in concrete construction*, SCI.

Bakharev, T., 2005. *Geopolymeric materials prepared using Class F fly ash and elevated temperature curing*. Cement and concrete research, 35(6), pp.1224-1232.

Ball, C., and Whitmore, D. W., 2009. *Embedded galvanic anodes for targeted protection in reinforced concrete structures*. Concrete Repair Bulletin, pp. 6-9.

Banthia, N., Zanotti, C. and Sappakittipakorn, M., 2014. *Sustainable fibre reinforced concrete for repair applications.* Construction and Building Materials, 67, pp. 405-412.

Banthia, N. and Gupta, R.., 2009. *Plastic shrinkage cracking in cementitious repairs and overlays.* Materials and structures, 42(5), pp. 567-579.

Bedi, R., Chandra, R. and Singh, S.P., 2014. *Reviewing some properties of polymer concrete*. Indian Concrete Journal, 88(8), pp.47-68.

Beeby, A.W., 1983. *Cracking, cover and corrosion of reinforcement*. Concrete International, 5(2), pp. 35-40.

Bentur, A. and Kovler, K., 2003. *Evaluation of early age cracking characteristics in cementitious systems*. Materials and Structures, 36(3), pp. 183-190.

Bentur, A., Berke, N. and Diamond, S., 1997. *Steel corrosion in concrete: fundamentals and civil engineering practice*. CRC Press.

Berry, M., Cross, D. and Stephens, J., 2009. *Changing the environment: an alternative "Green" concrete produced without Portland cement*. In Proc., World of Coal Ash Conf., Lexington, KY, USA.

Berry, M., Cross, D. and Stephens, J.E., 2009. *Performance of 100% fly ash concrete with 100% recycled glass aggregate*. In Transportation Research Board 88th Annual Meeting (No. 09-1570).

Bertolini, L., Elsener, B., Pedeferri, P., Redaelli, E. and Polder, R.B., 2013. *Corrosion of steel in concrete: prevention, diagnosis, repair*. John Wiley & Sons.

Beushausen, H.D. and Bester, N., 2016. *The influence of curing on restrained shrinkage cracking of bonded concrete overlays*. Cement and Concrete Research, 87, pp.87-96.

Beushausen, H.D. and Chilwesa, M., 2013. *Assessment and prediction of drying shrinkage cracking in bonded mortar overlays*. Cement and Concrete Research, 53, pp. 256-266.

Beushausen, H.D., Masuku, C. and Moyo, P., 2012. *Relaxation characteristics of cement mortar subjected to tensile strain*. Materials and structures, 45(8), pp.1181-1188.

Beushausen, H.D., 2010. *The influence of concrete substrate preparation on overlay bond strength*. Magazine of concrete research. 62(11) pp. 845-852.

Beushausen, H.D. and Alexander, M.G., 2009. Concrete Repair. Fulton's Concrete Technology. Chapter 27, Cement & Concrete Institute, South Africa.

Beushausen, H.D. and Alexander, M.G., 2007. *Performance of concrete patch repair systems*. In Advances in Construction Materials. Springer Berlin Heidelberg, pp. 255-262.

Beushausen, H.D. and Alexander, M.G., 2007. *Localised strain and stress in bonded concrete overlays subjected to differential shrinkage*. Materials and structures, 40(2), pp. 189-199.

Beushausen, H.D. and Alexander, M.G., 2006. *Failure mechanisms and tensile relaxation of bonded concrete overlays subjected to differential shrinkage*. Cement and Concrete Research. 36(10):1908-1914. DOI:http://dx.doi.org/10.1016/j.cemconres.2006.05.027.

Bignozzi, M.C., Saccani, A. and Sandrolini, F., 2002. *New polymer mortars containing polymeric wastes*. Part 2. Dynamic mechanical and dielectric behaviour. Composites Part A: applied science and manufacturing, 33(2), pp.205-211.Broomfield J.P., 1997. Corrosion of Steel in Concrete: Understanding, Investigation and Repair, E&FN SPON, London/New York.

Bignozzi, M.C., Saccani, A. and Sandrolini, F., 2000. *New polymer mortars containing polymeric wastes*. Part 1. Microstructure and mechanical properties. Composites Part A: applied science and manufacturing, 31(2), pp. 97-106.

Bissonnette, B., Courard, L., Fowler, D.W. and Granju, J.L. eds., 2011. *Bonded Cement-Based Material Overlays for the Repair, the Lining Or the Strengthening of Slabs Or Pavements*: State-of-the-Art Report of the RILEM Technical Committee 193-RLS (Vol. 3). Springer Science & Business Media.

Blaga, A. and Beaudoin, J.J., 1985. *Polymer concrete*. Concrete Institute for Research in Construction Publications. Canadian building digest, CBD-244.

Bockris, J., Conway, B., Yeager, E. and White, R. ed., 1981. *Comprehensive treatise of electrochemistry*. Electrochemical Materials Science, Vol. 4, Plenum Press: New York.

Browne, R.D., 1980. *Mechanisms of corrosion of steel in concrete in relation to design, inspection, and repair of offshore and coastal structures*. Special Publication, 65, pp. 169-204.

Bruns, M., and Raupach, M., 2009. *CP of the rear reinforcement in RC structures – Numerical modelling of the current distribution*. Concrete Repair, Rehabilitation and Retrofitting II – Alexander *et al* (Eds), Taylor & Francis Group, London, pp. 813-819.

Buenfeld, N. R., Shurafa-Daoudi, M. T. S., and McLoughlin, I. M., 1997. *Chloride transport due to wick action in concrete*. In Nilsson L. O., and Olliver J. P., Proceedings of RILEM international workshop on chloride penetration into concrete, Paris: RILEM.

Cabrera, J.G., 1996. *Deterioration of concrete due to reinforcement steel corrosion*. Cement and concrete composites, 18(1), pp. 47-59.

Castro P, Pazini E, Andrade C, Alonso C., 2003. *Macrocell activity in slightly chloride-contaminated concrete induced by reinforcement primers*. Corrosion, 59, pp. 535–46.

Chilwesa M., 2012. *Assessing the age at cracking of concrete repair mortars/overlays subjected to restrained drying shrinkage*. Master of Science thesis. Department of Civil Engineering Faculty of Engineering and Built Environment, University of Cape Town. South Africa.

Claisse, P., 2005. *Transport Properties of Concrete How movement on the molecular level affects design, construction, and durability*. Concrete international: Design & construction, (1), pp. 43-49.

Corral, R., Arredondo, S., Almaral, J. and Gómez, J., 2013. *Chloride corrosion of embedded reinforced steel on concrete elaborated from recycled coarse aggregates and supplementary cement materials.* Revista Ingeniería de Construcción, 28(1), pp.21-35.

Courard, L., Piotrowski, T. and Garbacz, A., 2014. *Near-to-surface properties affecting bond strength in concrete repair*. Cement and Concrete Composites, 46, pp. 73-80.

Courard, L., Lenaers, J.F., Michel, F. and Garbacz, A., 2011. *Saturation level of the superficial zone of concrete and adhesion of repair systems*. Construction and Building Materials, 25(5), pp.2488-2494.

Courard, L., 2002. *Evaluation of thermodynamic properties of concrete substrates and cement slurries modified with admixtures*. Materials and Structures, 35(3), pp.149-155.

Courard, L., 2000. *Parametric study for the creation of the interface between concrete and repair products*. Materials and structures, 33(1), pp.65-72.

Criado, M., Fernández-Jiménez, A. and Palomo, A., 2010. *Alkali activation of fly ash. Part III: Effect of curing conditions on reaction and its graphical description*. Fuel, 89(11), pp.3185-3192.

Cross, D., Stephens, J., Jones, W. and Leach, L., 2008. *Evaluation of the durability of 100 percent fly ash concrete*. Coal Combustion By-Products Consortium: Morgantown, WV.

Cross, D., Stephens, J. and Vollmer, J., 2005. *Structural applications of 100% fly ash concrete*. Proceedings, World of Coal Ash, Lexington, KY.

Cross, J. and Stephens, J., 2005. *An alternative to Portland cement concrete*. In Proceedings of the third international construction materials: performance, innovations and structural implications and mindess symposium conference on, Vancouver, Canada.

Cusson, D. and Mailvaganam, N., 1996. *Durability of repair materials.* Concrete International-Design and Construction, 18(3), pp. 34-38.

Czarnecki, L., 2008. *Adhesion–A challenge for concrete repair*. In Concrete Repair, Rehabilitation and Retrofitting II: 2nd International Conference on Concrete Repair, Rehabilitation and Retrofitting, ICCRRR-2, 24-26 November 2008, Cape Town, South Czarnecki L, Emmons PH. Repair and protection of concrete

Czarnecki, L. and Emmons, P.H., 2000. *Repair and protection of concrete structures*. Kraków: Polski Cement. pp. 193–202.

Dalven Products, n.d. *Waterblok rubberised bitumen emulsion waterproofing compound product sheet.* Cape Town, South Africa.

Davidovits, J., 1999. *Chemistry of geopolymeric systems, terminology*. In Geopolymer Vol. 99, No. 292. pp. 9-39.

Davidovits, J., 1988. *Geopolymer chemistry and properties*. In Geopolymer, Vol. 88, No. 1. pp. 25-48.

Denarié, E., Silfwerbrand, J., and Beushausen, H., 2011. *Structural behaviour. Bonded cement-based material overlays for the repair, the lining or the strengthening of slabs or pavements*. Bissonnette *et al* (Eds). State-of-the Art Report of the RILEM Technical Committee 193-RLS. Volume 3. Springer. pp. 81-106.

Diaz, E.I., Allouche, E.N. and Eklund, S., 2010. *Factors affecting the suitability of fly ash as source material for geopolymers*. Fuel, 89(5), pp.992-996.

Dillard, J.G., Glanville, J.O., Collins, W.D., Weyres, R.E. and Al-Qadi, I.L., 1993. *Concrete Bridge Protection and Rehabilitation: Chemical and Physical Techniques*. Feasibility Studies of New Rehabilitation Techniques (No. SHRP-S-665), Strategic Highway Research Program, Washington, DC, pp. 169.

Emberson, N.K. and Mays, G.C., 1990. *Significance of property mismatch in the patch repair of structural concrete Part 1: Properties of repair systems*. Magazine of Concrete Research, 42(152), pp. 147-160.

Emmons, P.H. and Sordyl, D.J., 2006. *The state of the concrete repair industry, and a vision for its future*. Concrete repair bulletin, pp. 7-14.

Emmons PH, Vaysburd AM., 1997. *Corrosion protection in concrete repair: myth and reality*. Concr Int;19 pp. 47–56.

Emmons, P.H., Vaysburd, A.M. and McDonald, J.E., 1993. *A rational approach to durable concrete repairs*. Concrete International-Detroit-, 15, pp. 40-40.

EN 1504, 2003. *Products and systems for the protection and repair of concrete structures – Definitions – Requirements – Quality control and evaluation of conformity*. CEN (Brussels).

Fernández-Jiménez, A. and Palomo, A., 2003. *Characterisation of fly ashes. Potential reactivity as alkaline cements*. Fuel, 82(18), pp.2259-2265.

Ferro, G., Tulliani, J.M., Lopez, A. & Jagdale, P., 2015. *New cementitious composite building material with enhanced toughness*. Theoretical and Applied Fracture Mechanics. 76:67-74. DOI:http://dx.doi.org/10.1016/j.tafmec.2015.01.005.

Fraczek, J., 1987. *Review of Electrochemical Principles as Applied to Corrosion of Steel in a Concrete or Grout Environment*. ACI Special Publication, pp. 13-24.

Fowler, D.W., 1999. *Polymers in concrete: a vision for the 21st century*. Cement and Concrete Composites, 21(5), pp. 449-452.

Foley, R., 1970. *Role of the Chloride Ions in Iron Corrosion*. Corrosion, 26(2), pp. 58-70.

Garbacz, A., Górka, M. and Courard, L., 2005. *Effect of concrete surface treatment on adhesion in repair systems*. Magazine of Concrete Research, 57(1), pp. 49-60.

Glass, G. K., Hassanein, A. M., and Buenfeld, N. R., 2001. *Cathodic protection afforded by an intermittent current applied to reinforced concrete*. Corrosion Science, 43, pp. 1111-1131

Gouda, V. K., 1970. C*orrosion and Corrosion Inhibition of Reinforcing Steel I: Immersed in Alkaline Solutions*. British Corrosion Journal. pp. 198-203.

Gouda , V. K. and Halaka, W. Y., 1970. *Corrosion and Corrosion Inhibition of Reinforcing Steel II: Embedded in Concrete*. British Corrosion Journal. pp. 204-208.

Gutsch, A. and Rostásy, F.S., 1994. *Young Concrete Under High Tensile Stresses-Creep, Relaxation and Cracking.* In Thermal Cracking in Concrete at Early Ages: Proceedings of the International RILEM Symposium (Vol. 25, p. 111). CRC Press.

Hassan, K.E., Brooks, J.J. and Al-Alawi, L., 2001. *Compatibility of repair mortars with concrete in a hot-dry environment*. Cement and Concrete Composites, 23(1), pp. 93-101.

Hansen, E.J. and Saouma, V.E., 1999. *Numerical simulation of reinforced concrete deterioration: Part II–steel corrosion and concrete cracking*. ACI Materials Journal, 96(3), pp. 331-338.

Hansson, C.M., Poursaee, A. and Jaffer, S.J., 2007. *Corrosion of reinforcing bars in concrete*. Portland Cement Association (PCA), PCA R&D Serial, (3013).

Hansson, C. M.and Sørensen, B., 1990. *The Threshold Concentration of Chloride in Concrete for the Initiation of Reinforcement Corrosion*. in Corrosion Rates of Steel in Concrete, Baltimore, Maryland, USA, ASTM STP 1065.

Heckroodt, R. O., 2002, *Guide to deterioration and failure of building materials*, published by Thomas Telford Ltd, 1 Heron Quay, London E14 4JD.

Hendrik Van Oss G., 2007. *Prepared for the US geological survey*. Mineral commodity summaries.

Holl, C.H. and O'Connor, S.A., 1997. *Cleaning and preparing concrete before repair*. Concrete International, 19(3).

Holt, E.E., 2001. *Early age autogenous shrinkage of concrete* (Vol. 446). Technical Research Centre of Finland. VTT Publications 446, Finland.

Hossain, A.B. and Weiss, J., 2004. *Assessing residual stress development and stress relaxation in restrained concrete ring specimens*. Cement and Concrete Composites, 26(5), pp. 531-540.

Jung, K.C., Roh, I.T. and Chang, S.H., 2015. *Thermal behaviour and performance evaluation of epoxy-based polymer concretes containing silicone rubber for use as runway repair materials*. Composite Structures, 119, pp. 195-205.

Katz, A., 1998. *Microscopic study of alkali-activated fly ash*. Cement and Concrete Research, 28(2), pp.197-208.

Kim, M.O., Bordelon, A., Lee, M.K. and Oh, B.H., 2016. *Cracking and failure of patch repairs in RC members subjected to bar corrosion*. Construction and Building Materials, 107, pp. 255-263.

Komljenović, M., Baščarević, Z. and Bradić, V., 2010. *Mechanical and microstructural properties of alkali-activated fly ash geopolymers*. Journal of Hazardous Materials, 181(1), pp.35-42.

Kovalchuk, G., Fernández-Jiménez, A. and Palomo, A., 2007. *Alkali-activated fly ash: effect of thermal curing conditions on mechanical and microstructural development–Part II*. Fuel, 86(3), pp.315-322.

Kristiawan, S.A., 2013. *Performance Criteria to Assess Shrinkage Cracking Tendency in Concrete Overlay*. Procedia Engineering, 54, pp. 82-100.

Lacombe, P. Beaupré, D. and Pouliot, N., 1999. *Rheology and bonding characteristics of selfleveling concrete as a repair material*. Materials and Structures, vol.32, no.222, pp. 593-600.

Latif, M.A., Naganathan, S., Razak, H.A. and Mustapha, K.N., 2015. *Performance of Lime Kiln Dust as Cementitious Material*. Procedia Engineering, 125, pp. 780-787.

Lee, M.G., Wang, Y.C. and Chiu, C.T., 2007. *A preliminary study of reactive powder concrete as a new repair material*. Construction and Building Materials, 21(1), pp. 182-189.

Leek, D. S. and Poole, A. S., 1990. T*he Breakdown of the passive film on high yield mild steel by chloride ions, Corrosion of Reinforcement in Concrete*. Society of Chemical Industry, Elsevier, London, pp. 65-73.

Li, M. and Li, V.C., 2011. *High-Early-Strength Engineered Cementitious Composites for Fast, Durable Concrete Repair-Material Properties*. ACI materials journal, 108(1).

Li, M., 2009. *Multi-scale design for durable repair of concrete structures*. Doctoral dissertation, Department of Civil Engineering. University of Michigan, United States.

Lohani, T.K., Jena, S., Dash, K.P. and Padhy, M., 2012. *An experimental approach on Geopolymeric recycled concrete using partial replacement of industrial by-product*. International Journal of Civil & Structural Engineering, 3(1), pp. 141-149.

Lukovic, M., Ye, G. and Van Breugel, K., 2012. *Reliable concrete repair: A critical review*. In 14th International Conference Structural Faults and Repair, Edinburgh, Scotland, UK, 3-5 July 2012.

Mackechnie, J.R. and Alexander, M.G., 2002. *Durability predictions using early-age durability index testing*. In Proc. Ninth Durability and Building Materials Conference, Australian Corrosion Association, Brisbane, Australia.

Mackechnie, J. R. and Alexander, M. G., 2001. *Repair principles for corrosion-damaged reinforced concrete structures*. Research monograph No. 5, Department of Civil Engineering, University of Cape Town.

Malhotra, V.M. and Ramezanianpour, A.A., 1994. *Fly Ash in Concrete*, second ed., CANMET, Ottawa.

Mangat, P.S. and O'Flaherty, F.J., 2000. *Influence of elastic modulus on stress redistribution and cracking in repair patches.* Cement and Concrete Research, 30(1), pp. 125-136.

Mapei, 2011. *Protection and Repair of concrete in compliance with European Standard UNI EN 1504, Technical Manual*. Milan, Italy.

Martinola, G., Sadouki, H. and Wittmann, F.H., 2001. *Numerical model for minimizing risk of damage in repair system*. Journal of materials in civil engineering, 13(2), pp. 121-129.

Matthews, S., Holton, I., Morlidge, J. and Pool, R., 2003. *ConRepNet: a thematic network on performance-based rehabilitation of reinforced concrete structures*. Concrete, 37(8).

Mauroux, T., Benboudjema, F., Turcry, P., Aït-Mokhtar, A., and Deves, O., 2012. *Study of cracking due to drying in coating mortars by digital image correlation*. Cement and Concrete Research, 42, pp. 1014-1023.

Mays, G.C. and Wilkinson, W.B., 1987. *Polymer repairs to concrete: their influence on structural performance.* Special Publication, 100, pp. 351-376.

Mehta, K.P. & Monteiro, P.J.M., 2006. *Dimension Stability. In Concrete: Microstructure, Properties and Materials*. Third ed. United States of America: McGraw-Hill Companies. 85.

Mehta, P.K., 2004. *High-performance, high-volume fly ash concrete for sustainable development*. In Proceedings of the international workshop on sustainable development and concrete technology (pp. 3-14). Ames, IA, USA: Iowa State University.

Michigan department of transportation (MDOT), 1996. *Research record evaluating pavement patching materials polymers and elastomeric concretes, issue number 81*. Michigan Department of Transportation's Materials and Technology Division. Available at: https://www.michigan.gov/documents/mdot_c&t_rr-81_67067_7.pdf. Accessed on the 18th of April 2016 @ 16:00pm.

Miyagawa, T., 1991. '*Durability design and repair of concrete structures: chloride corrosion of reinforcing and alkali aggregate reaction'*. Magazine of Concrete Research, 43(156), pp. 155-170.

Moghtadaei, R.M., Mohammadi, M., Samani, N.A. and Mousavi, S., 2015. *The impact of surface preparation on the bond strength of repaired concrete by metakaolin containing concrete*. Construction and Building Materials, 80, pp. 76-83.

Momayez, A., Ehsani, M.R., Rajaie, H. and Ramezanianpour, A., 2005. *Cylindrical specimen for measuring shrinkage in repaired concrete members*. Construction and Building Materials, 19(2), pp. 107-116.

Montoya, R., Aperador, W., and Bastidas, D. M., 2009. *Influence of conductivity on cathodic protection of reinforced alkali-activated slag mortar using the finite element method.* Corrosion Science, 51, pp. 2857-2862.

Morgan, D.R., 1996. *Compatibility of concrete repair materials and systems*. Construction and building materials, 10(1), pp. 57-67.

Naidu, P.V. and Pandey, P.K., 2014. *Replacement of Cement in Concrete.* International Journal of Environmental Research and Development. ISSN 2249-3131 Volume 4, Number 1 pp. 91-98 © Research India Publications http://www.ripublication.com/ijerd.htm.

Nilssson, L. O., Poulsen, E., Sandberg, P., Sorensen, H. E. and Klinghoffer, O., 1996. *Chloride penetration into concrete, state-of-the-art, transport processes, corrosion initiation, test methods and prediction models*. HETEK Report No. 53.

Nielsen, A., 1985. *Concrete Durability, The Concrete Book* (Beton Bogen), A.D. Herholdt, *et al*., Editors, Aalborg Portland.

Nkemba L., 2016. *Verbal communication*. Centre for Minerals Research, University of Cape Town.

Nóvoa, P.J.R.O., Ribeiro, M.C.S., Ferreira, A.J.M. and Marques, A.T., 2004. *Mechanical characterization of lightweight polymer mortar modified with cork granulates*. Composites science and technology, 64(13), pp. 2197-2205.

Oh, B.H., Kim, K.H. and Jang, B.S., 2009. *Critical corrosion amount to cause cracking of reinforced concrete structures*. ACI materials journal, 106(4), pp. 333-339.

Otieno, M., Alexander, M. and Beushausen, H., 2010. *Transport mechanisms in concrete, corrosion of steel in concrete and assessment of corrosion*. Research report, Concrete Materials and Structural Integrity Research Group, University of Cape Town, South Africa.

Otieno, M., *2008. Corrosion Propagation in Cracked and Uncracked Concrete*. Master of Science in Engineering dissertation, Faculty of Engineering and the Built Environment, University of Cape Town, South Africa.

Owens, G. ed., 2012. *Fundamentals of concrete*. Cement and Concrete Institute, South Africa, pp. 123-127.

Owens, G. ed., 2009. *Fulton's concrete technology*. Cement & Concrete Institute. Midrand, South Africa.

Pacheco-Torgal, F. and Labrincha, J.A., 2013. *The future of construction materials research and the seventh UN Millennium Development Goal: A few insights*. Construction and building materials, 40, pp. 729-737.

Paulsson, J. T. and Johan, S., 2002. *Estimation of chloride ingress in uncracked and cracked concrete using measured surface concentrations*. ACI Materials Journal, 99(1).

Perez, F., Morency, M., Bissonnette, B. and Courard, L., 2008. *Correlation between the roughness of the substrate surface and the debonding risk*. In Concrete Repair, Rehabilitation and Retrofitting II: 2nd International Conference on Concrete Repair, Rehabilitation and Retrofitting, ICCRRR-2, 24-26 November 2008, Cape Town, South Africa (p. 347). CRC Press.

Pretorius, J. and Kruger, D., 2001. *The influence of surface roughness on the bond strength of concrete repairs*. Proc. 10th ICPIC 2001, 13.

Puyate, Y.T. and Lawrence, C.J., 1999. *Effect of solute parameters on wick action in concrete*. Chemical engineering science, 54(19), pp. 4257-4265.

Qian, S., Zhang, J. and Qu, D., 2006. *Theoretical and experimental study of microcell and macrocell corrosion in patch repairs of concrete structures*. Cement and Concrete Composites, 28(8), pp. 685-695.

Quillin, K., 2001. *Performance of belite–sulfoaluminate cements.* Cement and Concrete Research, 31(9), pp. 1341-1349.

Rangan, B.V., Hardjito, D., Wallah, S.E. and Sumajouw, D.M., 2005. *Studies on fly ash-based geopolymer concrete*. In Proceedings of the World Congress Geopolymer, Saint Quentin, France Vol. 28, pp. 133-137.

Raupach, M., 2006. *Patch repairs on reinforced concrete structures–Model investigations on the required size and practical consequences*. Cement and Concrete Composites, 28(8), pp. 679-684.

Raupach, M., 2005. *Concrete repair according to the new European standard EN 1504*. Integrative Oncology: Principles and Practice, pp 6.

Raupach, M., 1996. *Chloride-induced macrocell corrosion of steel in concrete-theoretical background and practical consequences*. Construction Building Materials, 10, pp. 329–38.

Ribeiro, M.C.S., Meira-Castro, A.C., Silva, F.G., Santos, J., Meixedo, J.P., Fiúza, A., Dinis, M.L. and Alvim, M.R., 2013. *Re-use assessment of thermoset composite wastes as aggregate and filler replacement for concrete-polymer composite materials*: A case study regarding GFRP pultrusion wastes. Resources, Conservation and Recycling.

Rivera, F., Martínez, P., Castro, J. and López, M., 2015. *Massive volume fly-ash concrete: A more sustainable material with fly ash replacing cement and aggregates*. Cement and Concrete Composites, 63, pp. 104-112.

Roh, I.T., Jung, K.C., Chang, S.H. and Cho, Y.H., 2015. *Characterization of compliant polymer concretes for rapid repair of runways*. Construction and Building Materials, 78, pp. 77-84.

Rosenberg, A., Hansson, C.M. and Andrade, C., 1989. *Mechanisms of corrosion of steel in concrete*. Materials science of concrete, 1, pp. 285-314.

Santos, P.M. and Julio, E.N., 2007. *Correlation between concrete-to-concrete bond strength and the roughness of the substrate surface*. Construction and Building Materials, 21(8), pp. 1688-1695.

Saribiyik, M., Piskin, A. and Saribiyik, A., 2013. *The effects of waste glass powder usage on polymer concrete properties*. Construction and building materials, 47, pp. 840-844.

Sergi, G., and Page, C. L., 1999. *Sacrificial anodes for cathodic protection of reinforcing steel around patch repairs applied to chloride-contaminated concrete.* Eurocorr ’99, pp. 1-9.

Sharif, A., Loughlin, K. F., Azad, A. K. and Nawaz, C. M., 1999. *Determination of the effective diffusion coefficient in concrete via a gas diffusion technique*. Proceedings of the international conference on concrete durability and repair technology, Edited by Dhir R. K. and McCarthy M. J., published by Thomas Telford.

Shaw, M., n.d. *A Guide to the Concrete Repair European Standards BS EN 1504 Series*. Sika Limited, Watchmead, Welwyn Garden City, Hertfordshire, pp. 12-13.

Shekhovtsova, J., 2015. *Using South African fly ash as a component of alkali-activated binder*. Doctoral thesis. Faculty of Engineering, Built Environment and Information Technology. University of Pretoria, South Africa.

Shreir, L. ed., 1979. Corrosion Volume 1, Metal/Environment Reactions, Newnes-Butterworths: London cited by Scott A.N. (2004), *The Influence of Binder Type and Cracking on Reinforcing Steel Corrosion in Concrete*. PhD Thesis, University of Cape Town.

Silfwerbrand, J. & Beushausen, H-D., 2005. *Bonded concrete overlays – bond strength issue.* Proceedings of the international conference on concrete repair, rehabilitation and retrofitting ICCRRR, Cape Town. pp. 19-21.

Silfwerbrand, J., 2003. *Shear bond strength in repaired concrete structures*. Materials and structures. 36(6), pp. 419-424.

Silfwerbrand, J. and Paulsson, J., 1998. *Better bonding of bridge deck overlays*. Concrete International, 20(10), pp.56-61.

Sisomphon, K. and Franke, L., 2007. *Carbonation rates of concrete containing high volume of pozzolanic materials*. Cement and Concrete Research, 37, pp. 1647-1653.

Smith, J.L. and Virmani, Y.P., 2000. *Materials and methods for corrosion control of reinforced and prestressed concrete structures in new construction* (No. FHWA-RD-00-081).

Somna, K., Jaturapitakkul, C., Kajitvichyanukul, P. and Chindaprasirt, P., 2011. *NaOH-activated ground fly ash geopolymer cured at ambient temperature*. Fuel, 90(6). pp.2118-2124.

Song, G. and Shayan, A., 1998. C*orrosion of steel in concrete: causes, detection and prediction: a state-of-the-art review* (No. 4).

Soraru, G.D. and Tassone, P., 2004. *Mechanical durability of a polymer concrete: a Vickers indentation study of the strength degradation process*. Construction and Building Materials, 18(8), pp.561-566.

Taffesea, W.Z. and Sistonen, E., 2013. *Service life prediction of repaired structures using concrete recasting method: state-of-the-art*. Procedia Engineering, 57, pp. 1138-1144.

Talotti M., 2014. *Influence of Substrate Moisture Preparation on Concrete Overlay Bond Strength*. MSc Thesis. Department of Civil Engineering, Concrete Materials and Structural Integrity Research Unit, Faculty of Engineering and Built Environment. University of Cape Town, South Africa.

Tuutti K., 1982. *Corrosion of Steel in Concrete*. Swedish Cement and Concrete Research Institute.

Torres-Acosta A.A, Sagues A.A., 2004. *Concrete cracking by localized steel corrosion-Geometric effects*. ACI Materials Journal, 101(6), pp. 501-507.

CoMSIRU, 2010. *Durability Index Testing Procedure Manual*. Version 2.0. University of Cape Town.

USDoT., 2001. *Long-Term effectiveness of cathodic protection systems on highway structures*. Publication No. FHWA-RD-01-096, pp. 95.

Vaysburd, A. M. and Emmons, P.H., 2006. *Concrete repair – a composite system: philosophy, engineering and practice*. Proceedings of the international conference on concrete repair,

rehabilitation and retrofitting ICCRRR, Cape Town, 21-23 Nov. 2005. London: Taylor & Francis, pp. 9-11.

Vaysburd, Alexander M., 2006. *"Holistic system approach to design and implementation of concrete repair."* Cement and Concrete composites 28.8 pp. 671-678.

Vaysburd, A.M., Emmons, P.H., Mailvaganam, N.P., McDonald, J.E. and Bissonnette, B., 2004. *Concrete repair technology-a revised approach is needed*. Concrete international, 26(1), pp. 59-65.

Vu, K., Stewart, M.G. and Mullard, J., 2005. *Corrosion-induced cracking: experimental data and predictive models*. ACI structural journal, 102(5), pp. 719.

Winnefeld, F., Leemann, A., Lucuk, M., Svoboda, P. and Neuroth, M., 2010. *Assessment of phase formation in alkali activated low and high calcium fly ashes in building materials*. Construction and building materials, 24(6), pp.1086-1093.

Wittmann, F.H. and Martinola, G., 2003. *Decisive properties of durable cement-based coatings for reinforced concrete structures*. International Journal for Restoration of Buildings and Monuments, 9(3), pp.235-264.

Xu, H. and Van Deventer, J.S.J., 2000. *The geopolymerization of alumino-silicate minerals*. International Journal of Mineral Processing, 59(3), pp.247-266.

Zhu, Y., 1992. *Effect of surface moisture condition on bond strength between new and old concrete*. Department of Structural Mechanics and Engineering, Royal Institute of Technology, Stockholm, Bulletin No. 159.

Zhou, J., 2011. *Performance of engineered cementitious composites for concrete repairs*. TU Delft, Delft University of Technology.

Zhou, Q., Milestone, N.B. and Hayes, M., 2006. *An alternative to Portland cement for waste encapsulation—the calcium sulfoaluminate cement system*. Journal of hazardous materials, 136(1), pp. 120-129.

7 Appendices

Appendix A Raw experimental data

A1 Compressive strength and density tests

100% FA 7 days								
Cube No.	**Mass (kg)**	**Dimension (mm)**	**Dimension (mm)**	**Dimension (mm)**	**Volume (m^3)**	**Density (kg/m^3)**	**Strength (kN)**	**Strength (MPa)**
1	1,850	100	100	97	0,00097	1907	12,0	1,20
2	1,910	100	100	97	0,00097	1969	13,0	1,30
3	1,920	100	100	98	0,00098	1959	12,0	1,20
Average	1,893	100	100	97	0,00097	1945	12,3	**1,23**

100% FA 14 days								
Cube No.	**Mass (kg)**	**Dimension (mm)**	**Dimension (mm)**	**dimension (mm)**	**Volume (m^3)**	**Density (kg/m^3)**	**Strength (kN)**	**Strength (MPa)**
1	1,860	100	100	97	0,00097	1918	19,0	1,90
2	1,855	100	100	98	0,00098	1893	18,0	1,80
3	1,830	100	100	97	0,00097	1887	18,0	1,80
Average	1,848	100	100	97	0,00097	1899	18,3	**1,83**

100% FA 28 days								
Cube No.	**Mass (kg)**	**Dimension (mm)**	**Dimension (mm)**	**Dimension (mm)**	**Volume (m^3)**	**Density (kg/m^3)**	**Strength (kN)**	**Strength (MPa)**
1	1,825	100	100	99	0,00099	1843	14,0	1,40
2	1,855	100	100	99	0,00099	1874	16,0	1,60
3	1,840	100	100	99	0,00099	1859	16,0	1,60
Average	1,84	100	100	99	0,00099	1859	15,3	**1,53**

100% FA 60 days								
Cube No.	**Mass (kg)**	**Dimension (mm)**	**Dimension (mm)**	**Dimension (mm)**	**Volume (m^3)**	**Density (kg/m^3)**	**Strength (kN)**	**Strength (MPa)**
1	1,780	100	100	99	0,00099	1798	17,0	1,70
2	1,775	100	100	100	0,00100	1775	15,0	1,50
3	1,785	100	100	100	0,00100	1785	16,0	1,60
Average	1,780	100	100	100	0,00100	1786	16,0	**1,60**

80% FA 7 days								
Cube No.	**Mass (kg)**	**Dimension (mm)**	**Dimension (mm)**	**Dimension (mm)**	**Volume (m^3)**	**Density (kg/m^3)**	**Strength (kN)**	**Strength (MPa)**
1	2,090	100	100	99	0,00099	2111	32,0	3,20
2	2,050	100	100	99	0,00099	2071	34,0	3,40
3	2,030	100	100	99	0,00099	2051	31,0	3,10
Average	2,057	100	100	99	0,00099	2077	32,3	**3,23**

80% FA 14 days								
Cube No.	**Mass (kg)**	**Dimension (mm)**	**Dimension (mm)**	**Dimension (mm)**	**Volume (m^3)**	**Density (kg/m^3)**	**Strength (kN)**	**Strength (MPa)**
1	2,075	100	100	97	0,00097	2139	59,0	5,90
2	2,070	100	100	97	0,00097	2134	65,0	6,50
3	2,060	100	100	98	0,00098	2102	54,0	5,40
Average	2,068	100	100	97	0,00097	2125	59,3	**5,93**

80% FA 28 days								
Cube No.	**Mass (kg)**	**Dimension (mm)**	**Dimension (mm)**	**Dimension (mm)**	**Volume (m^3)**	**Density (kg/m^3)**	**Strength (kN)**	**Strength (MPa)**
1	2,035	100	100	97	0,00097	2098	80,0	8,00
2	2,115	100	100	99	0,00099	2136	79,0	7,90
3	2,045	100	100	97	0,00097	2108	82,0	8,20
Average	2,065	100	100	98	0,00098	2114	80,3	**8,03**

80% FA 60 days								
Cube No.	**Mass (kg)**	**Dimension (mm)**	**Dimension (mm)**	**Dimension (mm)**	**Volume (m^3)**	**Density (kg/m^3)**	**Strength (kN)**	**Strength (MPa)**
1	2,080	100	100	99	0,00099	2101	144,0	14,40
2	2,060	100	100	99	0,00099	2081	142,0	14,20
3	2,065	100	100	99	0,00099	2086	140,0	14,00
Average	2,068	100	100	99	0,00099	2089	142,0	**14,20**

60% FA 7 days								
Cube No.	**Mass (kg)**	**Dimension (mm)**	**Dimension (mm)**	**Dimension (mm)**	**Volume (m^3)**	**Density (kg/m^3)**	**Strength (kN)**	**Strength (MPa)**
1	2,065	100	100	99	0,00099	2086	99,0	9,90
2	2,135	100	100	100	0,00100	2135	107,0	10,70
3	2,095	100	100	99	0,00099	2116	96,0	9,60
Average	2,098	100	100	99	0,00099	2112	100,7	**10,07**

60% FA 14 days								
Cube No.	**Mass (kg)**	**Dimension (mm)**	**Dimension (mm)**	**Dimension (mm)**	**Volume (m^3)**	**Density (kg/m^3)**	**Strength (kN)**	**Strength (MPa)**
1	2,105	100	100	100	0,00100	2105	129,0	12,90
2	2,135	100	100	101	0,00101	2114	122,0	12,20
3	2,165	100	100	101	0,00101	2144	139,0	13,90
Average	2,135	100	100	101	0,00101	2121	130,0	**13,00**

60% FA 28 days								
Cube No.	**Mass (kg)**	**Dimension (mm)**	**Dimension (mm)**	**Dimension (mm)**	**Volume (m^3)**	**Density (kg/m^3)**	**Strength (kN)**	**Strength (MPa)**
1	2,100	100	100	98	0,00098	2143	176,0	17,60
2	2,110	100	100	99	0,00099	2131	164,0	16,40
3	2,115	100	100	100	0,00100	2115	181,0	18,10
Average	2,108	100	100	99	0,00099	2130	173,7	**17,37**

60% FA 60 days								
Cube No.	**Mass (kg)**	**Dimension (mm)**	**Dimension (mm)**	**Dimension (mm)**	**Volume (m^3)**	**Density (kg/m^3)**	**Strength (kN)**	**Strength (MPa)**
1	2,155	100	100	99	0,00099	2177	215,0	21,50
2	2,110	100	100	98	0,00098	2153	209,0	20,90
3	2,145	100	100	99	0,00099	2167	220,0	22,00
Average	2,137	100	100	99	0,00099	2166	214,7	**21,47**

Polymer-cement concrete 7 days								
Cube No.	**Mass (kg)**	**Dimension (mm)**	**Dimension (mm)**	**Dimension (mm)**	**Volume (m^3)**	**Density (kg/m^3)**	**Strength (kN)**	**Strength (MPa)**
1	2,155	100	100	101	0,00101	2134	4,0	0,40
2	2,055	100	100	99	0,00099	2076	5,0	0,50
3	2,135	100	100	99	0,00099	2157	4,5	0,45
Average	2,115	100	100	100	0,00100	2122	4,5	**0,45**

Polymer-cement concrete 14 days								
Cube No.	**Mass (kg)**	**Dimension (mm)**	**Dimension (mm)**	**Dimension (mm)**	**Volume (m^3)**	**Density (kg/m^3)**	**Strength (kN)**	**Strength (MPa)**
1	2,120	100	100	99	0,00099	2141	7,0	0,70
2	2,130	100	100	98	0,00098	2173	9,0	0,90
3	2,120	100	100	99	0,00099	2141	9,0	0,90
Average	2,123	100	100	99	0,00099	2152	8,3	**0,83**

Polymer-cement concrete 28 days								
Cube No.	**Mass (kg)**	**Dimension (mm)**	**Dimension (mm)**	**Dimension (mm)**	**Volume (m^3)**	**Density (kg/m^3)**	**Strength (kN)**	**Strength (MPa)**
1	2,080	100	100	99	0,00099	2101	14,0	1,40
2	2,170	100	100	99	0,00099	2192	14,0	1,40
3	2,090	100	100	96	0,00096	2177	15,0	1,50
Average	2,113	100	100	98	0,00098	2156	14,3	**1,43**

Polymer-cement concrete 60 days								
Cube No.	**Mass (kg)**	**Dimension (mm)**	**Dimension (mm)**	**Dimension (mm)**	**Volume (m^3)**	**Density (kg/m^3)**	**Strength (kN)**	**Strength (MPa)**
1	2,125	100	100	100	0,00100	2125	18,0	1,80
2	2,030	100	100	100	0,00100	2030	17,0	1,70
3	2,105	100	100	100	0,00100	2105	19,0	1,90
Average	2,087	100	100	100	0,00100	2087	18,0	**1,80**

Polymer-cement concrete (dried)								
Cube No.	**Mass (kg)**	**Dimension (mm)**	**Dimension (mm)**	**Dimension (mm)**	**Volume (m^3)**	**Density (kg/m^3)**	**Strength (kN)**	**Strength (MPa)**
1	2,085	100	100	98	0,00098	2128	43,0	4,30
2	2,065	100	100	99	0,00099	2086	36,0	3,60
3	2,140	100	100	100	0,00100	2140	45,0	4,50
Average	2,097	100	100	99	0,00099	2118	41,3	**4,13**

Control 7 days								
Cube No.	**Mass (kg)**	**Dimension (mm)**	**Dimension (mm)**	**Dimension (mm)**	**Volume (m^3)**	**Density (kg/m^3)**	**Strength (kN)**	**Strength (MPa)**
1	2,105	100	100	99	0,00099	2126	338,0	33,80
2	2,150	100	100	100	0,00100	2150	368,0	36,80
3	2,100	100	100	100	0,00100	2100	356,0	35,60
Average	2,118	100	100	100	0,00100	2125	354,0	**35,40**

Control 14 days								
Cube No.	**Mass (kg)**	**Dimension (mm)**	**Dimension (mm)**	**Dimension (mm)**	**Volume (m^3)**	**Density (kg/m^3)**	**Strength (kN)**	**Strength (MPa)**
1	2,115	100	100	99	0,00099	2136	421,0	42,10
2	2,105	100	100	99	0,00099	2126	428,0	42,80
3	2,130	100	100	100	0,00100	2130	400,0	40,00
Average	2,117	100	100	99	0,00099	2131	416,3	**41,63**

Control 28 days								
Cube No.	**Mass (kg)**	**Dimension (mm)**	**Dimension (mm)**	**Dimension (mm)**	**Volume (m^3)**	**Density (kg/m^3)**	**Strength (kN)**	**Strength (MPa)**
1	2,115	100	100	99	0,00099	2136	428,0	42,80
2	2,125	100	100	99	0,00099	2146	460,0	46,00
3	2,135	100	100	100	0,00100	2135	465,0	46,50
Average	2,125	100	100	99	0,00099	2139	451,0	**45,10**

Control 60 days								
Cube No.	**Mass (kg)**	**Dimension (mm)**	**Dimension (mm)**	**Dimension (mm)**	**Volume (m^3)**	**Density (kg/m^3)**	**Strength (kN)**	**Strength (MPa)**
1	2,125	100	100	97	0,00097	2191	435,0	43,50
2	2,065	100	100	96	0,00096	2151	432,0	43,20
3	2,035	100	100	96	0,00096	2120	437,0	43,70
Average	2,075	100	100	96	0,000963	2154	434,7	**43,47**

Substrate 28 days								
Cube No.	**Mass (kg)**	**Dimension (mm)**	**Dimension (mm)**	**Dimension (mm)**	**Volume (m^3)**	**Density (kg/m^3)**	**Strength (kN)**	**Strength (MPa)**
1	2,350	100	100	97	0,00097	2423	638,0	63,80
2	2,305	100	100	96	0,00096	2401	612,0	61,20
3	2,370	100	100	97	0,00097	2443	628,0	62,80
Average	2,342	100	100	97	0,00097	2422	626,0	**62,60**

A2 Restrained shrinkage (ring) tests

Specimen 1			
Material	**Crack date**	**Days to crack**	**No. of cracks**
Control	20 Sep & 22 Sep	8	2
60% FA	22 Sep & 23 Sep	10	2
80% FA	25 Sep & 26 Sep	13	2
100% FA	04 Oct	20	1
Polymer-cement concrete			

Specimen 2			
Material	**Crack date**	**Days to crack**	**No. of cracks**
Control	20 Sep & 20 Sep	7	2
60% FA	22 Sep & 23 Sep	10	2
80% FA	25 Sep	12	1
100% FA	8 Oct, 10 Oct & 11 Oct	26	3
Polymer-cement concrete			

Specimen 3			
Material	**Crack date**	**Days to crack**	**No. of cracks**
Control	20 Sep & 20 Sep	7	2
60% FA	23 Sep & 23 Sep	10	2
80% FA	25 Sep & 26 Sep	13	2
100% FA	10 Oct	26	1
Polymer-cement concrete			

Material	**Crack width specimen 1**			**Crack width specimen 2**			**Crack width specimen 3**			**Average crack width**
	(mm)			**(mm)**			**(mm)**			**(mm)**
Control	1,00	1,20	1,40	1,00	1,20	1,25	2,00	1,80	1,80	1,41
60% FA	0,60	0,60	0,80	0,60	0,60	0,70	0,80	0,80	0,90	0,71
80% FA	0,40	0,40	0,50	0,30	0,40	0,40	0,40	0,40	0,45	0,41
100% FA	0,40	0,60	0,45	0,10	0,15	0,10	0,20	0,10	0,10	0,24
Polymer-cement concrete	0,00	0,00	0,00	0,00	0,00	0,00	0,00	0,00	0,00	0,00

A3 Oxygen permeability index tests

Project:	MSc thesis Primesh Jassa
Sample ID:	100% FA
Date:	19 October 2016
Operator:	Primesh
Company:	UCT

Mean k (m/s):	1,925E-09
OPI (Based on mean k):	8,72
COV % (Mean k):	9,0
Variability Check:	Good

Sample 1		**Sample 2**		**Sample 3**		**Sample 4**	
Mean diameter (mm)	66,67	Mean diameter (mm)	67,24	Mean diameter (mm)	67,12	Mean diameter (mm)	67,18
Diameter 1 (mm)	66,64	Diameter 1 (mm)	67,00	Diameter 1 (mm)	67,17	Diameter 1 (mm)	67,11
Diameter 2 (mm)	66,98	Diameter 2 (mm)	67,26	Diameter 2 (mm)	66,91	Diameter 2 (mm)	67,25
Diameter 3 (mm)	66,23	Diameter 3 (mm)	67,33	Diameter 3 (mm)	66,98	Diameter 3 (mm)	67,47
Diameter 4 (mm)	66,81	Diameter 4 (mm)	67,36	Diameter 4 (mm)	67,42	Diameter 4 (mm)	66,88
Mean thickness (mm)	29,69	Mean thickness (mm)	29,75	Mean thickness (mm)	29,75	Mean thickness (mm)	29,64
Thickness 1 (mm)	29,56	Thickness 1 (mm)	29,93	Thickness 1 (mm)	29,21	Thickness 1 (mm)	29,50
Thickness 2 (mm)	30,07	Thickness 2 (mm)	29,87	Thickness 2 (mm)	29,98	Thickness 2 (mm)	29,90
Thickness 3 (mm)	29,53	Thickness 3 (mm)	29,73	Thickness 3 (mm)	29,74	Thickness 3 (mm)	29,70
Thickness 4 (mm)	29,60	Thickness 4 (mm)	29,48	Thickness 4 (mm)	30,05	Thickness 4 (mm)	29,44
Cell Volume (L)	4,60	Cell Volume (L)	4,60	Cell Volume (L)	4,60	Cell Volume (L)	4,60
k (m/s)	1,780E-09	k (m/s)	2,137E-09	k (m/s)	1,996E-09	k (m/s)	1,787E-09
r^2	0,9994	r^2	0,9988	r^2	0,9993	r^2	0,9953
r^2 Validity	Valid	r^2 Validity	Valid	r^2 Validity	Valid	r^2 Validity	Valid
OPI	8,75	OPI	8,67	OPI	8,70	OPI	8,75

Project:	MSc thesis Primesh Jassa
Sample ID:	80% FA
Date:	18 October 2016
Operator:	Primesh
Company:	UCT

Mean k (m/s):	4,526E-10
OPI (Based on mean k):	9,34
COV % (Mean k):	35,3
Variability Check:	Good

Sample 1		**Sample 2**		**Sample 3**		**Sample 4**	
Mean diameter (mm)	67,76	Mean diameter (mm)	67,77	Mean diameter (mm)	67,79	Mean diameter (mm)	67,92
Diameter 1 (mm)	67,76	Diameter 1 (mm)	68,01	Diameter 1 (mm)	67,69	Diameter 1 (mm)	68,01
Diameter 2 (mm)	67,72	Diameter 2 (mm)	67,85	Diameter 2 (mm)	67,90	Diameter 2 (mm)	67,74
Diameter 3 (mm)	67,97	Diameter 3 (mm)	67,75	Diameter 3 (mm)	67,75	Diameter 3 (mm)	68,04
Diameter 4 (mm)	67,59	Diameter 4 (mm)	67,47	Diameter 4 (mm)	67,82	Diameter 4 (mm)	67,89
Mean thickness (mm)	31,66	Mean thickness (mm)	31,76	Mean thickness (mm)	31,24	Mean thickness (mm)	31,36
Thickness 1 (mm)	31,70	Thickness 1 (mm)	31,30	Thickness 1 (mm)	31,17	Thickness 1 (mm)	31,49
Thickness 2 (mm)	31,57	Thickness 2 (mm)	31,50	Thickness 2 (mm)	31,20	Thickness 2 (mm)	31,16
Thickness 3 (mm)	31,64	Thickness 3 (mm)	32,18	Thickness 3 (mm)	31,27	Thickness 3 (mm)	31,30
Thickness 4 (mm)	31,71	Thickness 4 (mm)	32,07	Thickness 4 (mm)	31,32	Thickness 4 (mm)	31,48
Cell Volume (L)	4,60	Cell Volume (L)	4,60	Cell Volume (L)	4,60	Cell Volume (L)	4,60
k (m/s)	3,214E-10	k (m/s)	6,474E-10	k (m/s)	5,193E-10	k (m/s)	3,223E-10
r^2	0,9993	r^2	0,9964	r^2	0,9985	r^2	0,9989
r^2 Validity	Valid	r^2 Validity	Valid	r^2 Validity	Valid	r^2 Validity	Valid
OPI	9,49	OPI	9,19	OPI	9,28	OPI	9,49

Project:	MSc thesis Primesh Jassa
Sample ID:	60% FA
Date:	18 October 2016
Operator:	Primesh
Company:	UCT

Mean k (m/s):	1,242E-10
OPI (Based on mean k):	9,91
COV % (Mean k):	37,6
Variability Check:	Good

Sample 1		**Sample 2**		**Sample 3**		**Sample 4**	
Mean diameter (mm)	68,01	Mean diameter (mm)	67,93	Mean diameter (mm)	68,02	Mean diameter (mm)	68,05
Diameter 1 (mm)	68,07	Diameter 1 (mm)	67,98	Diameter 1 (mm)	67,93	Diameter 1 (mm)	67,98
Diameter 2 (mm)	68,01	Diameter 2 (mm)	67,96	Diameter 2 (mm)	68,04	Diameter 2 (mm)	68,04
Diameter 3 (mm)	68,09	Diameter 3 (mm)	68,00	Diameter 3 (mm)	67,94	Diameter 3 (mm)	68,12
Diameter 4 (mm)	67,86	Diameter 4 (mm)	67,79	Diameter 4 (mm)	68,16	Diameter 4 (mm)	68,06
Mean thickness (mm)	31,90	Mean thickness (mm)	31,65	Mean thickness (mm)	31,52	Mean thickness (mm)	31,98
Thickness 1 (mm)	31,30	Thickness 1 (mm)	31,49	Thickness 1 (mm)	31,54	Thickness 1 (mm)	31,71
Thickness 2 (mm)	31,71	Thickness 2 (mm)	31,72	Thickness 2 (mm)	31,69	Thickness 2 (mm)	32,02
Thickness 3 (mm)	32,09	Thickness 3 (mm)	31,74	Thickness 3 (mm)	31,46	Thickness 3 (mm)	32,06
Thickness 4 (mm)	32,51	Thickness 4 (mm)	31,66	Thickness 4 (mm)	31,38	Thickness 4 (mm)	32,13
Cell Volume (L)	4,60	Cell Volume (L)	4,60	Cell Volume (L)	4,60	Cell Volume (L)	4,60
k (m/s)	8,833E-11	k (m/s)	1,810E-10	k (m/s)	8,355E-11	k (m/s)	1,441E-10
r^2	0,9999	r^2	0,9989	r^2	0,9984	r^2	0,9986
r^2 Validity	Valid	r^2 Validity	Valid	r^2 Validity	Valid	r^2 Validity	Valid
OPI	10,05	OPI	9,74	OPI	10,08	OPI	9,84

Project:	MSc thesis Primesh Jassa
Sample ID:	Polymer-cement concrete
Date:	11 October 2016
Operator:	Primesh
Company:	UCT

Mean k (m/s):	7,071E-11
OPI (Based on mean k):	10,15
COV % (Mean k):	63,1
Variability Check:	Caution

Sample 1		**Sample 2**		**Sample 3**		**Sample 4**	
Mean diameter (mm)	67,68	Mean diameter (mm)	68,45	Mean diameter (mm)	68,05	Mean diameter (mm)	67,79
Diameter 1 (mm)	68,02	Diameter 1 (mm)	68,56	Diameter 1 (mm)	68,17	Diameter 1 (mm)	67,98
Diameter 2 (mm)	67,18	Diameter 2 (mm)	68,06	Diameter 2 (mm)	67,88	Diameter 2 (mm)	68,06
Diameter 3 (mm)	67,74	Diameter 3 (mm)	68,75	Diameter 3 (mm)	68,10	Diameter 3 (mm)	67,09
Diameter 4 (mm)	67,79	Diameter 4 (mm)	68,41	Diameter 4 (mm)	68,04	Diameter 4 (mm)	68,01
Mean thickness (mm)	26,08	Mean thickness (mm)	27,10	Mean thickness (mm)	27,52	Mean thickness (mm)	27,67
Thickness 1 (mm)	22,28	Thickness 1 (mm)	27,13	Thickness 1 (mm)	27,26	Thickness 1 (mm)	27,53
Thickness 2 (mm)	27,21	Thickness 2 (mm)	27,10	Thickness 2 (mm)	27,57	Thickness 2 (mm)	27,55
Thickness 3 (mm)	27,42	Thickness 3 (mm)	27,07	Thickness 3 (mm)	27,71	Thickness 3 (mm)	27,77
Thickness 4 (mm)	27,40	Thickness 4 (mm)	27,09	Thickness 4 (mm)	27,55	Thickness 4 (mm)	27,81
Cell Volume (L)	4,60	Cell Volume (L)	4,60	Cell Volume (L)	4,60	Cell Volume (L)	4,60
k (m/s)	4,905E-11	k (m/s)	2,392E-11	k (m/s)	1,270E-10	k (m/s)	8,292E-11
r^2	0,9944	r^2	0,9681	r^2	0,9929	r^2	0,9950
r^2 Validity	Valid	r^2 Validity	Invalid	r^2 Validity	Valid	r^2 Validity	Valid
OPI	10,31	OPI	10,62	OPI	9,90	OPI	10,08

Project:	MSc thesis Primesh Jassa
Sample ID:	Control
Date:	11 September 2016
Operator:	Primesh
Company:	UCT

Mean k (m/s):	9,124E-11
OPI (Based on mean k):	10,04
COV % (Mean k):	68,4
Variability Check:	Caution

Sample 1		**Sample 2**		**Sample 3**		**Sample 4**	
Mean diameter (mm)	68,51	Mean diameter (mm)	68,44	Mean diameter (mm)	68,63	Mean diameter (mm)	68,64
Diameter 1 (mm)	68,68	Diameter 1 (mm)	68,33	Diameter 1 (mm)	68,56	Diameter 1 (mm)	68,65
Diameter 2 (mm)	68,68	Diameter 2 (mm)	68,33	Diameter 2 (mm)	68,56	Diameter 2 (mm)	68,65
Diameter 3 (mm)	68,33	Diameter 3 (mm)	68,55	Diameter 3 (mm)	68,69	Diameter 3 (mm)	68,62
Diameter 4 (mm)	68,33	Diameter 4 (mm)	68,55	Diameter 4 (mm)	68,69	Diameter 4 (mm)	68,62
Mean thickness (mm)	32,06	Mean thickness (mm)	32,24	Mean thickness (mm)	31,82	Mean thickness (mm)	32,06
Thickness 1 (mm)	31,62	Thickness 1 (mm)	31,99	Thickness 1 (mm)	32,05	Thickness 1 (mm)	31,96
Thickness 2 (mm)	32,45	Thickness 2 (mm)	32,01	Thickness 2 (mm)	31,63	Thickness 2 (mm)	31,82
Thickness 3 (mm)	32,69	Thickness 3 (mm)	32,42	Thickness 3 (mm)	31,48	Thickness 3 (mm)	32,33
Thickness 4 (mm)	31,49	Thickness 4 (mm)	32,55	Thickness 4 (mm)	32,11	Thickness 4 (mm)	32,11
Cell Volume (L)	4,60	Cell Volume (L)	4,60	Cell Volume (L)	4,60	Cell Volume (L)	4,60
k (m/s)	4,612E-11	k (m/s)	1,437E-10	k (m/s)	1,461E-10	k (m/s)	2,899E-11
r^2	0,9993	r^2	0,9992	r^2	0,9999	r^2	0,9984
r^2 Validity	Valid	r^2 Validity	Valid	r^2 Validity	Valid	r^2 Validity	Valid
OPI	10,34	OPI	9,84	OPI	9,84	OPI	10,54

A4 Water sorptivity tests

Project:	MSc thesis Primesh Jassa
Sample ID:	100% FA
Date:	October 19, 2016
Operator:	Primesh
Company:	UCT

				Variability
Av. Sorptivity:	42,4	COV:	4,0	Good
Av. Porosity:	17,54	COV:	1,1	Good

	Sample 1	**Sample 2**	**Sample 3**	**Sample 4**
Diameter (mm)	66,67	67,24	67,12	67,18
Thickness (mm)	29,69	29,75	29,75	29,64
Time (min)	Mass (g)	Mass (g)	Mass (g)	Mass (g)
0	183,6	183,7	183,3	183,1
3	191,0	189,7	188,4	188,4
5	193,0	191,6	190,2	190,5
7	194,6	192,9	191,5	191,8
9	195,8	194,3	192,6	193,1
12	197,5	196,0	194,2	194,9
16	199,4	197,8	196,0	196,8
20	200,4	199,3	197,6	198,4
25	200,7	199,9	199,2	199,5
Saturated Mass (g)	202,0	202,1	201,9	201,3
R^2 (Must be >0.98)	0,9942	0,9888	0,9997	0,9955
Range	3-20 min	3-25 min	3-25 min	3-25 min
Sorptivity ($mm/hr^{0.5}$)	43,8	40,9	41,0	44,0
Porosity (%)	17,8	17,4	17,7	17,3

Project:	MSc thesis Primesh Jassa
Sample ID:	80% FA
Date:	October 18, 2016
Operator:	Primesh
Company:	UCT

				Variability
Av. Sorptivity:	13,2	COV:	19,2	Caution
Av. Porosity:	21,81	COV:	1,8	Good

	Sample 1	**Sample 2**	**Sample 3**	**Sample 4**
Diameter (mm)	67,76	67,77	67,79	67,92
Thickness (mm)	31,66	31,76	31,24	31,36
Time (min)	Mass (g)	Mass (g)	Mass (g)	Mass (g)
0	216,5	215,8	212,3	212,9
3	218,5	218,9	214,9	215,2
5	219,0	219,8	215,6	215,8
7	219,4	220,5	216,1	216,4
9	219,8	221,1	216,6	216,9
12	220,4	221,9	217,2	217,4
16	221,0	222,9	217,9	218,0
20	221,5	223,6	218,5	218,6
25	222,0	224,4	219,2	219,3
Saturated Mass (g)	240,9	240,7	237,5	237,7
R^2 (Must be >0.98)	0,9997	0,9992	0,9999	0,9996
Range	3-25 min	3-25 min	3-25 min	3-25 min
Sorptivity ($mm/hr^{0.5}$)	11,0	16,8	12,7	12,2
Porosity (%)	21,4	21,8	22,3	21,8

Project:	MSc thesis Primesh Jassa
Sample ID:	60% FA
Date:	October 18, 2016
Operator:	Primesh
Company:	UCT

				Variability
Av. Sorptivity:	10,0	COV:	16,2	Caution
Av. Porosity:	19,85	COV:	2,3	Good

	Sample 1	**Sample 2**	**Sample 3**	**Sample 4**
Diameter (mm)	68,01	67,93	68,02	68,05
Thickness (mm)	31,90	31,65	31,52	31,98
Time (min)	Mass (g)	Mass (g)	Mass (g)	Mass (g)
0	222,8	220,1	219,1	222,7
3	224,1	221,9	220,5	224,1
5	224,5	222,7	221,0	224,6
7	224,8	223,1	221,3	225,1
9	225,1	223,5	221,7	225,4
12	225,4	224,0	222,0	225,8
16	225,8	224,6	222,5	226,4
20	226,1	225,1	223,0	226,9
25	226,5	225,6	223,4	227,5
Saturated Mass (g)	245,2	243,5	241,9	245,6
R^2 (Must be >0.98)	0,9993	0,9976	0,9996	0,9995
Range	3-25 min	3-25 min	3-25 min	3-25 min
Sorptivity ($mm/hr^{0.5}$)	8,0	11,7	9,5	11,0
Porosity (%)	19,3	20,4	20,0	19,8

Project:	MSc thesis Primesh Jassa
Sample ID:	Polymer-cement concrete
Date:	October 11, 2016
Operator:	Primesh
Company:	UCT

				Variability
Av. Sorptivity:	11,4	COV:	13,7	Good
Av. Porosity:	2,50	COV:	8,6	Good

	Sample 1	**Sample 2**	**Sample 3**	**Sample 4**
Diameter (mm)	67,68	68,45	68,05	67,79
Thickness (mm)	26,08	27,10	27,52	27,67
Time (min)	Mass (g)	Mass (g)	Mass (g)	Mass (g)
0	222,6	226,3	213,0	226,0
3	222,8	226,5	213,1	226,1
5	222,9	226,6	213,1	226,2
7	222,9	226,6	213,2	226,2
9	223,0	226,7	213,3	226,3
12	223,0	226,7	213,3	226,3
16	223,1	226,9	213,4	226,4
20	223,1	227,0	213,4	226,5
25	223,2	227,0	213,5	226,5
Saturated Mass (g)	225,2	229,0	215,3	228,3
R^2 (Must be >0.98)	0,9807	0,9828	0,9821	0,9815
Range	3-25 min	3-25 min	3-20 min	3-25 min
Sorptivity ($mm/hr^{0.5}$)	9,5	12,8	12,4	10,7
Porosity (%)	2,7	2,7	2,3	2,3

Project:	MSc thesis Primesh Jassa
Sample ID:	Control
Date:	September 11, 2016
Operator:	Primesh
Company:	UCT

				Variability
Av. Sorptivity:	5,2	COV:	17,5	Caution
Av. Porosity:	14,53	COV:	5,7	Good

	Sample 1	**Sample 2**	**Sample 3**	**Sample 4**
Diameter (mm)	68,51	68,44	68,63	68,64
Thickness (mm)	32,06	32,24	31,82	32,06
Time (min)	Mass (g)	Mass (g)	Mass (g)	Mass (g)
0	231,8	238,9	231,8	236,3
3	232,4	239,4	232,4	236,8
5	232,6	239,5	232,5	236,9
7	232,7	239,6	232,7	237,0
9	232,9	239,8	232,9	237,1
12	233,0	239,9	233,0	237,3
16	233,3	240,1	233,3	237,4
20	233,5	240,3	233,6	237,5
25	233,7	240,4	233,9	237,6
Saturated Mass (g)	249,2	255,6	250,2	252,5
R^2 (Must be >0.98)	0,9970	0,9943	0,9870	0,9969
Range	3-25 min	3-25 min	3-25 min	3-25 min
Sorptivity (mm/hr$^{0.5}$)	5,5	5,0	6,3	4,1
Porosity (%)	14,7	14,1	15,6	13,7

A5 Chloride conductivity tests

Project:	MSc thesis Primesh Jassa
Sample ID:	100% FA
Date:	19 Oct 16
Operator:	Primesh
Company:	UCT

Sample 1		Sample 2		Sample 3		Sample 4	
Thickness	**Diameter**	**Thickness**	**Thickness**	**Thickness**	**Diameter**	**Thickness**	**Diameter**
29,53	66,93	29,45	66,53	30,62	66,85	30,25	67,18
29,93	66,54	29,84	66,52	30,75	66,76	29,55	66,76
29,95	66,57	29,36	66,41	29,61	67,01	30,81	67,01
29,56	66,83	29,46	66,58	29,45	66,73	29,45	66,06
29,74	**66,72**	**29,53**	**66,51**	**30,11**	**66,84**	**30,02**	**66,75**

Sample	Oven dry mass (g)	Saturated mass (g)	Thickness (mm)	Diameter (mm)	Voltage (V)	Current (mA)	Conductivity (mS/cm)
Sample 1	183,85	218,91	29,74	66,72	2,01	333,0	14,13
Sample 2	183,35	230,19	29,53	66,51	2,00	277,3	11,76
Sample 3	184,23	231,55	30,11	66,84	2,00	255,8	10,97
Sample 4	184,46	231,73	30,02	66,75	2,03	388,7	16,46

Average:	13,33
COV:	18,62
Rating:	Very Poor

Project:	MSc thesis Primesh Jassa
Sample ID:	80% FA
Date:	18 Oct 16
Operator:	Primesh
Company:	UCT

Sample 1		Sample 2		Sample 3		Sample 4	
Thickness	**Diameter**	**Thickness**	**Diameter**	**Thickness**	**Diameter**	**Thickness**	**Diameter**
31,02	67,93	31,03	67,66	31,15	67,53	31,20	67,78
31,35	67,57	31,34	67,84	31,02	67,95	31,44	67,50
31,57	67,71	31,55	67,81	31,10	67,45	30,86	67,85
30,82	67,98	31,57	67,67	31,35	67,92	31,12	67,76
31,19	**67,80**	**31,37**	**67,75**	**31,16**	**67,71**	**31,16**	**67,72**

Sample	**Oven dry mass (g)**	**Saturated mass (g)**	**Thickness (mm)**	**Diameter (mm)**	**Voltage (V)**	**Current (mA)**	**Conductivity (mS/cm)**
Sample 1	212,20	236,50	31,19	67,80	5,09	247,4	4,20
Sample 2	213,02	238,44	31,37	67,75	5,02	230,3	3,99
Sample 3	212,13	237,48	31,16	67,71	5,03	231,9	3,99
Sample 4	211,07	236,66	31,16	67,72	5,03	234,0	4,02

Average:	4,05
COV:	2,47
Rating:	Very Poor

Project:	MSc thesis Primesh Jassa
Sample ID:	60% FA
Date:	11 Oct 16
Operator:	Primesh
Company:	UCT

Sample 1		Sample 2		Sample 3		Sample 4	
Thickness	**Diameter**	**Thickness**	**Diameter**	**Thickness**	**Diameter**	**Thickness**	**Diameter**
31,66	68,08	31,24	68,04	31,57	67,93	31,11	67,94
31,43	68,02	31,42	68,03	31,66	68,00	30,95	68,00
31,74	68,00	31,82	68,20	31,47	67,96	31,13	67,96
31,92	68,04	32,21	67,95	31,53	67,84	31,22	67,91
31,69	**68,04**	**31,67**	**68,06**	**31,56**	**67,93**	**31,10**	**67,95**

Sample	Oven dry mass (g)	Saturated mass (g)	Thickness (mm)	Diameter (mm)	Voltage (V)	Current (mA)	Conductivity (mS/cm)
Sample 1	220,19	244,45	31,69	68,04	5,11	156,9	2,68
Sample 2	222,11	243,05	31,67	68,06	5,11	105,7	1,80
Sample 3	220,82	244,09	31,56	67,93	5,06	110,0	1,89
Sample 4	216,10	239,24	31,10	67,95	5,08	128,2	2,16

Average:	2,13
COV:	18,43
Rating:	Poor

Project:	MSc thesis Primesh Jassa
Sample ID:	Polymer-cement concrete
Date:	11 Oct 16
Operator:	Primesh
Company:	UCT

Sample 1		Sample 2		Sample 3		Sample 4	
Thickness	**Diameter**	**Thickness**	**Diameter**	**Thickness**	**Diameter**	**Thickness**	**Diameter**
27,05	68,14	25,79	67,89	26,76	67,86	27,31	68,10
26,87	69,02	26,35	68,19	26,47	67,90	27,61	67,99
26,89	68,16	26,13	67,82	26,56	67,87	27,82	67,89
26,82	68,08	25,66	68,12	26,76	67,99	27,41	67,92
26,91	**68,35**	**25,98**	**68,01**	**26,64**	**67,91**	**27,54**	**67,98**

Sample	**Oven dry mass (g)**	**Saturated mass (g)**	**Thickness (mm)**	**Diameter (mm)**	**Voltage (V)**	**Current (mA)**	**Conductivity (mS/cm)**
Sample 1	210,46	212,05	26,91	68,35	10,05	13,8	0,10
Sample 2	199,22	200,66	25,98	68,01	10,06	27,0	0,19
Sample 3	205,21	206,86	26,64	67,91	10,08	16,8	0,12
Sample 4	211,80	213,28	27,54	67,98	10,02	19,5	0,15

Average:	0,14
COV:	27,85
Rating:	Excellent

Project:	MSc thesis Primesh Jassa
Sample ID:	Control
Date:	11 Sep 16
Operator:	Primesh
Company:	UCT

Sample 1		Sample 2		Sample 3		Sample 4	
Thickness	**Diameter**	**Thickness**	**Diameter**	**Thickness**	**Diameter**	**Thickness**	**Diameter**
31,35	68,51	32,96	68,34	31,86	69,05	31,81	68,55
31,68	68,58	32,87	68,19	31,64	69,13	32,46	68,54
31,88	68,26	32,51	68,49	31,54	69,37	32,61	68,52
31,75	68,46	32,56	68,31	31,61	69,26	32,84	68,52
31,67	**68,45**	**32,73**	**68,33**	**31,66**	**69,20**	**32,43**	**68,53**

Sample	Oven dry mass (g)	Saturated mass (g)	Thickness (mm)	Diameter (mm)	Voltage (V)	Current (mA)	Conductivity (mS/cm)
Sample 1	231,72	247,73	31,67	68,45	10,13	132,1	1,12
Sample 2	229,66	246,46	32,73	68,33	10,14	172,4	1,52
Sample 3	230,79	246,74	31,66	69,20	10,07	147,1	1,23
Sample 4	235,55	251,08	32,43	68,53	10,08	134,6	1,17

Average:	1,26
COV:	14,00
Rating:	Good

A6 Accelerated drying shrinkage tests

Specimen	100% FA
Cast date	14.09.16
Dimensions	100x100x200 mm

Date	**21 Sep**		**28 Sep**		**30 Sep**		**02 Oct**		**04 Oct**	
	Initial		**7 days**		**7 days + 48 hrs**		**7 days + 96 hrs**		**7 days + 144 hrs**	
	L_0 /µm		L_1 /µm		L_2 /µm		L_2 /µm		L_2 /µm	
Prism	A	B	A	B	A	B	A	B	A	B
1	502	506	451	456	448	454	449	451	448	448
2	502	499	452	448	450	446	447	437	445	439
3	497	512	449	460	444	457	443	455	441	453
Strains	(µ-ε)		510	500	540	520	530	550	540	580
			500	510	520	530	550	620	570	600
			480	520	530	550	540	570	560	590
Average strain	µ-ε		503		532		560		573	
20% Avg strain	µ-ε		101		106		112		115	
Range	µ-ε		40		30		90		60	
Validity	-		OK		OK		OK		OK	

Specimen	80% FA
Cast date	21.09.16
Dimensions	100x100x200 mm

Date	**28 Sep**		**05 Oct**		**07 Oct**		**09 Oct**	
	Initial		**7 days**		**7 days + 48 hrs**		**7 days + 96 hrs**	
	L_0 /µm		L_1 /µm		L_2 /µm		L_3 /µm	
Prism	A	B	A	B	A	B	A	B
1	497	502	462	470	461	468	460	468
2	535	513	503	482	500	480	500	480
3	511	505	480	473	478	472	477	472
Strains	(µ-ε)		350	320	360	340	370	340
			320	310	350	330	350	330
			310	320	330	330	340	330
Average strain	µ-ε		322		340		343	
20% Avg strain	µ-ε		64		68		69	
Range	µ-ε		40		30		40	
Validity	-		OK		OK		OK	

Specimen	60% FA
Cast date	21.09.16
Dimensions	100x100x200 mm

Date	**28 Sep**		**05 Oct**		**07 Oct**		**09 Oct**	
	Initial		**7 days**		**7 days + 48 hrs**		**7 days + 96 hrs**	
	L_0 /µm		L_1 /µm		L_2 /µm		L_3 /µm	
Prism	A	B	A	B	A	B	A	B
1	505	526	477	500	475	499	475	498
2	513	503	485	478	484	474	484	474
3	499	529	473	505	470	502	470	498
Strains	(µ-ε)		280	260	300	270	300	280
			280	250	290	290	290	290
			260	240	290	270	290	310
Average strain	µ-ε		262		285		293	
20% Avg strain	µ-ε		52		57		59	
Range	µ-ε		40		30		30	
Validity	-		OK		OK		OK	

Specimen	Polymer-cement concrete
Cast date	28.10.16
Dimensions	100 x 100 x 200 mm

Date	**04 Nov**		**11 Nov**		**13 Nov**		**15 Nov**		**17 Nov**		**19 Nov**		**21 Nov**		**23 Nov**		**25 Nov**		**27 Nov**	
	Initial		**7 days**		**7 days + 48 hrs**		**7 days + 96 hrs**		**7 days + 144 hrs**		**7 days + 192 hrs**		**7 days + 240 hrs**		**7 days + 288 hrs**		**7 days + 336 hrs**		**7 days + 384 hrs**	
	L_0 /µm		L_1 /µm		L_2 /µm		L_3 /µm		L_4 /µm		L_3 /µm		L_4 /µm		L_4 /µm		L_4 /µm		L_4 /µm	
Prism	A	B	A	B	A	B	A	B	A	B	A	B	A	B	A	B	A	B	A	B
1	510	484	466	448	454	432	441	419	433	409	426	402	419	394	413	387	408	380	404	374
2	515	504	463	445	453	428	443	413	435	402	431	395	425	387	420	378	415	370	412	363
3	511	501	457	461	443	447	433	438	423	430	418	426	412	420	405	416	398	410	394	408
Strains	(µ-ε)		440	360	560	520	690	650	770	750	840	820	910	900	970	970	1020	1040	1060	1100
			520	590	620	760	720	910	800	1020	840	1090	900	1170	950	1260	1000	1340	1030	1410
			540	400	680	540	780	630	880	710	930	750	990	810	1060	850	1130	910	1170	930
Average strain	µ-ε		475		613		730		822		878		947		1010		1073		1117	
20% Avg strain	µ-ε		95		123		146		164		176		189		202		215		223	
Range	µ-ε		230		240		280		310		340		360		410		430		480	
Validity	-		INVALID		INVALID		INVALID		INVALID		INVALID		INVALID		INVALID		INVALID		INVALID	

- Note: The shrinkage readings for the polymer-cement concrete were all found to be invalid i.e. the difference in shrinkage values between the three prisms tested were too large. This was likely due to the long setting time of the material which resulted in slow and differential water loss.

Specimen	Polymer-cement concrete (continued)
Cast date	28.10.16
Dimensions	100 x 100 x 200 mm

Date	**29 Nov**		**01 Dec**		**03 Dec**		**05 Dec**		**07 Dec**		**09 Dec**		**11 Dec**		**13 Dec**		**15 Dec**		**17 Dec**		**19 Dec**	
	7 days + 432 hrs		**7 days + 480 hrs**		**7 days + 528 hrs**		**7 days + 576 hrs**		**7 days + 624 hrs**		**7 days + 672 hrs**		**7 days + 720 hrs**		**7 days + 768 hrs**		**7 days + 816 hrs**		**10 days + 864 hrs**		**7 days + 912 hrs**	
	$L_4/\mu m$		$L_4/\mu m$		$L_4/\mu m$		$L_4/\mu m$		$L_4/\mu m$		$L_4/\mu m$		$L_4/\mu m$		$L_4/\mu m$		$L_4/\mu m$		$L_4/\mu m$		$L_4/\mu m$	
Prism	A	B	A	B	A	B	A	B	A	B	A	B	A	B	A	B	A	B	A	B	A	B
1	400	370	394	364	391	359	387	355	382	350	378	346	373	340	369	336	367	333	366	332	366	332
2	409	358	403	351	399	346	396	341	392	335	389	332	385	325	381	322	378	319	377	319	377	318
3	389	404	383	398	379	395	373	391	369	387	365	385	359	379	356	377	352	374	350	373	349	373
Strains	1100	1140	1160	1200	1190	1250	1230	1290	1280	1340	1320	1380	1370	1440	1410	1480	1430	1510	1440	1520	1440	1520
	1060	1460	1120	1530	1160	1580	1190	1630	1230	1690	1260	1720	1300	1790	1340	1820	1370	1850	1380	1850	1380	1860
	1220	970	1280	1030	1320	1060	1380	1100	1420	1140	1460	1160	1520	1220	1550	1240	1590	1270	1610	1280	1620	1280
Average strain	1158		1220		1260		1303		1350		1383		1440		1473		1503		1513		1517	
20% Avg strain	232		244		252		261		270		277		288		295		301		303		303	
Range	490		500		520		530		550		560		570		580		580		570		580	
Validity	INVALID		INVALID		INVALID		INVALID		INVALID		INVALID		INVALID		INVALID		INVALID		INVALID		INVALID	

- Note: The shrinkage readings for the polymer-cement concrete were all found to be invalid i.e. the difference in shrinkage values between the three prisms tested were too large. This was likely due to the long setting time of the material which resulted in slow and differential water loss.

Specimen	Control
Cast date	07.09.16
Dimensions	100x100x200 mm

Date	**14 Sep**		**22 Sep**		**23 Sep**		**26 Sep**		**27 Sep**		**29 Sep**	
	Initial		**8 days**		**7 days + 48 hrs**		**7 days + 120 hrs**		**7 days + 144 hrs**		**7 days + 192 hrs**	
	L_0 /µm		L_1 /µm		L_2 /µm		L_3 /µm		L_4 /µm		L_4 /µm	
Prism	A	B	A	B	A	B	A	B	A	B	A	B
1	505	510	479	483	473	479	467	469	465	467	463	467
2	530	530	504	499	502	497	490	491	491	489	491	487
3	522	518	496	487	494	484	487	478	486	476	484	474
Strains	(µ-ε)		260	270	320	310	380	410	400	430	420	430
			260	310	280	330	400	390	390	410	390	430
			260	310	280	340	350	400	360	420	380	440
Average strain	µ-ε		278		310		388		402		415	
20% Avg strain	µ-ε		56		62		78		80		83	
Range	µ-ε		50		60		60		70		60	
Validity	-		OK		OK		OK		OK		OK	

Appendix B Product sheets

B1 Bitumen

DALVEN products

CAPE TOWN: P.O. Box 371, Eppindust 7475 Tel: 021 593 6790 Fax: 021 593 8650
JOHANNESBURG: P.O. Box 1358, Florida 1710 Tel: 011 472 4417 Fax: 011 472 1206
HEAD OFFICE: P.O. Box 26738, Hout Bay 7872 Tel: 021 790 2379 Fax: 021 790 3360
E-mail: info@dalven.co.za Website: www.dalven.co.za

WATERBLOK RUBBERISED BITUMEN

EMULSION WATERPROOFING COMPOUND

DESCRIPTION

WATERBLOK Rubberised Waterproofing Compound (R.W.P.C.).is a mineral filled emulsion of a refined grade of bitumen which contains a high percentage of rubber latex. It is a multi-purpose waterproofing and sealing compound. It is a water based emulsion and requires no heating. The product has the consistency of a soft paste and is thixotropic. It is thus very easy to apply with brushes or soft brooms.

TYPICAL USES

WATERBLOK R.W.P.C.after drying gives a highly elastic bituminous film which is impervious to water. It is an excellent sealing compound for walls, parapet walls, flashings, roofs, reservoirs and fish ponds etc. It may be applied to asphalt, asbestos cement, concrete, corrugated iron, lead, zinc, roofing felt and similar surfaces whether flat, sloping, or vertical. It can be used on its own when applied to sound surfaces that are free of cracks and joints, or in conjunction with geotextile fabric where there is any possibility of movement in cracks or joints.

SPECIAL CHARACTERISTICS

A high percentage of rubber latex imparts considerable elasticity to the dried film.

PREPARATION

Remove all dust, dirt and rust. Where moss and lichen etc. are present, this should be removed, and the surface treated with fungicide which should be allowed to dry before the WATERBLOK treatment proceeds. Stir contents of tin before use.

APPLICATION

WATERBLOK can be applied to both damp (and drying), and dry surfaces with soft brushes or brooms which should be dampened with water before, and occasionally during use, to avoid clogging and to ensure ease of application. To promote adhesion and spreading in very hot weather and on absorbent surfaces, dampen the surface with water.

Porous surfaces such as brickwork, concrete or asbestos-cement should first be primed with a coat of WATERBLOK R.W.P.C. diluted 50/50 with water. Allow to dry before proceeding.

WATERBLOK R.W.P.C. is brushed on but is not a paint. It is a waterproofing coating and should be applied at a thickness of approximately 1mm for best results. Recommended coverage is therefore 1litre per m^2 per layer to achieve desired film thickness.

A second application is recommended to waterproof porous surfaces and to provide a thoroughly durable covering. Each coat must be dry before the next is applied. Drying time will be approximately 2 - 3 hours in sunny weather.

Where joints, cracked or unstable areas need to be treated, it is advisable to embed non-woven polyester geofabric membrane into the first full strength coat of WATERBLOK immediately after application while the product is still wet. After drying, a further two coats should be applied over the membrane.

This system creates a very effective and flexible waterproof membrane. In cases where the product is used together with membrane the total application for all coats is approximately 3 litres per m^2 (excluding the prime coat).

When waterproofing cement dams or ponds, particularly where they are excavated below ground level, care should be taken to ensure that no free moisture is migrating through the wall and inhibiting the drying of the product. The surrounding ground should be dry and there should be no signs of dampness or moisture inside the pond. After applying the product, ensure that it is properly cured and dry before proceeding with following applications. There should be no wet, brown areas visible once the product has cured correctly. The use of membrane is recommended in area's which are very porous, or where cracks or joints are present.

NOTE:

Do not apply if rain appears probable within a few hours. Ideally WATERBLOK should be applied during the morning of a sunny day. To test for proper curing, rub the surface with a wet finger. Once dry, WATERBLOK R.W.P.C. will not cause brown staining.

WATERBLOK R.W.P.C. should not be applied to surfaces previously treated with tar-based materials unless such materials have weathered for two to three years.

Brushes or brooms should be washed in clean water immediately after use; if clogged, they can be cleaned with paraffin or white spirit. These solvents should not be used on brushes or brooms during application.

SPECIFICATION

Product Type	:	Bitumen emulsion containing rubber latex
Product Consistency	:	Soft thixotropic paste.
Colour	:	Black when dry.
Drying time	:	2-3 hours outdoors on a sunny day.
Water Permeability	:	Impervious to depths of 5m
Flash Point	:	Non inflammable
Fire Resistance	:	Low fire spread
Mass per litre	:	1.05 kilograms
Availability	:	1 litre, 5 litre, 20 litre, 200 litre containers
Effect of U.V.	:	Viaseal Waterblok film has withstood 500 hrs in SABS weatherometer. SABS 1134-77
Toxicity to water	:	None. SABS 1217
Elong.@ B. Point	:	100% SABS 952 - 1969
Acid Resistance	:	Unaffected by 30% sulphuric acid. (1 year @ 25^{o}C).
Softening point	:	91^{o}C
Ductility @ 10^{o}C	:	> 100 cm
Elastic Recovery @ 10^{o}C	:	47.5%
Solids Content	:	61%

B2 Polymer

FX2320

Technical Datasheet

1. Product Description

ELOTEX® FX2320 is a redispersible binder based on a copolymer of vinyl acetate and ethylene.

Protective colloid	Polyvinyl alcohol
Additives	Mineral anti-block agents
Plasticisers	none
Solvents	none
Film-forming agents	none

2. Specifications

Appearance	free-flowing, white powder
Bulk density	450 - 650 g/l
Residual moisture	maximum 1.0%
Ash TGA 1000°C	10.5% +/- 1.5%
pH value	6.0 – 9.0 (as a 10% dispersion in water)
Min. film building temp.	+ 0°C
Film properties	opaque, flexible

3. Application Areas

ELOTEX® FX2320 is a flexible redispersible binder for the modification of mortar and plaster systems, based on cement with/without hydrated lime.

a) Main application areas

– ETICS: adhesives and base coat renders
– Base coat renders and plasters
– Finishing renders and plasters, skim coats
– Non structural repair mortars

4. Key Properties

a) During processing

– Excellent redispersability
– Reduced water demand
– Excellent rheology and workability
– Good open time performance

b) In the cured state

– Increased adhesion, especially on EPS, XPS and MW boards
– Increased flexibility and impact resistance
– Increased cohesion
– Increased surface abrasion resistance
– Avoids crack formation
– Increased long-term performance

5. Powder Processing

ELOTEX® redispersible powders can be blended in all commercial positive mixers with other dry additives to produce finished products in powder form. Since ELOTEX® redispersible powders exhibit thermoplastic behaviour, mixing times should be as short as possible, and significant temperature rise caused by strong shear forces should be avoided. All hydraulically and non-hydraulically curing dry mixtures with ELOTEX® redispersible powder may be easily mixed with water before application. For mixing finished products in powder form, one usually places the required amount of mixing water in a suitable vessel and add the powder mixture under agitation. Too intensive agitation of the mixture may result in unwanted air inclusion. Before application, one should allow the mixture to stand for a short time. Depending on the properties of the other additives, the standing time will be in the range of approx. 1-5 minutes.

6. Packaging and Storage

Standard packaging: 25 kg paper sacks with polyethylene liners.
Other types of packaging such as Big Bags or silo wagons are possible on request.
As a basic rule it is recommended to store ELOTEX® redispersible powder in a dry location at temperatures below 25°C and to process within six months. Sacks that are stored under pressure, damaged or left open for an extended period tend to cause blocking of the redispersible powder.

7. Quality, Safety and Environment

ELOTEX® redispersible powders are non-toxic and are unclassified according to Regulation 88/379/EEC. We recommend all individuals using ELOTEX® redispersible powder, or coming in contact with it, to observe the separate Safety Data Sheets. Our safety specialists will be pleased to advise you regarding safety, health and environmental issues of our products. Akzo Nobel Chemicals AG has been certified according to DIN EN ISO9001 and DIN EN ISO14001.

Product Liability

The above information and recommendations are based upon our experience and are offered merely for advice. They do not absolve the consumer from making his own tests. Akzo Nobel Chemicals AG, their representatives or distributor organizations have no control over the conditions under which ELOTEX® redispersible powders are transported, stored, handled or used. Responsibility for damage arising from the use of our products cannot be derived from the recommendations given. The observance of any intellectual property rights of third parties is the responsibility of the consumer in each case.

Technical information may not be passed on to any third party without our previous consent.

Other Information

Version	5 / 11.3.2014
Replaces version from	1.11.2012
Date of issue	29.8.2002

Akzo Nobel Chemicals AG
Industriestrasse 17a, CH-6203 Sempach
Station T +41 41 469 69 69 F +41 41 469 69 00
contact.elotex@akzonobel.com www.akzonobel.com/elotex

AkzoNobel

Appendix C Ethics clearance form

EBE Faculty: Assessment of Ethics in Research Projects

Any person planning to undertake research in the Faculty of Engineering and the Built Environment at the University of Cape Town is required to complete this form before collecting or analysing data. When completed it should be submitted to the supervisor (where applicable) and from there to the Head of Department. If any of the questions below have been answered YES, and the applicant is NOT a fourth year student, the Head should forward this form for approval by the Faculty EIR committee: submit to Ms Zakiya Chikte (Zakiya.chikte@uct.ac.za); New EBE Building, Ph 021 650 5739).

Please note – It is important to keep a signed copy of this form as students must include a copy of the completed form with the dissertation/thesis when it is submitted for examination.

Name of Principal Researcher/Student: PRIMESH JASSA **Department:** CIVIL (COMSIRU)

If a Student: **Degree:** Civil Infrastructure management **Supervisor:** Professor Hans.

If a Research Contract indicate source of funding/sponsorship:

Research Project Title: Alternative patch repair material for rebar corrosion damage.

Overview of ethics issues in your research project:

Question 1: Is there a possibility that your research could cause harm to a third party (i.e. a person not involved in your project)?	YES	(NO)
Question 2: Is your research making use of human subjects as sources of data? If your answer is YES, please complete Addendum 2.	YES	(NO)
Question 3: Does your research involve the participation of or provision of services to communities? If your answer is YES, please complete Addendum 3.	YES	(NO)
Question 4: If your research is sponsored, is there any potential for conflicts of interest? If your answer is YES, please complete Addendum 4.	YES	(NO)

If you have answered YES to any of the above questions, please append a copy of your research proposal, as well as any interview schedules or questionnaires (Addendum 1) and please complete further addenda as appropriate.

I hereby undertake to carry out my research in such a way that

- there is no apparent legal objection to the nature or the method of research; and
- the research will not compromise staff or students or the other responsibilities of the University;
- the stated objective will be achieved, and the findings will have a high degree of validity;
- limitations and alternative interpretations will be considered;
- the findings could be subject to peer review and publicly available; and
- I will comply with the conventions of copyright and avoid any practice that would constitute plagiarism.

Signed by:

	Full name and signature	Date
Principal Researcher/Student: Signed by candidate	Signed by candidate	4/2/2016.

This application is approved by:

Supervisor (if applicable):	Signed by candidate	04/02/16
HOD (or delegated nominee): Final authority for all assessments with NO to all questions and for all undergraduate research.	Signed by candidate	05/02/'16
Chair : Faculty EIR Committee For applicants other than undergraduate students who have answered YES to any of the above questions.	Signed by candidate	